UNIVERSITY OF BIRMINGHAM

Exploring The Utility Of 3D-Skin Models To Evaluate Trans-dermal Uptake of Flame Retardants from Indoor Dust and Consumer Products

by

GOPAL PAWAR

M.Pharm (Pharmacology)

A thesis submitted to the University of Birmingham for the degree of:

DOCTOR OF PHILOSOPHY (Ph.D)

Division of Environmental Health and Risk Management

School of Geography, Earth and Environmental Sciences

College of Life and Environmental Sciences

University of Birmingham

United Kingdom

MARIE CURIE ACTIONS

A·TEAM

ADVANCED TOOLS FOR EXPOSURE ASSESSMENT AND BIOMONITORING

June 2017

ABSTRACT

The aim of this research was to evaluate the utility of innovative *in vitro* techniques as an alternatives for human/animal tissues to study the transdermal uptake of organic flame retardants from indoor dust and consumer products. Firstly, we successfully designed and applied an *in vitro* physiologically based extraction test to provide new insights into the dermal bioaccessibility of various FRs from indoor dust. These investigations revealed the bioaccessible fraction for the brominated flame retardants (BFRs) α-, β-and γ- HBCD and TBBPA to 1:1 (sweat/sebum) mixture to be 41 %, 47 %, 50 % and 40 %, respectively, while for the phosphate flame retardants (PFRs) TCEP, TCIPP and TDCIPP, the values were 10 %, 17 % and 19 %. With the exception of TBBPA, the presence of cosmetics had a significant effect ($p < 0.05$) on the bioaccessibility of our target FRs from indoor dust. The presence of cosmetics decreased the bioaccessibility of HBCDs from indoor dust, whereas shower gel and sunscreen lotion enhanced the bioaccessibility of target PFRs. Secondly, we developed a protocol for studying dermal uptake of legacy and novel brominated flame retardants using two 3D-HSE (three dimensional human skin equivalent tissue) models, EpiDerm™ and EPISKIN™ in compliance with the OECD guidelines 428. Overall, results showed a significant negative correlation between the permeability constant of FRs and their Log K_{OW} values. We also mimicked real life exposure scenarios by exposing the skin surface in turn to FR-containing dust, reference material plastics and upholstered fabrics. Our findings showed that under such scenarios dermal exposure to FRs was appreciable for UK adults and toddlers. For example, for dust exposure, our estimates of daily intake indicated toddlers to be 10 times more highly exposed than adults in the presence of sweat and sebum. This differential exposure is likely attributable to more dust adhering to toddler's skin and their higher exposed skin surface area to body weight ratio compared to adults.

ACKNOWLEDGMENTS

I would like to express my sincere gratitude to my PhD supervisor and A-TEAM project coordinator Prof. Stuart Harrad for the continuous support, his patience, motivation and his immense knowledge during my PhD study. His guidance helped me during my research and writing of this thesis. I would also like to thank my second supervisor and also a good friend, Dr. Mohamed Abdallah for his insightful comments and encouragement. I could not have imagined a better supervisors for my PhD work.

The A-TEAM project has provided me many opportunities for travel and collaboration with the collaborators across the Europe and also ADAPT project undertaken by Dr. Mohamed Abdallah. My sincere thanks also goes to Prof. Adrian Covaci and Dr. Malarvanan who guided me during these years.

Thank you Marie Curie –ITN program for funding my research work and big thanks to all the researchers in A-TEAM.

Thanks to my fellow friends in the lab Dr. Cassandra Rauert, Dr. Sandra Brommer, Dr.Yuning Ma, Dr. Fang Tao, Dr. William Stubbing, Dr. Layala, Dr. Tuan and soon to be Dr. Ana, Yessica, Salim Ali Sakaroun, Jiangmeng Kuang, Leon, Aristide & Hoang Nguyen.

I would like to greatfully acknowledge Dr. William Stubbing for providing the fabric samples for our study.

I couldn't have imagined my dream comes true without the inspirations from my ex-colleagues from Jubilant Drug discovery (India). A big-big thanks to Dr. Ramesh Mullangi, Dr. Shrikanth Kanagal and Dr. Sanjeev Giri.

Last but not the least I am immensely grateful to my family members and friends for their love & encouragement to pursue my dream.

TABLE OF CONTENTS

LIST OF TABLES

Chapter I: Introduction

Chapter II: Analytical methodology and validation

Chapter V Towards understanding the role of skin moisture and oiliness on dermal uptake of flame retardant chemicals

Chapter VI Dermal bioaccessibility and uptake of PBDEs from plastics

Chapter VII Dermal bioaccessibility and uptake of organophosphate flame retardants from upholstered fabrics

LIST OF FIGURES

Chapter I: Introduction

Chapter II: Analytical methodology and validation

Chapter III: Dermal bioaccessibility of flame retardants from indoor dust

CHAPTER IV Studies of dermal uptake of FRs applied as neat compounds to *in vitro* models

Chapter V Towards understanding the role of skin moisture and oiliness on dermal uptake of flame retardant chemicals

Chapter VI Dermal bioaccessibility and uptake of PBDEs from plastics

Chapter VII Dermal bioaccessibility and uptake of organophosphate flame retardants from upholstered fabrics

LIST OF PUBLICATIONS

1. Abou-Elwafa Abdallah M, **Pawar G**, Harrad S. Human dermal absorption of chlorinated organophosphate flame retardants; implications for human exposure. Toxicol Appl Pharmacol. 2016;291:28-37.
2. Abdallah MA-E, **Pawar G**, Harrad S. Evaluation of 3D-human skin equivalents for assessment of human dermal absorption of some brominated flame retardants. Environment International. 2015;84:64-70.
3. Abdallah MA, Zhang J, **Pawar G**, Viant MR, Chipman JK, D'Silva K, et al. High-resolution mass spectrometry provides novel insights into products of human metabolism of organophosphate and brominated flame retardants. Anal Bioanal Chem. 2015;407(7):1871-83.
4. **Pawar G**, Abdallah MA, de Saa EV, Harrad S. Dermal bioaccessibility of flame retardants from indoor dust and the influence of topically applied cosmetics. J Expo Sci Environ Epidemiol. 2017;27(1):100-5.
5. Abdallah MA, **Pawar G**, Harrad S. Evaluation of in vitro vs. in vivo methods for assessment of dermal absorption of organic flame retardants: a review. Environ Int. 2015;74:13-22.
6. Abdallah MA, **Pawar G**, Harrad S. Effect of Bromine Substitution on Human Dermal Absorption of Polybrominated Diphenyl Ethers. Environ Sci Technol. 2015;49(18):10976-83.

CONFERENCE PRESENTATIONS

OP = oral presentation; **PP** = Poster presentation and **CA** = contributing author.

1. **Pawar G**, Abdallah, MA, Harrad S. Exploring the utility of 3D synthetic skin models to evaluate the transdermal uptake of Flame retardants from indoor dust.*The 2nd UK & Ireland Exposure Science,*2014; Manchester UK (**PP)**
2. **Pawar G**, Abdallah, MA, Harrad S. Fire Master 550®- deep under the skin ??.*The 34th International symposium on Halogenated Persistent Organic pollutants-Dioxin*, 2014; Madrid, Spain **(PP)**
3. Abou-Elwafa Abdallah M, Harrad S, **Pawar G.**Application of 3D-Human skin equivalent model for in-vitro assessment of dermal absorption of brominated flame retardants. *The 34th International symposium on Halogenated Persistent Organic pollutants-Dioxin*, 2014; Madrid, Spain **(CA)**
4. Abou-Elwafa Abdallah M, Harrad S, **Pawar G.** Application of 3D-Human skin equivalent model for in-vitro assessment of dermal absorption of brominated flame retardants.*7th International symposium on Flame retardants.BFR,* 2015; Beijing, China **(CA)**
5. **Pawar G**, Abdallah, MA, Harrad S. Dermal bioaccessibility of flame retardants from indoor dust and the influence of topically applied cosmetics.The 35th International symposium on halogenated persistent organic pollutants.Dioxin 2015 ; Sao Paulo;Brazil **(OP) Otto Hutzinger Student Award**
6. **Pawar G**, Abdallah, MA, Harrad S. Invitro dermal upatke of PBDEs from plastics. *The 10th POPs conference***.**2016**;** Birmingham,UK.**(PP)**
7. Thuy Bui, Mohamed Abdallah,Georgios Giovanoulis, **Gopal Pawar**,Jorgen Magner,Anna Palm-Cousins, Stuart Harrad.Dermal uptake of pthalate esters and alternative plasticizers using 3D human skin equivalents (EPISKIN™).*The 10th POPs conference***.**2016**;** Birmingham,UK.**(CA)**

ABBREVIATIONS

BFR	Brominated flame retardants.
PBDE	Polybrominated diphenyl ethers.
HBCD	Hexabromocyclododecane.
TBBP-A	Tetrabromobisphenol A.
NBFR	Novel brominated flame retardants.
OPFRs	Organophosphate flame retardants.
HIPS	High impact polystyrene.
POPs	Persistent organic pollutants.
DBDPE	Decabromodiphenylethane.
BTBPE	1, 2-bis (2, 4, 6-tribromophenoxy) ethane.
BEHTEBP	Bis (2-ethylhexyl) tetrabromophthalate.
TCEP	Tris (2-chloroethyl) phosphate.
TCIPP	Tris (2-chloro-1-methylethyl) phosphate.
TDCPP	Tris (1, 3-dichloro-2-propyl) phosphate.
TPhP	Triphenyl phosphate.
T*o*CP	Tri-*o*-cresyl-phospahte.
T*m*CP	Tri-*m*-cresyl-phosphate.
T*p*CP	Tri-*p*-cresyl-phosphate.
EHDPP	2-Ethylhexyl diphenyl phosphate.
TnBP	Tri-n-butyl phosphate.
TEHP	Tris (2-ethylhexyl) phosphate.
TBOEP	Tris (2-butoxyethyl) phospahte.
PBEB	Pentabromoethylbenzene.
ECHA	European Chemical Agency.
EH-TBB	2-ethylhexyl-2, 3, 4, 5-tetrabromobenzoate.
HBB	Hexabromobenzene.
DPTE	3-dibromopropyl-2, 4, 6-tribromophenyl ether.
PBT	Pentabromotoluene.
PBBz	Pentabromobenzene.
TBECH	Tetrabromoethylcyclohexane.
***Syn/anti*- DP**	Syn/anti-Dechlorane plus.

SC	Stratum corneum.
OATP	Organic anion transporting polypeptides.
PK	Pharmacokinetics.
CYP-450	Cytochrome P-450.
PCB	Polychlorinated biphenyls.
US. EPA	United States Environmental Protection Agency.
HEPES	4-(2-hydroxyethyl)-1-piperazineethanesulfonic acid).
BPA	Bisphenol-A.
3D-HSE	3-Dimensional Human skin equivalent.
OECD	Organisation for Economic Co-operation and Development.
ECVAM	European Centre for Validation of Alternative Methods.
RHE	Reconstructed Human Epidermis.
FT	Full thickness.
KC	Keratinocytes.
FB	Fibroblasts.
LCs	Langerhans cells.
UDP-GT	Uridine diphosphate glucuronosyl transferase.
GST	Glutathione-S-transferases.
mRNA	Messenger ribonucleic acid.
FMOs	Flavin containing monooxygenase.
GSTP1	Glutathione- S-transferase P1.
COMT	Catechol-O-methyl transferase.
SULT2B1b	Steroid sulfotransferase.
NAT5	N-acetyl transferase 5.
LC-MS/MS	Liquid chromatography- mass spectrometry.
GC-MS	Gas chromatography-mass spectrometry.
WHO	World health organisation.
BLQ	Below limit of quantification.
AHH	Aryl hydrocarbon hydroxylase.
EROD	7-ethoxyresorufin O-dealkylase.
NAT	N-acetyl transferase.
COX	Cyclooxygenase.

NCI	Negative chemical ionisation.
SIM	Selected ion monitoring.
QA/QC	Quality assurance and quality control.
RRF	Relative response factor.
S/N	Signal to noise ratio.
RRT	Relative retention time.
RDS	Relative determination standard.
IS	Internal standard
SSSM	Synthetic sweat sebum mixture
NIST	National institute of standards and technology.
SRM-2585	Standard reference material.
SSFL	Skin surface film liquid.
LOD	Limits of detection.
FEV	Final extract volume.
VFEI	Volume of final extract injected.
SS	Sample size.
ANOVA	Analysis of variance.
ppm	Parts per million.
DED	Daily exposure dose
BSA	Body surface area.
FA	Fraction absorbed.
IEF	Indoor exposure fraction.
BW	Body weight.
NSRL	No significant risk level.
HBLVs	Health base limit values.
NOAEL	No observed adverse effect level.
RFD	Reference dose.
MM	Maintenance medium.
MPD	MatTek permeation device.
TEWL	Trans-epidermal water loss.

SD	Standard deviation.
TEER	Trans-epidermal electrical resistance.
MTT	3-(4, 5-dimethylthiazol-2-yl)-2, 5-diphenyltetrazolium bromide.
t_{lag}	Lag time.
K_p	Permeability coefficient.
J_{max}	Maximum flux.
M.Wt	Molecular weight.
2, 4, 6-TBP	2, 4, 6 Tribromophenol.
q.s	Quantity sufficient.
E&E	Electrical and electronics.
WEEE	Waste electrical and electronic equipment.
IRMM	Institute for Reference Materials and Measurements.
DCM	Dichloromethane.
RH	Relative humidity.
PP	Polypropylene.
LDPE	Low density polyethylene.
BSEF	Bromine science environmental forum
ER	Estrogenic forum
DMEM	Dulbecco's Modified Eagle's Medium

CHAPTER I
INTRODUCTION

Some passages in this chapter have been quoted verbatim from a review article:

Abdallah, MA-E, Pawar, G & Harrad, S 2015, 'Evaluation of in vitro vs. in vivo methods for assessment of dermal absorption of organic flame retardants: A review' Environment International, vol 74, pp. 13-22.

1.1: Flame retardants

Fire has been a major cause of property damage, injuries and death over many centuries. Efforts to reduce such fire hazards and to increase associated safety standards resulted in the development of flame retardants (FRs). FRs are a group of chemicals added during the manufacture of polymers and textiles to inhibit or delay the spread of fire by suppressing the chemical reactions in the flame or by the formation of a protective layer on the surface of a material. The most common classes of flame retardants are: Brominated, Phosphorous, Nitrogen, Chlorinated and Inorganic. Among the brominated group, the important ones are polybrominated diphenyl ethers (PBDEs), hexabromocyclododecane (HBCD), tetrabromobisphenol A (TBBP-A), novel brominated flame retardants (NBFRs), as well as organophosphate flame retardants (PFRs) (Ghosh, Hageman and Bjorklund 2011, van der Veen and de Boer 2012b)

PBDEs are a class of anthropogenic chemicals with 209 theoretical congeners (Fromme et al. 2016). They have been used as additive flame retardants in plastics, textiles, casings for electronic devices and circuitry. The fully brominated product (Deca-BDE) dominated the market worldwide with a global demand of 56,100 t in 2001 when compared

to 7,500 and 3,790 t for the less brominated Penta-BDE and Octa-BDE formulations, respectively (BSEF 2013).

The major application of Hexabromocyclododecane (HBCD) is polystyrene foams (expanded and extruded) used mainly for thermal insulation of buildings. It has also been applied in the back coating of fabrics for textiles and to a lesser extent in high impact polystyrene (HIPS) (KEMI (National Chemicals Inspectorate) 2008). Commercial HBCD formulations consist mainly of the γ-HBCD diastereoisomer (75–89%), while the α- and β-HBCD are present in considerably lower amounts (10–13% and 1–12%), respectively (Tao, Abdallah and Harrad 2016b). The global market demand for HBCD in 2001 (the last publicly available figures) was estimated at about 16,700 tons, 57% of which was in Europe (Covaci et al. 2006a)

TBBP-A is the most widely used BFR with a global market of 120,000 to 150,000 tons/year, including TBBP-A derivatives. It is applied mainly for epoxy resins used in printed circuit boards of consumer electronics (TVs, vaccum cleaners, washing machines etc), fax machines and photocopiers, vacuum cleaners, coffee machines and plugs/socket.(Wang et al. 2015, Covaci et al. 2009)

As is the case with PBDEs, HBCD and ~20% of the production of TBBP-A are blended physically within (and referred to as "additive" FRs) rather than bound chemically (and known as "reactive" FRs) to polymeric materials. Such additive FRs more readily migrate from products and their environmental persistence and bioaccumulative nature leads to contamination of the environment including humans (Harrad et al. 2010a). Hence, there is great concern owing to their potential health risks such as endocrine disruption, neuro-developmental and behavioural disorders, hepatotoxicity & possibly cancer (Darnerud 2008, Oulhote, Chevrier and Bouchard 2016, Wikoff and Birnbaum 2011), cryptorchidism (Main et al. 2007), thyroid hormone homeostasis (Turyk et al. 2008), effects on male hormones and

semen quality (Johnson et al. 2013, Meeker et al. 2009, Abdelouahab, Ainmelk and Takser 2011, Wikoff and Birnbaum 2011) and impaired fecundability in adult women (Harley et al. 2010a). Further, they lower birth weight and length (Chao et al. 2007, Lignell et al. 2013). Such evidence has contributed to complete EU bans for the Penta- and Octa-BDE formulations, and restrictions on the use of Deca-BDE. In addition, PBDEs associated with Penta and Octa-BDE are listed under the UNEP Stockholm Convention on POPs, while Deca-BDE is currently under consideration for listing under Annexes A, B and/or C of the convention (Stockholm Convention on POPs 2009). Furthermore, HBCD will be phased out following its recent listing under Annex A of the Stockholm Convention (Stockholm Convention on POPs 2013). Despite such restrictions on their production and use, human exposure to PBDEs and HBCD is likely to continue for some time, given the ubiquity of flame retarded products remaining in use and entering the waste stream, coupled with the environmental persistence of these BFRs. (Harrad and Diamond 2006)

These restrictions on the use of PBDEs and HBCD have paved the way for the use of so-called novel BFRs (NBFRs) as replacements with an estimated global production volume of 100,000 tonnes in 2009 (Covaci, Harrad and Abdallah 2011a). Major NBFRs are: DBDPE (Decabromodiphenylethane), BTBPE (1,2-bis(2,4,6 tribromophenoxy) ethane), EH-TBB (2-ethylhexyl 2,3,4,5-tetrabromobenzoate), and BEH-TEBP (Bis (2-ethylhexyl)tetrabromophthalate) (Table 1.3). These chemicals are either new to the market or have been detected recently in the environment. NBFRs are now being found as ubiquitously as PBDEs and they have been observed in indoor (Stuart et al. 2008, Covaci et al. 2011b, Ali et al. 2011, Karlsson et al. 2007) and outdoor environments (Shi et al. 2009, Ismail et al. 2009).Some NBFRs (EH-TBB,TBPH) have been reported to display endocrine disruption activity (Saunders et al. 2013, Patisaul et al. 2013a). However, very little is known about the toxicological properties and the pathways and magnitude of human exposure to NBFRs.

Nevertheless, several NBFRs bear striking structural similarity to PBDEs (e.g. DBDPE is a very close analogue of BDE-209) and are reported to have similarly low vapour pressures and water solubilities, as well as high K_{OW} values, and PBT characteristics. (Covaci et al. 2011b)

In addition to BFRs, PFRs have been associated with a wide range of applications (Table 1.4). Likely linked to the aforementioned restrictions on PBDEs, EU market demand for PFRs increased from 83,700 tons in 2004 to 91,000 tons in 2006 (EFRA 2007). Tris (2-chloroethyl) phosphate (TCEP), tris (2-chloro-1-methylethyl) phosphate (TCIPP) and tris (1, 3-dichloro-2-propyl) phosphate (TDCIPP) were all subject to an EU risk assessment process under an Existing Substances Regulation (EEC 793/93) (Regnery and Püttmann 2010). Despite lower stability and overall environmental persistence than PBDEs, they were classified as persistent organic compounds in the aquatic environment and reported to fulfil Persistent bioaccumulative and Toxic (PBT) criteria. In addition, several studies have reported them to display adverse effects including reproductive toxicity and carcinogenic effects on lab animals.(Regnery et al. 2011). Hence TCEP is classified by the EU as a "potential human carcinogen" (Regnery and Püttmann 2010), while TDCIPP is classified under regulation EC 1272/2008 as a category 2 carcinogen (ECHA 2010).

Fig 1.1: Chemical structure of PBDEs

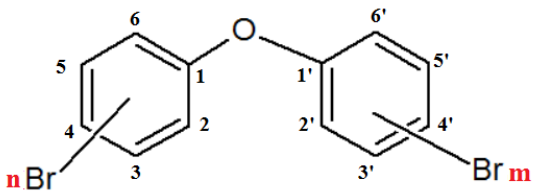

PBDE congeners are formed by substitution of H atom with Br atoms at 1,1',2,2',3,3'4,4',5,5',6,6' positions of benzene ring

Table 1.1: Molecular weights and LogKow values for PBDE congeners (Pubchem, National Center for Biotechnology Information. PubChem Compound Database)

BDE #	Bromine substitution	CAS NO	Mol.Wt (g/mol)	LogKow
28	2,4,4'-tri BDE	41318756	405.8	5.94
47	2,2',4,4'-tetra BDE	5436431	485.79	6.2
99	2,2',4,4',5-penta BDE	32534819	564.69	6.9
100	2,2',4,4',6-penta BDE	189084648	564.69	6.9
153	2,2',4,4',5,5'-hexaBDE	68631492	643.587	7.6
183	2,2',3,4,4',5'6-hepta BDE	207122165	722.483	8.3
209	2,2',3,3',4,4',5,5',6,6'-deca BDE	1163195	959.17	10.3

Fig 1.2: Chemical structures of selected brominated and phosphorus flame retardants

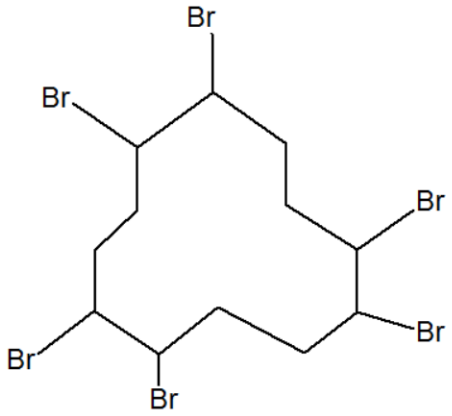

Hexabromocyclododecane

(HBCD)

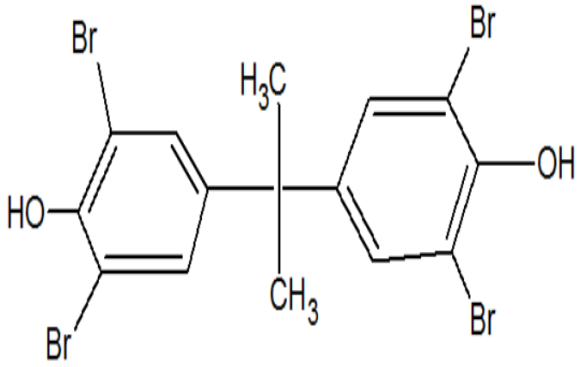

Tetrabromobisphenol-A

(TBBPA)

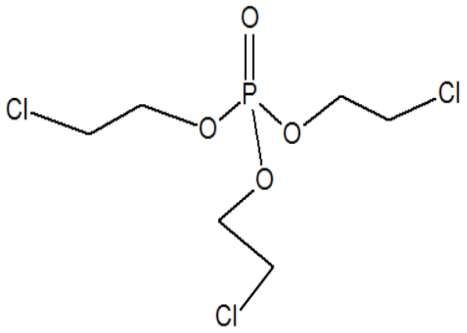

Tris (2-chloroethyl) phosphate

(TCEP)

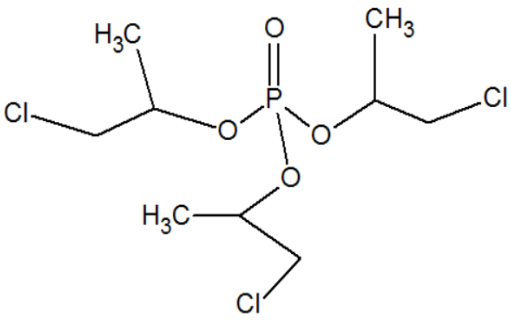

Tris (2-chloroisopropyl)phosphate

(TCIPP)

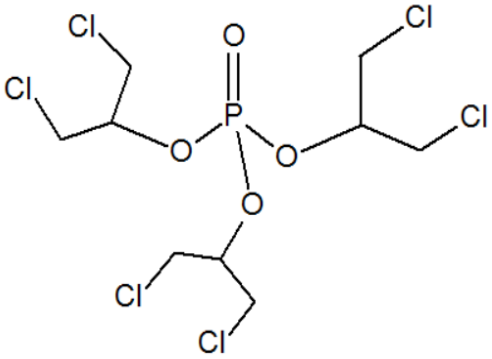

Tris(1,3-dichloroisopropyl)phosphate

(TDCIPP)

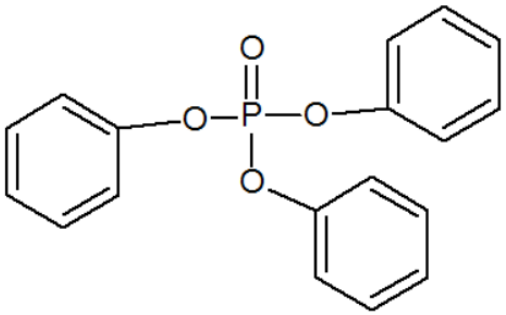

Triphenyl phosphate

(TPhP)

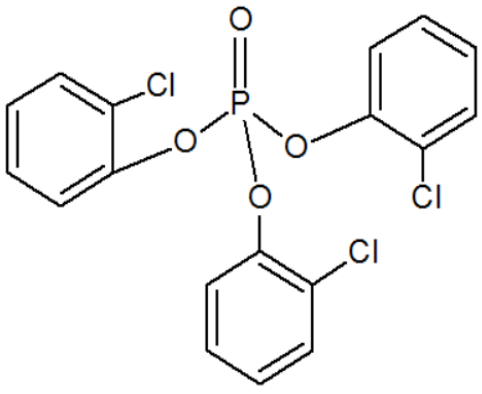

Tricresyl phosphate

(TCP)

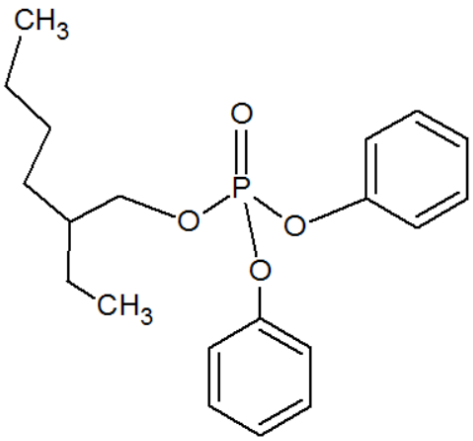

2-Ethylhexyl diphenyl phosphate

(EHDPP)

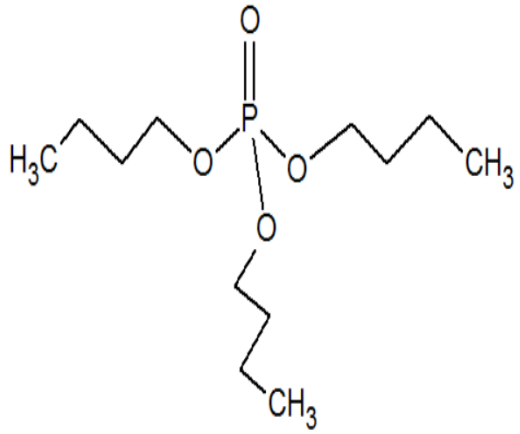

Tri-n-butyl phosphate

(TnBP)

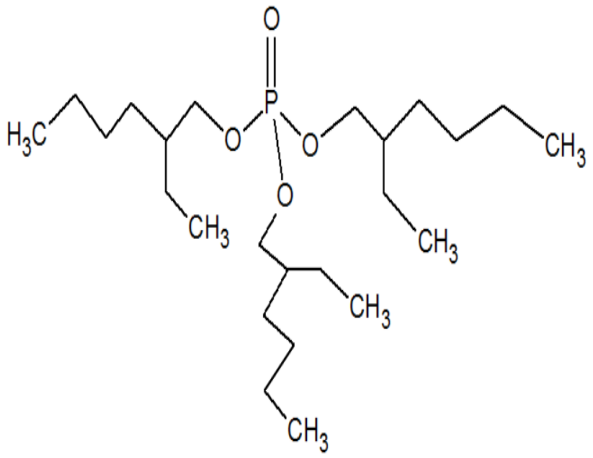

Tris (2-ethylhexyl) phosphate

(TEHP)

Table 1.2: Molecular weight and LogKow values of BFRs (Pubchem, National Center for Biotechnology Information. PubChem Compound Database)

BFRS	Abbrev.	CAS NO	Mol.Wt (g/mol)	Log Kow
α-Hexabromocyclododecane	α-HBCD	678970-15-5	641.7	5.07
β-Hexabromocyclododecane	β-HBCD	678970-16-6	641.7	5.12
γ-Hexabromocyclododecane	γ-HBCD	678970-17-7	641.7	5.47
Tetrabromobisphenol-A	TBBP-A	121839-52-9	543.9	5.90
Tris(2-chloroethyl)phosphate	TCEP	115-96-8	285.49	1.44
Tris(2-chloroisopropyl) phosphate	TCIPP	13674-84-5	327.57	2.59
Tris(1,3-dichloroisopropyl)phosphate	TDCIPP	13674-87-8	430.91	3.56
Triphenyl phosphate	TPhP	115-86-6	326.29	4.59
Tri-o-cresyl-phosphate	T*o*CP	78-30-8	368.37	6.34
Tri-m-cresyl-phosphate	T*m*CP	563-04-2	368.37	6.34
Tri-p-cresyl-phosphate	T*p*CP	78-32-0	368.37	6.34
2-Ethylhexyl diphenyl phosphate	EHDPP	1241-94-7	362.41	5.73
Tri-n-butyl phosphate	TnBP	126-73-8	266.32	4.0
Tris (2-ethylhexyl) phosphate	TEHP	78-42-2	434.65	9.49
Tris (2-butoxyethyl) phosphate	TBOEP	78-51-3	398.48	3.75

Fig 1.3: Chemical structures of Novel brominated flame retardants.

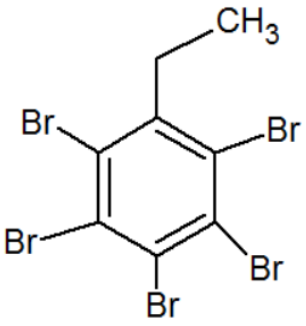

Pentabromoethylbenzene

(PBEB)

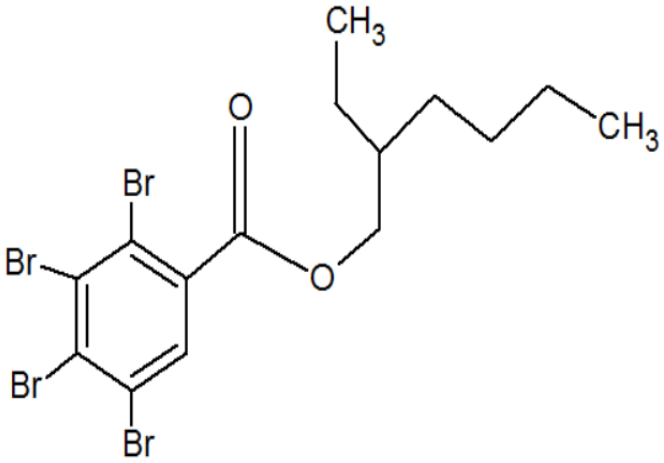

2-ethylhexyl-2,3,4,5 tetrabromobenzoate

(EHTBB)

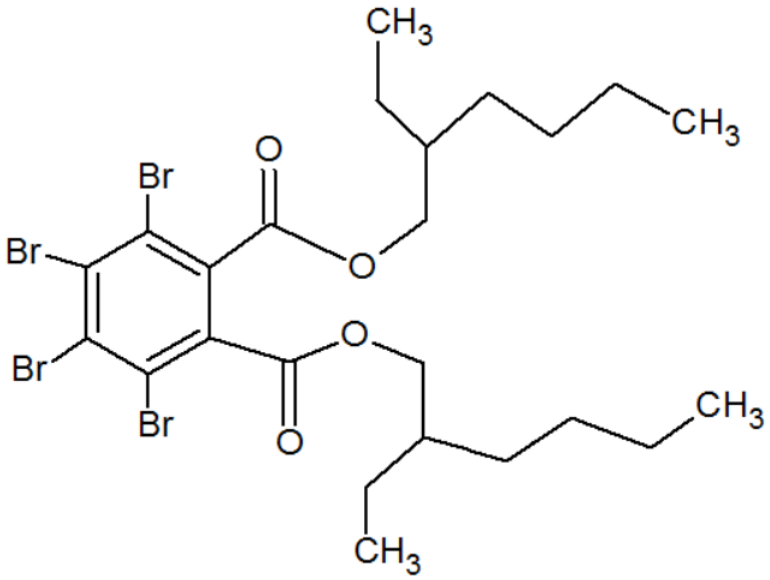

Bis (2-ethylhexyl)-2,3,4,5-tetrabromophthalate

BEHTEBP

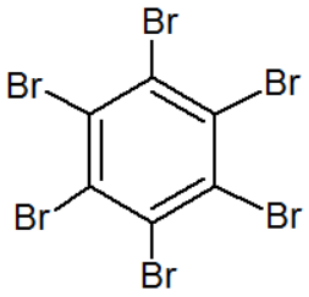

Hexabromobenzene

(HBB)

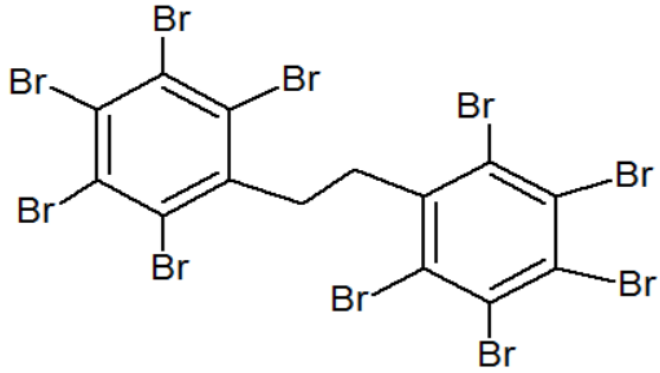

Decabromodiphenylethane

(DBDPE)

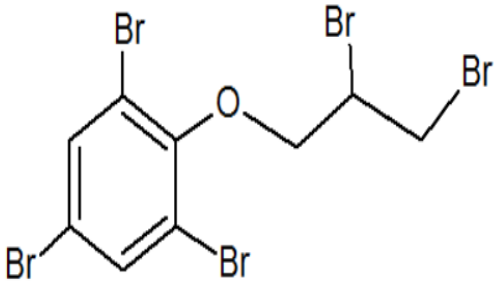

2,3-dibromopropyl-2,4,6-tribromophenyl ether

(DPTE)

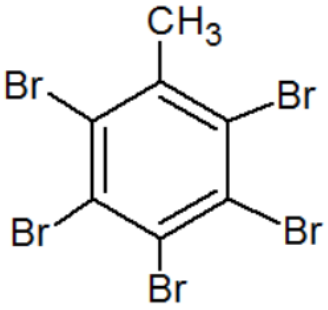

Pentabromotoluene

(PBT)

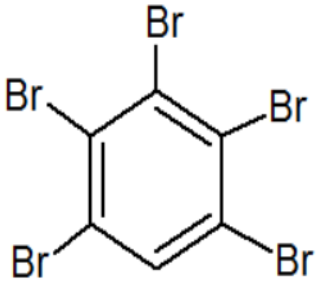

Pentabromobenzene

(PBBz)

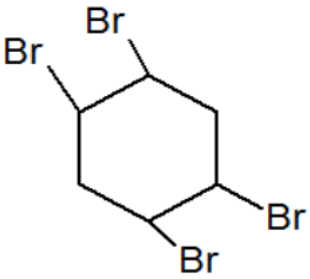

1,2,4,5-Tetrabromocyclohexane

(TBECH)

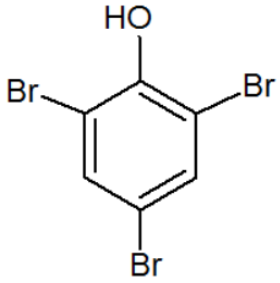

2,4,6-Tribromophenol

(2,4,6-TBP)

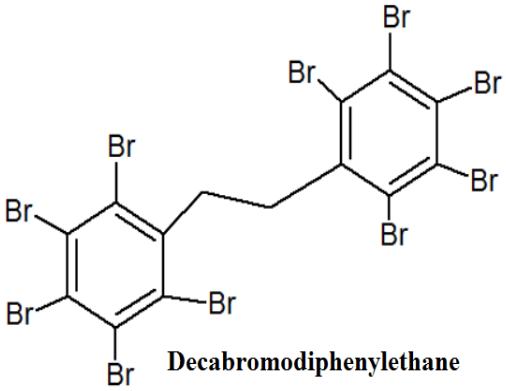

Decabromodiphenylethane

(DBDPE)

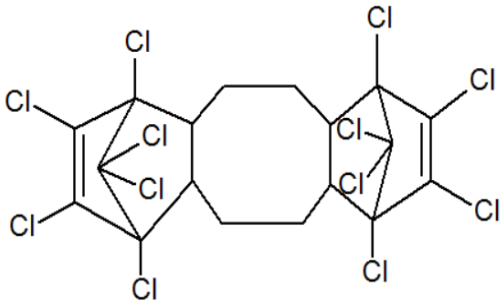

Dechlorane plus

(DP)

Table 1.3: Physicochemical properties of Novel brominated flame retardants

NBFRs	Abbrev.	CAS NO	Mol.Wt (g/mol)	Log K_{OW}
Pentabromoethylbenzene	PBEB	85-22-3	500.645	7.96
2-ethylhexyl-2,3,4,5-tetrabromobenzoate	EH-TBB	183658-27-7	549.9	7.73
Bis (2-ethylhexyl)-2,3,4,5-tetrabromophthalate	BEHTEBP	26040-51-7	706.2	11.95
1,2-Bis(2,4,6-tribromophenoxy)ethane	BTBPE	37853-59-1	687.6	9.1
Hexabromobenzene	HBB	87-82-1	551.49	6.07
2,3-dibromopropyl-2,4,6-tribromophenyl ether	DPTE	35109-60-5	530.67	6.34
Pentabromotoluene	PBT	87-83-2	486.621	5.87
Pentabromobenzene	PBBz	608-90-2	472.59	5.4
Tetrabromoethylcyclohexane	TBECH	3322-93-8	399.74	3.73
Decabromodiphenylethane	DBDPE	84852-53-9	971.22	13.6
Dechlorane plus	Syn/anti DP	13560-89-9	653.72	9.0

Note : some of the molecular weight and log K_{OW} values have been estimated by ACD/Labs software

Table 1.4: Applications, concentrations in Indoor dust and different human matrices and potential toxicity of key flame retardants.

Target Compounds	Applications /conc. in consumer goods	Concentrations in UK Home (H) and Office (O) dust	Concentrations in human matrices	Potential Toxic Effects
BDE-28	< 0.2% by weight in Penta-BDE commercial products.[1]	**H** = (<0.5 – 2.10 µg/kg)[4] (<0.03-15 ng/g ,n =45)[5] **O**=(dl-11)*(<0.03-22ng/g, n=47)[5]	**UK** Serum (<0.03-0.55 ng/g lw, n=20)[2], breast milk (0.02-0.31 ng/g lw, n=6)[2], **China** hair (0-5 ng/g,dw & serum(0-7ng/g lw)[3], **Spain** Cord serum (nd-0.03 ng/ml, n=308)[6],placenta (nd-0.04 ng/g ,n=49)[6],maternal serum (nd-0.02 ng/ml, n=308)[6] **US**[56] hair =(0.23-8.6 ng/g,n=50), fingernail=(0.22-8.5 ng/g, n=50) ,toenail(0.21-8.5ng/g,n=50), serum=(0.36-6.6 ng/g lw, n=50)	Potential liver toxicity, thyroid toxicity, developmental toxicity, and developmental neurotoxicity
BDE-47	38-42 % in Penta-BDE commercial products	**H** = (1.2-58 ng/g)[4] (0.04-50 ng/g ,n =45)[5] **O** = (2.6-380 ng/g)*(7.1-660, n=47 ng/g)[5]	**UK** Breast milk (0.17-14.65 ng/g lw)[7] Serum (<0.36-4.87 ng/g lw, n= 20)[2], breast milk (0.32-13.0 ng/g lw, n=6)[2], **China** hair (2-400 ng/g,dw & serum(14-148 ng/g lw)[3], **Spain** Cord serum (nd-0.0.28 ng/ml, n=308)[6],placenta (nd-0.008 ng/g ,n=49)[6],maternal serum (nd-0.13 ng/ml, n=308)[6] **US**[56] hair =(5.2-890 ng/g,n=50), fingernail=(4.5-8.5 ng/g, n=50) ,toenail (3.9-910 ng/g,n=50), serum=(4.3-240 ng/g lw, n=50) **Egypt**[57] **serum** = (<LOQ-8.31 ng/glw,n=32)	Inhibits the cells viability, increase LDH leakage, and induces cell apoptosis in fibroblastic cell lines[8] & disrupts hypothalamic–pituitary thyroid function[9], ↓thyroid hormone T4[10].Alters growth, and morphology, cardiac and neural development in zebrafish[11].

BDE-99	Polyurethanes (10-18%) Major component in DE-71 or Penta Technical product (50-62%)	**H**= (2.8-180 ng/g)[4] (5-92 ng/g ,n =45)[5] **O**=(4.2-490)[4] (15-480,n=47 ng/g)[5]	**UK** Breast milk (<0.06-3.43 ng/g lw)[7], Serum (<0.26-5.61 ng/g lw, n= 20)[2], breast milk (0.12-3.74 ng/g lw, n=6)[2], **China** hair (1-569 ng/g,dw & serum (nd -22 ng/g lw)[3], **Spain** Cord serum (nd-0.22 ng/ml, n=308)[6],placenta (nd-0.005 ng/g ,n=49)[6],maternal serum (nd-0.16 ng/ml, n=308)[6] **US[yy]** hair =(2.2-1020 ng/g,n=50), fingernail=(2.1-1460 ng/g, n=50) ,toenail (2.1-1600 ng/g,n=50), serum=(1.1-108 ng/g lw, n=50) **Egypt[57] Serum** = (<LOQ-6.11 ng/glw,n=32)	In rats (oral,28 days) disturbed redox homeostasis, induced liver microsomal enzymes & fatty degeneration in liver.[12] In rodents-thyroid hormone disruption, developmental neurotoxicity, some changes of fetal development, and hepatotoxic effects.[13] -In male rats reduced sperm production and delayed onset of puberty.[14]
BDE-100	Polyurethanes (10-18%) Present in (7.8-13%)	**H**= (<dl-17 ng/g)[4] (0.75-16 ng/g ,n =45)[5] **O** = (<dl-79)[4] (1.9-120, n=47 ng/g)[5]	**UK** Breast milk (<0.05-1.86 ng/g lw)[7] Serum (0.57-80 ng/g lw, n= 20)[2], breast milk (0.07-2.19 ng/g lw, n=6)[2] **China** hair (0-98 ng/g,dw & serum (nd -19 ng/g lw ,n =32)[3] **US[56]** hair =(0.48-176 ng/g,n=50), fingernail=(0.74-274 ng/g, n=50) ,toenail (0.99-304 ng/g,n=50), serum=(0.49-32 ng/g lw, n=50) **Egypt[57] Serum** = (<LOQ-3.29 ng/glw,n=32)	Penta-BDE is more toxic than octa- and deca-BDE -**LD_{50} in rats -0.5-5g/kg**[13] Induces mitochondrial impairment.[15] Immune modulating effects[16]

BDE-153	Plastics,textiles,coatings and electrical & electronic appliances	**H** = (<dl-110 ng/g)[4] (0.025-24 ng/g ,n =45)[5] **O**=(<dl-99)[4](0.025-190,n=47 ng/g)[5]	**UK** Breast milk (<0.06-4.57 ng/g lw)[7], Serum (0.12-4.0 ng/g lw, n= 20)[2], breast milk (0.70-1.68 ng/g lw, n=6)[2] hair (1-62 ng/g,dw **China** serum (5 -82 ng/g lw, n=32)[3] **Belgium** Adipose tissue (0.70-25.1 ng/g lw, n=53)[18] **US**[56] hair =(1.4-78 ng/g,n=50), fingernail=(2.2-135 ng/g, n=50) ,toenail (3.3-180 ng/g,n=50), serum=(2.7-55 ng/g lw, n=50) **Egypt**[57]**Serum** = (<LOQ-3.78 ng/glw,n=32)	In neonatal mice impairs learning, memory and decreases hippocampal cholinergic receptors in adult mice.
BDE-183	Styrene Copolymers (12-15%)	**H** = (<dl-550 ng/g)[4] (<0.13-51 ng/g ,n =45)[5] **O** = (<dl-24)[4](0.065-220, n=47 ng/g)[5]	**UK** Serum (<0.03-0.33 ng/g lw, n= 20)[2], breast milk (0.02-0.23 ng/g lw, n=6)[2] **China** hair (1-11 ng/g,dw & serum (3 -162 ng/g lw, n=32)[3] **Belgium** Adipose tissue (<Decision limit-15.4 ng/g lw, n=53)[18] **Egypt**[57]**Serum** = (<LOQ-2.22 ng/glw,n=32)	"may cause harm to unborn child", and "possible risk of impaired fertility".(IRIS, EPA) Decrease in serum thyroxine T4 in rats. Delayed neurotoxic effects.
BDE-209	HIPS (11-15%) Polyamides (13-16%) Polyolefins (5-8%)	**H**= (<dl-2200000 ng/g)[4] (160-370000-51 ng/g,n =45)[5] **O**=(620-280000)[4](200-110000, n=47 ng/g)[5]	**UK** Breast milk (<0.06-0.92 ng/g lw)[7] Serum (<0.03-0.33 ng/g lw, n= 20)[2], breast milk (0.02-0.23 ng/g lw, n=6)[2] **China** hair (1-11 ng/g,dw & serum (3 -162 ng/g lw, n=32)[3] **US**[56] hair =(1.2-950 ng/g,n=50), fingernail=(1.8-706 ng/g, n=50) ,toenail (1.9-840 ng/g,n=50), serum=(3.1-44.0 ng/g lw, n=50) **Egypt**[57]**Serum**=(<LOQ-21.39 ng/glw,n=32)	Suggestive evidence of carcinogenic potential (EPA,2006b) Decrease in serum T3,increase in TSH[19] Changes in sperm's motion velocity, sperm count[20] Liver enlargement, induced hepatic EROD,PROD and UGT activities.[21]

HBCD	Thermal insulation XPS & EPS), Fabrics, Furniture and casing of electronics (HIPs) (0.8-4%)	∑HBCD **H** = (140-140000 ng/g)[4] (50-110000-51ng/g,n =45)[5] **O**=(90-6600)[4] (150-6400, n=47 ng/g)[5]	**USA** Adipose tissue (n=20)-<0.0026-2.41 ng/glw)[22] **Sweden** Milk (<0.20-2.4 ng/g lw, n=33)[23],(0.4-20 ng/g lw,n=85)[23], **Netherland** cord serum (<0.16-4.2 ng/g lw,n=12)[23], Maternal serum (<0.16-7.0 ng/g lw,n=78)[23]	HBCDs are cytotoxic in Hep G2 cells –γ-HBCD >β-HBCD > α-HBCD by ROS formation.[24] Developmental toxic.[25] HBCD induces liver fatty acids and modulates thyroid hormone receptors genes [26]
TBBP-A	Epoxy resin (19-33%) Polycarbonate & phenolic resins in printed circuit boards	**H** = (<0.06-382 ng/g, n =35)[27] **O** = (<0.06-382 ng/g, n =140)[27]	**USA** Adipose tissue (n=20)-<0.0033-0.464 ng/glw)[22] **UK** Milk = (<0.04-0.65 ng/glw, n=34)[29] **France** Milk = (34-9400 pg/g lw,n =26)[30] Maternal serum = (2-783 pg/g fw,n =26)[30] cord serum = (2-1012 pg/g fw, n=26) [30]	LD50 > 5 g/kg in rats, acts as a thyroid and oestrogen agonist, neurotoxic, immunotoxic (endocrine disruption)[28] Reduced fetal weight, increased malformations, and increased fetal death in rats.(WHO,1995)
TCEP	Additive plasticiser, PUF and upholstered fabrics & textiles (furniture),roof insulation	**H** = (<0.06-28 µg/g, n =10)[31] **H** = (138-6265 ng/g, n =10)[32]	**China** Serum = (200.0–958.2 ng/g lipid, n=10)[33] **Japan** Milk (ND-20 ng/g lw, n =20) **Payatas** (ND-152 ng/g lw, n =20) **US**[yy] hair =(60-2740 ng/g,n=50), fingernail=(93-1860 ng/g, n=50) toenail (100-150 ng/g,n=50),	Carcinogenic for animals (WHO 1998) is a neurotoxin in rats and mice.[34] TCEP increased both 17-estradiol (E2) and testosterone (T) concentrations in H295R cells.[35]
TCIPP	Polyurethane (PU) rigid and flexible foam	**H** = (2.4-370 µg/g, n =10)[31] **H** = (18331-1010000 ng/g, n =10)[32]	**U.S** BCIPP Urine =Mothers (<0.12-0.64 pg/ml, n=22)[36], children (<0.12-0.46 pg/ml, n=26)[36] **U.S** Hand wipe = (Geo mean 45.4 2 ng ,max = 255 ng, n=38)[54] BCIPP Urine = max = 0.57 ng, n=40)[54] **US**[yy] hair =(100-9840 ng/g,n=50), fingernail=(74-2410 ng/g, n=50) toenail (90-5150 ng/g,n=50),	Potentially Carcinogenic.[37] It increases both 17-estradiol (E2) and testosterone (T) concentrations in H295R cells. and could alter sex hormones.[38]

TDCIPP	flexible polyurethane foams for upholstered furniture and automotive products (EU, 2009)	**H** = (0.11-740 µg/g, n =10)[31] **H** = (346-3792 ng/g, n =10)[32]	**U.S** BDCIPP Urine =Mothers (0.37-11.0 pg/ml, n=22)[36], children (0.89-251 pg/ml, n=26)[ee] Hand wipe = (Geo mean 108.3 ng ,max = 535 ng, n=38)[54] BDCIPP Urine = (Geo mean 2.321 ng max = 21.21 ng, n=40)[54] **Norway** Female (Finger nails = 63.5 ± 52, n=4) (Toenails = 41.9 ± 26, n=4) Male (Finger nails = 54.0 ± 72, n=5) (Toenails = 27.9 ± 6, n=2) [55] **US** hair =(70-10490 ng/g,n=50) fingernail=(90-1410 ng/g, n=50) toenail (75-2300 ng/g,n=50) [56]	Developmental toxicity in zebrafish[39] and showed neurotoxicity in rats[40]
TPhP	Vinyl automotive upholstery and in cellulose acetate articles; also as ingredient in FM-550 flame retardant formulation	**H** = (0.27-170 µg/g, n =10)[31] **H** = (190-9549 ng/g, n =10)[32]	**China** Serum = (1.3–4.2 ng/g lipid, n=10)[33] **U.S** DPHP Urine =Mothers (<0.18-68.7 pg/ml, n=22), children (0.68-140 pg/ml, n=26)[36] **U.S** Hand wipe = (Geo mean =22.41ng ,max=416.7 ng, n=38)[54] DPHP Urine = (Geo mean =1.137 ng max= 26.77 ng, n=40)[54] **Norway** Female (Finger nails DPHP = 40002 ± 106, n=4) (Toenails = 6815 ± 209, n=4) Male (Finger nails DPHP = 80.5 ±180, n=5) (Toenails = 18.5 ± 66, n=2) [55] **US**[yy] hair =(70-4710 ng/g,n=50) fingernail=(110-59800 ng/g, n=50) toenail (54-232900 ng/g,n=50)	ER and/or ER agonistic activity. Immunomodulating agent and immunotoxic.[42] neurotoxic[43]

TCP	Additive in plastics and lubricant oils (Pubchem)	**H** = (0.01-5.6 µg/g, n =10)[31] **H** = (83-1052 ng/g, n =10)[32]	**China** TmCP Serum = (3.3–23.1 ng/g lipid, n=10)[33] **Norway** Sum of all isomers Hair =Mothers(<2-134 ng/g, n=48)[50], children (<2 -74 ng/g, n=54)[50]	Induces immunotoxicity,testicular toxicity and neurotoxicity in animals. Inhibition of esterases enzyme- AChE and also inhibits neurotoxic esterases[45] **OPIDN**– paralysis of lower and upper extremities. Saligenin cyclic-o-tolyl phosphate (SCOTP), an activated metabolite of TOCP (one of the isomer of TCP), markedly inhibited NTE activity in spermatogonial stem cells and decreases the sperm count in mouse testis)[44]
EHDPP	Primarily as a flame retardant in plastics and flexible PVC and food packaging in US.(Environment agency 2009a)	**H** = (0.29-11 µg/g, n =10)[31] **H** = (292-9172 ng/g, n =10)[32]	**Sweden** blood donor plasma 0.73-1.2 µg/g plasma , n=3 **Norway** Hair =Mothers(5-265ng/g, n=48)[50], children (2-346 ng/g, n=54)[50]	Dose related changes in blood, liver, kidney, adrenal glands, testes and ovaries in rats (375-425 mg/kg day in diet for 90 days study.(UK environ. Risk evaluation report).
TnBP	Plasticizer nitrocellulose & cellulose acetate	**H** = (< 0.03-1.2 µg/g, n =10)[31] **H** = (210-479 ng/g, n =10)[32]	**China** Serum = (1.8–46.5 ng/g lipid, n=10)[33] **Germany** Metabolite-DPP found in crew members in airlines, 0.2-1.1µg/L in urine.[49] **Norway** Hair =Mothers(5-672 ng/g, n=48)[50], children (3-150 ng/g, n=54)[50]	urinary bladder hyperplasia,[47] AR/GR antagonistic activity & PXR agonistic activity.[48]

TEHP	Plasticiser in PVC in low temperature applications and in clothing. (OEHHA,2011a)	**H** = (96.2-465 ng/g, n =10)[32]	**Norway** Hair =Mothers (<1.0-53ng/g, n=48)[50], children (<1.0-114 ng/g, n=54)[50]	Follicular cell hyperplasia of the thyroid gland in male and female B6C3F1 mice, some evidence of carcinogenicity in female B6C3F1 mice (1,000 mg/kg).[51]
TBOEP	Floor polishes, rubber stopper & plastics	**H** = (225-58745 ng/g, n =10)[32]	**Norway** Serum = (Mean 5.7 ng/g lipid, n=10)[33] Hair =Mothers(14-1253ng/g, n=48)[50], children (34-2411 ng/g, n=54)[50] **Norway** Female (Finger nails = 3.8 ng/g, n=1) (Toenails <2.2 ng/g) Male (Finger nails = <2.2 ng/g , n=1) (Toenails =4.1 ng/g, n=1)[55]	PXR agonist.[52] Increases both 17-estradiol (E2) and testosterone (T) concentrations in H295R cells and could alter steroidogenesis or estrogen metabolism.[53]
PBEB	Thermoset Polyster resins and thermoplastic resins.	**H**= (< 0.010-21 ng/g,n =45)[5] **O**=(0.36-10, n=47 ng/g)[5]	**US**[56] hair =(0.1-2.6 ng/g,n=50), fingernail=(0.25-1.1 ng/g, n=50) ,toenail (0.20-1.1 ng/g,n=50), serum=(ND)	It is a brominated analogue of ethylbenzene which is listed as known to cause cancer under Proposition 65.
EH-TBB	Widely used in furniture foam. Found in baby products containing polyurethane foam. Component of FM-550 (40-70%)	**H**= (< 0.010-85 ng/g,n =45)[5] **O**=(<0.010-2000, n=47 ng/g)[5] **H** = (2.5-32.0 ng/g, n =10)[32]	**US** hair =(7.6-4540 ng/g,n=50), fingernail=(11.0-1210 ng/g, n=50) ,toenail (13.0-2310 ng/g,n=50), serum=(1.3-54.0 ng/g lw, n=50)[56] Urine TBBA = Mothers (<3.0-62.2 pg/ml ,n=22) TBBA Children (<3.0-84.9 pg/ml,n=26) **Canada**[63] maternal serum = (ND-68 ng/g lw, n= 102), milk = ND-24 ng/g lw, n= 105	EH-TBB affects fecundity in medaka fish.Invitro tests showed that EHTBB modulate endocrine function through interactions with estrogen (ER) and androgen receptors (AR) and via alterations to synthesis of 17-β-estradiol (E2) and testosterone (T).[58]

BEH-TEBP	polyurethane foam in furniture and juvenile products, often as a replacement for pentaBDE	**H**= (16-3500 ng/g,n =45)[5] **O**=(54-25000, n=47 ng/g)[5] **H** = (18.0-234 ng/g, n =10)[32]	**US**[56] hair =(13-2600 ng/g,n=50), fingernail=(18-1120 ng/g, n=50) ,toenail (18-1990 ng/g,n=50), serum=(19-69 ng/g lw, n=50) **Canada**[63] maternal serum = (ND-164 ng/g lw, n= 102), milk = ND-19 ng/g lw, n= 105)	Endocrine disruptive compound.[58,62] In a porcine primary testicular cell mode TBPH produces greater conc. of Testosterone and Estradiol by regulation of CYP11A.[59]
BTBPE	acrylonitrile-butadiene-polystyrene, and high impact polystyrene	**H** = (<dl-1900 ng/g)[4] (0.01-110 ng/g ,n =45)[5] **O** = (<dl-40)*(0.019-4700000, n=47 ng/g)[5] **H** = (<1.3-100.0 ng/g, n =10)[32]	**Canada**[63] maternal serum = (3.9-16 ng/g lw, n= 102), milk = n.d	Metabolism of BTBPE by ingestion in mammals, ether cleavage of BTBPE may yield 2, 4,6-tribromophenol which is a neurotoxicant in Sprague Dawley rat.[60] Induced AhR- and CXR mediated CYP responses, in addition to affecting deiodinase transcription in in vitro-in ovo toxicity testing.[61]
HBB	Used in manufacturing of paper,woods,textiles,plastics and electronic goods	**H**= (< 0.0030-12 ng/g,n =45)[5] **O**=(<0.030-84, n=47 ng/g)[5]	**US**[56] hair =(0.11-9.0 ng/g,n=50), fingernail=(0.20-3.0 ng/g, n=50) ,toenail (0.24-5.3 ng/g,n=50), serum=(2.1 ng/g lw, n=50) **Japan** adipose tissue = 2.1-4.1 ng/g wet wt & 1,2,4,5 TBB metabolite.[65]	Elevation in GST activity in zebrafish embryo model.[64] effects on liver, enzyme inhibition, induction, or change in blood or tissue levels and on esterases in rats when given oral continuously.[66]
DPTE	Flame retardant in extrusion grade polypropylene.	Not detected in indoor dust	Not found any study	Substructures similar to both 2, 3,-dibromo-1-propanol and 2, 4, 6-TBP. 2, 3-Dibromo-1-propanol is listed under Proposition 65 as known to cause cancer. 2,4,6-TBP is a thyroid hormone disrupting chemical.[69]

PBT	Unsaturated polyesters, polyethylene,polypropylenes,polystyrene, SBR-latex, textiles, rubbers, ABS (NPCA TA-2462/2008)	**H**= (< 0.010-90 ng/g,n =45)[5] **O**=(<0.010-59, n=47 ng/g)[5]	**China Serum =** (Highest 5.7 ng/g lipid, n=10)[33]	Subacute and subchronic studies mild dose-dependent histopathological changes were observed in the thyroid, liver and kidney of rats fed PBT diets.[68]
PBBz	Not available	**H**= (< 0.010-12 ng/g,n =45)[5] **O**=(< 0.010-23, n=47 ng/g)[5]	**Serum =** (Highest 10.0 ng/g lipid, n=10)[33] **US** [56] hair =(0.33-4.9 ng/g,n=50), fingernail=(0.90-1.3 ng/g, n=50) ,toenail (0.72-2.9 ng/g,n=50), serum=(0.99-3.7 ng/g lw, n=50)	Not available
TBECH **(DBE-DBCH)**	used as an additive in polystyrene and polyurethane products	α-TBECH–**H** (<0.7-5.6 ng/g, n=10)[32] β-TBECH-**H**(<0.6-1.7ng/g, n=10)[32]	Not found	TBECH is an endocrine disrupting chemical in humans, to bind and activate human androgen receptors (hAR), γ- and δ-isomers are more potent activators of hAR than the α- and β-isomers, induce prostate specific antigen at 100 nM amounts in vitro.[69]
DBDPE	electrical and electronic equipment, wire, textile coatings and blends, and polyester products, high impact polystyrene (HIPS)	**H** = (<dl-3400 ng/g)[4] (<1.2-2300 ng/g ,n =45)[5] **O**=(<dl-860)[4](<1.20-17000,n=47 ng/g)[5] **H** (<531-39221 ng/g, n =10)[32]	**Canada**[63] maternal serum = (ND-123 ng/g lw, n= 102), milk = (n.d-25 ng/g lw, n= 105)	Its ill effects on hepatocyte detoxification metabolism and its oestrogenicity were confirmed by using the in vitro hepatocyte assay.[70]

Syn/anti DP	Thermoplastic materials (PE, PVA, PP) in electronic wire and cable applications (5-35%) (ECHA 2007)	**Syn-DP H**= (<0.26-28 ng/g,n =45)[5] **O**=(< 0.26-640, n=47 ng/g)[5] **Anti-DP H**= (<0.15-170 ng/g,n =45)[5] **O**=(< 0.15-2100, n=47 ng/g)[5]	**Syn –DP US**[56] hair =(0.10-4.0 ng/g,n=50), fingernail=(0.22-1.3 ng/g, n=50) ,toenail (0.24-2.3 ng/g,n=50), serum=(0.69-1.3 ng/g lw, n=50) **Anti–DP US**[56] hair =(0.36-3.7 ng/g,n=50), fingernail=(0.70-3.4 ng/g, n=50) ,toenail (0.59-5.4 ng/g,n=50), serum=(0.98-1.0 ng/g lw, n=50)	DP interferes with metabolism and was associated with proteins related to apoptosis and cell differentiation. effects on the generalized stress response, small G-protein signal cascades, Ca^{2+}signaling pathway, and metabolic process, and may induce apoptosis in the liver of juvenile Chinese sturgeon.[72] DP accumulates in the liver when rats were exposed at 10 and 100 mgkg /g.[73]
2,4,6 TBP	Epoxy resins, phenolic resins, polyester resins, polyolefins	Not found	Nicaraguan women waste disposal sites increases TBP levels	Oral LD50 -1995 (Male) and 1819 mg/kg (Female) Signs of toxicity included decreased motor activity, nasal discharge, lacrimation, tremors, prostration, clonic convulsions and developmental abnormalities and behavioral changes of the newborn pup.[71]

1- (Alaee et al. 2003) **2-** (Bramwell et al. 2014) **3**- (Zheng et al. 2014) **4-** (Stuart et al. 2008) **5** - (Tao et al. 2016b) **6** - (Vizcaino et al. 2014) **7** - (Abdallah and Harrad 2014) 8- (Jin et al. 2010), 9-(Chan and Chan 2012), **10**-(Hallgren et al. 2001), **11** -(Lema et al. 2007) **12** -(Bruchajzer et al. 2010) **13**- (Gill et al. 2004) **14**- (Kuriyama et al. 2005) **15** - (Pereira, de Souza and Dorta 2013) **16**-(Mynster Kronborg et al. 2016) **17**-(Viberg,

Fredriksson and Eriksson 2003) **18** -(De Saeger et al. 2005) **19** -(Lee et al. 2010) **20**- (Tseng et al. 2006) **21**- (Zhou et al. 2001) **22**- (Johnson-Restrepo, Adams and Kannan 2008) **23**- (Covaci et al. 2006b) **24**- (Zhang et al. 2008) **25**- (Du et al. 2012) 26-(Yamada-Okabe et al. 2005) **27**- (Abdallah, Harrad and Covaci 2008a) **28**- (Kitamura et al. 2002), **29**- (Abdallah and Harrad 2011a) **30** - (Antignac et al. 2008) **31** -(Harrad, Brommer and Mueller 2016) **32**-(Kademoglou et al.) **33**-(Li et al. 2017) **34**-(Tilson et al. 1990, Umezu et al. 1998) **35**-(Liu, Ji and Choi 2012) **36**-(Butt et al. 2014b), **37**- (Ni, Kumagai and Yanagisawa 2007) **38**-(Liu et al. 2012) **39**-(Wang et al. 2013) **40** -(Dishaw et al. 2011) **41**- (Kojima et al. 2013) **42**-(Fautz and Miltenburger 1994, Esa, Warr and Newcombe 1988) **43** -(Veronesi, Padilla and Newland 1986) **44**-(Chen et al. 2012) **45** -(Abou-Donia 1981) **46**- (Jonsson and Nilsson 2003) **47**-(Auletta, Weiner and Richter 1998) **48**- (Kojima et al. 2013) **49**- (Schindler et al. 2014) **50**-(Kucharska et al. 2015a) **51**-(1984) **52**-(Kojima et al. 2013) **53**-.(Liu et al. 2012) **54**-(Hammel et al. 2016) **55**-(Alves, Covaci and Voorspoels 2017) **56**-(Liu et al. 2016) **57**- (Abdallah, Zaky and Covaci), **58**-(Saunders et al. 2015),**59**-(Mankidy et al. 2013) **60**-(Lyubimov, Babin and Kartashov 1998) **61**-(Egloff et al. 2011) **62**-(Patisaul et al. 2013b) **63**- (Zhou et al. 2014), **64**-(Usenko et al. 2016), **65**-(Yamaguchi et al. 1988b) **66**-(Yamaguchi, Kawano and Tatsukawa 1988a) **67**-(Hamers et al. 2006, Suzuki et al. 2008, Yamaguchi et al. 1988b), **68**-(Chu et al. 1987), **69**-(Khalaf et al. 2009), **70**-(Nakari and Huhtala 2010). **71**- Simonsen et al.**72**-(Liang et al. 2014) **73**-(Li et al. 2013)

1.2: Routes of Human Exposure to FRs

While it is established that the diet (consumption of contaminated food) constitutes and important source of non-occupational exposure to BFRs, it appears that ingestion of indoor dust, dermal contact with dust/consumer products and inhalation of indoor air could also be substantial pathways of exposure (Abdallah et al. 2008a, Frederiksen et al. 2009, Watkins et al. 2011). Contact with indoor dust has been highlighted as an important contributor especially for young children because they spend a large portion of their time on the floor exploring their environment and they tend to place their hands or other objects or dust in their mouth. However, there remains uncertainty about how such contact with dust occurs. The principal pathway highlighted to date is oral ingestion. Various studies have reported on levels of different FRs in various environmental and human matrices (Covaci et al. 2011b, Covaci et al. 2009, Harrad et al. 2010b, Law et al. 2014, van der Veen and de Boer 2012b). Studies from North America report indoor dust (via ingestion or dermal contact) as the major exposure pathway for all age groups to PBDEs contributing 70-80% to the average overall daily exposure (Trudel et al. 2011b, Lorber 2007). In contrast to PBDEs, only a few studies are available that address human exposure to NBFRs and PFRs (Covaci et al. 2011b, Stapleton et al. 2011, Ali et al. 2012c). Ingestion of FRs is observed particularly more in toddlers and young children while other exposure pathways make substantial contributions to the overall adult intake of BFRs (Abdallah et al. 2008a, Harrad et al. 2010b, Harrad et al. 2008).Furthermore, the observed association between BFRs in dust and body burdens may at least partly arise because BFRs in dust are an indicator of (an)other exposure hazard that influences body burdens. Specifically, body burdens may be influenced by dermal uptake via direct contact with materials containing FRs. Hence, furthering understanding of dermal uptake of FRs from dust and FR-treated materials is an important research gap.

Current thinking about exposure via dust ingestion for FRs is that although we think there is a correlation between FRs in indoor dust and human body burdens, we do not yet know the exact mechanisms(s) via which FRs transfer from dust into the body (e.g. whether it is ingestion or dermal uptake, most attention to date has focused on ingestion), or indeed whether dust is just an indicator of the levels in consumer materials and the "real" link is between such materials and body burdens. This paucity of information was evident in the EU risk assessment reports on TBBPA (EU Risk Assessment Report 2006) and BDE-209 (EU Risk Assessment Report 2002) where the lack of experimental data has led to the assumption of dermal absorption efficiencies based on consideration of compound-specific physicochemical properties and extrapolation from data available for PCBs. Furthermore, several authors have discussed the absence of experimental data on dermal absorption of various FRs and highlighted the potential inaccuracies of current estimates of human exposure to these FRs owing to a general lack of knowledge on the percutaneous route (Boyce, et al.2009;U.S EPA 1992) (Garner and Matthews 1998, Trudel et al. 2011b). Therefore, the lack of experimental information on human dermal uptake of FRs from dust and source materials represents an important research gap that hampers accurate assessment of human exposure to FRs. However, efforts to fill this gap are hindered by several difficulties including: ethical issues encountered with human studies, inter-species variation in dermal structure and uptake that cast doubt on the accuracy of extrapolation or allometric scaling of animal data to humans, and tighter regulations on *in vivo* tests involving animals.(Gibbs et al. 2013, Kandarova et al. 2013, Tornier et al. 2010)

Fig 1.4: Major pathways of human exposure to FRs.

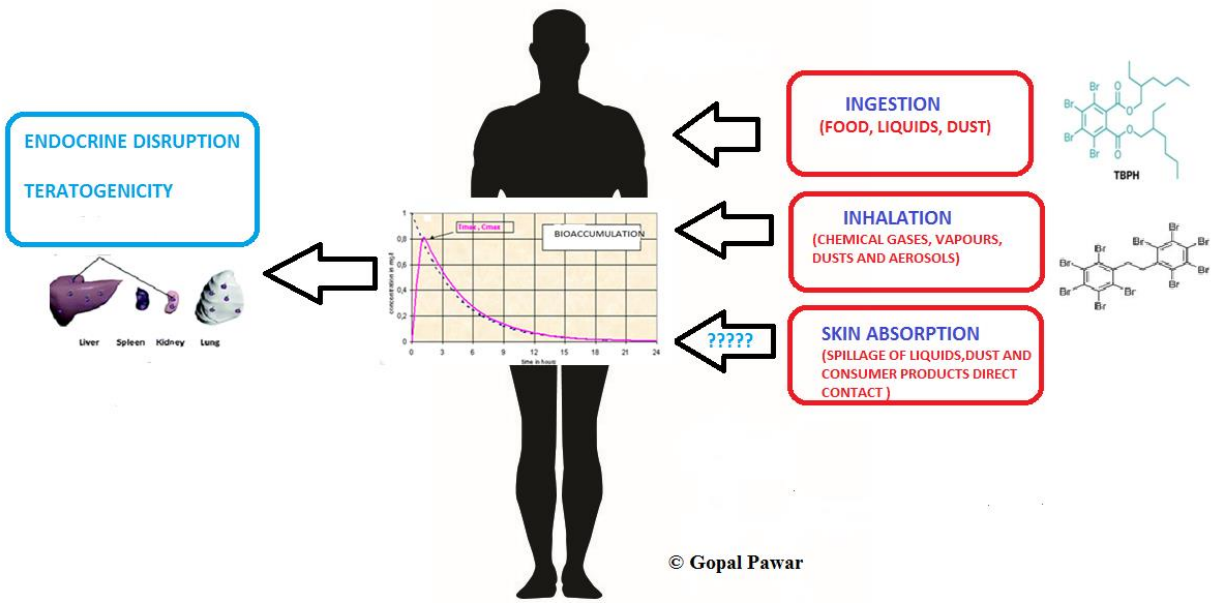

1.3: The skin as a barrier for systemic exposure to xenobiotic chemicals.

Skin is multi-layered and is the largest body organ with a surface area of ~ 2 m^2 and weighing about 5 kg in adult humans (Godin and Touitou 2007). It protects the body from the surrounding environment, thus forming an efficient barrier for hazardous chemicals. Human skin is formed of 3 main layers, namely: the epidermis, dermis and hypodermis (Figure 1.2). The epidermis is the outermost layer and is a non-vascular layer with a protective role as a barrier to penetration of chemicals to the underlying vascular dermis. The healthy human epidermis is further classified into 4 layers (stratum corneum, stratum granulosum, stratum spinosum and stratum basale) separated from the dermis by the basement membrane (Breitkreutz et al. 2013).The barrier properties of the skin lie mainly within the stratum corneum (SC), which has about 16 layers and takes about two weeks to completely desquamate (Hoath and Leahy 2003). The SC is linked to the protein-enriched corneocyte layers and the intercellular membrane lipids, mostly composed of ceramides, cholesterol, and free fatty acids (Proksch, Brandner and Jensen 2008). This highly hydrophobic layer is composed of differentiated non-nucleated cells, corneocytes, which are filled with keratins

and embedded in the lipid domain. Percutaneous penetration of molecules through the SC occurs mainly via passive diffusion but may also occur via sweat glands and hair follicles directly to the dermis. Although little is known about the expression and function of influx transport proteins in human skin and their role in dermal uptake of xenobiotics, the role of organic anion transporting polypeptides (OATP) in mediating the active transport process of large organic cations via human keratinocytes has been highlighted (Schiffer et al. 2003). Chemical residues limited to the epidermis will be eliminated from the exposed skin by desquamation and will not be available for systemic distribution (Aggarwal et al. 2014).

Fig 1.5: Anatomy of the human skin.

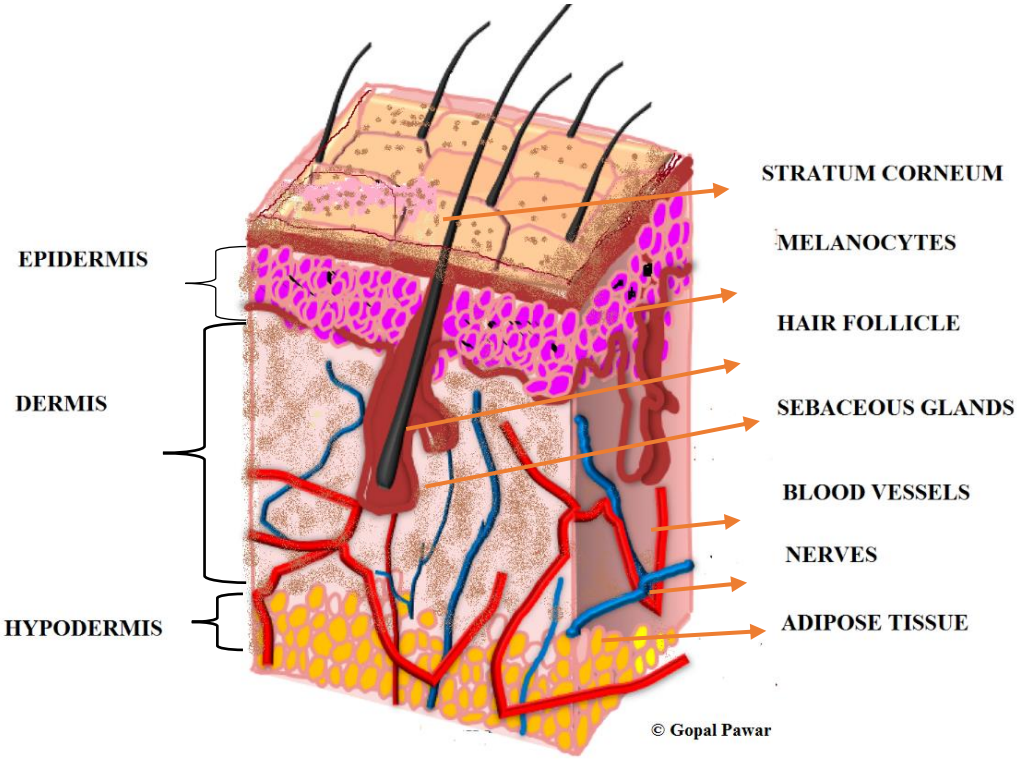

1.4: Significance of dermal absorption as a pathway of human exposure to FRs.

While numerous studies have highlighted the importance of indoor dust ingestion as a pathway for human exposure to various FRs, few reports have discussed human dermal exposure to such contaminants (Stapleton et al. 2012a, Stapleton et al. 2008b, Watkins et al. 2011). Watkins et al. 2011 reported a strong positive correlation between PBDE levels on hand wipes (assumed to result from hand contact with contaminated dust or flame-retarded products) and PBDE concentrations in serum from American adults. While concentrations of PBDEs in indoor dust were strongly correlated with those in hand wipes, and infrequent hand-washers had 3.3 times the levels of PBDEs in their hand wipes than the frequent hand-washers; correlation could not be established directly between PBDE concentrations in indoor dust and their levels in serum. Similarly, Stapleton et al. 2014 (Stapleton et al. 2014) found that PBDE residues measured on children's hand wipes were a strong predictor of serum PBDE levels. Carignan, et al. 2013 (Carignan et al. 2013), reported 2-3 times increase of median concentrations of penta-BDE, EH-TBB, and BEH-TEBP in paired hand wipe samples of 11 gymnasts before and after practice. In a more recent contribution, significant associations between concentrations of TCEP, TCIPP, TDCIPP, HBCD, EH-TBB, and BEH-TEBP in children's hand wipes and house dust were observed (Stapleton et al. 2014). This opens up the possibility that FRs in dust may also be an indicator of another exposure pathway, such as direct dermal uptake of FRs present in treated goods (e.g. games consoles, remote controls, and fabrics). A pivotal issue for risk assessment studies is the influence of indoor contamination with FRs on human body burdens. Understanding of this remains incomplete. One approach is that of Lorber (2008), who used a simple pharmacokinetic (PK) model to predict the body burdens of PBDEs in American adults using intake data from different exposure pathways. Predicted body burdens were compared with measured data and the relationship between external and internal exposure discussed. Since then, a few studies

have applied similar PK models with slight adjustments to further understanding of the relationship between concentrations of PBDEs, HBCD and TBBP-A in the environment and human body burdens (Abdallah and Harrad 2011b, Johnson-Restrepo and Kannan 2009, Trudel et al. 2011b). As well as identifying various research gaps including the bioavailability of FRs following ingestion of indoor dust and the elimination half-lives of these compounds in human, one major outcome of such PK studies is the highlighted potential importance of dermal contact with indoor dust and/or FR-containing items as a pathway of exposure to BFRs. To illustrate, dermal uptake was reported as the 2nd most important contributor (following dust ingestion) to PBDE body burdens of Americans. This was despite a very conservative assumption – *made in the absence of experimental data for PBDEs* - that only 3 % of PBDEs with which dermal contact occurred (via adherence of indoor dust to the skin) were absorbed (Lorber 2008a). Moreover, a recent PK model reported ingestion of diet and dust, as well as dermal exposure to dust to constitute the major factors influencing human body burdens of PBDEs in both Americans and Europeans. Once again, these conclusions were founded on low assumed values of dermal absorption efficiency (2.5-4.8%) (Trudel et al. 2011b). Neither study considered potential dermal absorption following contact with FR-treated items and assumed percutaneous penetration fractions based on values reported for dermal absorption of dioxins and PCBs from soil in laboratory animal models (Trudel et al. 2011b, Lorber 2008a). Boyce et al. (2009) applied a Monte Carlo-based mathematical approach for assessment of human exposure to TBBPA, DBDPE and BDE-209 via indoor dust ingestion and dermal contact. Based on physicochemical properties, analogy with data for PCBs and the absence of any chemical-specific studies, dermal absorption values of 10%, 0.1% and 1% were used for TBBPA, DBDPE and BDE-209, respectively. Results revealed dermal contact with indoor dust made significant contributions (15 - 40%) to estimates of overall human exposure to these BFRs in North America and Europe. The

authors highlighted that at such significant contribution levels; inaccuracies in the dermal absorption factors applied could have dramatic effects on exposure assessments (Boyce, et al. 2009).

1.5: Transdermal metabolism of xenobiotics.

In the past few years, the cutaneous metabolic activity of skin has been identified and widely studied. Evidence shows that active enzymes in viable skin tissues have a capacity for bio-transforming topically applied compounds, with a consequence of an altered pharmacological effect (Zhang and Michniak-Kohn 2012). The SC, which contains a mixture of cholesterol, fatty acids, and ceramides not only act as epidermal barrier but also help in xenobiotic metabolizing. There is increasing evidence that xenobiotic metabolizing enzymes and transport proteins function as a second biochemical barrier of the skin (Gundert-Remy et al. 2014, Esser and Gotz , Wiegand et al. 2014)

Extensive literature exists on the capacity of human skin to metabolise various chemical compounds, however, very little is known about the transdermal metabolism of flame retardant chemicals. Human skin cells express at least five different esterases which act on simple ester bonds in organophosphate compounds (e.g. paraoxon and bis (4-nitrophenyl) phosphate). Recent findings indicate that human skin possesses not only multiple cytochrome P450 isoenzymes, but also influx and efflux transporter proteins. While the pattern of cytochrome P450 isoenzymes in the skin differs from the pattern in the liver. It seems likely that the skin can participate in both Phase I (e.g. oxidation, reduction and hydrolysis) and Phase II (e.g. glucuronidation and acetylation) metabolic reactions (Gundert-Remy et al. 2014, Merk 2009).Garner and Matthews confirmed extra hepatic dermal metabolism of mono- to hexa- PCBs in F-344 male rats (Garner and Matthews 1998). Similarly, Hughes, et al. 2001 reported *in vitro* dermal metabolism of BDE-209 and TDCPP in adult female mice.

The literature suggests that dermal biotransformation may play an important role in the ultimate fate and bio-availability of FRs in the skin.

1.6: *In vivo* dermal bioavailability studies

Human dermal uptake of environmental contaminants (e.g. polycyclic aromatic hydrocarbons, phthalates and pesticides) from soil and sediment has been reviewed (Spalt et al. 2009), however very little is known about the uptake of flame retardants via skin (Table 1.5). In this regard, Schmid et al. 1992 studied the dermal absorption of PCBs in one human volunteer (52 year old male, 65 kg body weight) (Schmid, Bühler and Schlatter 1992). The volunteer was exposed to a mixture of 8 tetra- to hepta- ^{13}C-PCBs for different time spans using cotton cloth and aluminium foil as carrier materials to mimic real life situations of skin contact with PCB-contaminated clothes or metal surfaces. After exposure the skin was washed subsequently with water and ethanol. Non-absorbed ^{13}C-PCBs were determined in the washing solvents and in the carrier materials, while the bioavailable fraction was measured in plasma samples collected at 0.5-6 days post-exposure. Results revealed low percutaneous absorption (PA) of target PCBs equivalent to 6 % of the absorption after oral intake of the same amount. The absorption rate was largely dependent on the site of administration, on the carrier material (higher from the aluminium foil than the cotton cloth) and almost not on the duration of exposure where the percentage uptake remained constant at long (8 hours) and short (10 min) exposure times.

Assessment of human dermal absorption of FRs involving human volunteers is limited due to ethical issues (Jakasa and Kezic 2008). In this regard, animal models are used when human volunteers are not available. *In vivo* animal models especially rats have long been used by different industrial and regulatory institutions to provide data on various toxicokinetic and toxicodynamic parameters, as well as dermal absorption (Zendzian 2000).

Table 1.5: Summary of *in vivo* and *in vitro* methods applied for studying dermal absorption of FR chemicals.

Compound	Skin Type	Study type	Dosing	Exposure time	Absorption (% of administered dose)	Ref.
BDE-47	Female C57BL/6 mice	*In vivo*	1 mg/kg bw applied to 2 cm^2 of skin	5 days	62%	(Staskal, et al. 2005)
BDE-209 and TDCPP	female mice (SKH1)	*In vitro*	6, 30 and 60 nmol in THF for BDE-209; 20, 100 and 200 pmol in acetone for TDCPP	24 hrs	2–20% in skin, 0.07-0.34% in receptor fluid for BDE-209. 39–57% in skin and 28–35% in receptor fluid for TDCPP	(Hughes, et al. 2001)
BDE-47	Human and rat skin (350–410 µm)	*In vitro*	10 mg/cm^2 applied in acetone.	24 hrs	2-15% in 0.9% NaCl receptor fluid; 57% and 33% remained in cells for human and rat skin, respectively.	(Roper, et al. 2006)
BISPHENOL-A (Precursor to TBBP-A)	Pig Ear Skin and Human skin	*In vitro*	50, 100, 200, 400 and 800 nmol were applied in 60 µL ethanol/phosphate buffer (pH 7.4)	24, 48 and 72 h	Human skin (45.6 ± 6.2%), pig skin (65.3 ± 8.2%) BPA–glucuronide formed in human skin , corresponding to 7 ± 2, 16 ± 3 and 30.± 3 nmol at 24, 48 and 72 h, respectively.	(Zalko, et al. 2011)
TBBPA	Human skin & rat skin	*In vitro*	100 nmol/cm^2 C-14 TBBPA in 10 µL acetone	24 h	0.2 % penetrated,3.4 % absorbed into the Human skin 3.5% penetrated,9.3% absorbed (rat skin)	(Knudsen et al. 2015)

EH-TBB	Rat	*In vivo*	100 nmol/cm^2 & 1000 nmol/cm^2 -[^{14}C]-TBBPA (100 µL/Kg) in acetone	24 h 72 h	7.7 % penetrated,13.6 % absorbed (~ 100 nmol/cm^2) 5.3 % penetrated,5.1 % absorbed (~ 1000 nmol/cm^2) 30% penetrated,40 % absorbed (~ 1000 nmol/cm^2)	(Knudsen et al. 2015)
	Human & rat skin	*In vitro*	100 nmol/cm^2 –[^{14}C] EH-TBB in toluene ((5µL)	24 h	0.2 % penetrated,24 % absorbed, Flux = 11.0 pmol-eq/cm^2/h -human skin 2 % penetrated, 51% absorbed, Flux = 102 pmol-eq/cm^2/h-Rat	(Knudsen et al. 2016b)
	Rat	*In vivo*	100 nmol/cm^2 [^{14}C] EH-TBB in toluene (5µL)	24 h	27.5 % absorbed and 13% reached systemic circulation (Flux= 464 pmol-eq/cm^2/h)	(Knudsen et al. 2016b)
BEH-TEBP	Human & rat skin	*In vitro*	100 nmol/cm^2 [^{14}C] BEH-TEBP in toluene (5µL)	24 h	Penetration <0.01 % in both 12 % absorption in humans (0.3 pmol-eq/cm^2/h) 41 % in rats (1.0 pmol-eq/cm^2/h)	(Knudsen et al. 2016b)
	Rat	*In vivo*	100 nmol/cm^2 [^{14}C]-BEH-TEBP in toluene ((5µL)	24 h	27% absorption, 1.2% reached systemic circulation (16.0 pmol-eq/cm^2/h)	(Knudsen et al. 2016b)
TBP-DBPE	Human skin	*In vitro*	10-100 and 50-300 ng/cell (500 µL ethanol with 20% isooctane residue)	72 h	Receptor fluid = <0.1% Epidermis = 11% Dermis = 1.6 %	(Frederiksen et al. 2016)
EH-TBB	Human skin (0.8 mm) N =5 F	*In vitro*	10-100 and 50-300 ng/cell (500 µL ethanol with 20% isooctane residue)	72 h	Receptor fluid = 0.2% Epidermis = 10 % Dermis = 0.6 % Kp = 0.16-2.5 * 10^{-4}cm/h	-do-

BTBPE	Human skin	*In vitro*	10-100 and 50-300 ng/cell (500 µL ethanol with 20% isooctane residue)	72 h	Receptor fluid = 0.1 % Epidermis = 10 % Dermis = 0.7 % Kp = 0.16-2.4 * 10^{-4}cm/h	-do-
DBDPE	Human skin	*In vitro*	10-100 and 50-300 ng/cell (500 µL ethanol with 20% isooctane residue)	72 h	Receptor fluid = <0.5 % Epidermis = 10 % Dermis = 1.0 % Kp = 0.11-2.2 * 10^{-4}cm/h	-do-
BEH-TEBP	Human skin	*In vitro*	10-100 and 50-300 ng/cell (500 µL ethanol with 20% isooctane residue)	72 h	Receptor fluid = 0.04 % Epidermis = 9.5 % Dermis = 0.5 % Kp = 0.13-1.4 * 10^{-4}cm/h	-do-
***syn*-DP**	Human skin	*In vitro*	10-100 and 50-300 ng/cell (500 µL ethanol with 20% isooctane residue)	72 h	Receptor fluid = <0.1 % Epidermis = 8.4 % Dermis = 0.5 % Kp = 0.11-1.9 * 10^{-4}cm/h	-do-
***anti*-DP**	Human skin	*In vitro*	10-100 and 50-300 ng/cell (500 µL ethanol with 20% isooctane residue)	72 h	Receptor fluid = 0.2 % Epidermis = 7.9 % Dermis = 0.8 % Kp = 0.16-1.8 * 10^{-4}cm/h	-do-
***α*-HBCD**	Human skin	*In vitro*	10-100 and 50-300 ng/cell (500 µL ethanol with 20% isooctane residue)	72 h	Receptor fluid = 0.1 % Epidermis = 11 % Dermis = 1.0 % Kp = 0.22-2.7 * 10^{-4}cm/h	-do-
***β*-HBCD**	Human skin	*In vitro*	10-100 and 50-300 ng/cell (500 µL ethanol with 20% isooctane residue)	72 h	Receptor fluid = <0.1 % Epidermis = 11 % Dermis = 0.8 % Kp = 0.17-2.5* 10^{-4}cm/h	-do-
***γ*-HBCD**	Human skin	*In vitro*	10-100 and 50-300 ng/cell (500 µL ethanol with 20% isooctane residue)	72 h	Receptor fluid = 0.1 % Epidermis = 10 % Dermis = 0.8 % Kp = 0.15-2.3 * 10^{-4}cm/h	-do-

Similarly, Mayes, et al. 2002 reported PA values of 3.4-4.5 % in Rhesus monkeys exposed to PCB-contaminated soil for 24 h.

The difference between the calculated PA values for PCBs from soil in this study and the 14% dermal absorption factor used by the USEPA (U.S. EPA 1992) was attributed mainly to soil organic content in addition to particle size, skin residence time and contaminant "aging" in the soil. The percutaneous absorption of ^{14}C-Aroclor 1260 in test monkeys was determined by measuring the radioactivity in excreta (equation 1) (Mayes et al. 2002).

$$\%\ \text{Dose Absorbed} = \left(\frac{\%\ \text{Topical Dose Excreted}_{(^{14}\text{C-urine} + ^{14}\text{C feces})}}{\%\ \text{Intravenous Dose Excreted}_{(^{14}\text{C-urine} + ^{14}\text{C feces})}} \right) \times 100 \quad \textbf{....(1)}$$

An important point is that the model used in equation 1 and in all *in vivo* studies in humans or surrogate species where the animal is not sacrificed, cannot account for any test compounds sequestered within the skin (Mayes et al. 2002, Spalt et al. 2009). This may lead to substantial underestimation of the actual dermal uptake of persistent lipophilic compounds which would eventually (within days) be systemically absorbed from the skin depot of the exposed organism. For such compounds, for which the outcome of concern is typically not acute toxicity, inclusion of skin burden is necessary (Spalt et al. 2009). While adjustment for excretion following intravenous administration may be employed, this has associated uncertainty and presumes no difference in the excretory pattern associated with dermal and intravenous administration used as a reference. The importance of this concept of contaminant skin depot was confirmed by (Garner and Matthews 1998). These authors applied 0.4 mg/kg body weight of a mixture of radiolabelled mono- to hexa- PCBs in acetone to a 1 cm^2 hairless skin area at the back of adult male F-344 rats. Distribution of radioactivity in the dose site and selected tissues was determined by serial sacrifice at time points up to 2 weeks. Results revealed the dermal penetration of test compounds to vary inversely with degree of chlorination and at 48 h ranged from ca. 100 % for mono-PCB to ca. 30 % for

hexa-PCB. Although the maximum internal exposure to mono-PCB was at 4 h (37 % of the dose present in tissues), only 0.2 % of the absorbed dose remained in the tissues after 2 weeks. In contrast, tetra-PCB internal exposure was the greatest with ca. 85 % of the total absorbed dose present in tissues 72 h post administration. Furthermore, hexa-PCB equivalents in tissues continued to rise through 2 weeks postdose (~15 % of absorbed dose) since systemic absorption from epidermis depots was still incomplete when the study was terminated. While rat skin favoured the rapid absorption of lower chlorinated PCBs; their relatively rapid metabolism and elimination, suggests lower body burdens of the less chlorinated congeners compared to higher molecular weight PCBs which penetrate less rapidly, but persist at the site of exposure and slowly enter the systemic circulation (Garner and Matthews 1998). In another contribution, (Garner, Demeter and Matthews 2006a) used the same animal model to study the disposition of mono- to hexa- PCBs following dermal administration. Results confirmed higher chlorinated PCBs to be slowly absorbed and accumulated in the adipose and skin. Interestingly, excretion and metabolic profiles following dermal dosing tended to differ from profiles following equivalent intravenous doses. This was attributed to first pass metabolism occurring at the dermal dose site. The study further suggested that the rate of absorption, and consequently disposition of PCBs following dermal exposure, may be mediated, either in part or fully, by transdermal metabolism (Garner et al. 2006a).

The dermal absorption of the flame retardant resorcinol bis-diphenylphosphate (RDP) was investigated in rats and monkeys. Sprague-Dawley rats and cynomolgus monkeys were dermally exposed to 100 mg of ^{14}C-RDP spread over a shaved area representing about 20 % of the animal's surface area. Results revealed ~ 20 % of the dermal dose was absorbed in rats, whereas primates absorbed only 10 % of the applied dermal dose (Freudenthal et al. 2000). Very little is known about the dermal absorption of BFRs. In an early report, Ulsamer et al.

studied the dermal absorption of the banned flame retardant tris (dibromopropyl) phosphate (TRIS) in rabbits. The test animals were exposed to radiolabelled ^{14}C-TRIS via sections of fabric (10 x 12 cm) placed in contact with skin for 96 h. Results revealed that up to 17 % of the applied dose was absorbed when the fabric was wetted with urine. Only 6 % of the dose was absorbed when the cloth was wetted with simulated sweat, which was slightly higher than the absorption (4 %) from a dry cloth (Ulsamer, Porter and Osterberg 1978). A more recent study used a female C57BL/6 mice model to assess the dermal bioavailability of BDE-47. Test animals were exposed to 1 mg/kg body weight of ^{14}C-BDE 47 in acetone applied to a hairless 2 cm^2 skin patch. Results revealed ~62 % absorption of the administered dose after 5 days while 15 % remained at the site of application where skin and adipose were reported as the major depot tissues (Staskal et al. 2005). Though the animal models have substituted human volunteers but, ethical and technical issues arising from them their use has been discouraged (Jakasa and Kezic 2008).

1.7: Paradigm shift – *in vivo* to *in vitro* dermal bioavailability studies

Due to the ethical and technical issues arising from the use of lab animals in toxicology studies, the use of *in vivo* animal models is strongly discouraged (Jakasa and Kezic 2008).Therefore, much more emphasis is given to finding an alternative. I*n vitro* test methods provide a better platform for development of predictive pharmacokinetic models. Several guidance documents for conducting *in vitro* skin absorption studies (OECD 2004; U.S. EPA 2004; WHO 2006) are currently available. Various types of diffusion cells and different types of skin are used, for example, human excised skin from surgery or from cadavers (*ex vivo* skin) or animal (e.g. pig) skin. Similarly, Hughes, et al. 2001 used skin from adult hairless female mice (SKH1) mounted in flow-through diffusion cells to study the absorption of ^{14}C-BDE-209 and ^{14}C-TDCIPP at 3 concentration levels. HEPES ((*4-(2-hydroxyethyl)-1-piperazineethanesulfonic acid*))-buffered Hanks' balanced salt solution (pH 7.4) with 10 %

fetal bovine serum was used as receptor fluid. Following 24 h exposure, the skin patches were washed with solvent prior to analysis of receptor fluid, skin wash and skin for chemical-derived radioactivity. BDE-209 showed low penetration (0.3 %) into the receptor fluid while up to 20 % of the dose remained in skin after 24 h. TDCIPP displayed higher penetration (39–57 %) to the receptor fluid, while 28–35 % of administered dose remained in the skin. This was mainly attributed to its lower molecular weight and K_{OW} than BDE-209 (Hughes et al. 2001). The dermal absorption of BDE-47 was studied using *in vitro* split-thickness skin membranes (350–410 μm, stratum corneum uppermost) of human and rat skin exposed to a single dose of ca. 10 mg/cm^2 of ^{14}C-BDE-47 for 24 h. The skin patches were mounted in flow-through cells while receptor fluid (NaCl, 0.9 %, w/v in water) was pumped through the receptor chambers at ca. 1.5 ml/h (Roper et al. 2006).The dose recovered from the receptor fluid was 2 % and 15 % of administered BDE-47 to human and rat skin, respectively. The difference between the results of this *in vitro* study (Roper et al. 2006) and the higher (62 %) sorption observed in an *in vivo* study of dermal absorption in mice (Staskal et al. 2005) (Table 1.5) may be attributed mainly to the use of 0.9% NaCl solution in water as a receptor fluid, as this may greatly reduce diffusion of the lipophilic BDE-47 to the receptor fluid (Wilkinson and Williams 2002) and does not accurately mimic actual biological conditions. Possible evidence of this is provided by the high residual levels of BDE-47 detected in the cells (57 % and 33 % for human and rat skin, respectively) that appeared not to diffuse to the receptor fluid (Roper et al. 2006). While no data exists on dermal absorption of TBBP-A, a recent *in vitro* study reported on the percutaneous bioavailability of its precursor, bisphenol A (BPA) from human and pig skin (Zalko et al. 2011). Viable human and pig skin patches (500 μm thickness) were maintained at the air/liquid interface using Transwell inserts while dermal/epidermal feeding was achieved via diffusion of nutrients from a modified Dulbecco's Eagle culture medium which kept the cells alive during 72 h exposure

experiments. BPA was efficiently absorbed (65 % and 46 % from pig and human skin, respectively) and metabolised by the cultured skin indicating the trans-dermal route contributes substantially to human exposure to BPA (Zalko et al. 2011). However, it should be noted that TBBP-A has a much higher molecular weight and consequently, different physicochemical properties (e.g. water solubility, partition co-efficient and vapour pressure) than BPA. Furthermore, the lack of halogen atoms in BPA is likely to enhance the rate of its percutaneous absorption compared to its tetra-brominated derivative (Garner and Matthews 1998).

Given the growing evidence that suggest dermal absorption to be a potentially significant pathway of human exposure to FRs, the paucity of data on dermal bioavailability of such ubiquitous contaminants may be attributed to a combination of ethical, technical and economic issues. One alternative method with the potential to overcome such difficulties is the use of 3D human skin equivalent (HSE) models which provide a relatively cheap, commercially available, ethical, and reliable method for dermal absorption studies that is capable of producing data of relevance to human exposure.

1.8: Human Skin Equivalent models (HSE)

1.8.1 Rationale. Although the Organisation for Economic Co-operation and Development (OECD) and the European Centre for Validation of Alternative Methods (ECVAM) describe methods for assessing dermal absorption using excised *in vitro* human and animal skin, the lack of correlation in transdermal permeation of chemicals across species imparts a high degree of uncertainty when extrapolating results from animal models to humans. This is mainly due to variations in the stratum corneum thickness, intercellular subcutaneous lipids and/or between-species differences in metabolic enzymes and their activity (Schafer-Korting et al. 2006). Therefore, excised *in vitro* human skin is preferable to animal skin (e.g. rat or pig skin) for dermal absorption testing, but is clearly less available. To overcome this shortage,

HSE models have been developed to provide an alternative to human skin in testing of compounds for transdermal permeability (Mertsching et al. 2008). A protocol was developed and validated according to the OECD guidelines for percutaneous absorption by using commercially available HSE models (Table 1.6). The permeability of tested HSE models were compared to that of excised human epidermis, pig skin and bovine udder skin, using 9 compounds widely varying in physicochemical characteristics, including the OECD standards: testosterone, caffeine and benzoic acid. Results revealed HSE models closely mimic the histological and physiological character of viable human skin, allowing their use for *in vitro* skin penetration studies (Hartung et al. 2004, Schafer-Korting et al. 2008). Consequently, several validated methods using HSE models have been approved by OECD and ECVAM for testing skin absorption, phototoxicity, corrosion and irritation by xenobiotic chemicals.(Ackermann et al. 2010, Buist et al. 2010)

1.8.2: *Composition.* HSE models can be generally classified into 2 main types:

1- Reconstructed Human Epidermis (RHE): RHE is a human skin tissue obtained from human keratinocytes cultured on an inert polycarbonate medium. One key advantage is that it permits growth of donor epidermal cells in a serum-free culture environment. After rapidly proliferating preparative keratinocyte cultures have been obtained, the epidermal cells yielded are seeded on inert filter substrates, which are then raised to the air-liquid interface in a humidified-air incubator. A fully-defined nutrient medium feeds the basal cells through the filter substratum. After 14 days, a stratified epidermis is formed that closely resembles human epidermis *in vivo* (Boelsma et al. 2000)

Morphologically, these cultures exhibit a well-stratified epithelium and cornified epidermis with significantly improved barrier function and metabolic activity (Boelsma et al. 2000). Differentiation markers such as suprabasal keratins, integrin b4, integrin a6, fibronectin, involucrinyt, filaggrin, trichohyalin, type I, III, IV, V, VII collagen and laminin

Table 1.6: Characteristics of commercially available HSE models.

Brand Name	Scaffold material	Source	Dermis	Manufacturer
Episkin™	Collagen (0.38 cm^2)	Keratinocytes(Mammary/ Abdominal samples obtained from healthy consenting Donors during plastic surgery)	NO	L'Oréal, Nice, France
Skinethic™	Polycarbonate membrane (0.5 cm^2)	Keratinocytes (neonatal foreskin tissue or adult breast tissue)	No	L'Oréal, Nice, France
Epiderm™	Collagen coated Polycarbonate (9mm diameter)	Human keratinocytes (neonatal foreskin adult breast skin)	No	MatTek Corporation, MA, USA
EpidermFT™	Collagen	Human keratinocytes (neonatal foreskin adult breast skin) human fibroblasts (neonatal skin, adult skin)	Yes	MatTek Corporation, MA, USA
EST-1000	Polycarbonate membrane	Keratinocytes (neonatal foreskin)	No	Cell Systems, Troisdorf Germany
AST-2000	Collagen	Human Keratinocytes	Yes	Cell Systems, Troisdorf Germany
Phenion® FT Model	Bovine, cross linked, lyophilized collagen (1.3 cm dia)	Primary human keratinocytes (neonatal foreskin), human fibroblasts (neonatal foreskin)	Yes	Henkel, Duesseldorf, Germany
StrataTest®	Collagen I (0.6 cm^2)	immortalized, human NIKS® keratinocytes dermal fibroblasts	Yes	Stratatech Corporation Madison WI,

				USA
Epistem ® LSE	Collagen	Primary human keratinocytes and dermal fibroblasts.	Yes	Epistem limited, Manchester, UK.
StratiCell® EPI/001	Polycarbonate membrane	Primary human keratinocytes	No	Straticell Corporation, Gembloux, Belgium.
StratiCell® Mel/001	Polycarbonate membrane	Primary human keratinocytes and melanocytes.	No	Straticell Corporation, Gembloux, Belgium.

sulfate and membrane-bound transglutaminase are expressed similar to those of the human epidermis.

1.8.3: ***Evaluation of 3D-HSE Skin models.***

1.8.3.1: ***Barrier function:*** The evaluation of permeability potential of chemicals or cosmetic formulations is a critical step in risk assessment or product development. The 3D-HSE models replaced in-vitro keratinocytes in culture as these models closely resemble the skin morphology. A validation study (Schafer-Korting et al. 2008) was performed to assess whether the RHE models like EPISKIN, Epiderm and SkinEthic were suitable for percutaneous permeability testing. The study tested the permeability of 9 compounds with a wide range of physicochemical properties and the results were compared with the recommended ex-vivo human epidermis and pig skin by OECD test guideline 428. Some of the main outcomes of this validation work are given below:

- The lag-times of the studied drugs for the HSE models were in the order of minutes to few hours, the maximum being 2 h whereas the lag-times were high (4.47 h with nicotine to 11.05 h with digoxin)

- For testosterone, the following order of permeability (P_{APP}) was found: SkinEthic RHE >Epiderm >EPISKIN, however for caffeine, SkinEthic and EPISKIN exceeded in permeability than the Epiderm model, *ex vivo* human skin and pig skin.
- Flufenamic acid and nicotine showed the highest permeability as compared to the other compounds which could be due to its low molecular weight 281.2 and moderate lipophilicity (4.80). A very lipophilic clotrimazole permeated through HES and pig skin less than flufenamic acid and nicotine where as the hydrophilic compound, Mannitol permeation was non-homogenous. The integrity and the barrier function of HSE models were well verified with high molecular weight compounds (>500) and the results indicated that ivermectin did not permeate at all whereas digoxin's permeability was very low. This suggested that there were no differences between the RHE models and the OECD approved skin preperations with respect to the molecular weight cut-off.

Permeation through the HSE model was two fold higher for testosterone and 10 fold higher in case of clotrimazole as compared to the pig skin at infinite concentrations. However, at finite dosing, the results were comparable for the distribution of testosterone and caffeine between donor, skin and receptor fluid. Thus the validation results support the use of RHE models as an alternative means for human and animal skin for dermal absorption and permeability testing.

1.8.3.2: Characterising Metabolising Enzymes or activities:

It is imperative to measure the levels of phase I and phase II enzymatic activities in skin models that are used in safety evaluation studies. Many studies have assessed the suitability of epidermal models for studies involving biotransformation by comparing the profiles of metabolising enzymes with the human skin. (Table 1.7 & Table 1.8)

EPISKIN *Phase* I enzymes activates the lipophilic compounds by adding a polar group to the compound and thus making it more hydrophilic. Then phase II enzymes like UDP-glucuronosyl transferases, glutathione-S-transferases and sulfotransferases which add conjugate groups (glucuronosyl, thiol and sulfate respectively) to the intermediate hydroxylate compounds to increase their polarity and excretable.

(Luu-The et al. 2009) compared the mRNA expression of Phase I and Phase II enzymes in Episkin and FTM with the human epidermis, dermis and total skin using real time PCR. The data indicated that CYP450 & FMOs were expressed at low levels and phase II metabolizing enzymes like glutathione- S-transferase P1 (GSTP1), catechol-O-methyl transferase (COMT), steroid sulfotransferase (SULT2B1b) and N-acetyl transferase (NAT5) at much higher levels. These data strongly supports that the Episkin and FTM represent reliable and valuable alternative *in vitro* models to study the function of phase I and II metabolizing enzymes in xenobiotic metabolisms.

1.9*: General Protocol for in vitro percutaneous absorption studies.* (Fig: 1.7)

Each HSE model is supplied with its respective receptor/culture fluid and its percutaneous absorption protocol. Generally, the protocol involves mounting the fully-developed skin patches at the air-liquid interface of a permeation device (e.g. Franz-cell type diffusion cells, Mattek® permeation device) while in contact with the receptor fluid. The test compound is then applied to the surface of the stratum corneum and incubated for the required exposure time (usually 24 h). The receptor fluid is sampled and replaced at fixed time intervals. At the end of the exposure period, the skin surface is washed/wiped clean of any residual contaminant remaining, prior to collection of the receptor fluid and cell culture for chemical analysis.

Table 1.7: Representative CYP & non –CYP –xenobiotic –metabolizing enzyme activities^ in human skin and human reconstructed skin models (^ = Constitutive; number after slash: induced (highest reported induced activity)

Activity	Human Skin	Skin microsomes	Episkin™	EpiDerm™	Units/Abbreviations	Reference
CYP1 Family	0.24-1.35* (AHH) BLQ-35* (EROD) 3.0 ± 1.2$		7.8 ± 0.4$ FTM -2.6 ± 0.3$	BLQ/ 1.7 ± 0.8#	*pmol/min/mg microsomal protein $ = pmol of products/6 h/mg protein (sum of 7,500g supernatant + medium) # = pmol/min/mg intact model protein AHH = Aryl hydrocarbon hydroxylase EROD = 7-ethoxyresorufin O-dealkylase	(Oesch et al. 2014)
CYP3A	BLQ-76 ± 41* (BQOD)		BLQ	94 ± 13*/5.5 ± 0.9#	*pmol/min/mg microsomal protein # = pmol/min/mg intact model protein BQOD = benzyloxyquinoline O-dealkylase	(Oesch et al. 2014)
CYP2C9	0.46 ± 0.05e$ (Tolbutamide 4		~≤ 0.5 (MFCOD)	BLQ	pmol/h/mg microsomal protein	

	hydroxylation)			MFCOD = 7-methoxy-4 trifluoromethylcoumarin O dealkylase	
CYP1A2		BLQ/0.7 ± 0.3[@] < 0.16	0.7 ± 0.3	@ = pmol/min/mg intact model protein	
CYP2E1	2.83 ± 0.34 [**] (Chlorzoxazone 6-hydroxylation)	< 0.11		** pmol/h/mg microsomal protein	
CYP3A4	2.35 ± 0.23[**] (Mi|dazolam 1-hydroxylation)	< 0.23		** pmol/h/mg microsomal protein	
CYP3A5		< 0.08		** pmol/h/mg microsomal protein	
Phase-II Enz					
GST-α	20 ± 6.8[*d]		307.99[##]		
NAT-1	Slow =0.63 0.94[*d] Fast = 1.73-3.03[*d]		11.24 ± 4.15 (microsome)	nmol/min/mg protein	(Jackh et al. 2011)

UGT	1.3 ± 0.2[*d]		1.98 ± 0.17 (microsome)	nmol/min/mg protein	(Jackh et al. 2011)
Non-CYP					
FMO			5.95 ± 1.06 (Benzydamine) (microsome)	nmol/min/mg protein	(Jackh et al. 2011)
COX	23.5 ± 8.7[#] (ARACHIDONIC ACID)		3.6 ± 1.9d[#]/~8[#]	# = pg prostaglandin E2 formed/min/mg microsomal protein	Jackh, Blatz et al. 2011)
NQR	7-10[h],~11[h,I] (Menadione)	~ 11	~ 3.6	nmol/min/mg cytosolic protein	Jackh, Blatz et al. 2011)
GST	~ 290*, 15 ± 3** (20 ± 6.8)[&] CDNB	~180-430 [&] 51 ± 2 ** FTM = 112 ± 12**	~ 410.-920[&] (~62) [&]	*= nmol/min/mg cytosolic protein (epidermis scrapped from skin surgical samples) ** = pmol/min/mg protein (sum of 7,500g supernatant + medium) & = nmol/min/mg cytosolic protein	

				CDNB =1-chloro-2,4 dinitrobenzene
UGT (4-MU)	1.3 ± 0.2[c] 18 ± 11[d]	68 ± 3[d] FTM = 54 ± 3[d]	~ 1.8 -1.98 [c]	C = nmol/min/mg microsomal protein d = pmol/min/mg protein (sum of 7,500g supernatant + medium)
NAT (PABA)	33 ± 8 [d]	21 ± 2 [d] FTM = 47 ± 3[d]	11.2 ± 4.1[e]	d = pmol/min/mg protein (sum of 7,500g supernatant + medium) e = nmol/min/mg S9 protein
Para Toluidine -NAT	0.63-3.03[f]		~ 0.68[f]	f = nmol/min/mg cytosolic protein

Table 1.8 : Expression profiles (copies/µg of total RNA)(x1000) of phase I and phase II metabolizing enzymes in human skin and the Episkin models (Luu-The et al. 2009)

Genes profiling	Total human skin (n=10)	Human dermis (n= 6)	Human epidermis (n =10)	Episkin Model (n =6)	FTM (Episkin) (n= 3-8)
Phase I					
CYP4B1	106 ± 21.61	55.57 ± 22.87	114.99 ± 25.14	137.36 ± 25.46	44.80 ± 2.90
CYP26B1	65.84 ± 9.51	151.22 ± 102.21	80.58 ± 17.01	7.42 ± 3.21	36.16 ± 7.12
CYP39A1	64.83 ± 7.12	13.60 ± 4.10	41.0 ± 7.69	14.67 ± 2.46	18.70 ± 7.06
CYP2J2	44.66 ± 8.07	6.97 ± 1.01	45.35 ± 7.88	21.46 ± 7.18	42.70 ± 6.87
CYP4FB	38.66 ± 18.65	31.23 ± 17.01	3.63 ± 0.57	7.53± 3.40	1.67 ± 0.82
CYP4F12	36.33 ± 5.73	13.45 ± 8.76	29.33 ± 6.11	6.58 ± 3.59	18.74 ± 6.74
CYP27A1	33.99 ± 6.30	52.51 ± 6.49	10.48 ± 1.32	ND	ND
CYP7B1	22.70 ± 3.02	20.18 ± 4.41	16.97 ± 4.60	27.61 ± 2.46	15.33 ± 2.46
CYP2B6	18.47 ± 5.29	12.99 ± 3.47	3.98 ± 1.01	7.38 ± 6.81	3.98 ± 1.13
CYP2D6	15.19 ± 3.15	7.88 ± 3.02	4.79 ± 0.76	9.39 ± 2.90	7.31 ± 2.71
CYP2E1	14.10 ± 3.91	3.65 ± 2.76	7.50 ± 4.96	46.33 ± 21.44	11.44 ± 2.64
CYP1A1	12.56 ± 7.28	2.81 ± 1.17	18.82 ± 11.07	10.13 ± 6.14	1.14 ± 0.26
CYP1B1	6.58 ± 0.85	10.25 ± 3.85	7.85 ± 1.76	48.39 ± 24.41	5.56 ± 2.47
CYP27B1	1.95 ± 0.26	1.95 ± 0.26	1.96 ± 1.32	50.25 ± 9.81	97.66 ± 20.9
CYP46A1	6.49 ± 1.59	8.84 ± 3.94	1.59 ± 0.26	6.49 ± 2.94	1.18 ± 0.32
CYP2C18	5.41 ± 0.94	1.33 ± 0.26	6.80 ± 1.76	27.89 ± 6.76	10.65 ± 6.8
CYP2C8	4.34 ± 1.00	3.34 ± 2.97	6.96 ± 3.58	9.96 ± 3.88	12.93 ± 4.26
CYP21A2	3.97± 0.88	13.70 ± 4.46	2.01 ± 0.50	4.01 ± 1.97	1.48 ± 0.85
CYP2C9	3.34 ± 0.68	1.55 ± 1.47	1.40 ± 0.38	2.29 ± 0.68	0.94 ± 0.53
CYP2F1	3.23 ± 0.62	3.97 ± 1.39	1.37 ± 0.33	4.57 ± 2.29	2.85 ± 1.11
CYP4F2	3.25 ± 0.92	0.79 ± 0.34	1.51 ± 0.44	7.15 ± 3.18	5.39 ± 0.83
CYP1A2	2.36 ± 1.5	0.68 ± 0.18	5.60 ± 1.32	0.68 ± 0.29	0.64 ± 0.26
CYP3A5	2.4 ± 1.90	ND	7.71 ± 2.16	18.58 ± 7.98	2.63 ± 1.21
CYP4F3	1.64 ± 0.74	1.32 ± 1.18	1.81 ± 1.13	1.36 ± 0.16	0.66 ± 0.15
CYP3A7	1.49 ± 0.33	0.45 ± 0.11	1.74 ± 0.30	5.55 ± 2.27	0.68 ± 0.15
CYP11A1	1.36 ± 0.21	2.95 ± 0.47	ND	0.57 ± 0.14	0.23 ± 0.13
CYP26A1	0.93 ± 0.16	0.93 ± 0.43	ND	ND	ND

ADH1B	1500.0 ± 300.0	3000.0 ± 700	ND	ND	ND
EPHX1	473.54 ± 70.5	881.54 ± 111.11	91.42 ± 15.22	63.1 ± 12.35	75.36 ± 67.48
HADH2	202.56 ± 207.33	245.96 ± 25.84	431.73 ± 36.46	576.73 ± 85.85	893.71 ± 145.57
EPHX2	210.71 ± 40.77	66.60 ± 21.25	226.24 ± 51.97	24.13 ± 4.88	78.98 ± 16.94
AKR1C1	204.77 ± 28.42	354.36 ± 57.71	91.96 ± 11.77	814.62 ± 90.44	323.39 ± 41.34
AKR1C2	193.65 ± 43.7	155.77 ± 39.33	98.36 ± 16.94	686.66 ± 91.87	422.24 ± 113.41
DHRS8	88.94 ± 10.5	215.85 ± 27.85	14.89 ± 6.60	10.2 ± 3.45	11.18 ± 4.2
FMO1	41.9 ± 8.18	11.37 ± 2.84	43.55 ± 9.62	0.59 ± 0.46	1.29 ± 0.42
STS	17.93 ± 2.7	24.14 ± 6.21	12.73 ± 3.65	25.99 ± 6.60	40.98 ± 6.14
FMO4	13.46 ± 2.42	10.16 ± 4.11	8.58 ± 1.90	6.37 ± 0.67	21.28 ± 2.39
FMO5	12.89 ± 1.37	16.43 ± 6.0	15.63 ± 3.9	1.34 ± 0.39	7.13 ± 2.46
FMO3	8.25 ± 1.58	13.90 ± 3.23	ND	ND	ND
FMO2	5.9 ± 1.30	6.91 ± 0.70	44.46 ± 20.0	141.50 ± 11.48	141.15 ± 11.48
NOS1	4.45 ± 1.30	1.96 ± 0.32	13.89 ± 2.88	5.15 ± 1.51	1.29 ± 0.32
ADH7	1.35 ± 0.31	0.82 ± 0.42	1.28 ± 0.31	1.59 ± 0.35	2.54 ± 0.77
NOS2A	1.10 ± 0.38	1.69 ± 0.42	1.02 ± 0.35	0.36 ± 0.35	BLQ
AKR1CA	0.95 ± 0.49	BLQ	ND	ND	ND
Phase II					
GSTP1	2833.43 ± 507.22	2249.79 ± 550.48	2579.28 ± 398.79	8825.94 ± 1175.6	6593.73 ± 216.1
SULT2B1b	653.537 ± 134.14	107.787 ± 94.309	1242.21 ± 187.96	1937.9 ± 606.19	2477.83 ± 408.96
COMT	397.247 ± 71.274	271.551 ± 31.708	355.072 ± 60.164	716.641 ± 122.22	1278 ± 115.0
GST1	305.177 ± 80.758	435.579 ± 231.707	198.773 ± 51.22	88.2553 ± 8.130	227.874 ± 27.1
SULT1A1	216.636 ± 38.752	384.165 ± 37.128	26.4931 ± 6.504	21.12 ± 9.75	111.149 ± 7.101
GST M5	143.3 ± 28.99	521.101 ± 243.063	10.04 ± 5.96	ND	ND

NAT5	177.28 ± 29.81	95.165 ± 16.529	130.446 ± 31.43	106.37 ± 30.81	102.905 ± 33.875
SULT1E1	16.24 ± 5.20	2.12 ± 0.49	6.62 ± 1.25	9.6 ± 1.60	35.37 ± 8.35
NAT1	11.23 ± 2.60	7.33 ± 1.527	3.21 ± 0.94	6.35 ± 0.99	7.50 ± 1.50
UGT2B28	10.13 ± 8.91	2.87 ± 1.69	ND	0.99 ± 0.43	ND
UGT2B4	4.82 ± 1.54	28.19 ± 16.71	0.48 ± 0.55	0.86 ± 0.35	0.47 ± 0.18
UGT1A10	2.64 ± 0.80	1.94 ± 0.94	1.3 ± 0.57	1.45 ± 0.24	3.80 ± 1.32
UGT2B17	1.25 ± 1.7	4.96 ± 5.94	ND	1.13 ± 0.94	ND
UGT2B15	0.51 ± 0.22	1.42 ± 1.3	ND	ND	ND
SULT1B1	0.36 ± 0.20	0.44 ± 0.28	ND	0.82 ± 0.63	0.41 ± 0.33
SULT2A1	0.74 ± 0.35	0.43 ± 0.28	ND	ND	ND
NAT2	ND	ND	0.73 ± 0.37	ND	ND

Note – Values are extracted from the publication figures using using GetData software tool

Fig 1.6: General stages of development of HSE model.

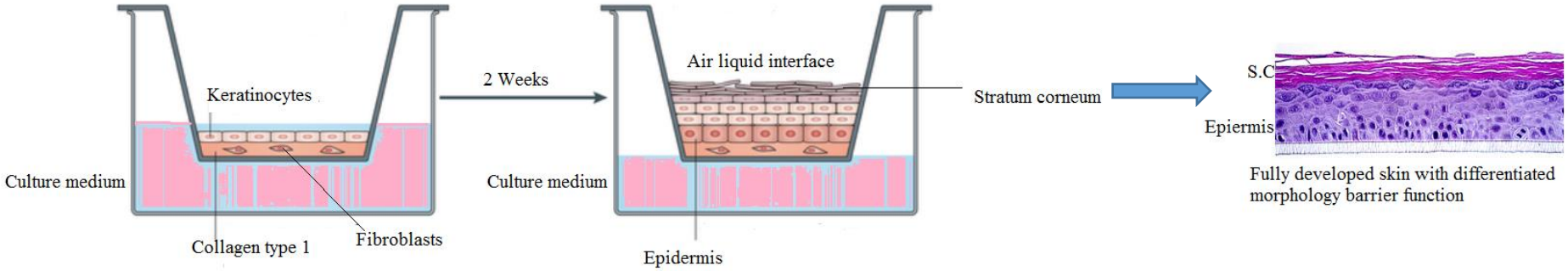

a) Keratinocytes and fibroblasts were pre seeded onto the scaffold/matrix before being assembled together using inserts. Ensuring that the agarose gel was sandwiched between the upper (keratinocyte) and bottom (fibroblast) layers.

b) Then the entire construct was placed onto the plastic platform insert with sufficient medium added to each well to ensure an air-liquid surface. (Chau et al.2013)

Fig 1.7 : General protocol for percutaneous absorption studies using *in vitro* 3D HSE models

Step-1 **Equilibration of 3D-HSE with receptor medium**

Step-2 **Exposure of the contaminant on the stratum corneum**

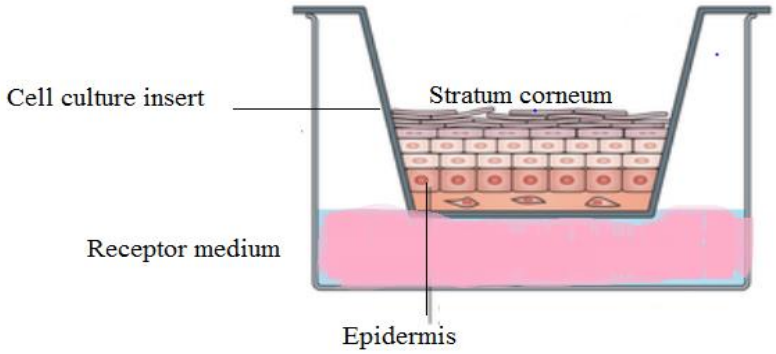

Step-3 **Receptor medium is collected (& replaced) at serial time points**

Step-4 **At the end of the exposure experiment, the stratum corneum surface is washed thoroughly, all the receptor fluid is collected & the cell culture is stored at -80'C untill analysis**

1.10: HYPOTHESIS and AIMS

The overriding hypothesis that this work tests is that dermal uptake of FRs is a significant pathway of human exposure. To address these gaps, the aims of the current study are to:

- Develop and validate analytical methods for FRs using LC-MS/MS and GCMS
- Assess the bioaccessibility of the studied FRs from indoor dust to synthetic sweat/sebum under physiological conditions.
- Evaluate the validity of HSE models (EpiDerm^{TM} & EPISKIN ^{TM}) against human *ex vivo* skin samples for measuring human dermal exposure to FRs.
- Develop and validate sampling and analytical methodology for determination of FRs in several samples like receptor fluid, cotton bud, skin tissue etc.
- Understand the role of skin moisture and oiliness on dermal uptake of FRs from the dust
- Conduct exposure experiments involving the application of consumer product samples like upholstered fabrics and plastics to 3D-HSE models under different exposure scenarios (dry, wet skin and in presence of moisturising cream)
- Assess external and internal human exposure to target FRs via dermal exposure using the following data for all the age groups:
    - Bioaccessible fraction of FRs from indoor dust, plastics and fabrics to the human sweat/sebum on the skin surface.
    - Bioavailable fraction of FRs when the skin models are exposed to indoor dust, plastics and upholstered fabrics.

CHAPTER II
ANALYTICAL METHODOLOGY AND VALIDATION

This chapter contains some material taken verbatim from Pawar, G., M. A. Abdallah, et al. (2016). Dermal bioaccessibility of flame retardants from indoor dust and the influence of topically applied cosmetics. J Expo Sci Environ Epidemiol 6 (10): 84.

2.1: Instrumental analysis

2.1.1: GC-NCI /MS Analysis for PBDEs

Quantification of target PBDEs was performed using a TRACE 1310™ GC coupled to a ISQ™ Single Quadrupole mass spectrometer (Thermo Fisher Scientific, Austin, TX, USA) operated in negative chemical ionisation (NCI) (Harrad et al. 2008, Abdallah, Pawar and Harrad 2015b). Separation of target PBDEs was performed on Agilent DB-5 capillary column (15 m x 0.25 mm; 0.1 µm). The mass spectrometer was run in selected ion monitoring (SIM) with ion source, quadrupole and mass transfer line temperatures set at 230, 150 and 300 °C, respectively. Helium was used as carrier gas at constant flow (1.0 mL/min) with methane as moderating (or reagent) gas. One µL of the extract was injected in solvent vent mode (injector temperature at 90 °C for 0.06 min, then increased at 700 °C/min to 305 °C, vent time 0.04 min, vent flow 50 mL/min). The splitless time was 1.5 min. The GC temperature program started at 90 °C for 1.5 min, then ramped linearly at 15 °C/min to 295 °C, which was kept for 15 min. Dwell times were 30 ms. Ions m/z 79 and 81, together with ions m/z 484.7/486.7 and 494.7/496.7 for BDE 209 and $^{13}C_{12}$-BDE 209, respectively, were monitored for the entire run. Analyte identification was based on retention times relative to the respective internal standard used for quantification, ion chromatograms and intensity ratios of the monitored ions. A deviation of ion intensity ratios in sample peaks of more than 20% of mean values observed in calibration standards was not accepted.

Fig 2.1: GC-ECNI/MS chromatograms of all PBDE congeners (1 ng/µL of each in iso-octane)

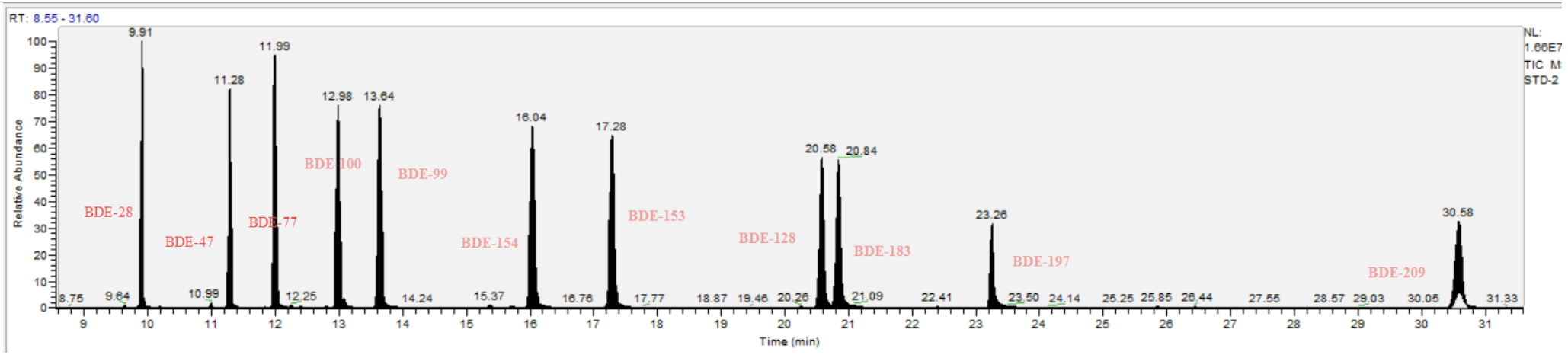

2.1.2: LC-MS/MS Analysis for HBCDs and TBBP-A

Separation of α-, β- and γ HBCDs and TBBP-A was achieved using a dual pump Shimadzu LC-20AB Prominence liquid chromatograph equipped with a SIL-20A autosampler, a DGU-20A3 vacuum degasser and a Varian Pursuit XRS3 C_{18} reversed phase analytical column (150 mm × 2 mm i.d., 3 µm particle size) according to (Abdallah, Pawar and Harrad 2015). A mobile phase program based upon (a) 1:1 methanol/water and (b) methanol at a flow rate of 150 µL min^{-1} was applied for elution of the target compounds; starting at 50% (b) then increased linearly to 100% (b) over 4 min, held for 7 min followed by a linear decrease to 60% (b) over 4 min, held for 1 min and finishing with 100% (a) for 10 min. TBBP-A and the three HBCD diastereomers were baseline separated with retention times of 9.0, 10.6, 11.2 and 11.7 min for TBBP-A, α-, β- and γ-HBCD, respectively.

Mass spectrometric analysis was performed using a Sciex API 2000 triple quadrupole mass spectrometer operated in electrospray negative ionization mode. MS/MS detection operated in the MRM mode was used for quantitative determination based on m/z 640.6→79, m/z 652.4→79 and m/z 657.7→79 for the native, ^{13}C-labelled and d_{18}-labelled HBCD diastereomers, respectively and m/z 540.8→79, m/z 552.8→79 for the native and ^{13}C-labelled TBBP-A, respectively. Specific instrumental calibration parameters are given in table 2.1

Table 2.1: Optimized MS/MS parameters* for the analysis of HBCDs and TBBP-A.

Parameter	Value (units)
Curtain gas	35 (a.u.)
Turbo gas temperature	500 (°C)
Ion spray voltage	- 4500 (V)
Declustering potential	-5 (V)
Focusing potential	-365 (V)
Collision gas	5 (a.u.)
Collision energy	40 (eV)
Cell entrance potential	-6 (V)
Collision cell exit potential	-10(V)

a.u. – arbitrary units

Fig 2.2: Illustrative LC-MS/MS chromatogram of native and ^{13}C-labelled HBCDs.

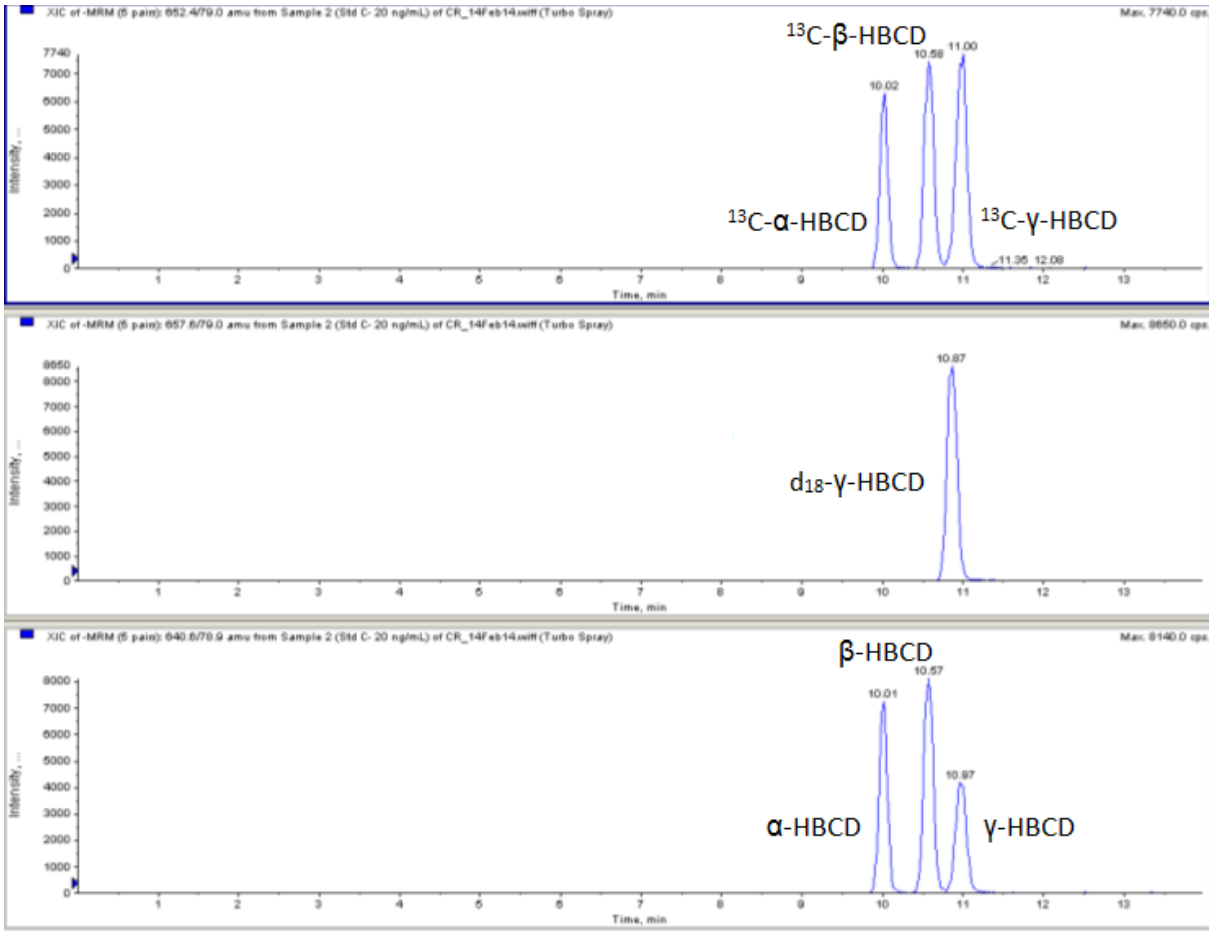

2.1.3: GC-EI/MS Analysis for PFRs

GC-EI/MS analysis of PFRs was performed using a Trace 1310 GC coupled to a ISQ mass spectrometer (Thermo Fisher Scientific, Austin, TX, USA) operated in electron ionization (EI) mode according to a previously described method (Abou-Elwafa Abdallah, Pawar and Harrad 2016). Separation of target analytes was performed on Agilent DB-5 capillary column (30 m x 0.25 mm; 0.25 μm) using helium as the carrier gas. One μL of purified extract was injected using cold split less injection. The injection temperature was set at 90 °C, hold 0.03 min, ramp 700 °C/min to 290 °C. Injection was performed using a pressure of 1 bar until 1.25 min and purge flow to split vent of 50 $mLmin^{-1}$ after 1.25 min. The GC temperature program was 90 °C, hold 1.25 min, ramp 10 °C/min to 240 °C, ramp 20 °C/min to 310 °C, hold 16 min. Helium was used as a carrier gas with a flow rate of 1.0 mL/min. The mass spectrometer was run in selected ion monitoring (SIM) mode. Dwell times ranged between 20 and 30 ms in different acquisition windows. The ion source, quadrupole and interface temperatures were set at 230, 150 and 300 °C, respectively, and the electron multiplier voltage was at 2200 V. TCEP, TCIPP and TDCIPP were quantified using the ions m/z 249, 277 and 381, respectively.

TnBP, TiBP, TEHP, EHDPP and TCP isomers analysis was conducted by a method developed on an Agilent 5975C GC/MS fitted with a 30 m DB-5 MS column (0.25 mm id, 0.25 μm film thickness) (Brommer et al. 2012b). Helium was used as carrier gas with a constant flow rate of 1.0 mL/min. The injector temperature was set at 290 °C under splitless conditions and the MS operated with a solvent delay of 3.8 min. The ion source, quadrupole and interface temperatures were set at 230 °C, 150 °C and 300 °C respectively. The GC temperature programme was 90°C, hold for 1.25 min, ramp 10 °C/min to 170, ramp 5 °C/min to 240 °C, hold for 10 min, ramp 20 °C/min to 310 °C, hold for 10 min. Resulting total run

time was 46.75 min. The MS was operated in selected ion monitoring (SIM) mode. (Table 2.2)

Fig 2.3: GC-MS chromatogram of TCEP, TCIPP, TDCPP and TPhP-d_{15} (IS) at 1 ng/µL in Iso-octane.

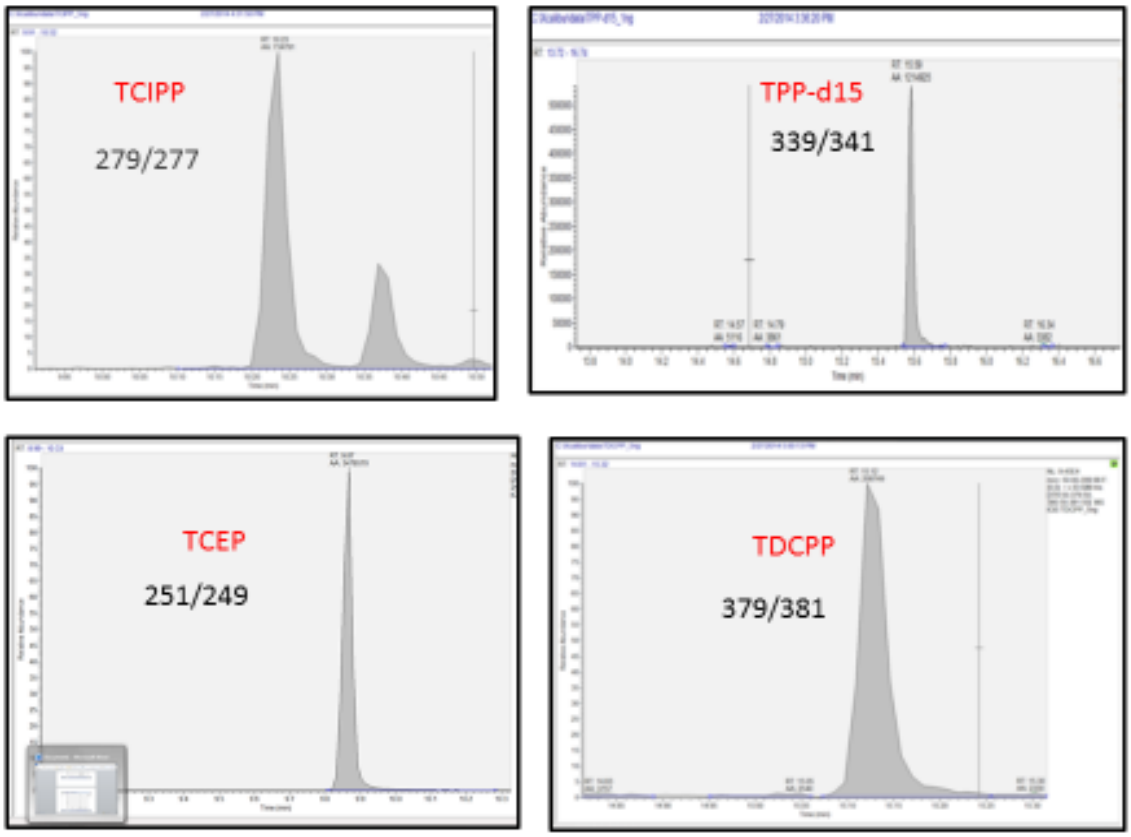

Fig 2.4: GC-MS chromatograms of TCP isomers.

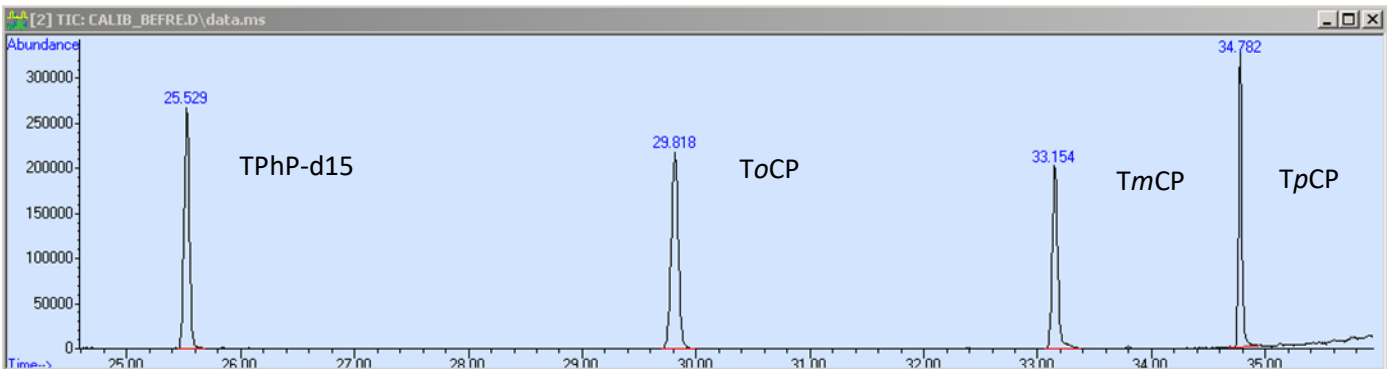

Table 2.2: Ions (m/z) monitored for some of the PFRs

Analyte	Quantification Ion	Identification Ion
TnBP	211	155
TiBP	211	155
TCEP	249	251
TCIPP	277	279
TDCIPP	381	379
EHDPP	251	250
TEHP	211	99
ToCP	368	367
TmCP	368	165
TpCP	368	367
d_{27}- TnBP	103	167
d_{15}-TPhP	341	339

2.1.4: Determination of NBFRs

GC-NCI /MS Analysis for NBFRs and other Flame retardants

Quantification of target NBFRs was performed using a TRACE 1310™ GC coupled to a ISQ™ Single Quadrupole mass spectrometer (Thermo Fisher Scientific, Austin, TX, USA) operated in negative chemical ionisation (NCI). Separation of target NBFRs was performed on an Agilent DB-5 capillary column (15 m x 0.25 mm; 0.1 µm). The mass spectrometer was run in selected ion monitoring (SIM) with ion source, quadrupole and mass transfer line temperatures set at 230, 150 and 280 °C, respectively. Helium was used as carrier gas at constant flow (2.0 mL/min) with methane as moderating (or reagent) gas. One µL of the extract was injected in solvent vent mode (injector temperature at 90 °C for 0.06 min, then increased at 700 °C/min to 305 °C, vent time 0.04 min, vent flow 50 mL/min). The splitless time was 1.5 min. The GC temperature program started at 100 °C for 2.0 min, then ramped

linearly at 25 °C/min to 270 °C, which was kept for 5 min and then ramped at 5°C/min to 270°C and finally at 20 °C/min to 320°C for 19 min. Dwell times were 30 ms. Ions m/z 79 and 81 for α-TECH,β-TBECH together with ions m/z 356.8/358.8, 420.7/421,464.0/464.7, 484.6/486.6,499.0/499.7, 653.8/655.8 for BTBPE,EH-TBB,TBPH, DBDPE,PBEB and DP, respectively, were monitored for the entire run. Analyte identification was based on retention times relative to the respective internal standard used for quantification, ion chromatograms and intensity ratios of the monitored ions. A deviation of ion intensity ratios more than 20% of mean values of calibration standards was NOT accepted.

Fig 2.5: GC-MS chromatograms of *syn*-Dechlorane plus and *anti*-Dechlorane plus

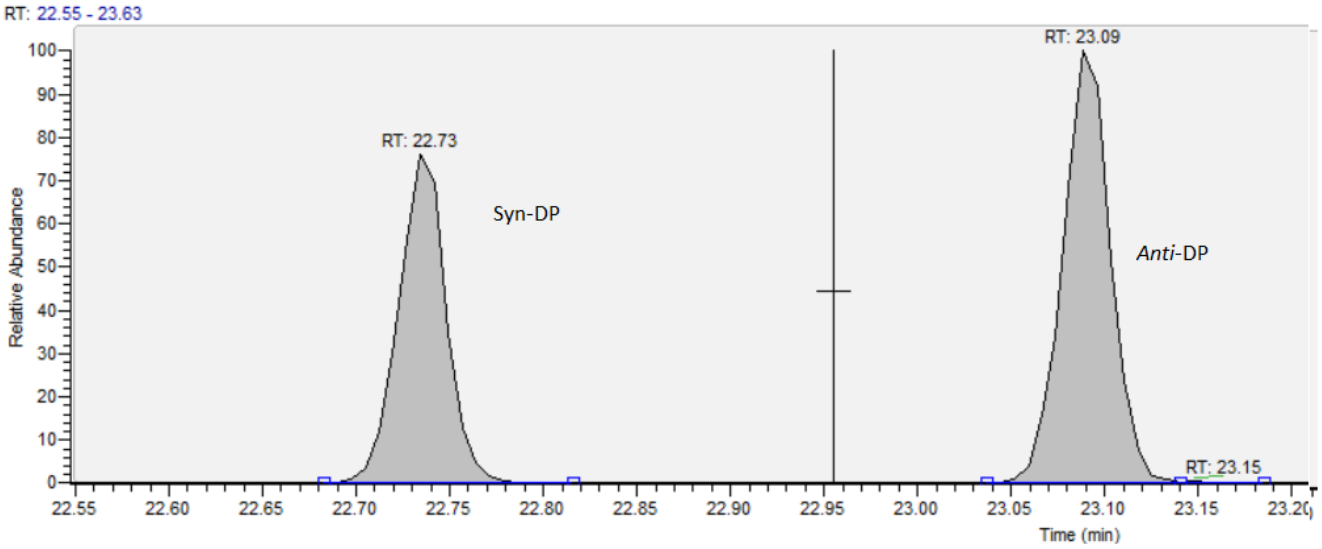

Fig 2.6: GCMS chromatograms of NBFRs.

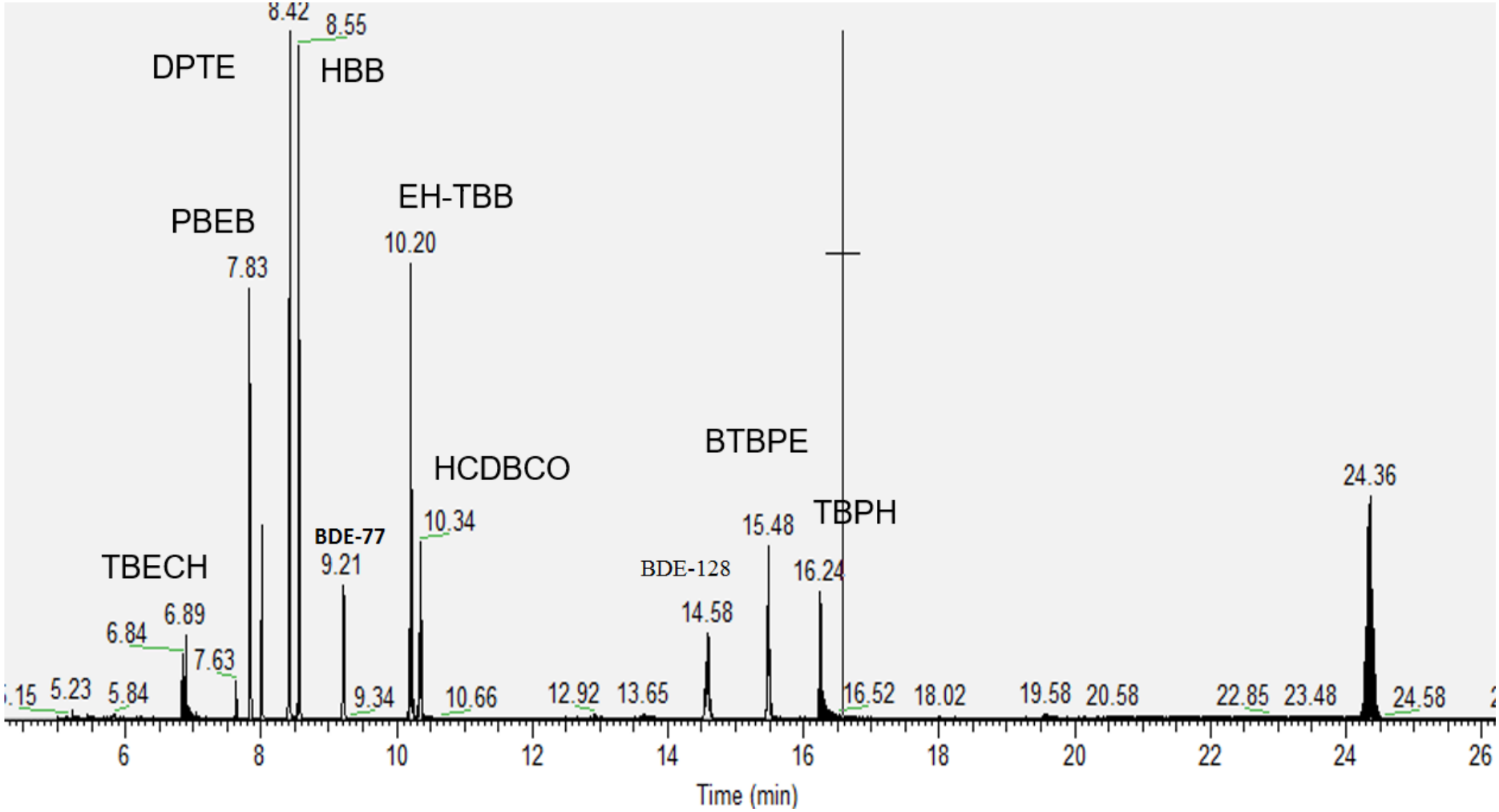

2.2: METHOD VALIDATION AND QA/QC CRITERIA

2.2.1 Identification and Quantification

Target compounds were identified and confirmed by specific retention time (tR) for each compound by injecting 2 ng pure standard on column. A full 5 point calibration was conducted for each of the studied compounds in a concentration range of 20-5000 pg/µL to assess the linearity of MS response. To compensate for the MS instrumental fluctuations and matrix effect, ^{13}C- labelled isomers were used as internal standard for each of the compound. Excellent linearity (R^2>0.99) was observed for each of the target compounds. Based on the 5 point calibration, relative response factors (RRF) for each compound were calculated. The RRF is the instrument response for a unit amount of the target compound relative to the same amount of the internal standard (IS).The relative response factor (RRF) was calculated, using equation (2.1) for each calibration standard and for each compound

$$RRF_N = \left(\frac{A_{NAT}}{A_{IS}}\right) \times \left(\frac{M_{IS}}{M_{NAT}}\right) \quad \text{..... (2.1)}$$

RRF_N refers to the relative response factor of the native compound, A_{NAT} is the peak area of the native in the calibration standard, A_{IS} is the peak area of the IS in the calibration standard, M_{IS} is the mass (ng) of IS added to the calibration standard and M_{NAT} is the mass (ng) of native analyte added to the calibration standard. An average of the calculated RRF_N of the five calibration standards was taken for the final RRF value of each analyte. The %RSD for each compound did not exceed 15%. The calculated RRFs were then used in equation (2.2) to calculate the concentration of the analyte (ng g^{-1}) in the sample.

$$C_N = \left(\frac{A_{NAT}}{A_{IS}}\right) \times \left(\frac{M_{IS}}{SM}\right) \times \left(\frac{1}{RRF_N}\right) \quad \text{.....(2.2)}$$

Where A_{NAT} refers to the analyte peak area in the sample, A_{IS} is the peak area of the internal standard in the sample, M_{IS} is the mass of IS added to the sample and SM is the sample mass extracted. For a given compound's chromatograph the signal to noise ratio (S/N) must exceed

3:1.The bromine isotope ratios must be within ± 20% of the average for the 2 calibration standards run at the start and at the end of the sample batch. The relative retention time (RRT) of the peak in the sample must be within the ± 0.2% of the average value determined for the same analyte in the 2 calibration standards ran before and after the sample batch.

2.2.2: Recovery Determination standard (RDS)

To compensate for any losses during the sample processing i.e. extraction and clean-up, internal standards (IS) were added prior to extraction and a recovery determination standard (RDS) was added to the final sample extract just before injection on the GCMS or LC-MS/MS. Calculation of the recoveries of IS were carried out. The RRF for each IS was calculated from the calibration standards using equation (2.3).

$$RRF_{IS} = \left(\frac{A_{IS}}{A_{RDS}}\right) \times \left(\frac{M_{RDS}}{M_{IS}}\right) \quad \text{.....(2.3)}$$

A_{RDS} is the peak area of the recovery determination standard (RDS) in the calibration standard and MRDS is the mass of RDS added to the calibration standard (ng). Again an average of the RRF_{IS} from all five calibration standards was calculated for the final, average RRF value of each IS used in equation (2.4) to calculate the % recovery of the IS.

$$\%\ IS\ Recovery = \left[\left(\frac{A_{IS}}{A_{RDS}}\right) \times \left(\frac{M_{RDS}}{RRF_{IS}}\right) \times \left(\frac{1}{M_{IS}}\right)\right] \times 100 \quad \text{.....(2.4)}$$

A_{IS} is the peak area of the IS in the sample, A_{RDS} is the peak area of the RDS in the sample, M_{RDS} is the mass of RDS added to the sample (ng) and M_{IS} is the actual mass of IS added to the sample (ng).For ^{13}C-α, β, and γ-HBCDs, average recoveries ranged from 71 to 92 % in bioaccessibility experiments (Table 2.3), while for ^{13}C-TBBPA, PBDE 77 and PBDE 128 average recoveries ranged > 85% in dust samples (Table 2.4).

Table 2.3: Representative table showing the % recovery of IS for the samples generated from Bioaccessibility experiments

Sample type	^{13}C-α-HBCD	^{13}C-β-HBCD	^{13}C-γ-HBCD	^{13}C-TBBP-A	d_{15}-TPhP
100% sweat	86.29 ± 6.50	87.32 ± 1.22	91.85 ± 3.22	90.33 ± 3.14	89.23 ± 8.16
99:1 sweat:sebum	89.36 ± 5.90	81.30 ± 4.59	92.24 ± 7.27	88.82 ± 2.50	80.41 ± 6.12
95:5 sweat:sebum	78.68 ± 4.03	78.18 ± 5.67	91.52 ± 10.03	90.40 ± 1.58	76.43 ± 5.18
9:1 sweat:sebum	89.75 ± 3.26	83.29 ± 6.88	79.49 ± 1.82	81.30 ± 3.60	79.76 ± 9.52
8:2 sweat:sebum	88.77 ± 7.07	84.73 ± 7.57	82.36 ± 1.32	83.34 ± 7.80	88.99 ± 8.82
1:1 sweat:sebum	86.15 ± 8.46	74.92 ± 8.94	72.79 ± 7.22	91.17 ± 6.35	70.94 ± 7.43
100% sebum	79.18 ± 18.03	83.74 ± 3.32	92.14 ± 2.50	78.88 ± 1.23	73.32 ± 5.72
Dust/SSSM (1:1)/ Moisturising Cream	72.84 ± 6.01	85.86 ± 7.96	88.28 ± 7.12	73.25 ± 4.70	70.84 ± 6.12
Dust/SSSM (1:1)/Body Spray	71.18 ± 8.76	73.36 ± 1.34	80.24 ± 11.95	81.94 ± 6.40	76.37 ± 5.64
Dust/SSSM (1:1)/Sun Screen Lotion	83.97 ± 13.09	78.34 ± 8.65	70.60 ± 5.71	88.03 ± 5.70	70.67 ± 5.70
Dust/SSSM (1:1)/Shower Gel	72.09 ± 1.48	75.30 ± 2.15	76.31 ± 1.23	85.83 ± 1.56	80.28 ± 7.29

Table 2.4: Summary of recoveries (expressed as %) of ^{13}C-labelled internal standards added to the studied dust samples.

Compound	Dust samples	
	Average	SD
^{13}C-α-HBCD	88	9
^{13}C-β-HBCD	85	5
^{13}C-γ-HBCD	86	12
^{13}C-TBBP-A	88	10
BDE-77	84	7
BDE-128	87	6

2. 3: ACCURACY AND PRECISION

2.3.1: Matrix spike method

Matrix spiking is a technique that is used to assess the performance of analytical procedures when testing a specific analyte in a matrix like dust or any other biological samples.

The NIST dust standard reference material (SRM) 2585 was analysed on a regular basis. Certified PBDE concentrations are published for this SRM, while only indicative HBCD concentrations are available. Due to the lack of an appropriate reference material for HBCDs, this SRM was analysed with concentrations compared to the indicative values. One SRM was analysed with every 20 samples as an ongoing method performance check. The mean concentration ± standard deviation (SD), %RSD, certified PBDE and indicative HBCD values are listed in Table 2.5. As the % RSDs are below 20%, the repeatability of the method is acceptable. Good recoveries (83 ± 9%) of the labelled IS was obtained. None of the target

analytes were detected in method blanks (n=3) consisted of sodium sulphate (~0.1 g) treated as a dust sample. Furthermore, our results compared favourably to previously reported concentrations of the target PFRs in SRM 2585 (Table 2.5, Chapter V).

Good recovery was obtained in case of the bioaccessibility experiment (Chapter III) for the sweat and sebum matrices at 3 different concentration levels. HBCDs, TBBPA & PFRs were ranged from 80-92% (Table 2.7) and the PBDEs recovery ranged from 87-93% (Table 2.8)

Method performance under the applied experimental conditions was tested via matrix spikes of the EPISKIN™ tissues, ex-vivo skin, receptor fluid at 3 different concentration levels of the target FRs (Table 2.9, 2.10, 2.11, Chapter IV).

ERM-EC 590 (low density polyethylene; LDPE) and ERM-EC 591 (Polypropylene; PP) were used in determining the method accuracy in the Episkin-microplastic bioaccessibility and bioavailability experiments (Chapter VI) Five replicate analyses of each CRM were conducted before the analysis of any bioaccessibility and skin exposure samples. Satisfactory recovery data was obtained with %RSD below 20% in compliance with EC Directive 2002/657/EC. (Table 2.12)

No known SRM or CRM is available for PFR-treated textiles or fabrics. To the author's knowledge, there are no studies conducted or published analyses on the same materials. However the fabrics were spiked with ^{13}C-labelled analytes that were satisfactorily recovered (80-92%) (Chapter VII).

Table 2.5: Mean ± standard deviation of BFRs in SRM 2585, %RSD and Certified and Indicative values (* Indicative values from (Abdallah, Harrad and Covaci 2008b), ** indicative values from (Brandsma et al. 2013), # certified values from NIST SRM-2585, ## indicative values from (Ali et al. 2012b)

Target compound	This study (n=5)		Certified Values/Indicative Values	
	Average	± SD	Average	± SD
α-HBCD	22.3	3.4	20 *	3.1
β-HBCD	4.4	0.8	4.3*	0.5
γ-HBCD	127.2	21.1	121.0*	19.0
TBBP-A	234.2	9.4	NM	NM
TCEP	711	56	792.0**	170
TCIPP	788	109	844.0**	100
TDCIPP	1928	124	1556.0**	280
BDE -28	48.3	6.0	46.9#	4.4
BDE -47	465.0	36.0	497.0#	46
BDE -99	858.3	31.3	892.0#	53
BDE-100	141.8	11.7	145.0#	11
BDE- 153	115.0	15.0	119.0#	1.0
BDE- 154	85.3	13.5	83.5#	2.0
BDE- 183	46.0	6.6	43.5#	3.5
BDE- 209	2345.9	18.0	2510.0#	190
EH-TBB	35.8	3.6	40.0##	-
BTBPE	41.2	7.4	32.0##	-

Table 2.6: Standard addition method results for TBBP-A in SRM 2585.

Mass added (ng)	Mass recovered (ng)	Recovery (%)	RSD (%) (n=5)
10	8.5	85	2.8
40	37.3	92.5	3.2
80	79.1	98.8	3.1

Table 2.7: Summary of standard addition "matrix spike" analysis results for target FRs in different formulations of skin surface film liquid (SSFL) (Pawar et al. 2016).

Spiking Level	Congener	100% sweat		1:1 sweat:sebum		100% sebum	
		Recovery (%)	RSD* (n=5)	Recovery (%)	RSD (n=5)	Recovery (%)	RSD (n=5)
10 ng BFRs, 100 ng PFRs	α-HBCD	88.4	5.1	83.2	4.3	83.4	5.4
	β-HBCD	85.3	4.0	81.4	5.2	80.7	3.9
	γ-HBCD	83.6	6.3	85.6	6.7	81.2	6.2
	TBBP-A	85.9	4.2	88.2	3.9	84.5	5.8
	TCEP	92.4	4.3	81.9	4.6	82.8	6.1
	TCIPP	92.6	4.3	80.2	6.1	80.5	4.6
	TDCIPP	86.5	5.2	84.2	5.2	82.3	4.9
40 ng BFRs, 400 ng PFRs	α-HBCD	91.0	5.8	87.3	5.5	84.8	6.1
	β-HBCD	81.2	4.1	88.9	4.8	82.4	4.5
	γ-HBCD	88.7	4.3	83.5	3.6	87.6	3.8
	TBBP-A	89.3	5.6	85.8	4.4	85.8	5.3
	TCEP	82.2	5.9	90.4	5.1	87.2	5.8
	TCIPP	88.1	6.6	91.6	4.9	83.1	6.7
	TDCIPP	81.6	5.3	86.7	6.2	85.6	6.8
80 ng BFRs, 800 ng PFRs	α-HBCD	83.8	6.2	83.5	3.9	91.3	5.6
	β-HBCD	89.6	5.3	87.3	4.1	86.2	6.4
	γ-HBCD	86.4	5.9	87.8	5.3	87.1	5.4
	TBBP-A	87.5	6.7	84.9	4.7	88.9	4.9
	TCEP	91.8	6.0	82.1	6.1	90.4	5.2
	TCIPP	90.2	5.3	88.3	5.9	85.7	6.1
	TDCIPP	88.4	6.4	85.4	5.6	89.2	6.4

Table 2.8: Summary of standard addition "matrix spike" method results for PBDEs in formulation of skin surface film liquid (SSFL).

Mass added (ng)	Congener	Mass recovered (ng)	Recovery (%)	RSD (%) (n=5)
50	BDE-28	42.1	88.2	6.3
	BDE-47	41.0	87.0	4.2
	BDE-99	43.5	89.0	4.3
	BDE-153	46.0	90.3	5.3
	BDE-183	43.8	89.1	4.3
	BDE-209	41.7	88.7	5.2
500	BDE-28	435.0	89.4	5.8
	BDE-47	461.0	92.2	4.1
	BDE-99	455.0	93.0	4.3
	BDE-153	428.9	87.7	5.6
	BDE-183	475.0	89.0	5.3
	BDE-209	420.0	86.0	6.2
1000	BDE-28	889.0	88.0	8.3
	BDE-47	860.8	93.1	5.9
	BDE-99	870.0	87.5	8.3
	BDE-153	897..7	89.7	9.4
	BDE-183	877.8	92.8	10.3
	BDE-209	899.0	85.9	8.6

Table 2.9: Summary of standard addition "matrix spike" method results for PBDEs in Receptor fluid. (Abdallah et al. 2015b)

Mass added (ng)	Congener	Mass recovered (ng)	Recovery (%)	RSD (%) (n=5)
50	BDE-1	44.6	89.1	5.1
	BDE-8	44.9	89.8	4.0
	BDE-28	44.1	88.2	6.3
	BDE-47	43.5	87.0	4.2
	BDE-99	44.5	89.0	4.3
	BDE-153	45.2	90.3	5.3
	BDE-183	44.5	89.1	4.3
	BDE-209	44.3	88.7	5.2
500	BDE-1	447.0	89.4	5.8
	BDE-8	461.1	92.2	4.1
	BDE-28	465.0	93.0	4.3
	BDE-47	438.7	87.7	5.6
	BDE-99	466.0	93.2	5.9
	BDE-153	443.8	88.8	6.6
	BDE-183	445.0	89.0	5.3
	BDE-209	430.2	86.0	6.2
1000	BDE-1	879.5	88.0	8.3
	BDE-8	930.8	93.1	5.9
	BDE-28	864.8	86.5	9.7
	BDE-47	907.0	90.7	7.8
	BDE-99	875.1	87.5	8.3
	BDE-153	896.7	89.7	9.4
	BDE-183	927.8	92.8	10.3
	BDE-209	859.3	85.9	8.6

Table 2.10: Representative table of standard addition "matrix spike" method results for PFRs. (Abou-Elwafa Abdallah et al. 2016)

Mass added (ng)	Matrix	Congener	Recovery (%)	SD (n=3)
50	EPISKIN™	TCEP	96.1	5.1
		TCIPP	91.8	4.0
		TDCIPP	93.2	6.3
	Ex vivo skin	TCEP	87.5	4.2
		TCIPP	89.0	4.3
		TDCIPP	90.3	5.3
	Receptor fluid	TCEP	97.1	4.3
		TCIPP	98.7	3.9
		TDCIPP	94.7	5.2
500	EPISKIN™	TCEP	98.6	5.8
		TCIPP	94.2	5.4
		TDCIPP	93.0	4.8
	Ex vivo skin	TCEP	88.7	5.6
		TCIPP	93.2	5.9
		TDCIPP	90.8	7.6
	Receptor fluid	TCEP	96.2	5.7
		TCIPP	98.1	6.3
		TDCIPP	95.4	6.6
1000	EPISKIN™	TCEP	92.8	8.3
		TCIPP	93.1	5.9
		TDCIPP	91.2	9.7
	Ex vivo skin	TCEP	90.7	7.8
		TCIPP	87.5	8.3
		TDCIPP	89.4	8.4
	Receptor fluid	TCEP	92.8	9.3
		TCIPP	95.1	7.8
		TDCIPP	91.9	8.6

Table 2.11: Matrix spike method for PFRs in cotton bud for skin experiments.

Mass added (ng)	Mass recovered (ng)	Recovery (%)	RSD (%) (n=5)
TCEP			
50	43.4	86.8	3.7
100	83.6	83.6	4.9
1000	800.0	80.0	2.7
TCIPP			
50	46.5	93.0	2.7
100	91.3	91.3	2.2
1000	825.0	82.5	4.1
TDCIPP			
50	39.8	79.6	3.7
100	85.6	85.6	1.9
1000	861.8	86.18	2.1

Table 2.12: Recovery (%) and RSD (%) for PBDE congeners from ERM-EC590 & ERM-EC591.

Target compound	This study (n=5)		Certified Values (gkg^{-1})		% RSD
	Average (ppm)	± SD	Average (ppm)	± SD	
ERM-EC590 (LDPE)					
BDE -47	0.177	0.06	0.23	0.04	1.34
BDE -99	0.285	0.09	0.30	0.030	4.67
BDE-100	0.056	0.01	0.063	0.005	4.11
BDE- 153	0.046	0.01	0.047	0.006	15.32
BDE- 154	0.023	0.003	0.026	0.0026	4.44
BDE- 183	0.10	0.009	0.13	0.012	16.0
BDE- 209	0.63	0.10	0.65	0.10	18.9
ERM-EC591 (PP)					
BDE -28	0.191	0.05	0.0025	0.0006	20.0
BDE-47	0.258	0.08	0.25	0.023	1.76
BDE -99	0.294	0.07	0.32	0.04	6.8
BDE-100	0.0056	0.001	0.066	0.007	0.29
BDE- 153	0.0422	0.003	0.044	0.006	18.42
BDE- 154	0.021	0.008	0.026	0.004	13.0
BDE- 183	0.069	0.02	0.087	0.008	14.0
BDE- 209	0.73	0.15	0.78	0.09	20.0

Table 2.13: Average recoveries (expressed as percent) of the internal (surrogate) standards.

Internal standard	Average recovery (%) ± SD
Fabric-E	**92 ± 9**
Fabric-C	**87 ± 11**
Fabric-O	**81 ± 17**

2.3.2: Limit of detection (LOD) and limit of quantification (LOQ)

Instrumental limits of detection (LOD) were calculated for each of the studied compounds based on a 10:1 signal to noise ratio (Table 2.14).

$$LOQ = \frac{LOD \times FEV}{VFEI \times SS} \times \frac{100}{\%\ IS\ RECOVERY} \quad \ldots\ldots\ldots\ldots\ldots\ldots\ldots\ldots\ldots\ldots\ldots\ldots (2.5)$$

Where FEV = final extract volume; VFEI = volume of final extract injected; SS = sample size (g or L); and % IS Recovery is % recovery of internal standard used to quantify the target. For dust method blanks 0.2 g of pre-extracted Na_2SO_4 was used). None of the studied compounds were above the limit of detection (LOD) in the field blank samples.

A "field" blank, comprising a skin tissue exposed to solvents only (omitting the dust, reference material plastics and the upholstered fabrics) and treated as a sample, was performed with each sample batch (n= 9). Blank values were subtracted from samples in the same batch if the blank contamination was more than 5% of the sample concentration.

2.4: Statistical analysis

Statistical analysis of the data was conducted using Excel (Microsoft Office 2003) and SPSS version 13.0. In all instances, where concentrations were below the LOQ, concentrations were assumed to equal half the LOQ. The results revealed concentrations in all data sets to be log-normally distributed. Hence, further ANOVA and t-tests were performed on log transformed concentrations. Levene test of homogeneity of variances and the F-test were performed on log-transformed data to evaluate statistical significance of the differences in variance between the tested data sets. The differences in means among the studied data sets were statistically evaluated using the suitable posthoc test (e.g. Bonferroni test if equal variances assumed). Confidence limits were preset to 95% while the significance levels in SPSS were set at 0.05.

Table 2.14: LOD (ng on coloumn) and LOQ (conc) values of HBCDs (LC-MS/MS), TBBPA (LC-MS/MS), PFRs (LC-MS/MS), PBDEs (GCMS) and NBFRs (GCMS)

Analyte	LOD (ng on coloumn)	Method LOQs					
		Dust (ng/g)	SSFL (ng/mL)	Skin (ng/cm^2)	Receptor fluid (ng /mL)	ERM-EC590/591 (ng/g)	Fabrics (ng/g)
α-HBCD	0.027	3.40	0.06	0.034	0.071	NM	NM
β-HBCD	0.030	3.80	0.07	0.035	0.078	NM	NM
γ-HBCD	0.029	3.6	0.07	0.036	0.076	NM	NM
TBBPA	0.07	8.92	0.18	0.041	0.18	NM	NM
TCEP	0.006	15.30	0.30	9.18	0.32	NM	4.7
TCIPP	0.004	10.20	0.20	6.10	0.21	NM	3.16
TDCIPP	0.008	20.40	0.40	12.24	0.42	NM	6.32
BDE-28	0.078	0.17	0.003	0.10	0.003	0.13	NM
BDE-47	0.10	1.60	0.03	0.96	0.033	1.24	NM
BDE-99	0.13	2.42	0.04	1.45	0.05	1.87	NM
BDE-100	0.15	2.5	0.05	1.5	0.051	1.93	NM
BDE-153	0.21	0.54	0.01	0.32	0.01	0.414	NM
BDE-154	0.22	0.56	0.01	0.33	0.01	0.434	NM
BDE-183	0.20	0.51	0.01	0.30	0.01	0.394	NM
BDE-209	0.24	0.61	0.01	0.36	0.01	0.473	NM
TPhP	0.56	1.42	0.028	0.857	0.02	NM	NM
EH-TBB	0.49	1.25	0.025	0.75	0.025	NM	NM
TBPH	0.95	2.42	0.048	1.45	0.05	NM	NM
BTBPE	2.3	5.86	0.11	3.52	0.12	NM	NM
DBDPE	4.8	12.24	0.24	7.34	0.25	NM	NM

CHAPTER III

DERMAL BIOACCESSIBILITY OF FLAME RETARDANTS FROM INDOOR DUST

This chapter contains some material taken verbatim from Pawar, G., M. A. Abdallah, et al. (2016). Dermal bioaccessibility of flame retardants from indoor dust and the influence of topically applied cosmetics. J Expo Sci Environ Epidemiol 6 (10): 84.

3.1: INTRODUCTION

Concerns exist over possible adverse health impacts following numerous reports of exposure to BFRs through inhalation, dermal contact and ingestion of both diet and settled dust. Physiologically-based *in vitro* bioaccessibility tests have emerged as an alternative method to study the availability for dermal uptake of several xenobiotics including heavy metals (Stefaniak et al. 2014, Hedberg, Midander and Wallinder 2010, Kulthong et al. 2010, Duling et al. 2012, Hillwalker and Anderson 2014) and pesticides (Ertl and Butte 2012a). Such bioaccessibility tests have been incorporated in regulatory frameworks such as the European standard for the release of nickel in artificial sweat (BS EN 1811, 2011). Bioaccessibility may be defined as "***the fraction of the total dose of a specific chemical/contaminant present in a matrix that becomes liberated into the body fluids and hence, is available for absorption"*** (Ruby et al. 1996). In other words, a combination of data on bioaccessibility and subsequent dermal uptake is required to determine the ability of a chemical (e.g. BFR) present in a matrix (e.g. dust), to be released from that matrix and be subsequently absorbed by an organ of the human body like the skin (Ertl and Butte 2012a). Bioaccessibility data from *in vitro* studies are considered conservative estimates, because not all the mass of a given chemical released into the body fluid (i.e. the bioaccessible fraction) will likely be absorbed through the

biological membrane (e.g. skin) to reach the systemic circulation (i.e. bioavailable) (Abdallah et al. 2012). Under physiological conditions, the outermost surface of the human skin, the *stratum corneum*, is covered with a skin surface film liquid (SSFL) mixture which consists of varying proportions of sweat and sebum (Buckley and Lewis 1960, Nicolaides 1974). Sweat is aqueous in nature and functions mainly to regulate the body temperature. It consists of electrolytes, organic acids, amino acids, vitamins and other nitrogenous substances. Sebum is a clear, oily substance secreted by sebaceous glands and forms a 0.5 to >4.0 μm thick layer to protect the skin from drying out. It mainly consists of squalene, wax esters and triglycerides, as well as free fatty acids, with a small amount of cholesterol and cholesterol esters (Stefaniak and Harvey 2008).

Cosmetics (e.g. sunscreen creams) may contain certain ingredients (e.g. surfactants) which can remain on the skin and become incorporated within the SSFL. This in turn, may alter the lipid domain of the skin, by interacting with the proteins in the barrier, or hydration, thereby increasing partitioning of chemicals to the SC (Lane 2013). Previous studies have shown certain sunscreen lotions to act as inadvertent penetration enhancers for potentially harmful chemicals (Pont, Charron and Brand 2004, Walters et al. 1997). Therefore, it is important to investigate the effect of topically-applied cosmetics on the dermal bioaccessibility of FRs in indoor dust.

Against this background, this chapter investigates the dermal bioaccessibility of selected organic FRs present in house dust in the presence of varying proportion of physiologically-relevant mixtures of sweat and sebum and topically-applied cosmetic products.

Figure 3.1: Schematic illustration depicting the structure of the skin and the absorption process for FRs in indoor dust in the presence of sweat/sebum mixture and topically applied cosmetics.

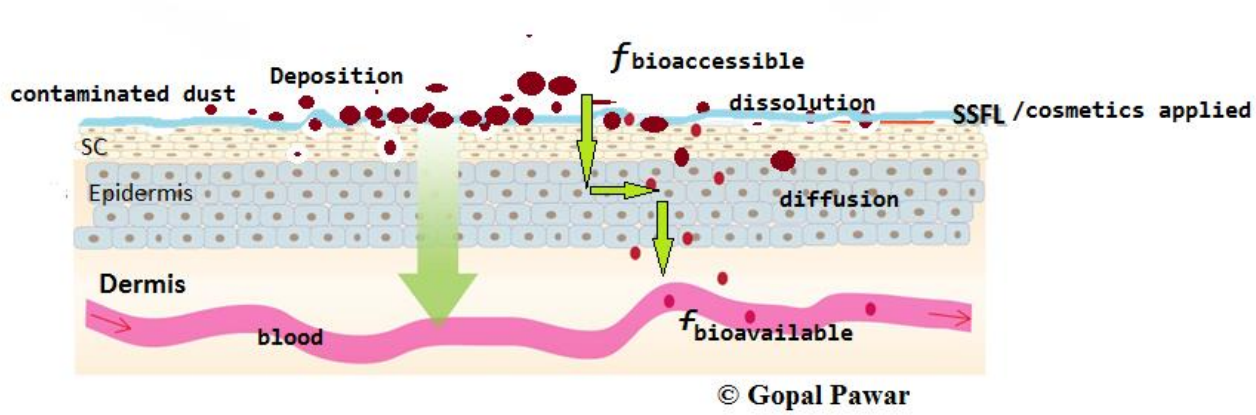

3.2: EXPERIMENTAL METHODOLGY

3.2.1: CHARACTERISATION OF THE STUDIED HOUSE DUST

SRM 2585 is intended for use in evaluating analytical methods for the determination of certified and indicative values of target FRs (organics in house dust, particle size < 100 µm and total moisture content =2.11 ± 0.06 %) was purchased from NIST (Gaithersburg, MD, USA). Aliquots (n=5, ~0.1 g each) of SRM2585 were analysed for target FRs using previously reported methods by our research group (Abdallah et al. 2008b, Brommer et al. 2012a). Results compared well with the indicative and reported levels of target FRs in this SRM. (Chapter 2 Section 2.2.3 Table 2.5)

3.2.2: PREPARATION OF SYNTHETIC SWEAT/SEBUM MIXTURE

Physiologically-simulated artificial sweat and sebum mixture (SSSM) was prepared according to a previously reported method and US patent (Stefaniak and Harvey 2008) using over 25 different chemical components given in table.3.1

We prepared 1 L of artificial sweat. To do so, initially 500 mL of fully aerated 18MΩ-cm distilled and deionized water were warmed to 32ºC to match human skin temperature and stirred continuously in an Erlen Meyer flask. Then the appropriate masses of electrolytes and other ionic constituents (given in table 3.1) were added followed by organic acids and carbohydrates.The pH was adjusted to that of normal human skin (5.3 ± 0.1) by adding 5 M NaOH dropwise using pH electrode, the volume was made up to 1 L and filtered through 0.2 µM pore size filter and preserved at 4°C.

Sebum was prepared according to Stefaniak and Harvey (2008) by dissolving the following constituents: squalene, palmityl palmitate saturated, triolein unsaturated, cholesteryl oleate, free cholesterol in concentrations found in physiological conditions in 500 mL of hexane in a sterilized 1000 mL Erlen Meyer flask with a magnetic stirrer bar. Synthetic sweat and sebum were mixed in different physiologically-relevant proportions using Tween 80 to mimic the naturally secreted surface active agents in the SSSM.

3.3: Dermal bioaccessibility *in vitro* test protocol

Briefly, ~60 mg of NIST SRM2585 dust and (when tested) 6 mg of cosmetics (moisturising cream, shower gel, sun screen lotion, and body spray were each examined separately) were accurately weighed and transferred into a clean dry test tube. In the absence of definitive data on the dust to sweat ratio on human skin, which is greatly influenced by variations of sweat secretion and dust loadings, we adopted a previously reported method (Ertl and Butte 2012) to mimic “wet skin conditions” using 1:1000 w/v dust to sweat ratio (i.e. 6 mL of the SSSM applied for each 60 mg of dust). The mixture was then gently agitated on a heated magnetic-stirrer plate maintained at physiological skin temperature (32°C). After 1 hour, phase separation was achieved by centrifugation at 3000 rpm for 15 mins. The dust (solid residue) and SSSM (supernatant) samples were analysed separately.

Table 3.1: Chemical composition of synthetic sweat and sebum mixture (SSSM)

Sweat Ingredients	Measured Qty.		Company
Electrolytes and Ionic Constituents	(g/L)	(µL/L)	
Sodium Sulfate	0.05826		Sigma Aldrich
Copper Chloride anhydrous		803	Merck
Ammonium Hydroxide		186	Fisher
Iron sulfate Heptahydrate	0.00272		Fisher
Sulfur	0.0737		Fisher
Lead- Reference Solution 1000 ppm		1243.0	Sigma Aldrich
Manganese- Reference Solution 1000 ppm		691.4	Sigma Aldrich
Nickel- Reference Solution 1000 ppm		1232.0	Sigma Aldrich
Zinc - Reference Solution 1000 ppm		0.77	Sigma Aldrich
Sodium Bicarbonate	0.252		FSA
Potassium chloride	0.4546		VWR
Magnesium Chloride Hexahydrate	0.01667		Sigma Aldrich
Sodium Phosphate Anhydrous Monobasic	0.04836		Sigma Aldrich
Calcium Chloride Dihydrate	0.7654		Fisher
Sodium chloride	0.05844		Fisher
Organic Acids and Carbohydrates			
Acetic Acid	0.00781		Sigma Aldrich
Butyric Acid		0.22	Sigma Aldrich
D(+) –Glucose	0.0306		Sigma Aldrich
Lactic Acid		2011	Sigma Aldrich
Essential Amino Acid Mix	0.01-0.1		Sigma Aldrich
DL-Alanine ($C_3H_7NO_2$)			
L-(+)-Arginine ($C_6H_{14}N_4O_2$)			
L-(+)-Aspartic acid ($C_4H_7NO_4$)			
L-(+)-Citrulline ($C_6H_{13}N_3O_3$)			
L-(+)-Glutamic acid ($C_5H_9NO_4$)			
Glycine ($C_2H_5NO_2$)			
L-Histidine ($C_6H_9N_3O_2$)			
L-Isoleucine ($C_6H_{13}NO_2$)			
L-Leucine ($C_6H_{13}NO_2$)L-(+)-Lysine MonoHCL			
($C_6H_{14}N_2O_2$°HCl)			
L-(+)-Omithine Hydrochloride ($C_5H_{12}N_2O_2$°HCl)			
L-Phenylalanine ($C_9H_{11}NO_2$)			
L-Threonine ($C_4H_9NO_3$)			
L-(-)-Tryptophan ($C_{11}H_{12}N_2O_2$)			
L-Tyrosine ($C_9H_{11}NO_3$)L-Valine ($C_5H_{11}NO_2$)			

Nitrogenous Substances		
Ammonium Chloride	0.00992	Fisher
Urea	0.6006	Sigma Aldrich
Creatinine	1357.0	Sigma Aldrich
SEBUM		
Squalene	0.5151	Sigma Aldrich
Palmityl Palmitate (saturated)	0.9718	Sigma Aldrich
Triolein (Unsaturated)	0.5345	Sigma Aldrich
Cholesteryl Oleate	0.0972	Sigma Aldrich

Figure 3.2: *In vitro* Dermal Bioaccessibility experimental configuration

3.4: Extraction and Clean-up

3.4.1: Determination of HBCDs & TBBPA

All solvents and reagents were purchased from Sigma-Aldrich (Poole, UK) of the highest available quality (e.g., analytical grade). Native α-, β-, and γ- HBCD, TBBPA, isotope-labelled ^{13}C- and d_{18}-α-, β-, and γ-HBCDs, ^{13}C -TBBPA were purchased from Wellington Laboratories (Guelph, ON, Canada).

Dust/SSSM/cosmetic samples were spiked with 30 µL of ^{13}C-isotopically labelled α-HBCD, β-HBCD, γ-HBCD and TBBPA (1ng/µL), prior to extraction with 3 mL of hexane: ethyl acetate (1:1 v/v) using a QuEChERS-based method.

Sample tubes were vortexed on a multi-positional mixer for 5 mins, followed by ultra-sonication for 5 mins and centrifugation at 3000 rpm for 5 mins. The extraction cycle was repeated twice before the pooled supernatant was collected in a clean tube and evaporated to ~ 1 mL under a stream of N_2. The crude extract was washed with ~ 2 mL of 95 % H_2SO_4 to remove lipids. The organic layer and washings were combined and evaporated to incipient dryness under N_2. Target analytes were reconstituted in 150 µL of methanol containing 50 pg /µL of d_{18}-α-HBCD used as recovery determination standard (RDS) prior to LC-MS/MS analysis using previously reported methods. (Abdallah et al. 2014a)

3.4.2: Determination of PFRs

Native TCEP, TCIPP and TDCIPP and d_{15}-triphenyl phosphate (d_{15}-TPHP) were purchased from Wellington Laboratories (Guelph, ON, Canada). Dust/SSSM/cosmetic samples were spiked with 30 µL of d_{15}-TPHP (10 ng/µL) used as internal (surrogate) standard prior to extraction with hexane: ethyl acetate (1:1 v/v, 3 mL) using the same procedure applied for HBCDs. The crude extract (~1 mL) was cleaned up by loading onto a Florisil SPE cartridge (pre-conditioned with 6 mL of hexane). Fractionation was achieved by eluting with 8 mL of hexane (Fraction 1 (F1), discarded) followed by 10 mL of ethyl acetate, Fraction 2 (F2). F2 was evaporated to incipient dryness under N_2. Target PFRs were reconstituted in 100 µL of isooctane containing ^{13}C-BDE-100 used as RDS prior to GC/MS analysis according to a previously reported method. (Abdallah and Covaci 2014a).

3.4.3: Determination of PBDEs and novel BFRs

Native PBDE congeners, TBB, BTBPE, ^{13}C-BDE-47, and ^{13}C-BDE-153 were purchased from Wellington Laboratories (Guelph, ON, Canada). Dust/SSSM were spiked with 30 µL of

^{13}C-BDE-47 & ^{13}C-BDE-153 (1 ng/µL) used as internal (surrogate) standards prior to extraction with hexane: ethyl acetate (1:1 v/v, 3 mL) and subjected to agitation on a multi-positional vortex mixer for 5 mins. Extraction of target BFRs was achieved via ultra-sonication of the samples for 5 mins and centrifugation at 3000 rpm for 5 minutes. The resulting supernatant liquid was aliquoted to clean test tubes. The extraction steps were repeated twice using fresh solvent mixture every time. The pooled supernatant fluid was subjected to evaporation under N_2 stream until ~ 2 mL.Two mL of 95 % of H_2SO_4 were added to remove the lipid content with a slightly manual agitation and the resulting supernatant liquid transferred to a clean tube. The sulfuric acid phase was washed twice with 1 mL of hexane and pooled them with the previous one. The clean extract was subjected to complete dryness under N_2 stream and reconstituted in 150 µL of the correspondent RDS containing 50 pg/µL of ^{13}C-BDE-100 and analysed by GC-MS.

3.5: Assessment of dermal bioaccessibility

In this study, bioaccessibility is expressed as $f_{bioaccessible}$, calculated (equation 3.1) as the percentage of each target FR present in the dust that was found in the supernatant at the end of each bioaccessibility experiments (all experiments were carried out in triplicate, hence average values were used)

$$f_{bioaccessibile}\,(\%) = \frac{\textbf{Average mass of FR in supernatant}}{\textbf{Average mass of FR in dust}} \times 100 \ldots \ldots\ldots\ldots\ldots\ldots\ldots\ldots\ldots\ldots (3.1)$$

3.6: RESULTS

3.6.1: Dermal bioaccessibility of HBCD, TBBPA and PFRs

In general, $f_{bioaccesssible}$ of HBCDs and TBBPA increased with increasing sebum content of the SSFL (Table 3.3). At 100% sweat, the $f_{bioaccesssible}$ of γ-HBCD (1.4 ± 0.1%) was less than that of β–HBCD (1.6 ± 0.6%) and α-HBCD (2.3 ± 0.2%). However, the reverse trend was observed at 100% sebum, where the $f_{bioaccesssible}$ was highest for γ-HBCD (67.2 ± 3.37%), followed by β–HBCD (60.4 ± 10.1%) and α-HBCD (50.5 ± 7.0%). This behaviour is

consistent with the lower water solubility of the γ-isomer (2 µg/L) compared to that of β–HBCD (15 µg/ L) and α-HBCD (49 µg/ L) (Abdallah et al. 2012).We recorded $f_{bioaccesssible}$ values for TBBPA of 3.5 ± 0.5 % and 55.7 ± 8.5 % in 100% sweat and 100% sebum, respectively. Compared to HBCDs, the higher $f_{bioaccesssible}$ value for TBBPA in 100% sweat is likely attributable to the higher water solubility of TBBPA (1.26 x 10^3 µg/L). Compared to the aqueous-based sweat, the substantially higher bioaccessibility of the studied BFRs in sebum can be attributed to the enhanced solubility of these lipophilic chemicals in the oily sebum.

In general, PFRs were more bioaccessible in sebum than sweat. In 100 % sweat, $f_{bioaccesssible}$ values for the studied PFRs were 16.0 ± 1.2% (TCEP), 12.4 ± 4.4% (TCIPP) and 11.9 ± 3.6% (TDCIPP); while in 100% sebum, the corresponding values were 22.3 ± 2.3% (TCEP), 26.9 ± 6.4% (TCIPP), and 28.1 ± 0.6 % (TDCIPP). This concurs with the physicochemical properties of our target PFRs (Table 3.2). In particular, the water solubility of TCEP, TCIPP and TDCIPP was reported as 7 x 10^3, 1.6 x 10^3 and 1.5 mg/L, respectively (van der Veen and de Boer 2012a).

Compared to the studied BFRs, PFRs show higher bioaccessibility in sweat and lower bioaccessibility in sebum (Table 3.3), which can be attributed to the differences in log K_{ow} and water solubility among these two classes of FRs (Table 3.2). Overall, under the more physiologically abundant SSFL composition (1:1 sweat: sebum) studied here, BFRs showed higher dermal bioaccessibility than PFRs, which may be attributed to increased partitioning of the more lipophilic BFRs from dust to the oily sebum.

Table 3.2: Physicochemical properties of target FRs relevant to dermal exposure (KEMI 2008, EU Risk Assessment Report 2006, van der Veen and de Boer 2012a).

Full name	Acronym	Water Solubility (µg/L, 25°C, pH=7)	Log K_{ow}
Tetrabromobisphenol- A	TBBPA	1.26×10^3	4.50
1,2,5,6,9,10-hexabromocyclododecane	HBCD	48.8 α-HBCD 14.7 β-HBCD 2.1 γ-HBCD 66 ΣHBCDs	5.07 ± 0.09 α-HBCD 5.12 ± 0.09 β-HBCD 5.47 ± 0.10 γ-HBCD
Tris(2-chloroethyl)phosphate	TCEP	7×10^6	1.44
Tris(chloroisopropyl)phosphate	TCIPP	1.6×10^6	2.59
Tris(1,3-dichloro-2-propyl)phosphate	TDCIPP	1.5×10^3	3.80

3.6.2: Effect of cosmetics on the dermal bioaccessibility of HBCD, TBBPA and PFRs in indoor dust

To investigate the influence of commonly applied cosmetics on the dermal bioaccessibility of FRs in indoor dust, we determined $f_{bioaccesssible}$ values of target FRs from reference dust into 1:1 sweat: sebum mixture, in the presence of (separately) moisturizing cream, sunscreen lotion, body spray, and shower gel. Results for each target compound were compared to a control group comprising reference dust exposed only to 1:1 sweat: sebum mixture without any surfactant or cosmetics. Except for TBBPA, statistically significant differences ($P<0.05$; ANOVA) were observed between $f_{bioaccesssible}$ values of target FRs in the presence of various cosmetics compared to the control group (Figure 3.3).

Table 3.3: Effect of the composition of SSFL on the bioaccessibility ($f_{bioaccessible}$) of target FRs from indoor dust

	$f_{bioaccessible}$ (%) for different SSSM compositions						
Compound	**100% Sweat**	**99:1 sweat: sebum**	**95:5 sweat: sebum**	**9:1 sweat: sebum**	**8:2 sweat: sebum**	**1:1 sweat: sebum**	**100% Sebum**
α-HBCD	2.3 ± 0.2	2.4 ± 0.2	12.0 ± 6.0	20.0 ± 2.8	36.1 ± 2.7	40.9 ± 2.9	50.5 ± 7.0
β-HBCD	1.6 ± 0.6	3.6 ± 0.7	10.1 ± 1.3	14.5 ± 5.7	29.7 ± 0.6	46.9 ± 3.4	60.4 ± 10.1
γ-HBCD	1.4 ± 0.1	4.1 ± 1.8	11.4 ± 2.2	19.0 ± 5.4	23.2 ± 6.5	49.6 ± 5.8	67.2 ± 3.37
Σ-HBCD	1.8 ± 0.2	3.3 ± 0.89	11.47± 4.1	18.7 ± 4.0	30.0 ± 4.2	45.2 ± 4.1	58.5 ± 5.7
TBBPA	3.5 ± 0.5	4.8 ± 1.9	9.6 ± 4.2	25.2 ± 7.1	32.4 ± 5.4	39.5 ± 4.3	55.7 ± 8.5
TCEP	16.0 ± 1.22	15.8 ± 0.8	14.8 ± 0.9	12.2 ± 1.0	11.2 ± 1.4	10.4 ± 1.8	22.3 ± 2.3
TCIPP	12.4 ± 4.4	15.4 ± 2.8	20.6 ± 3.2	8.4 ± 2.2	11.9 ± 1.9	17.4 ± 2.7	26.9 ± 6.4
TDCIPP	11.9 ± 3.6	12.0 ± 0.5	13.0 ± 0.4	10.5 ± 0.4	12.4 ± 0.3	18.6 ± 0.8	28.1 ± 0.6

Interestingly, the presence of cosmetics seems to decrease the bioaccessibility of HBCDs from indoor dust (Figure 3.3). This is in agreement with the reported slight decrease in dermal bioaccessibility of PCBs from house dust in the presence of skin cream (Ertl and Butte 2012b), which was attributed to possible retention of the lipophilic chemicals by skin cream lipids. Our results also show that while shower gel and sunscreen lotion enhanced the bioaccessibility of target PFRs, body spray significantly decreased the $f_{\text{bioaccesssible}}$ value of TDCIPP from indoor dust (Figure 3.3). To summarise, our results agree with previous reports that cosmetics contain various ingredients that can alter the composition of the SSFL and affect the availability of dust-bound FRs for dermal uptake. However, it is also evident that the nature and magnitude of this effect is substance-specific and highly dependent on the composition of the cosmetic preparation. The effect of surfactants - that are common ingredients of most cosmetics - on the dermal absorption of various chemicals has been previously highlighted (Pont et al. 2004, Walters et al. 1997). In addition, we hypothesize that the lipid content, ionic strength and skin contact period of these cosmetics can also influence the bioaccessibility of FRs from indoor dust. Detailed studies are required to test this hypothesis and fully investigate the factors affecting the bioaccessibility of FRs and ultimately their dermal uptake in the presence of various cosmetic preparations.

Figure 3.3: Effect of applied cosmetics on the bioaccessibility ($f_{bioaccessible}$ %) of target FRs from indoor dust.

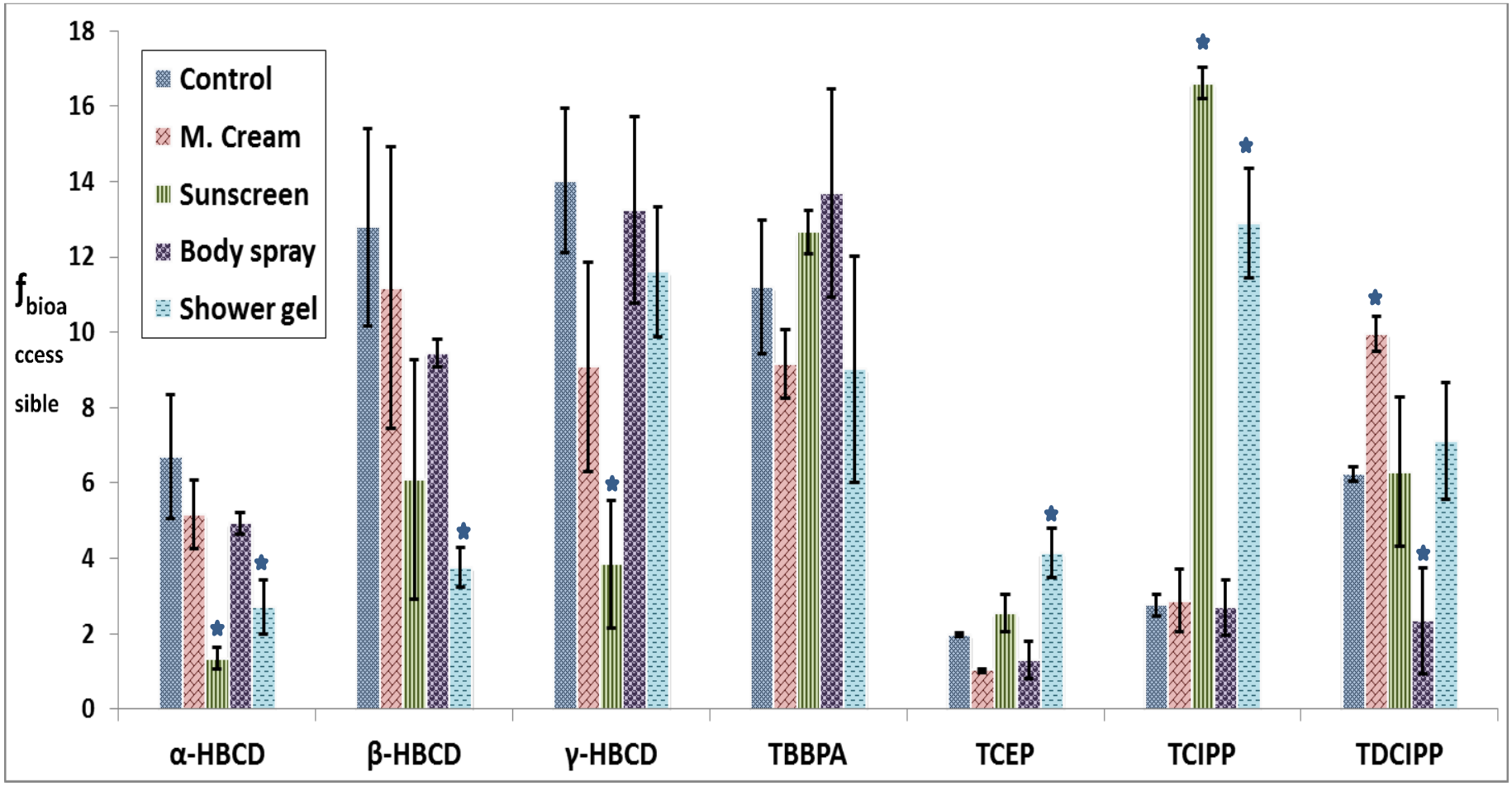

***** Denotes a statistically significant difference ($P < 0.05$) from the control group.

3.6.3: Dermal bioaccessibility of PBDEs

In general, $f_{bioaccesssible}$ of PBDEs increased with increasing sebum content of the SSFL (Table 3.5). At 100% sweat, the $f_{bioaccesssible}$ of BDE-209 (0.04 ± 0.01%) was found to be lowest which could be due to its low water solubility (<0.0001 mg/L) as compared to other congeners. (Table 3.5).However, the reverse trend was observed at 100% sebum, where the $f_{bioaccesssible}$ was highest for BDE-209 (98.5 ± 7.78%), followed by BDE-28 (98.2 ± 7.08%) and BDE-47 (87.18 ± 3.13%). At the most abundant physiologically relevant proportion i.e. 1:1 sweat sebum mixture, $f_{bioaccesssible}$ was highest for BDE-209 (79.37 ± 7.66%). The results show no negative correlation between the degree of congener bromination and the $f_{bioaccesssible.}$ This could be due to the equal proportion of aqueous and lipid content of the SSFL. Compared to the aqueous-based sweat, the substantially higher bioaccessibility of the studied BFRs in sebum can be attributed to the enhanced solubility of these lipophilic chemicals in the oily sebum.

3.6.4: Effect of cosmetics on the dermal bioaccessibility of PBDEs in indoor dust

The dermal bioaccessibility of PBDEs in presence of cosmetics, when compared to a control group comprising reference dust exposed only to 1:1 sweat: sebum mixture without any surfactant or cosmetics indicated that the presence of cosmetics seems to decrease the bioaccessibility of PBDEs from indoor dust (Table 3.6) which could be attributed to possible retention of the lipophilic chemicals by skin cream products like moisturising cream, sun screen lotion and shower gel. Interestingly there was no significant decrease in the bioaccessibility of PBDEs in presence of body spray which could be due to the gaseous form of the formulation.

Table 3.4: Physicochemical properties of PBDEs relevant to dermal exposure

	Mol. wt.	Water Solubility (mg/L)	Log K_{ow}
BDE-28	406.8	0.07	5.94
BDE-47	485.8	0.002	6.81
BDE-99	564.7	0.0024	7.32
BDE-153	643.6	0.0009	7.9
BDE-183	722.5	0.0015	8.27
BDE-209	959.2	<0.0001	10.3

Table 3.6: Effect of applied cosmetics on the bioaccessibility ($f_{bioaccessible}$ %) of target FRs from indoor dust.

PBDEs	Control	Dust/SSSM (1:1)/ Moisturising Cream	Dust/SSSM(1:1)/ Body Spray	Dust/SSSM(1:1)/ Sun screen Lotion	Dust/SSSM(1:1)/ Shower Gel
BDE-28	73.5 ± 8.9	65.0 ± 13.0	72.0 ± 8.5	68.0 ± 15.0	72.0 ± 11.2
BDE-47	72 ± 11.9	63.5 ± 8.0	71.0 ± 6.0	59.0 ± 16.3	70.0 ± 20.0
BDE-99	63.16 ± 11.28	58.0 ± 5.0	61.0 ± 6.2	55.0 ± 2.8	56.0 ± 13.2
BDE-100	71.9 ± 8.9	66.0 ± 8.5	70.0 ± 2.8	63.5 ± 19.3	60.0 ± 2.2
BDE-153	67.98 ± 10.8	64.0 ± 2.3	62.5 ± 2.6	59.5 ± 18.2	61.0 ± 11.8
BDE-183	50.8 ± 10.11	45.0 ± 11.0	50.0 ± 3.8	47.0 ± 12.0	43.0 ± 15.0
BDE-209	79.37 ± 7.66	70.0 ± 17.0	77.0 ± 18.0	68.0 ± 13.7	66.0 ± 10.0

Table 3.5: Effect of the composition of synthetic sweat and sebum mixture (SSSM) on the bioaccessibility ($f_{bioaccessible}$) of target FRs from indoor dust.

	$f_{bioaccessible}$ (%) for different SSSM compositions						
Compound	**100% Sweat**	**99:1 sweat: sebum**	**95:5 sweat: sebum**	**9:1 sweat: sebum**	**8:2 sweat: sebum**	**1:1 sweat: sebum**	**100% Sebum**
BDE-28	**3.1 ± 1.6**	**13.0 ± 3.4**	**33.5 ± 9.85**	**46.2 ± 19.72**	**58.9 ± 4.19**	**73.5 ± 8.9**	**98.2 ± 7.08**
BDE-47	**3.25 ± 0.04**	**3.97 ± 0.5**	**58.73 ± 11.8**	**63.59 ± 7.3**	**88.26 ± 19.35**	**72 ± 11.9**	**87.18 ± 3.13**
BDE-99	**4.44 ± 2.09**	**4.04 ± 1.07**	**26.15 ± 11.54**	**49.69 ± 6.96**	**60.51 ± 13.76**	**63.16 ± 11.28**	**69.61 ± 6.06**
BDE-100	**6.1 ± 1.6**	**13.4 ± 9.35**	**42.94 ± 7.11**	**58.36 ± 5.13**	**66.3 ± 3.18**	**71.9 ± 8.9**	**75.39 ± 10.58**
BDE-153	**1.5 ± 0.92**	**4.4 ± 0.92**	**36.75 ± 3.26**	**48.6 ± 23.24**	**64.64 ± 18.48**	**67.98 ± 10.8**	**74.75 ± 16.11**
BDE-183	**0.89 ± 0.17**	**2.79 ± 1.84**	**4.04 ± 1.21**	**12.42 ± 5.24**	**17.54 ± 7.8**	**50.8 ± 10.11**	**79.37 ± 7.66**
BDE-209	**0.04 ± 0.01**	**0.17± 0.07**	**0.19 ± 0.17**	**1.7 ± 0.15**	**4.84 ± 3.39**	**79.37 ± 7.66**	**98.5 ± 7.78**

3.7: Comparison of digestive and dermal bioaccessibility

Despite the vast differences between the digestive and dermal body fluids in terms of both composition and function, it is instructive to compare our results to previously reported bioaccessibilities of target FRs via the oral route. This can shed some light on the relative importance of dermal uptake versus ingestion as pathways of human exposure to FRs in indoor dust. Abdallah et al. (Abdallah et al. 2012) reported on the gut bioaccessibility of HBCDs and TBBPA from indoor dust using a colon enhanced-physiologically based extraction test (CE-PBET). On average, $f_{bioaccessible}$ values of 92%, 80%, 72% and 94% were reported for α-, β-, γ-HBCDs and TBBPA, respectively. These are almost twice the dermal $f_{bioaccesssible}$ values for the same BFRs in our study (Table 3.3)

The gut bioaccessibility of PFRs following ingestion of indoor dust was also studied using a modified version of the CE-PBET mentioned above (Fang and Stapleton 2014). Mean $f_{bioaccessible}$ values for TCEP, TCIPP and TDCIPP from 17 house dust samples were 80%, 82% and 85%, respectively, which are substantially higher than the corresponding dermal $f_{bioaccessible}$ values for the same PFRs (Table 3.3).

The substantially higher gut bioaccessibility of FRs may be attributed to several factors. These include the strong acidic medium in the stomach (pH = 1), the bile salts and digestive enzymes in the small intestine, the presence of carbohydrates to simulate the fed status, coupled with the long contaminant residence time in the models used (~13 - 21.5 hours) (Abdallah et al. 2012, Fang and Stapleton 2014) compared to the 1 h dermal exposure period used in this study. More research is required to fully understand the influence of prolonged dermal exposure times on the bioaccessibility of FRs from indoor dust and examine the kinetics of the release of various FRs from indoor dust to the sweat/sebum mixture. (Abou-Elwafa Abdallah et al. 2012) reported the % of bioaccessibility to be 58 ± 3.7,41 ± 3.4, 53 ± 2.2, 48 ± 2.3, 32 ± 2.5, 44 ± 2.9, 14.0 ± 1.3 for BDE-47, BDE-99, BDE-100, BDE-153, BDE-

154, BDE-183 and BDE-209 respectively using a colon enhanced-physiologically based extraction test (CE-PBET). Another study by Fang et al (Fang and Stapleton 2014) carried out the bioaccessibility assessment for organophosphate flame retardants and PBDEs from dust however their study lacked a colon compartment in their model but they used tenax as a sink which resulted in an increase in the bioaccessible fraction.

These value ranged from ~ 60% for low molecular weight congeners to ~ 25% for BDE-209 Interestingly these values are lower than that of our dermal bioaccessibility results at 1:1 seat/sebum mixture. The substantially higher dermal bioaccessibility of PBDEs may be attributed to several factors. These include the presence of both the aqueous and lipid phase of sweat/sebum formulation, in addition to the electrolytes and salts that might have contributed to enhanced dissolution and partitioning of all the PBDE congeners from dust to the simulated biological fluid. More research is required to fully understand the influence of prolonged dermal exposure times on the bioaccessibility of FRs from indoor dust and examine the kinetics of the release of various FRs from indoor dust to the sweat/sebum mixture.

3.8: Assessment of human dermal exposure to FRs in indoor dust

The results of dermal bioaccessibility experiments obtained in this study (Table 3.3 & Table 3.4) were used to gain some insight on the internal dose of the target FRs arising from dermal exposure to contaminated indoor dust. Results revealed $f_{\text{bioaccesssible}}$ values for the studied FRs in indoor dust were significantly influenced by the presence of various cosmetic preparations. However, incorporation of our data into risk assessment models is hampered by the current lack of reliable information on the exact amount of cosmetics remaining on the skin after application and on the skin residence time of such formulations. Therefore, exposure assessment estimations were performed without such data.

Human dermal exposure to our target FRs was estimated using the general equation:

$$DED = \frac{C \times BSA \times DAS \times F_A \times IEF}{BW \times 1000} \quad \text{..... (3.2)}$$

Where DED = Daily exposure dose (ng/kg bw/day), C = FR concentration in dust (ng/g), BSA = Body surface area exposed (cm^2), DAS = Dust adhered to skin (mg/cm^2), F_A = fraction absorbed by the skin (unitless), IEF = indoor exposure fraction (hours spent over a day in an indoor environment) (unitless), BW = Body weight (kg).

We estimated the dermal exposure of 2 age groups (adults and toddlers) using three exposure scenarios. We used data previously reported by our research group on the minimum, median and maximum concentrations (Table 3.8 & 3.9) of target FRs in indoor dust from several UK microenvironments (Brommer 2014, Abdallah et al. 2008b) & (Tao, Abdallah et al. 2016**)** to estimate low, average and high exposure, respectively.

The parameter F_A in equation 3.2 was replaced by the experimental values of $f_{\text{bioaccesssible}}$ obtained in this study for each target FR at the most physiologically abundant sweat: sebum

Table 3.7: Parameters used in dermal exposure assessment of target FRs in indoor dust (USEPA 2011).

Parameter	Adult	Toddler
Age	>18 years	2-3 years
Body weight	70 Kg	15 Kg
Body surface area	1.94 m^2	0.6 m^2
Skin surface exposed	4615 cm^2 (head, forearms, hands and feet)	2564 cm^2 (head, extremities including hands and feet)
Dust adhered to skin	0.01 mg/cm^2	0.04 mg/cm^2
Indoor exposure fraction (Abdallah et al. 2008b)		
House	63.8%	86.1%
Office	22.3%	-
Car	4.1%	4.1%

mixture (1:1) (Table 3.5). Values for other parameters in equation 2 were obtained from the USEPA exposure factors handbook (USEPA 2011) and summarized in table 3.6

Our dermal exposure estimates (Table 3.10 & 3.11) highlight the potential importance of the dermal route as a pathway of human exposure to FRs in indoor dust. The average scenario estimate of dermal exposure of UK adults and toddlers to the target BFRs ranged from (99-110%) and (44-59%) respectively, of their estimated exposure via dust ingestion (Abdallah et al. 2008b) (Figure 3). For PFRs, the estimated average dermal exposure corresponded to (26-42%) and (28-45%) of previously reported exposure via dust ingestion (Brommer 2014).

However, it should be noted that our dermal exposure estimates assume a fixed body area undergoing constant exposure to FRs in indoor dust for a constant period daily at a fixed absorbed fraction derived from 1 h dermal contact time with indoor dust. Such rigid assumptions are likely unrealistic and introduce uncertainty to our estimates of dermal exposure. A further significant caveat is that our estimates account only for bioaccessibility – i.e. the efficiency of release of FRs from dust into sweat/sebum. While this is important, reliable data are not yet available on the subsequent dermal transfer of the studied FRs from sweat/sebum across the epidermis to the systemic circulation. Such transfer will very likely be <100%, and thus the true influence of dermal exposure to dust will likely be appreciably lower than the values shown in Table 3.10. While noting this caveat, we also note that our estimates of exposure via dust ingestion assume 100 % efficiency of transfer from dust into gut fluids and thence across the gastro-intestinal tract.

In a risk assessment context, an extensive survey of the available literature revealed a No Significant Risk Level (NSRL) of 5.4 µg/day for TDCIPP listed as a carcinogen under the State of California safe drinking water and toxic enforcement act of 1986, PROPOSITION 65 (OEHHA 2015). No other health based limit values (HBLVs) of legislative standing for our target FRs were found in the literature. However, based on a chronic no observed adverse

effect level (NOAEL) divided by an uncertainty factor of 1,000, HBLVs of 22,000 and 80,000 ng/kg bw/day were derived for TCEP and TCIPP respectively (Ali et al. 2012a). Our worst-case scenario exposure estimates for dermal exposure of adults and toddlers fall far below these HBLV values even under our high-end dermal exposure scenario. However, as noted by Ali et al. (Ali et al. 2012a), the HBLV values cited here were based on relatively old toxicological studies and it is possible that future research may erode the margin of safety.

Table 3.11 summarises the exposure estimates of UK adults and toddlers to the studied PBDEs via dermal exposure via indoor dust. It is instructive to compare our estimated exposure values with currently available health-based limit values (HBLVs) for PBDEs. US EPA recommended HBLV values for BDE-47 and BDE-99 as 0.1 μg/kg/d (IRIS 2008a, b). Our results for BDE-47 and BDE-99 were found to be below HBLV of 0.1 μg/kg/d. The reference dose (RfD) of daily oral exposure to BDE-209 of 7 μg/kg bw/day is considered to be without appreciable risk of deleterious effects (U.S. EPA, 2008). This comparison revealed the estimated exposures for BDE-209 via dermal exposure pathways fell below the HBLV values. It is obvious that the human skin poses an extra barrier to these hazardous chemicals, however the dermal pathway should definitely be considered, along with other routes, when assessing the overall human exposure to FRs and the potential risk arising from it. In conclusion, notwithstanding the various caveats noted above, the results of this *in vitro* bioaccessibility study provide some important first insights into human dermal exposure to various FRs present in indoor dust. The composition (i.e. sweat: sebum ratio) of skin fluids, as well as the presence/absence of commonly used skin cosmetics is demonstrated to exert a insignificant influence on the efficiency with which our target FRs are released from dust and rendered available for dermal uptake.

Table 3.8: Concentrations of target FRs (ng/g dry weight) in UK indoor dust from different microenvironments (Brommer 2014, Abdallah et al. 2008b).

	Homes*			Offices[$]			Cars[#]		
FR	**Min**	**Median**	**Max**	**Min**	**Median**	**Max**	**Min**	**Median**	**Max**
α-HBCD	22	380	6600	15	220	2900	54	2000	8800
β-HBCD	9	93	2600	11	84	1300	16	740	5200
γ-HBCD	70	670	7500	36	470	3700	27	9600	56000
TBBPA	0.03	62	382	0.03	36	140	0.03	2	25
TCEP	<60	810	28000	<60	870	160000	<60	1230	8700
TCIPP	3700	21000	100000	3600	33000	230000	2400	53000	370000
TDCIPP	60	710	14000	<30	480	51000	110	31000	740000

* n = 35 for BFRs and 32 for PFRs. [$] n = 28 for BFRs and 19 for PFRs. [#] n = 20 for BFRs and 21 for PFRs.

Table 3.9: Concentrations of target PBDEs (ng/g dry weight) in UK indoor dust (Tao, Abdallah and Harrad 2016a)

	Offices (n = 47)		
PBDEs	**Min**	**Median**	**Max**
BDE-28	<0.03	2.6	22.0
BDE-47	7.1	37.0	660
BDE-99	15.0	77.0	480
BDE-100	1.9	12.0	120
BDE-153	0.025	9.2	190
BDE-183	0.065	9.8	220
BDE-209	200	2700	110000

Table 3.10: Assessment of human dermal exposure (ng/kg bw/day) to FRs present in indoor dust upon contact with a skin surface film composed of 1:1 sweat: sebum

FR/ Scenario	UK Adult			UK Toddler		
	Low	Average	High	Low	Average	High
α-HBCD	0.1	1.0	14.1	0.1	1.1	16.9
β-HBCD	<0.1	0.3	6.7	<0.1	0.4	7.9
γ-HBCD	0.2	3.0	25.8	0.2	3.3	29.7
TBBPA	<0.1	0.1	0.7	<0.1	0.1	0.9
TCEP	<0.1	0.1	3.7	<0.1	0.5	17.4
TCIPP	0.3	0.5	6.4	3.9	4.7	46.8
TDCIPP	<0.1	0.1	2.2	<0.1	0.9	19.2

Table 3.11: Assessment of human dermal exposure (ng/kg bw/day) to PBDEs present in indoor dust upon contact with a skin surface film composed of 1:1 sweat: sebum

FR/ Scenario	UK Adult			UK Toddler		
	Low	Average	High	Low	Average	High
BDE-28	0.000009	0.0008	0.0069	0.0001	0.0113	0.0957
BDE-47	0.0022	00.0112	0.2005	0.0301	0.1566	2.7942
BDE-99	0.0040	0.0205	0.1276	0.0556	0.2852	1.7781
BDE-100	0.0006	0.0036	0.0365	0.0080	0.0508	0.5080
BDE-153	0.000007	0.0026	0.0593	0.0001	0.0368	0.7597
BDE-183	0.000014	0.021	0.0687	0.0002	0.0294	0.6597
BDE-209	0.0667	0.9000	37.0	0.9291	12.5423	510.98

Fig 3.4: Comparison for (a) UK adults and (b) toddlers of exposure (ng/kg bw. day) to FRs in indoor dust via dermal contact (this study, average exposure scenario) and dust ingestion (Abdallah et al. 2008b, Brommer 2014)

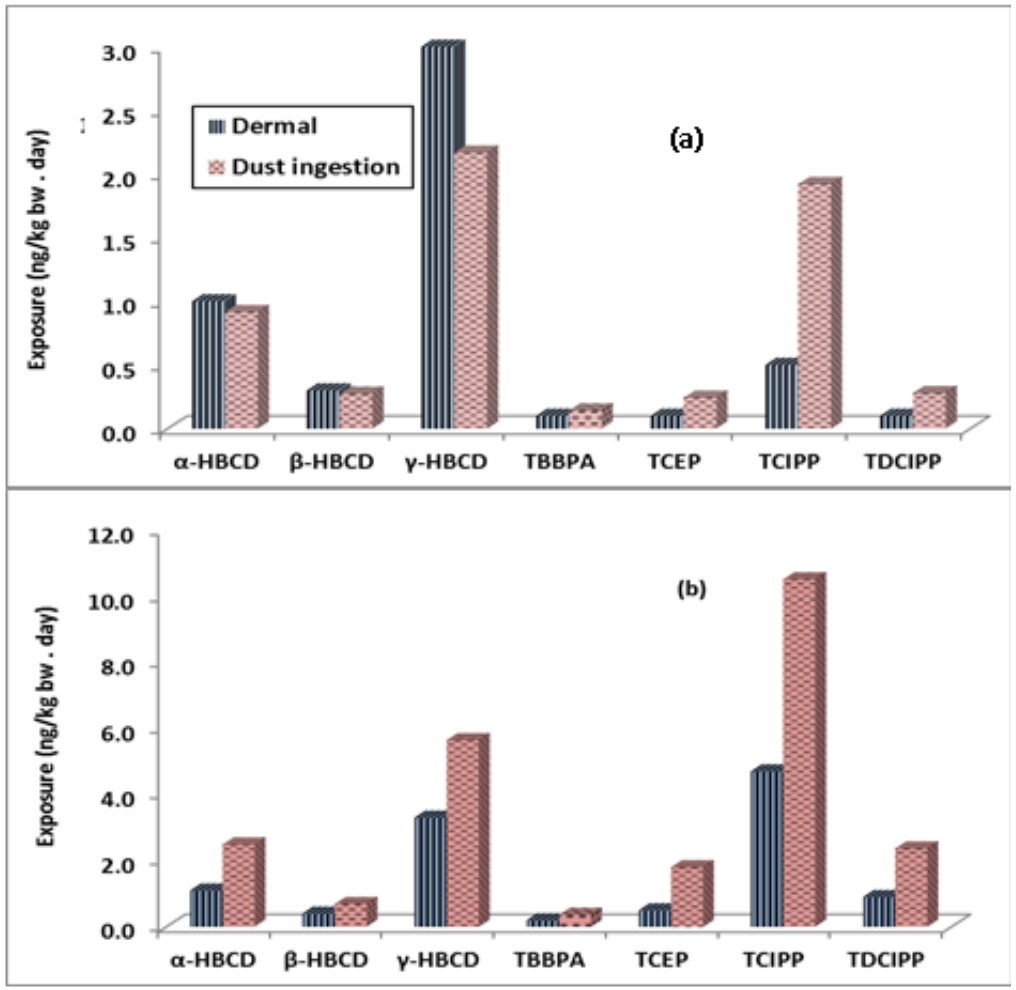

CHAPTER IV

Studies of dermal uptake of FRs applied as neat compounds to *in vitro* models

Introduction

This chapter reports the results of a series of experiments designed to study the dermal fate of a number of halogenated and phosphorus flame retardant chemicals applied as neat compounds (pure form of a chemical in a solvent) to *in vitro* 3D-HSE models. Results obtained using 2 commercially available 3D-HSE models were compared with each other and with those obtained from parallel experiments conducted using a commercially available *ex vivo* human skin model.

4.1: NEAT COMPOUND APPLICATION TO 3D-HSE MODELS

4.1.1: MATTEK'S EpiDerm™

The EpiDerm™ EPI-212X-3D kit was obtained from MatTek Corporation (Ashland, MA). EpiDerm™ EPI-212 tissue constructs are 0.26 cm^2 human skin equivalents resembling the normal human epidermis (www.mattek.com). The kit includes maintenance medium (MM) which is a proprietary DMEM-based medium that allows acceptable differentiated morphology of the EpiDerm™ EPI-212-X tissue for at least five days upon receipt (Figure 4.1). **Fig 4.1: Microscopic view of MatTek EpiDermis™**

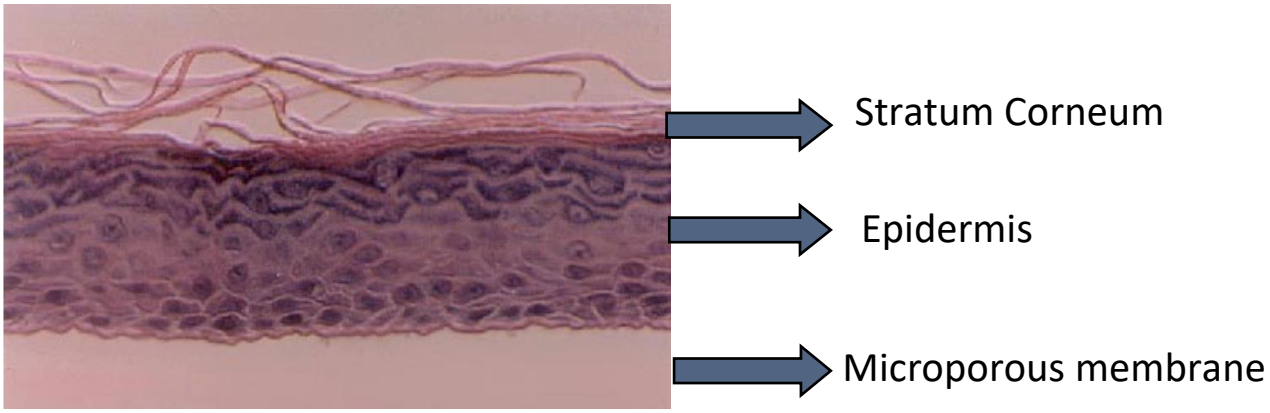

4.1.1.A: Storage & Equilibration: Upon receipt at Birmingham, sterile forceps were used to remove the tissues from the package, adhered agarose to the outside of the cell culture insert (if any) was removed by either sterile forceps or directly wiped on the sterile gauze supplied with the kit. The 12 skin patches with the inserts were cultured overnight in 12-costar well plates containing 1 mL of MM media at 5 ± 1% CO_2 and 37±1 °C before use in exposure experiments (Figure 4.2).

Fig 4.2: EpiDerm™ EPI-212X-3D kit

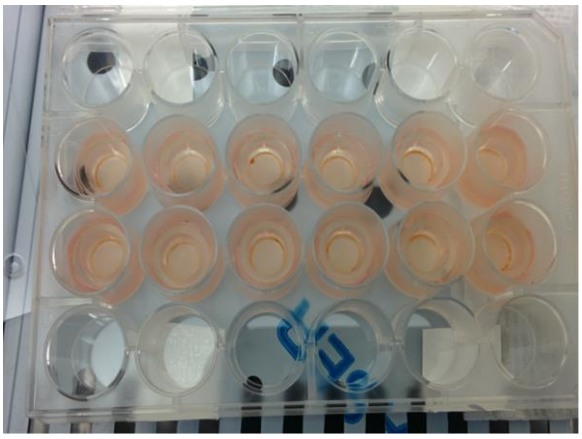

4.1.1.B: Preparation of Epiderm for Percutaneous Absorption measurement:

A MatTek Permeation device (MPD, part no. EPI-100-FIX, Figure 4.3) was used to mount the tissues directly with the inserts. The cell culture inserts which contain the Epiderm tissue with underlying microporous membrane were inserted between the 2 pieces of the device and the 4 screws/nuts tightened to create a seal between the bottom rim of the device's inner annulus and stratum corneum. The MPD was reused after washing and sterilization by soaking in 70% ethanol for 30 minutes.

Fig 4.3: Mattek Permeation Device

4.1.1.C: Experimental setup

The donor solution volume for MPD device for mounting the EPI-212-X is 0.4 mL. Sufficient donor volume (typically 100µL) of dosing vehicle was used so that the donor concentration would not drop more than 5% throughout the course of the permeation experiment. Five mL of a DMEM-based culture medium was used as a receptor solution in a 6 well plate (Figure 4.4). To comply with the OECD guidelines, 5% bovine serum albumin (BSA) was added to the receptor fluid (Table 4.1) to enhance the solubility of target analytes, while the levels of test compounds in the donor solution were chosen to ensure that the concentrations in the receptor fluid during the experiment did not exceed 10% of the saturation solubility.

Fig 4.4: Permeability Configuration using MatTek Permeation Device (MPD) illustrating exposure of donor solution to the surface of EpiDerm tissue and receptor compartment containing DMEM culture medium.

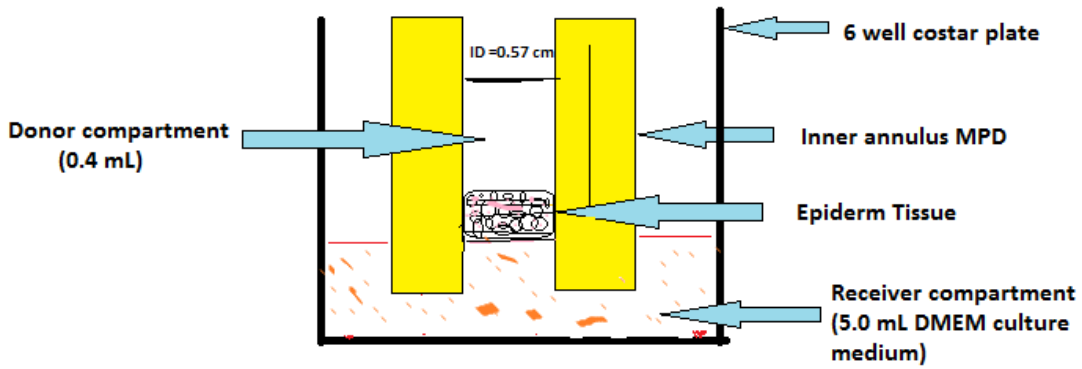

4.1.1. D: Equilibration and dosing of neat compound

Before dosing, the permeation device containing the tissue was equilibrated to the desired physiological temperature of 37°C in the incubator. According to OECD guidelines (OECD, 2004), the target compounds given in table below 4.1 were prepared in acetone and applied to each of the investigated skin tissues using an appropriate volume (100 µL) of dosing solution. The applied doses fall within the range of potential human exposure to the studied BFRs via contact with indoor dust (Abdallah et al. 2008a). Acetone was selected as the dosing vehicle on the basis of its ability to dissolve the test compounds at the desired levels and its minimal effect on skin barrier functions (Abrams et al. 1993). A previous study of the effect of organic solvents on the trans-epidermal water loss (TEWL) as an indicator of skin barrier revealed no significant differences in the behaviour of acetone and hexane compared to that of water, while a mixture of chloroform and methanol [2:1 (v/v)] caused the most significant increase in TEWL (Abrams et al. 1993). All experiments were performed in triplicate.

Table 4.1: Components of the modified DMEM (D0422, Sigma-Aldrich, UK) medium used as maintenance/receptor fluid for the investigated tissues.

Component	D0422
Inorganic Salts	g/L
Calcium Chloride	0.2
Cupric Sulfate • $5H_2O$	0.0000001
Ferric Nitrate • $9H_2O$	0.0000001
Magnesium Chloride • $4H_2O$	0.0000001
Magnesium Sulfate (anhydrous)	0.0977
Potassium Chloride	0.4
Sodium Bicarbonate	2.2
Sodium Chloride	6.8
Sodium Phosphate Monobasic (anhydrous)	0.122
Zinc Sulfate • $7H_2O$	0.0000002
Amino Acids	
L-Alanine	0.09
L-Arginine (free base)	0.05
L-Asparagine • H_2O	0.02
L-Aspartic Acid	0.03
L-Cysteine (free acid)	0.04
L-Cystine	0.02
L-Glutamic Acid	0.0445
L-Glutamine	—
Glycine	0.05
L-Histidine (free base)	0.015
L-Isoleucine	0.05
L-Leucine	0.075
L-Lysine • HCl	0.08746
L-Methionine	0.015
L-Phenylalanine	0.025
L-Proline	0.03
L-Serine	0.01
L-Threonine	0.04
L-Tryptophan	0.01
L-Tyrosine • 2Na • $2H_2O$	0.05045
L-Valine	0.05
Vitamins	
Ascorbic Acid • Na	0.00227
D-Biotin	0.0005
Calciferol	0.0001
Choline Chloride	0.0015
Folic Acid	0.001

Myo-Inositol	0.002
Menadione (sodium bisulfite)	0.00001
Niacinamide	0.001
D-Pantothenic Acid (hemicalcium)	0.001
Pyridoxal • HCl	0.001
Retinol Acetate	0.0001
Riboflavin	0.0001
Thiamine • HCl	0.001
DL-α-Tocopherol Phosphate • Na	0.00001
Vitamin B12	0.0002
Other	
D-Glucose	2
Glutathione (reduced)	0.00005
Methyl Linoleate	0.00003
Phenol Red • Na	0.0107
Pyruvic Acid • Na	0.025
bovine serum albumin (BSA)	5% v/v
Penicillin and streptomycin	100 U penicillin and 100 µg streptomycin/Ml

Fig 4.5: Figure displaying the *In vitro* permeability set-up.

(6-well plate containing the receptor fluid and the epidermis)

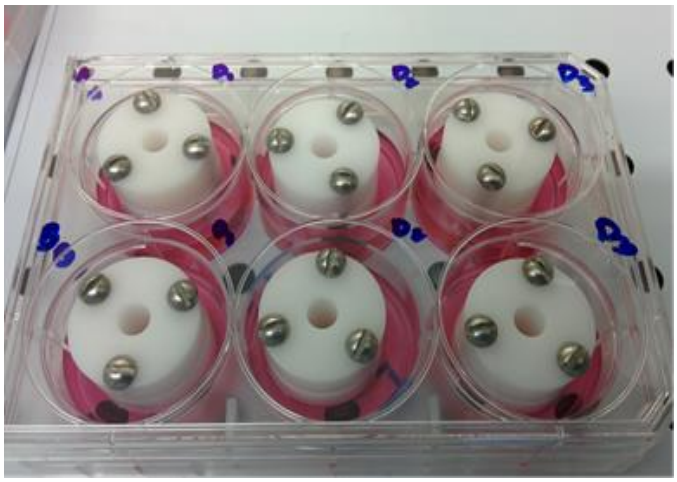

Fig 4.6: Incubation – 37 °C at 5% CO_2 and 98% relative humidity for 24 hr.

4.1.1 E: Sampling

At fixed time points (0.25, 0.5, 0.75, 1, 2, 4, 6, 10, 12, 18, 20, 24, and 30 hrs) depending on the compound studied, aliquots of receptor fluid (2.5 mL) were collected from the receptor compartment and immediately replaced with 2.5 mL fresh fluid. After 30 h, the entire receptor fluid was collected and the skin surface washed thoroughly with cotton buds impregnated in (1:1) hexane: ethyl acetate (5 times). The tissues were removed from the permeation devices and both the donor and receptor compartments were washed separately (5 × 2 mL) with PBS. All samples were stored at −20 °C until chemical analysis.

Fig 4.7: Donor Compartment with the skin insert.

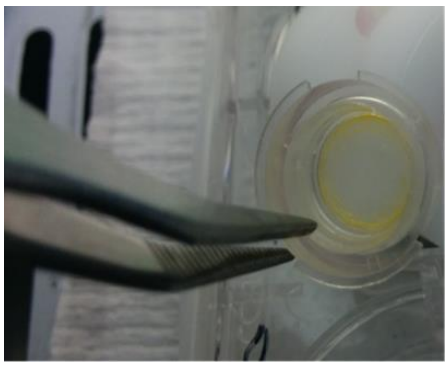

Fig 4.8: Skin wash with cotton bud.

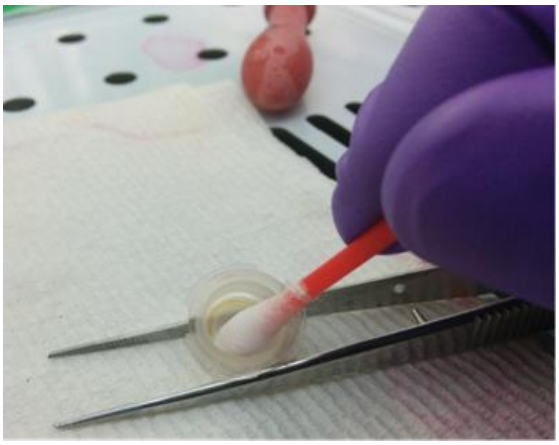

4.1.1 F: Sample Extraction and Clean-up

Each permeation assay generated five different types of samples comprising: receptor fluid, skin tissue, cotton buds (used to thoroughly wipe the skin surface), donor and receptor compartment washes. The receptor fluid, skin tissue and cotton buds samples were extracted according to a previously reported QuEChERs method (Abdallah et al., 2015). Briefly, each sample was spiked with 30 ng of isotopically labelled internal (surrogate) standards. Extraction was performed using 2 mL of (1:1) hexane: ethyl acetate mixture and vortexing for 2 minutes, followed by ultrasonication for 5 minutes and centrifugation at 4,000 g for 3 minutes. This extraction cycle was repeated twice before the combined organic extracts were evaporated under a gentle stream of N_2 and reconstituted into 100 µL of recovery (syringe) standard for QA/QC purposes. The donor and receptor compartment washes were spiked with 30 ng of the ^{13}C-labelled internal standard mixture prior to direct evaporation under a gentle stream of N_2. Target analytes were reconstituted into 100 µL of methanol containing recovery (syringe) standard for QA/QC purposes.

4.1.1.G: Modelling of percutaneous penetration using Epiderm® human skin equivalent

For infinite-dose condition, the cumulative amount of chemical penetrating the skin, Q, as a function of time, may be modelled using the appropriate version of Fick's second law; where Kp is the chemical's permeability coefficient, t_{lag} its lag time and *Cv*° its concentration in the

$$Q(t) = Cv°Kp[t - tlag - {}^{12tlag}/_{\pi^2} \sum_{n=1}^{\infty} \frac{(-1)^n}{n^2} exp\,[-\frac{n^2\pi^2 t}{6tlag}]$$

Solution. At steady state, the exponential term is negligible

$$Qss(t) = Cv°Kp(t - tlag)$$

Thus the cumulative amount of chemical at steady state (Qss) is a linear function of time. The derivative as a function of time, defines the maximum flux, which is constant at steady state

$$\frac{dQss\,(t)}{dt} = Jss = Cv°Kp$$

J_{ss} is the flux (ng/cm^2/hr) for the chemical and determined by plotting the cumulative absorption versus the time profile. The slope of the regression line represents the flux. Steady-state conditions were indicated by a linear regression line [$R^2 \geq 0.9$; $P \leq 0.05$.]

When using infinite-dose configurations, i.e., in which the donor concentration far exceeds the concentration in the receptor compartment ($C_D >> Cv°$), *Cv*° can be replaced by C_D

Permeation data was summarised by determining the lag time, steady state flux, and cumulative amount after 24 hr (Q24). Results are presented as the arithmetic mean of three replicates ± the standard deviation (SD). Statistical analysis was performed using SPSS 13.0. Differences in skin permeation were evaluated by the paired Student's t test between two data sets. A Games−Howell test was used for analysis of variance (ANOVA) among several data sets with equal variances not assumed; $p < 0.05$ was regarded as indicating a statistically significant difference.

Fig 4.9: Flowchart of the algorithm applied for identification of the steady state range as described by Niedorf et al. (Niedorf, Schmidt and Kietzmann 2008b)

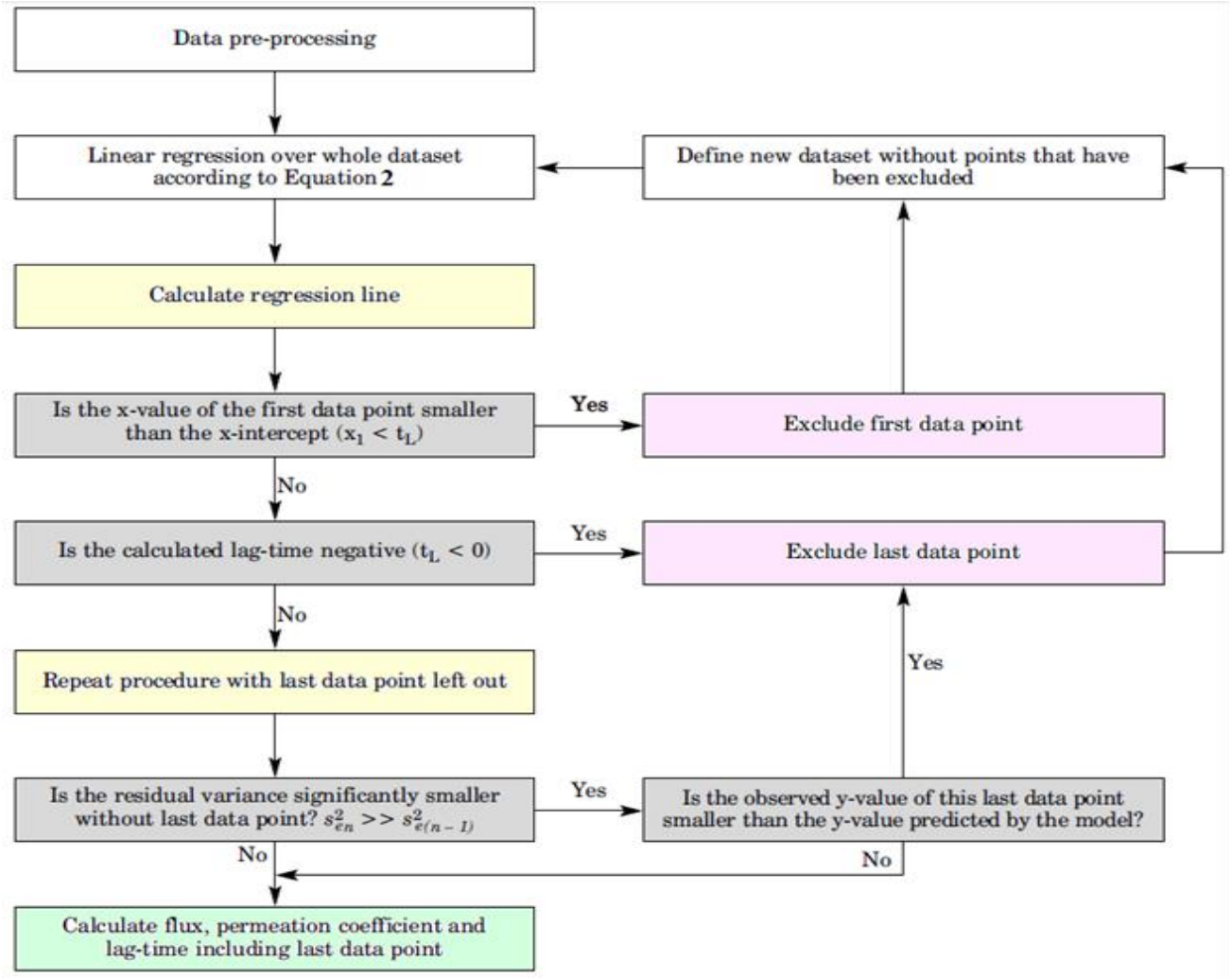

4.2: NEAT COMPOUND APPLICATION USING 3D-HSE EPISKINTM MODEL

Reconstructed skin models Episkin® 1.07 were provided by Skin Ethics (Lyon, France). Episkin is an *in vitro* reconstructed human epidermis from normal human keratinocytes cultured on a collagen matrix at the air-liquid interface. This model is histologically similar to the *in vivo* human epidermis. The human keratinocytes are obtained from healthy consenting donors during plastic surgery. HIV 1 & 2, B and C hepatitis tests are carried out on the donor blood as well as verification of the bacteriological & fungal sterility of the cells and absence of mycoplasma. (www.episkin.com). Episkin are provided as a kit consisting of 12 plastic insert where the epidermis patch is grown on a collagen matrix and kept firm in its place with the help of outer "o" ring. This feature is an extra value added advantage in Episkin model where the skin are ready to use immediately by placing the insert with the skin in a costar well plate containing the receptor fluid.

Fig 4.10: Episkin set-up.

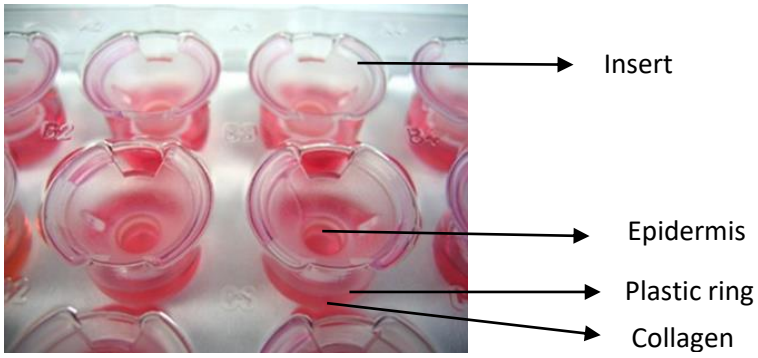

Fig 4.11 EPISKIN® PROTOCOL

12 reconstructed Epidermis placed in maintenance medium & incubated at 37°C with 5% CO_2 and 98% RH for 24 hrs

Dosing of neat compound in acetone

Collection of Receptor fluid every 4 hrs

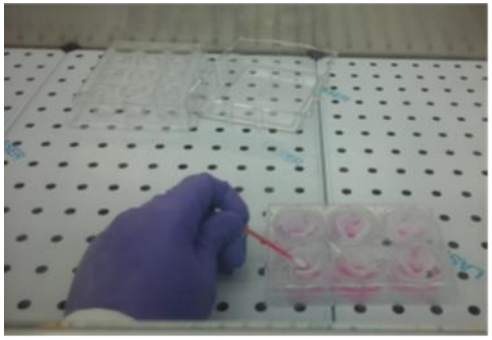

Cotton buds soaked in hexane: ethyl acetate (3:1) and the surface of the skin was swept for residual quantity and walls of the well for non specific binding

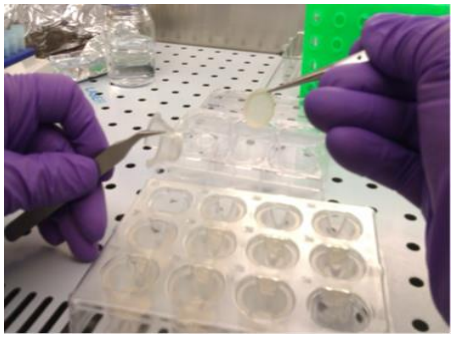

Skin Removed –Placed in hexane: ethyl acetate in clean test tubes

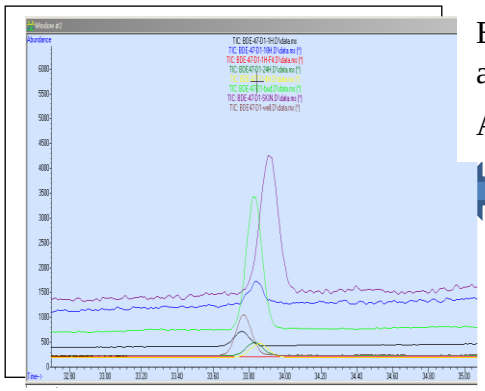

Extraction and Clean-up

Analysis

Table 4.2: Concentrations of target compounds applied on Episkin/Mattek Epidermis in acetone.

Target Analyte	M.Wt (g/mol) & Log K_{ow} (unitless)	3D-HSE SKIN MODEL	Mass per unit area (ng/cm^2) Study	Exposure Time (hr)
BDE-1	249.1 (4.28)	Episkin™	500,1000	24
BDE-8	----------	Episkin™	500,1000	24
BDE-28	327.9 (5.94)	Episkin™	500,1000	24
BDE-47	485.8 (6.81)	Episkin™	500,1000	24
BDE-99	564.7 (7.32)	Episkin™	500,1000	24
BDE-153	643.6 (7.9)	Episkin™	500,1000	24
BDE-183	722.5 (8.27)	Episkin™	500,1000	24
BDE-209	959.2 (10.3)	Episkin™	500,1000	24
α-HBCD	641.7 (5.07)	Episkin™ EpiDerm™ 212-X	500,1000	24
β-HBCD	641.7 (5.12)	Episkin™ EpiDerm™ 212-X	500,1000	24
γ-HBCD	641.7 (5.47)	Episkin™ EpiDerm™ 212-X	500,1000	24
TBBPA	543.9 (4.50)	Episkin™ EpiDerm™ 212-X	500,1000	24
TCEP	285.49 (1.44)	Episkin™ EpiDerm™ 212-X	250,500,1000	24
TCIPP	327.57 (2.59)	Episkin™ EpiDerm™ 212-X	250,500,1000	24
TDCIPP	430.91 (3.65)	Episkin™ EpiDerm™ 212-X	250,500,1000	24
TPhP	326.29 (4.59)	Episkin™ EpiDerm™ 212-X	250,500,1000	24

TBOEP	398.48 (3.75)	Episkin™	500,1000	24
TEHP	434.65 (9.49)	Episkin™	500,1000	24
ToCP	368 (5.1)	Episkin™	500,1000	24
TmCP	368 (5.1)	Episkin™	500,1000	24
TpCP	368 (5.1)	Episkin™	500,1000	24
PBEB	550.65 (6.76)	Episkin™	500,1000	24
α/ β -TBECH	399.74 (3.73)	Episkin™	500,1000	24
β-TBECH	399.74 (3.73)	Episkin™	500,1000	24
EHTBB	549.9 (7.73)	Episkin™ EpiDerm™ 212-X	500,1250,2500	30
BEHTEBP	706.2 (11.95)	Episkin™ EpiDerm™ 212-X	500,1250,2500	30
BTBPE	687.6 (9.10)	Episkin™ EpiDerm™ 212-X	500,1000	24
DBDPE	971.2 (11.1)	Episkin™	500,1250	24
***Syn*-DP**	653.72(9.0)	Episkin™	500,1000	24
***Anti*-DP**	653.72(9.0)	Episkin™	500,1000	24
HBB	551.49 (6.07)	Episkin™	500,1000	24
PBBz	472.59 (5.4)	Episkin™	500,1000	24
PBEB	500.64 (7.96)	Episkin™	500,1000	24
PBT	486.621 (5.87)	Episkin™	500,1000	24

Note : Pure standards for all FRs investigated in this study were purchased from Wellington labs

4.3: Evaluation of 3D HSE Models using human *ex vivo* skin mounted on Franz Diffusion cell

The measurement of dermal absorption of chemicals for consumer products intended for application to the skin or the xenobiotics is an important part of risk assessment. *In vitro* - Franz diffusion cells are applied to assess the skin permeability testing. (Bartosova and Bajgar 2012, Davies et al. 2015, Franz 1975). For the purpose of our skin permeation experiments, we procured custom-made Franz diffusion cells made of borosilicate glass components from the University of Birmingham professional glass-blower workshop. The cell comprises two compartments: the ***donor compartment***, which contains the sample to be tested and ***the receptor compartment*** containing the receptor fluid. The two compartments are separated by the mounted viable excised human skin, which acts as a conduit for diffusion. The effective diffusion area of the Franz cells was 0.2 cm^2, receptor volume was 5.0 mL with other dimensions shown in Figure 4.12. The receptor temperature was maintained at 37 °C to mimic the physiological temperature. Testing was conducted for 24 hr, during which the receptor fluid was collected via the sampling port and replaced with an equal volume of fresh receptor fluid at each time point. Fresh excised human upper breast skin was obtained via Caltag Medsystems Ltd. (Buckingham, UK) from 3 consented female adults (aged 36, 33 and 37 years) following plastic surgery. Selection criteria included: Caucasian, no stretchmarks, no scars and no hair. Full thickness skin without adipose tissue and an overall thickness of 550 ± 80 µm was used. Upon receipt, the *ex vivo* skin samples were equilibrated for 1 h with 3 mL of DMEM-based (Sigma-Aldrich, UK) culture medium (Table 4.1) at 5% CO_2 and 37 ˚C before use in permeation experiments. The study protocol received the required ethical approval (# ERN_12-1502) from the University of Birmingham's Medical, Engineering and Mathematics Ethical Review Committee.

Fig 4.12: Sketch of a typical custom-made Franz cell

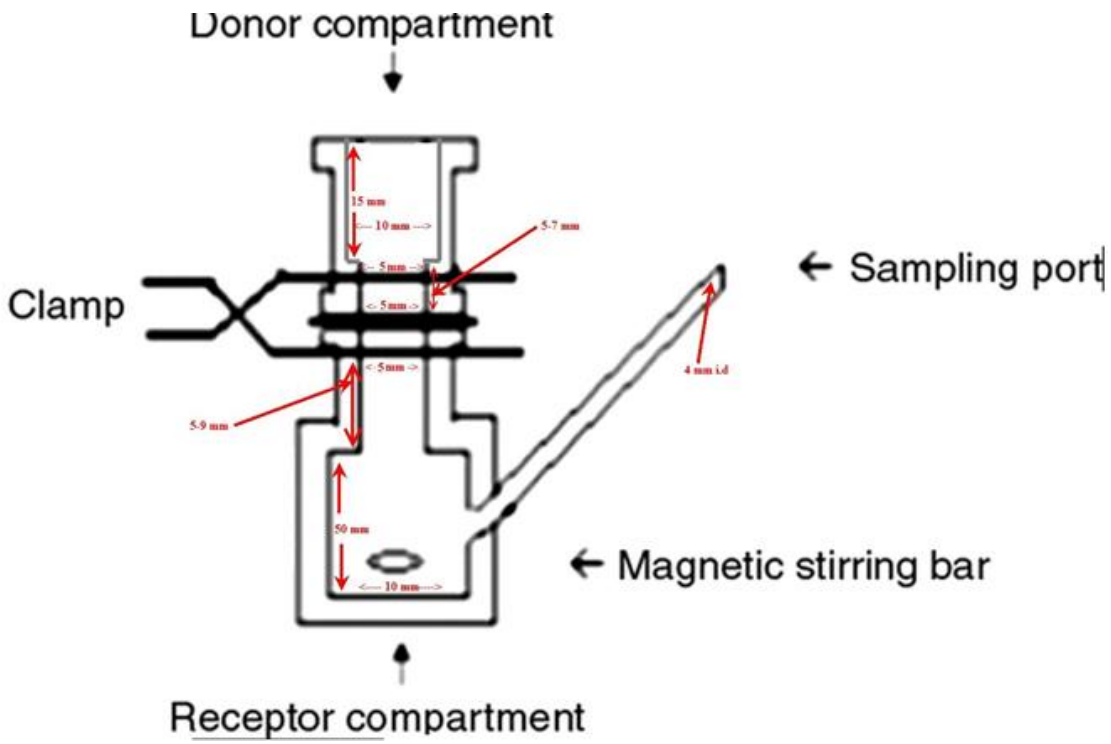

Fig 4.13: Histological comparison of excised human breast skin and 3D-HSE Episkin model.

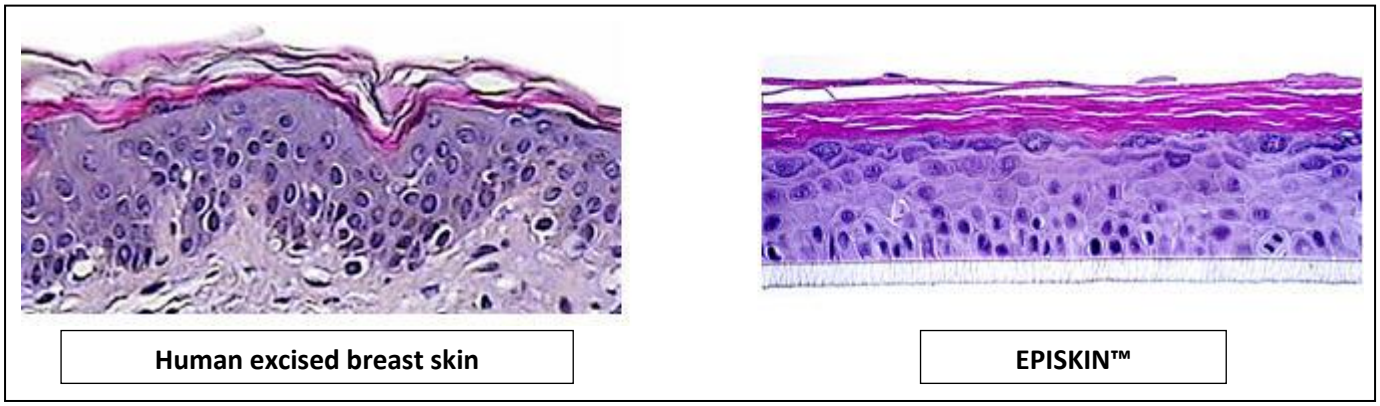

4.4: QA/QC

All tissues were visually inspected and if physical imperfections were noted by the manufacturer or via the following end –use testing, then the respective tissue was excluded.

Viability: Tissues are exposed to 1% Triton X-100 for 24 hours. The time of exposure required to reduce the tissue viability (ET-50) using the MTT (3-(4, 5-dimethylthiazol-2-yl)-2, 5-diphenyltetrazolium bromide) viability assay was determined for each tissue batch. Acceptable MTT results (i.e. Formazan concentration ≥1.5 mg/mL) were achieved following 24 h of exposure.

Functionality: Both positive and negative control experiments were carried out alongside each sample batch. Positive controls involved the exposure of the test tissue to Triton-X-100 (0.01% solution in deionised water) which showed ~100% permeation (n = 5; 97 ± 4%), while negative controls showed 0% penetration of decabromodiphenyl ethane (0.01% solution in acetone) after 24 hour exposure.

Integrity: The integrity of the skin membrane was tested using the standard trans-epidermal electrical resistance (TEER) and methylene blue (BLUE) standard methods (Guth et al. 2015) Furthermore, histological testing was performed randomly to evaluate the full differentiation of the human skin equivalent tissues (Figure 4.14).

Fig 4.14: Evaluation of histology for Episkin model.

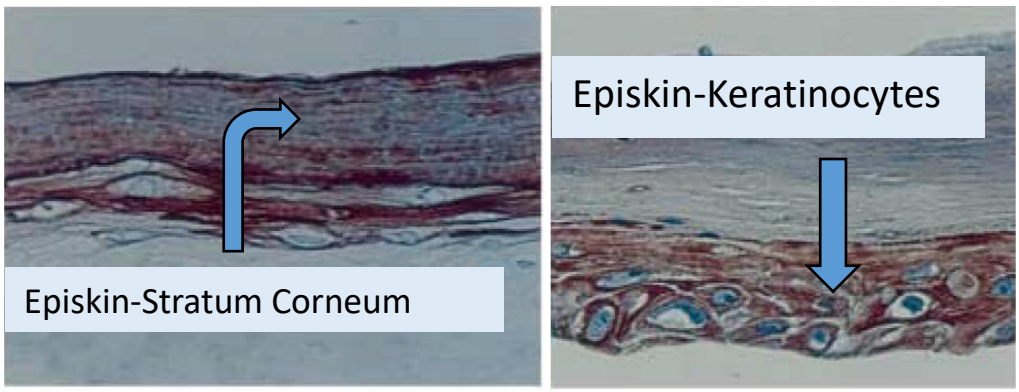

Table 4.3: Summary of QA/QC tests for Epiderm® model. (Provided by the SkinEthics Lyon, France).

Quality Control	Test	Specification	Result
	Histology Scoring	≥ 19.5	21.0 ± 0.3 (CV =1.5%)
		Well differentiated epidermis consisting of a basal layer, several spinous and granular layers and a thick stratum corneum	Satisfactory
	MTT test (IC50)	≥ 1mg/ml	1.5 mg/ml
	Statistical Analysis: Histology – Probability 0.95 that 100% of the batch >20 IC50: probability 0.95 that IC50 ≥ 1.4 mg/ml		
BIOLOGICAL SAFETY	On Blood of the same donors, verified ; The absence of HIV1 and 2 antibodies The absence of hepatitis C antibodies The absence of hepatitis B antigens HBs On Epidermal cells of the same donors, verified ; The absence of bacteria, fungus and mycoplasma		

The efficiency of the experimental approach was investigated using a mass balance exercise.

$$\% \text{ Recovery} = \frac{M_{\text{Cotton Bud}} + M_{\text{skin}} + M_{RF} + M_{\text{well wash}}}{\text{Initial Donor mass}}$$

Where

$M_{Cotton\ Bud}$ = Amount (ng) of Analyte remained on skin surface removed with the Cotton Buds soaked in Hexane

M_{skin} = Amount (ng) of Analyte remained in the skin upto 24 hr

M_{RF} = Cumulative amount in the receptor fluid over 24 hr

$M_{well\ wash}$ = Non-specific binding obtained after well wash with PBS after 24 hr

4.5: RESULTS

4.5.1: Evaluation of 3D-Human Skin Equivalents (Abdallah et al. 2015)

We have developed and applied a protocol for the evaluation of dermal absorption of HBCDs and TBBPA using 2 commercially available 3D-HSE models (EPISKIN™ and EpiDerm™) according to the OECD guidelines and subsequently the results were compared to the data obtained from ex-vivo skin. The results of the permeation experiments were grouped under three major compartments: the directly absorbed dose (cumulative concentration in the receptor fluid over 24 h + receptor compartment rinse), the skin (concentration in the skin tissue after 24 h) and the unabsorbed dose (concentration in the skin surface wipes after 24 h + donor compartment rinse) (Table 4.5) .The results revealed the overall recoveries from the mass balance exercise exceeded 85% for all the tested chemicals for all the models.

Flux (Jss) of HBCDs ranged from 0.8–1.5 ng/cm^2·h, 0.9–1.5 ng/cm^2·h and 0.7–1.3 ng/cm^2·h for the EPISKIN™, EpiDerm™ and human *ex vivo* skin, respectively. α-HBCD showed a consistently higher flux across skin than γ-HBCD at the studied doses. The Jss for TBBP-A was approximately the same value for both Episkin and Epiderm models (1.47 ng/cm^2·h) but was slightly lower (1.29 ng/cm^2·h) for the *ex vivo* model.

The directly absorbed fraction was found to be 6.29 % in case of TBBP-A followed by α-HBCD (5.81 %), β-HBCD (3.86 %) and γ-HBCD (3.42 %) when dosed at 500 ng/cm^2. A similar trend was observed at the higher dosing level (1 µg/cm^2). This could be attributed to the physicochemical properties of the tested compounds, where TBBP-A has a lower mass

and higher water solubility than HBCDs. Furthermore, a statistically significant correlation ($P < 0.05$) was observed between the 24 h cumulative absorbed dose and the log K_{OW} (Table 1.2) of the studied BFRs in all the tested *in vitro* models. This highlights the influence of physicochemical properties on the human dermal bioavailability of a chemical.

The estimated P_{app} (Table 4.4) values showed greater resistance of human *ex vivo* skin to the penetration of target BFRs than the EPISKIN™ and EpiDerm™ models. However, this difference was not statistically significant. In addition, both 3D-HSE models and human *ex vivo* skin displayed increasing resistance to the penetration of BFRs in the same order of γ-HBCD > β-HBCD > α-HBCD > TBBP-A. The lag time for β-HBCD and α-HBCD was found to be approx. 1 hr or more than 1 hr in all the three models. The lag time for β-HBCD was found to be similar for Episkin and Epiderm models (approx. 0.80 hr) and 0.85 hr for the *ex vivo* skin model. The lag time increased for TBBPA in the following order: Epiderm < Episkin <Human *ex vivo*. **Higher permeation of all target compounds in the following order: EpiDerm™ >EPISKIN™ > Human *ex vivo* skin was observed at the two concentration levels studied. However, statistical analysis showed no significant differences ($P > 0.05$) between the levels of target analytes in the 3 major compartments of the examined tissues.** Border line statistical significance values ($P = 0.053$ and 0.056) were observed between the results for human *ex vivo* skin and those for EpiDerm™ for β-HBCD and EPISKIN™ for TBBPA, respectively. The EpiDerm™ model displayed the largest permeation difference from human *ex vivo* skin with a ~25% increase in the permeated dose of β-HBCD over 24 hours exposure. We investigated the potential effect of the acetone, 30% acetone in water, and 20% Tween 80 in water on the percutaneous penetration of BFRs for the human *ex vivo* and Episkin models. Results indicated higher levels of target compounds absorbed from 20% Tween 80, which was also evident for TBBP-A and α-HBCD. Schafer-Korting et al. (Schafer-Korting et al. 2006) reported less penetration

of testosterone in pig and bovine skin (0.07 and 0.13 % of applied dose) compared to human skin (0.32 %), while EPISKIN™ and EpiDerm™ models showed higher permeations (0.53 and 2.36, respectively). However, the EPISKIN™ and EpiDerm™ models used in this study are listed under the "enhanced barrier function" category, which is different from those used in the 2006 study.

Table 4.4: Steady state flux, permeation coefficient and lag time values estimated for the target BFRs using different *in vitro* skin models.

	Flux ($ng/cm^2.h$)	Permeation coefficient (cm/h)	Lag time (h)
EPISKIN™			
α-HBCD	1.25	2.50×10^{-04}	0.80
β-HBCD	0.84	1.69×10^{-04}	1.01
γ-HBCD	0.78	1.56×10^{-04}	1.21
TBBPA	1.47	2.93×10^{-03}	0.72
EpiDerm™			
α-HBCD	1.33	2.74×10^{-04}	0.77
β-HBCD	0.88	1.77×10^{-04}	0.97
γ-HBCD	0.85	1.72×10^{-04}	1.13
TBBPA	1.48	2.97×10^{-03}	0.60
Human *ex vivo* skin			
α-HBCD	1.08	2.16×10^{-04}	0.85
β-HBCD	0.74	1.47×10^{-04}	1.17
γ-HBCD	0.69	1.37×10^{-04}	1.26
TBBPA	1.29	2.58×10^{-03}	0.79

Fig 4.15: Cumulative dose (ng/cm^2) absorbed into the receptor fluid following exposure of (from top to bottom): (a) human *ex vivo* skin, (b) EPISKIN™ and (c) EpiDerm™ to 1000 ng/cm^2 of target BFRs over 24 h.

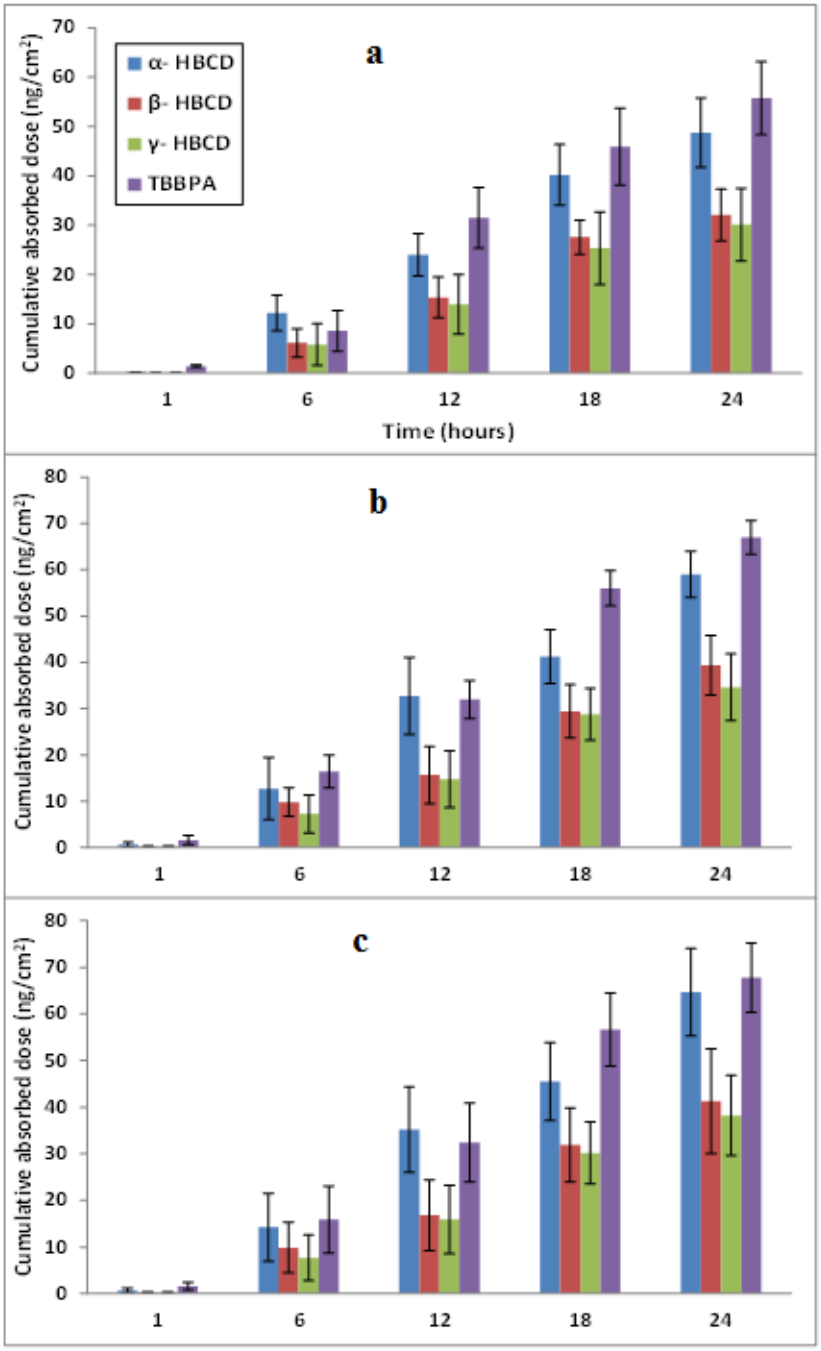

Table 4.5: Distribution of target BFRs (expressed as % of exposure dose) in different compartments of the *in vitro* diffusion system following 24 hour exposure to 500 ng/cm^2 of α-, β-, γ-HBCDs and TBBP-A in acetone.

	α-HBCD	β-HBCD	γ-HBCD	TBBP-A
	EPISKIN™			
Receptor fluid (24h)	5.81 ± 1.04	3.86 ± 0.78	3.42 ± 0.94	6.29 ± 0.65
Receptor rinse	0.10 ± 0.02	0.07 ± 0.02	0.11 ± 0.02	0.41 ± 0.28
Directly absorbed fraction	5.90 ± 1.06	3.94 ± 0.82	3.46 ± 0.96	6.70 ± 0.92
Skin-Epidermis (Depot)	30.06 ± 2.42	27.18 ± 2.28	23.66 ± 3.16	24.18 ± 2.54
Skin wash (unabsorbed)	44.34 ± 4.04	51.47 ± 3.72	56.82 ± 4.58	53.53 ± 3.46
Donor rinse (unabsorbed)	5.13 ± 0.64	3.16 ± 0.82	2.38 ± 1.06	4.93 ± 2.08
Total Recovery	85.43 ± 8.16	85.75 ± 7.64	86.32 ± 9.76	89.34 ± 9.02
	EpiDerm™			
Receptor fluid (24h)	6.35 ± 0.92	4.02 ± 1.04	3.74 ± 0.82	6.44 ± 0.59
Receptor rinse	0.11 ± 0.04	0.10 ± 0.08	0.09 ± 0.04	0.34 ± 0.16
Directly absorbed fraction	6.46 ± 0.94	4.13 ± 1.12	3.82 ± 0.86	6.78 ± 0.74
Skin-Epidermis (Depot)	28.19 ± 3.18	24.39 ± 2.22	21.02 ± 3.52	23.79 ± 2.42
Skin wash (unabsorbed)	45.73 ± 4.02	53.91 ± 3.44	58.84 ± 4.38	55.04 ± 4.29
Donor rinse (unabsorbed)	5.07 ± 0.62	2.39 ± 0.52	1.97 ± 0.74	4.11 ± 1.27
Total Recovery	85.45 ± 8.76	84.82 ± 7.30	85.65 ± 9.50	89.72 ± 8.72
	Human *ex vivo* skin			
Receptor fluid (24h)	4.88 ± 1.44	3.21 ± 1.06	3.01 ± 1.02	5.37 ± 0.65
Receptor rinse	0.07 ± 0.02	0.11 ± 0.02	0.06 ± 0.02	0.21 ± 0.28
Directly absorbed fraction	4.95 ± 1.44	3.32 ± 1.06	3.07 ± 1.48	5.57 ± 0.92
Skin-Epidermis (Depot)	30.59 ± 2.28	27.82 ± 2.38	24.16 ± 2.24	24.71 ± 2.96
Skin wash (unabsorbed)	47.05 ± 4.44	51.19 ± 4.68	56.48 ± 3.28	56.53 ± 4.46
Donor rinse (unabsorbed)	5.23 ± 1.48	3.37 ± 1.02	2.07 ± 0.66	3.83 ± 2.08
Total Recovery	87.82 ± 7.84	85.70 ± 6.28	85.78 ± 7.38	85.65 ± 10.42

Fig 4.16: A representative curve showing cumulative permeation (ng/cm^2) of target BFRs in the EPISKIN™ model at the linear-range region ($R^2 \geq 0.9$). Error bars represent 1 standard deviation.

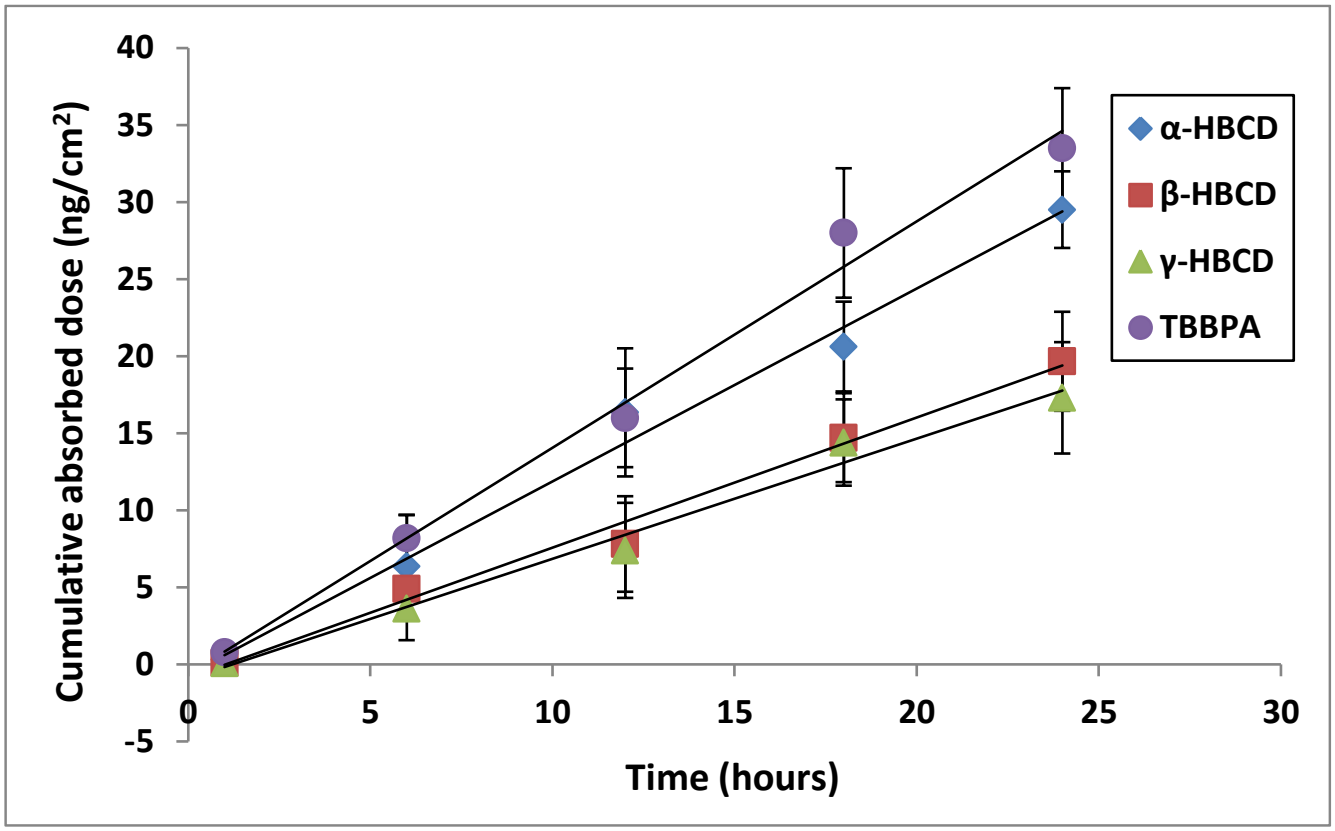

Figure 4.17: Cumulative permeation (ng/cm^2) into the receptor fluid following exposure of human *ex vivo* skin to 500 ng/cm^2 of target BFRs in (A) acetone, (B) 30% acetone in water, and (C) 20% Tween 80 in water for 24 h

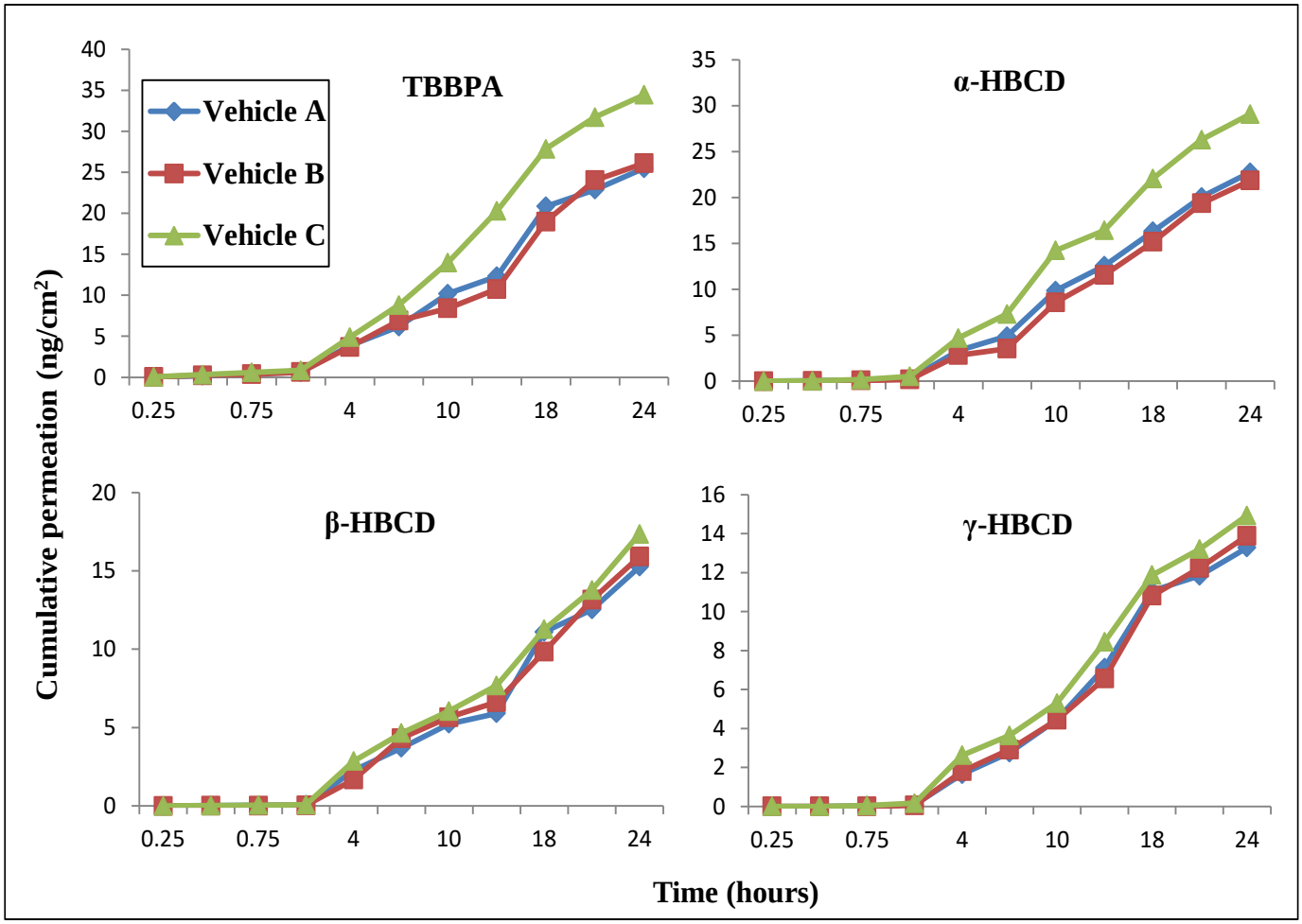

4.5.2: Human dermal absorption of PBDEs and effect of bromine substitution.(Abdallah et al. 2015b)

When Episkin was exposed to PBDE congeners at two different levels 500 ng/cm^2 and 1000 ng/cm^2, results (Table 4.7 & 4.8) indicated that the degree of permeation was inversely proportional to the degree of bromination.BDE-1 was absorbed at 30% of the applied dose after 24 hrs of exposure whereas the environmentally abundant BDE-47 and BDE-99 showed absorption values of 3% and 2% respectively. All target PBDEs accumulated in the skin to varying degrees. The proportion of accumulation increased with the increase of bromine substitution from BDE-1 (~18%) to BDE-153 (~37%) and decreased steeply from BDE-183 (~13) to BDE-209 (8%) (Fig 4.17).This behaviour could be due to the physicochemical properties of PBDEs i.e. more polar mono-PBDEs penetrated faster through the water-rich viable epidermis and octa-PBDEs were accumulated for longer in the lipid-rich *stratum corneum* prior to diffusion through the viable epidermis at a slower rate. Our results were in good agreement with a previously reported study (Garner, Demeter and Matthews 2006b) on PCBs (*in vivo* rat model). The low dermal accumulation values for BDE-183 and BDE-209 are due to their large molecular weight which hinders their partitioning to the stratum corneum and subsequent absorption by keratinocytes (Choy and Prausnitz 2011). Results also revealed a significant positive correlation ($P<0.05$) between the Papp values (Table 4.6) for mono to hexa PBDEs and water solubilities and vapour pressure of these congeners, with a significantly negative inverse relationship observed between Papp and both Log K_{ow} and molecular weight of the studied congeners. Because of the slow penetration of BDE-183 and BDE-209, P_{app} values could not be calculated. The estimated lag times (t_{lag}) varied between 0.25 and 1.26 h for BDE-1 and BDE-153, respectively. This is due to the fact that less brominated congeners diffuse quickly through the dermal tissue while lipophilic (more brominated) congeners are likely to accumulate within the stratum corneum. This retained

BFR mass constitutes a depot that may be available for subsequent release into the receptor fluid (systemic circulation) provided there is no loss in the skin by metabolism, irreversible binding to keratinocyte proteins, evaporation or desquamation.

Fig 4.18: Percent of applied dose (500 ng/cm^2) of target PBDEs absorbed (present in the receptor compartment), un-absorbed (remaining in the donor compartment and on skin surface) and accumulated in the skin tissue following 24 h exposure.

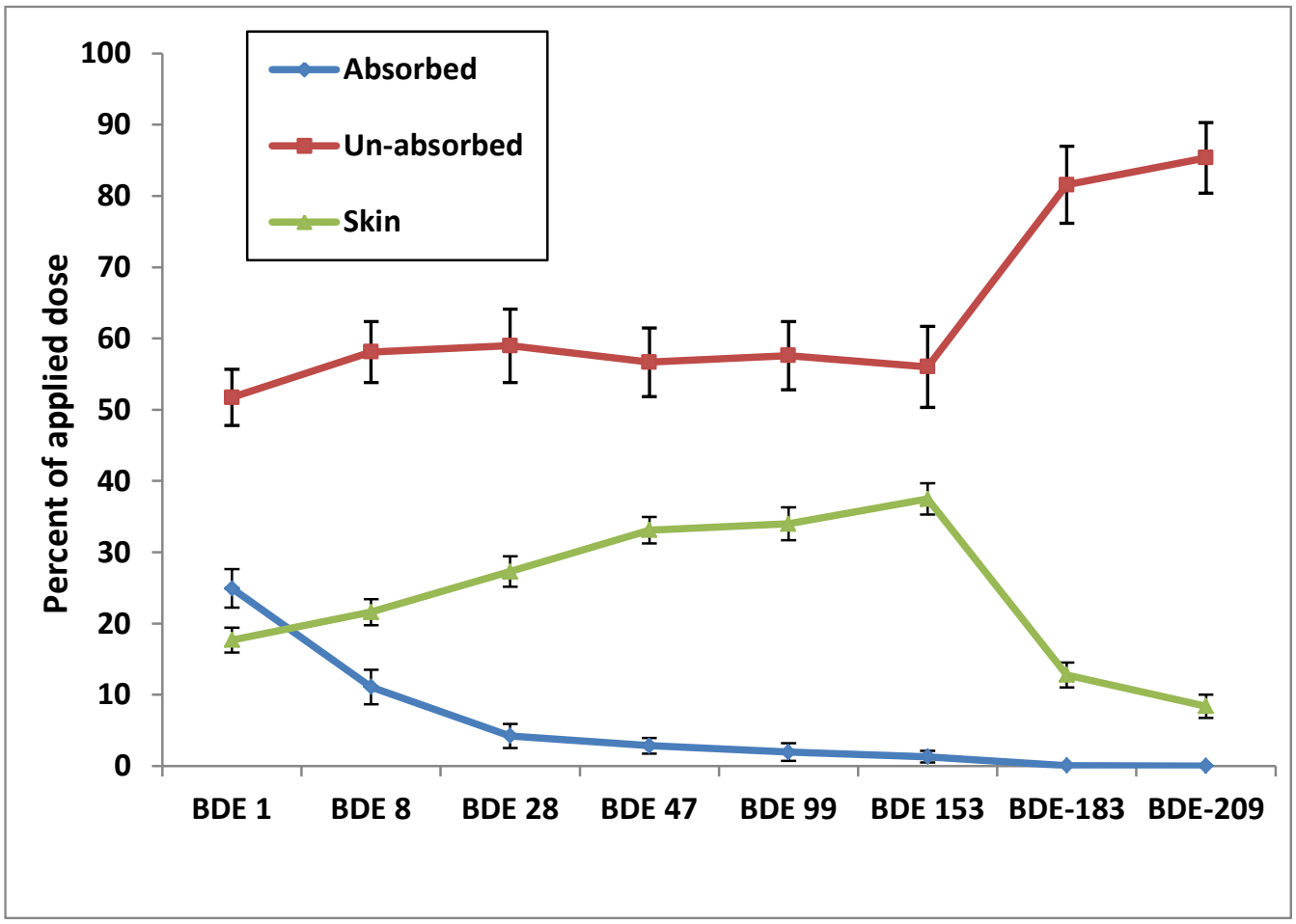

Table 4.6: Steady state flux, permeation coefficient and lag time values estimated from exposure of EPISKIN™ to 500 ng/cm^2 of target PBDEs for 24 h.

	Flux (ng/cm^2.h)	Permeation coefficient (cm/h)	Lag time (h)
BDE 1	5.45	1.09×10^{-2}	0.25
BDE 8	2.42	4.84×10^{-3}	0.42
BDE 28	0.88	1.76×10^{-3}	0.82
BDE 47	0.63	1.26×10^{-3}	0.90
BDE 99	0.40	8.00×10^{-4}	1.10
BDE 153	0.20	4.00×10^{-4}	1.26

Table 4.7: Cumulative levels (expressed as average percentage ± standard deviation of applied dose) of target PBDEs in the receptor fluid following exposure of EPISKIN™ to 500 ng/cm^2 of target PBDEs.

Time (hours)	BDE-1	BDE-8	BDE-28	BDE-47	BDE-99	BDE-153	BDE-183	BDE-209
0.25	ND*	ND	ND	ND	ND	ND	ND	ND
0.50	0.25 ± 0.09	0.10 ± 0.04	0.07 ± 0.03	0.04 ± 0.01	ND	ND	ND	ND
1.00	1.06 ± 0.28	0.41 ± 0.05	0.20 ± 0.02	0.13 ± 0.02	0.08 ± 0.01	0.03 ± 0.01	ND	ND
2.00	1.98 ± 0.61	0.82 ± 0.07	0.31 ± 0.09	0.21 ± 0.09	0.07 ± 0.04	0.04 ± 0.01	ND	ND
6.00	5.07 ± 1.07	1.88 ± 0.65	0.46 ± 0.31	0.48 ± 0.32	0.43 ± 0.15	0.13 ± 0.05	ND	ND
10.00	10.20 ± 1.89	4.34 ± 1.72	1.59 ± 1.56	0.97 ± 0.82	0.57 ± 0.77	0.33 ± 0.03	ND	ND
12.00	14.24 ± 2.12	6.75 ± 2.24	2.19 ± 1.36	1.56 ± 0.89	0.86 ± 0.84	0.46 ± 0.02	0.03 ± 0.01	ND
18.00	20.43 ± 2.54	8.68 ± 2.17	2.77 ± 1.43	2.23 ± 0.88	1.29 ± 1.07	0.68 ± 0.04	0.04 ± 0.01	ND
24.00	24.92 ± 2.71	11.08 ± 2.43	4.23 ± 1.68	2.85 ± 1.09	1.96 ± 1.26	0.89 ± 0.11	0.05 ± 0.01	ND

* Not detected (less than 0.02% of applied dose for all congeners, or 0.05% for BDE-209).

Table 4.8: Distribution of target BFRs (expressed as average percentage ± standard deviation of exposure dose) in different fractions of the *in vitro* diffusion system following 24 h exposure to 500 ng/cm^2 of the studied PBDEs.

	BDE 1	BDE 8	BDE 28	BDE 47	BDE 99	BDE 153	BDE-183	BDE-209
Absorbed*	24.9 ± 2.71	11.0 ± 2.43	4.2 ± 1.68	2.8 ± 1.09	1.9 ± 1.2	0.89 ± 0.11	0.05 ± 0.01	ND[$]
Unabsorbed[#]	51.7 ± 3.93	58.1 ± 4.28	58.9 ± 5.16	56.6 ± 4.81	57.6 ± 4.7	56.0 ± 5.67	81.57 ± 5.41	85.35 ± 4.95
Skin	17.6 ± 1.75	21.6 ± 1.83	27.2 ± 2.14	33.1 ± 1.87	33.9 ± 2.3	37.4 ± 2.18	12.78 ± 1.24	8.38 ± 1.31
Sum	94.3 ± 7.52	90.7 ± 8.31	90.4 ± 8.91	92.6 ± 7.68	93.5 ± 8.2	94.3 ± 7.90	94.40 ± 6.62	93.73 ± 6.22

***** Comprises cumulative concentrations in the receptor fluid over 24 h + receptor compartment rinse.

[#] Comprises concentrations in the skin surface wipes after 24 h + donor compartment rinse.

[$] Not detected (less than 0.02% of applied dose for all congeners, or 0.05% for BDE-209)

4.5.3: Human dermal absorption of chlorinated organophosphate flame retardants (Abou-Elwafa Abdallah et al. 2016)

Finite Dosing: Using human *ex vivo* skin for TCEP, the cumulative absorption detected in receptor fluid was found to be 28% of the applied dose (500 ng/cm^2), with lower absorbed fractions of 25% and 13% observed for TCIPP and TDCIPP respectively (Table 4.9). Analysis of the skin tissues showed recoveries of 15%, 11% & 7% of the applied dose for TCEP, TCIPP, and TDCIPP respectively after 24 h exposure. Statistical analysis revealed a significant ($P< 0.05$) positive correlation between the absorbed fractions of PFRs and their water solubility but a significant negative correlation between the cumulative 24 hr absorption of target compounds and their log K_{ow}. Similar results were obtained using the Episkin-HSE model. No statistically significant differences ($P>0.05$) were obtained between the two in vitro models. However, the Episkin™ tissues were more permeable to all target compounds than the human *ex vivo* skin. TCEP, TCIPP and TDCIPP showed respectively 16%, 11% and 9% greater absorption in experiments using the Episkin model compared to those using the human *ex vivo* skin model (Fig 4.18 & 4.19).

Infinite Dosing: Infinite dose application maximizes the concentration gradient and diffusion/penetration through the skin becomes the rate-limiting step, therefore it permits calculation of the permeability constant (Kp) for each compound. (OECD, 2004).

In the first 8 h of exposure both TCEP and TCIPP showed a rapid increase in the absorbed dose and the rate declined until 24 hr but TDCIPP showed a slower and yet more consistent rate of absorption throughout the 24 hr exposure period. This behaviour could be attributed to the higher lipophilicity of TDCIPP (log K_{ow} = 3.8) compared to TCIPP (log k_{ow} = 2.6) and TCEP (log K_{ow} = 1.4), resulting in slower mass transfer rate across the lipophilic stratum corneum.

Results revealed a significant negative correlation between Kp and log K_{ow} (Table 4.10) Differences in the barrier function (ΔKp) decreased with decreasing polarity in the order: TCEP (ΔKp = 0.8) > TCIPP (ΔKp = 0.6) > TDCIPP (ΔKp = 0.2). However, more studies covering a greater range of chemicals with a wider variety of physicochemical properties are required to confirm this observation.

Effect of hand washing: After 6 hrs of finite dosing (500 ng/cm^2) to *ex vivo* skin, the surface was washed thoroughly with a neutral detergent solution, while monitoring the absorbed dose in the receptor fluid continued until 24 h. Results (Fig 4.20) showed the absorption rate decreased markedly after washing, percutaneous penetration of the studied PFRs continues from the skin depot. A statistically significant difference ($P<0.05$) was observed in the absorption rate of TCEP and TCIPP with and without washing over a 24 h exposure period. The difference for TDCIPP was not significant ($P = 0.12$). In general our results indicate that hand-washing reduce overall dermal absorption of PFRs, albeit to varying degrees depending on the physicochemical properties of the FRs.

Effect of exposure vehicle: After 24 h exposure, results revealed an increase in the absorbed dose of the 3 target compounds from 20 % Tween 80 solution in water compared to acetone (Figure 4.20) but none of them showed a statistically significant difference ($P>0.05$) between the studied exposure vehicles. In general, a vehicle may hydrate the stratum corneum (SC), extract critical barrier components out of the skin, or damage the skin because it is a strong acid or base. Removing SC lipids may increase percutaneous absorption of the drugs.

Table 4.9: Distribution of target PFRs (expressed as average percentage ± standard deviation of exposure dose) in different fractions of the *in vitro* diffusion system following 24 h exposure to 500 ng/cm^2 of the studied compounds.

Human *ex vivo* skin	**TCEP**	**TCIPP**	**TDCIPP**
Absorbed*	28.3 ± 2.3	24.7 ± 1.4	12.7 ± 1.2
Unabsorbed#	6.8 ± 1.1	10.8 ± 1.2	14.8 ± 1.4
Skin	55.3 ± 3.5	53.1 ± 2.9	62.3 ± 4.3
Sum	90.30 ± 6.9	88.61 ± 5.5	89.79 ± 6.7
EPISKIN™	**TCEP**	**TCIPP**	**TDCIPP**
Absorbed*	33.7 ± 2.5	27.7 ± 1.9	13.9 ± 1.5
Unabsorbed#	6.8 ± 1.4	10.8 ± 1.0	14.8 ± 1.3
Skin	49.3 ± 3.9	50.3 ± 3.2	61.5 ± 4.6
Sum	89.7 ± 7.8	88.8 ± 6.1	90.2 ± 7.5

***** Comprises cumulative concentrations in the receptor fluid over 24 h + receptor compartment rinse.# Comprises concentrations in the skin surface wipes after 24 h + donor compartment rinse

Table 4.10: Flux rates (Jss, ng/cm^2 h), permeability constants (Kp, cm/h), lag times (t_{lag},h) and linear ranges (h) estimated from infinite exposure of human *ex vivo* skin and EPISKIN™ to 1000 ng/cm^2 of target PFRs for 24 h.

	Human *ex vivo* skin					**EPISKIN™**				
	J_{ss}	**K_p x 10^{-2}**	**t_{lag}**	**Range**	**R^{2*}**	**J_{ss}**	**K_p x 10^{-2}**	**t_{lag}**	**Range**	**R^2**
TCEP	21.9	2.2	0.28	0.5 – 8	0.97	30.1	3.0	0.21	0.5 – 8	0.98
TCIPP	15.5	1.6	0.29	0.5 – 10	0.98	21.7	2.2	0.23	0.5 – 10	0.96
TDCIPP	5.4	0.5	2.9	4 – 22	0.96	7.4	0.7	2.9	4 – 22	0.98

* R^2 is the linearity coefficient. A minimum value of 0.9 combined with a *P*-value < 0.05 was required to express linearity (Niedorf, Schmidt and Kietzmann 2008a).

Fig 4.19: Distribution of the studied PFRs applied as finite dose (500 ng/cm^2) to: (a) *ex vivo* human skin and (b) EPISKIN™ tissues following 24 h exposure. Error bars represent 1 standard deviation (n=3).

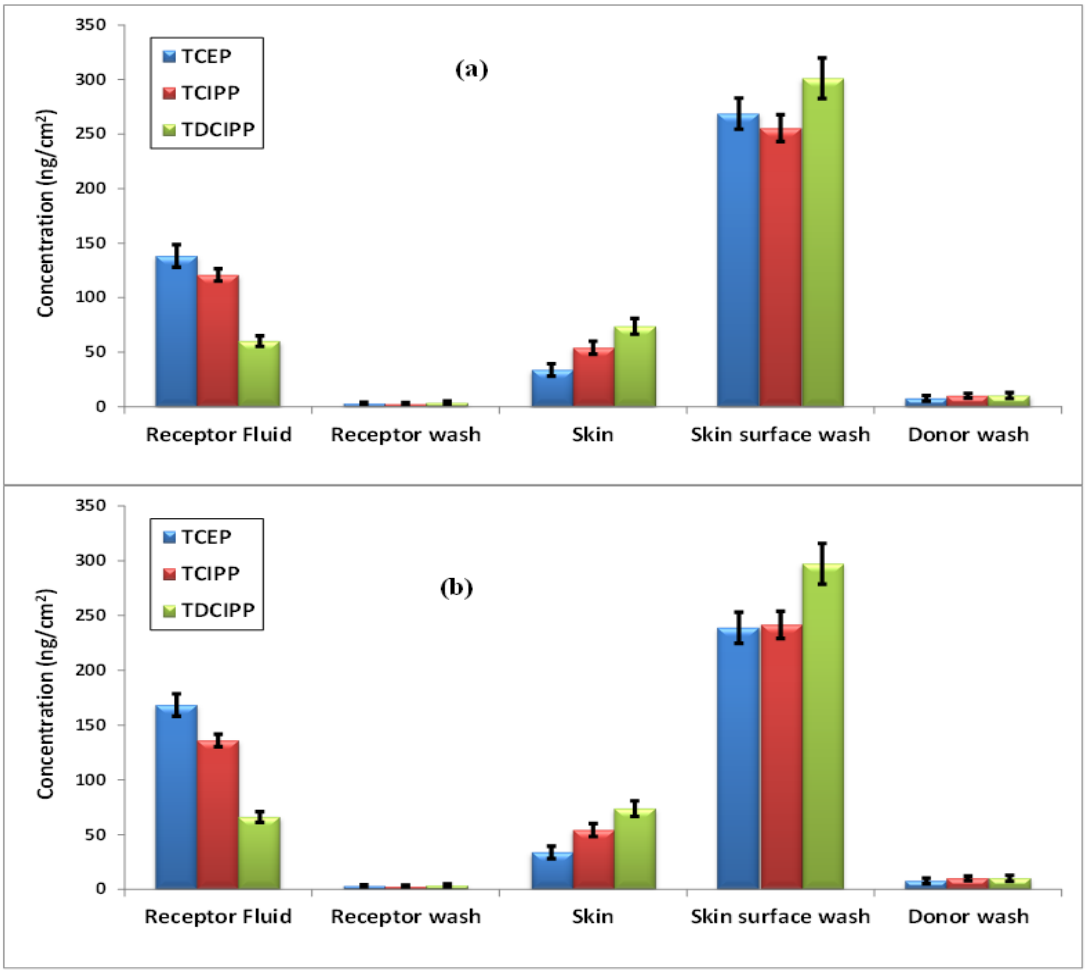

Fig 4.20: Cumulative absorbed dose of the target PFRs following 24 h exposure of: (a) human *ex vivo* skin and (b) EPISKIN™ to 1000 ng/cm^2 of the tested compounds (infinite dose).

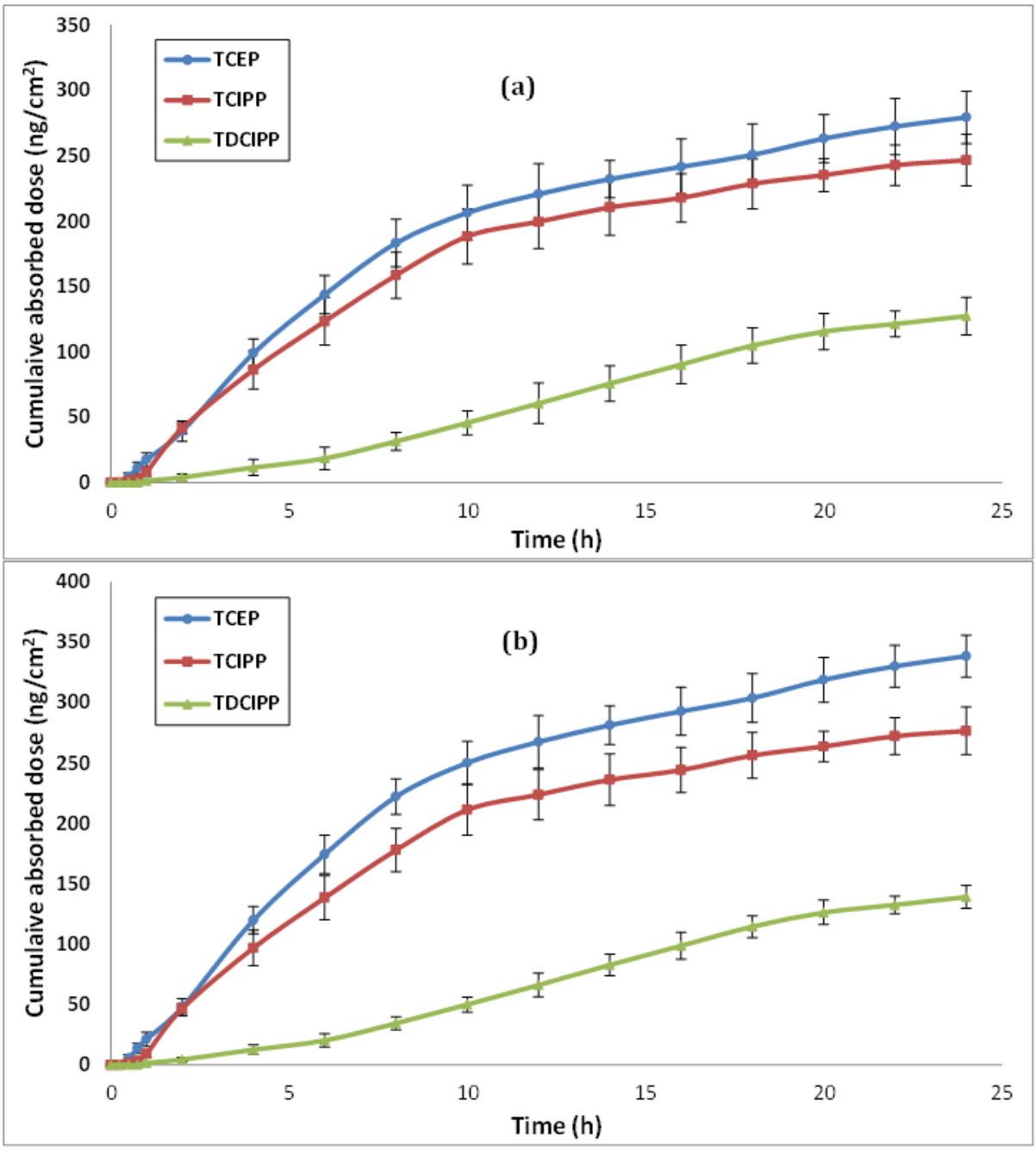

Fig 4.21: Cumulative absorbed dose of (a) TCEP, (b) TCIPP and (c) TDCIPP applied to *ex vivo* human skin at 500 ng/cm^2 each (finite dose). The skin surface in 3 cells was washed with detergent after 6 h (red line), while the other 3 cells were not washed (blue line).

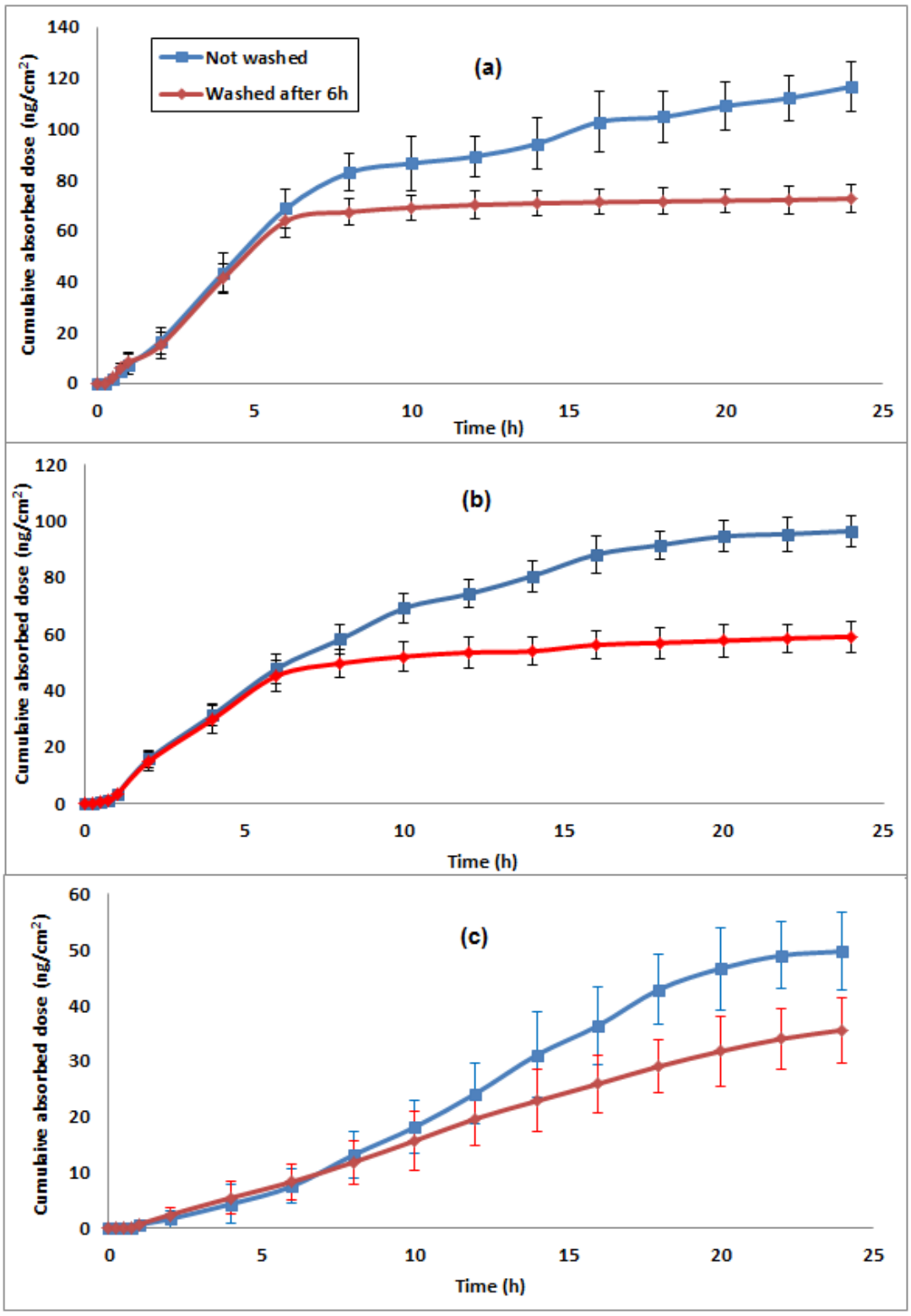

Fig 4.22: Distribution of: (a) TCEP, (b) TCIPP and (c) TDCIPP following 24 h exposure of human *ex vivo* skin to 500 ng/cm^2 of each compound in (i) acetone and (ii) 20% Tween 80 solution in water. Error bars represent 1 standard deviation (n=3).

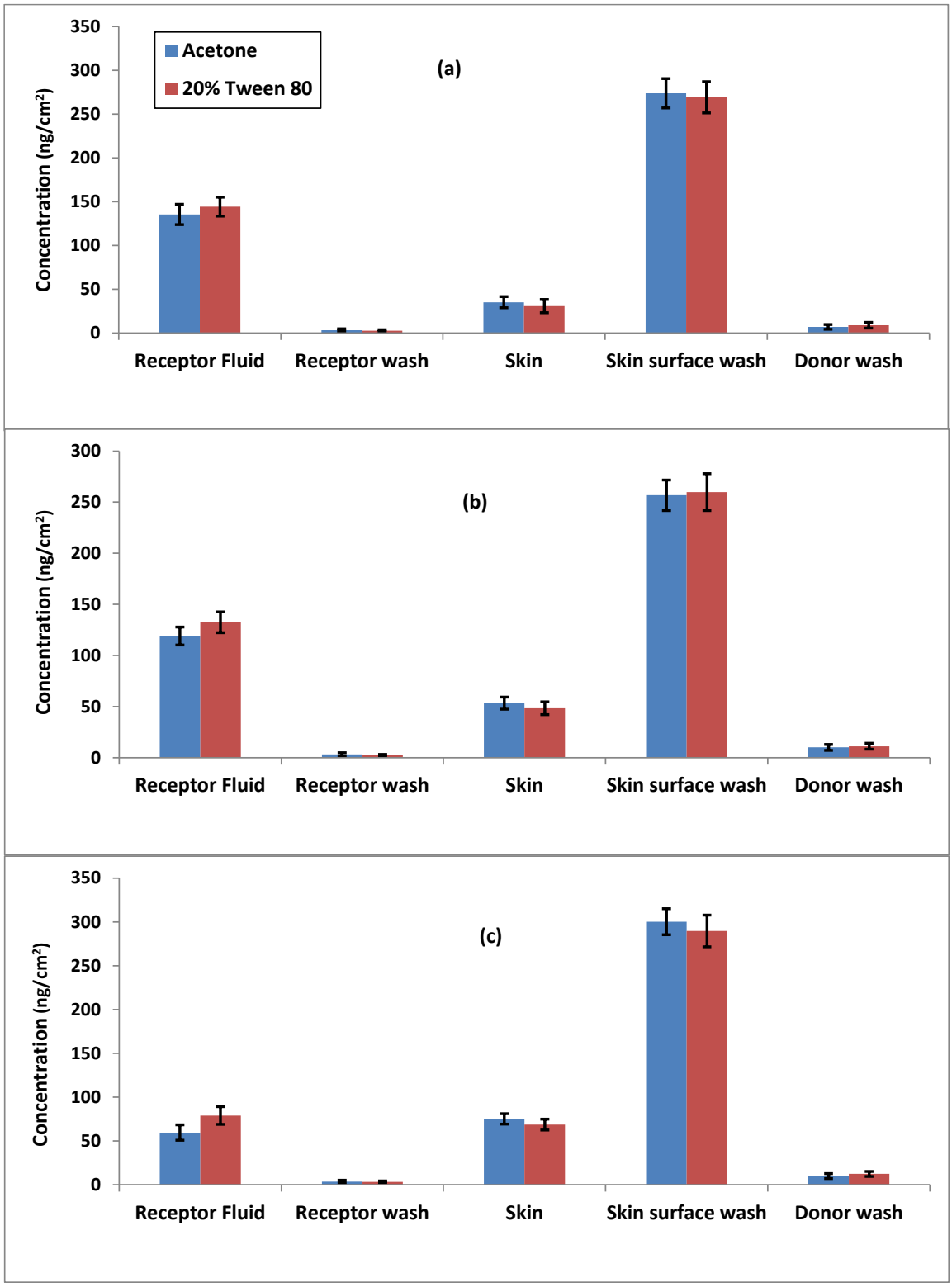

Fig 4.23: Linear cumulative permeation range (ng/cm^2) of target PFRs following infinite exposure of EPISKIN™ to 500 ng/cm^2 for 24 hours.

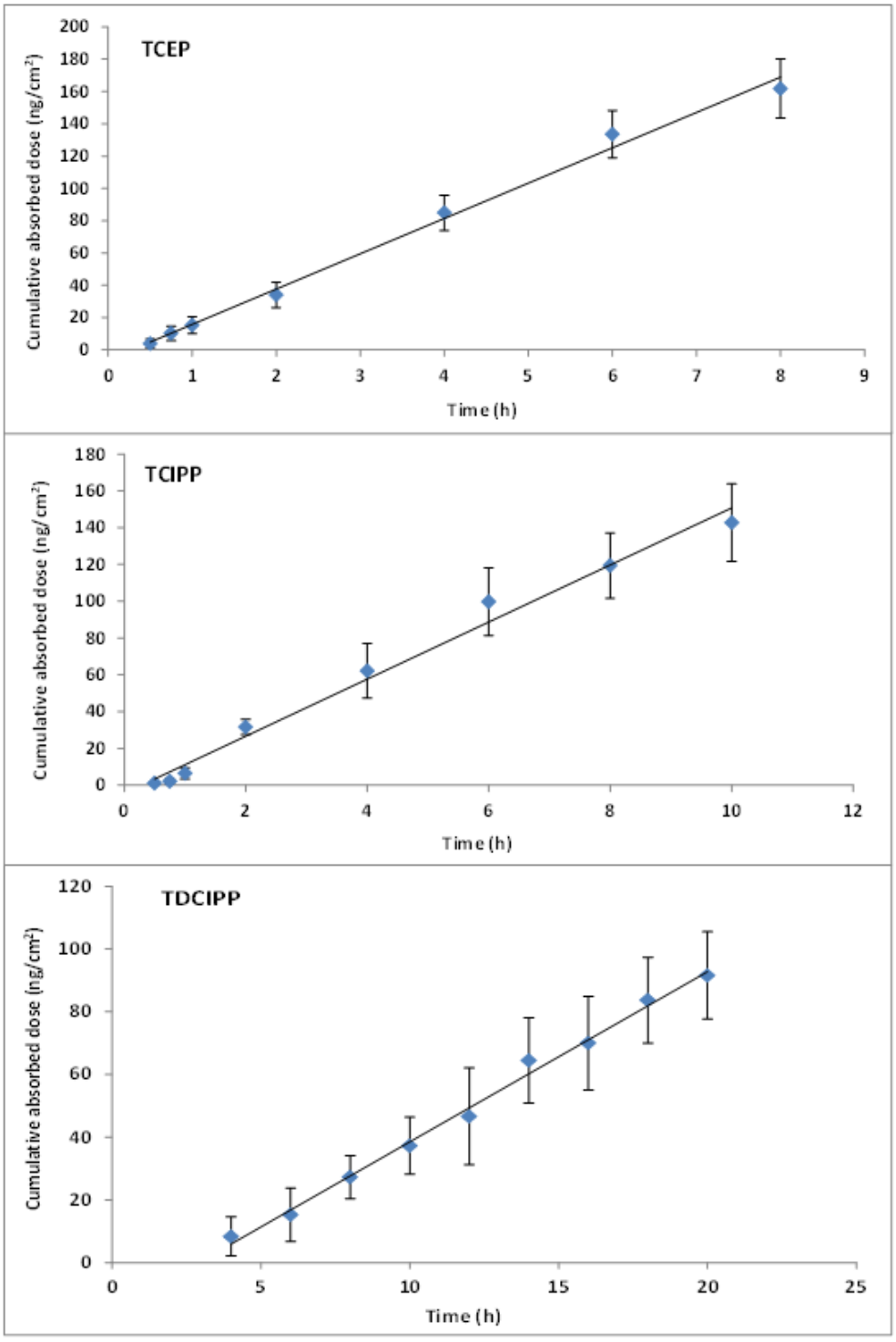

Fig 4.24: Linear cumulative permeation range (ng/cm^2) of target PFRs following infinite exposure of human *ex vivo* skin to 1000 ng/cm^2 for 24 hours. Error bars represent 1 standard deviation.

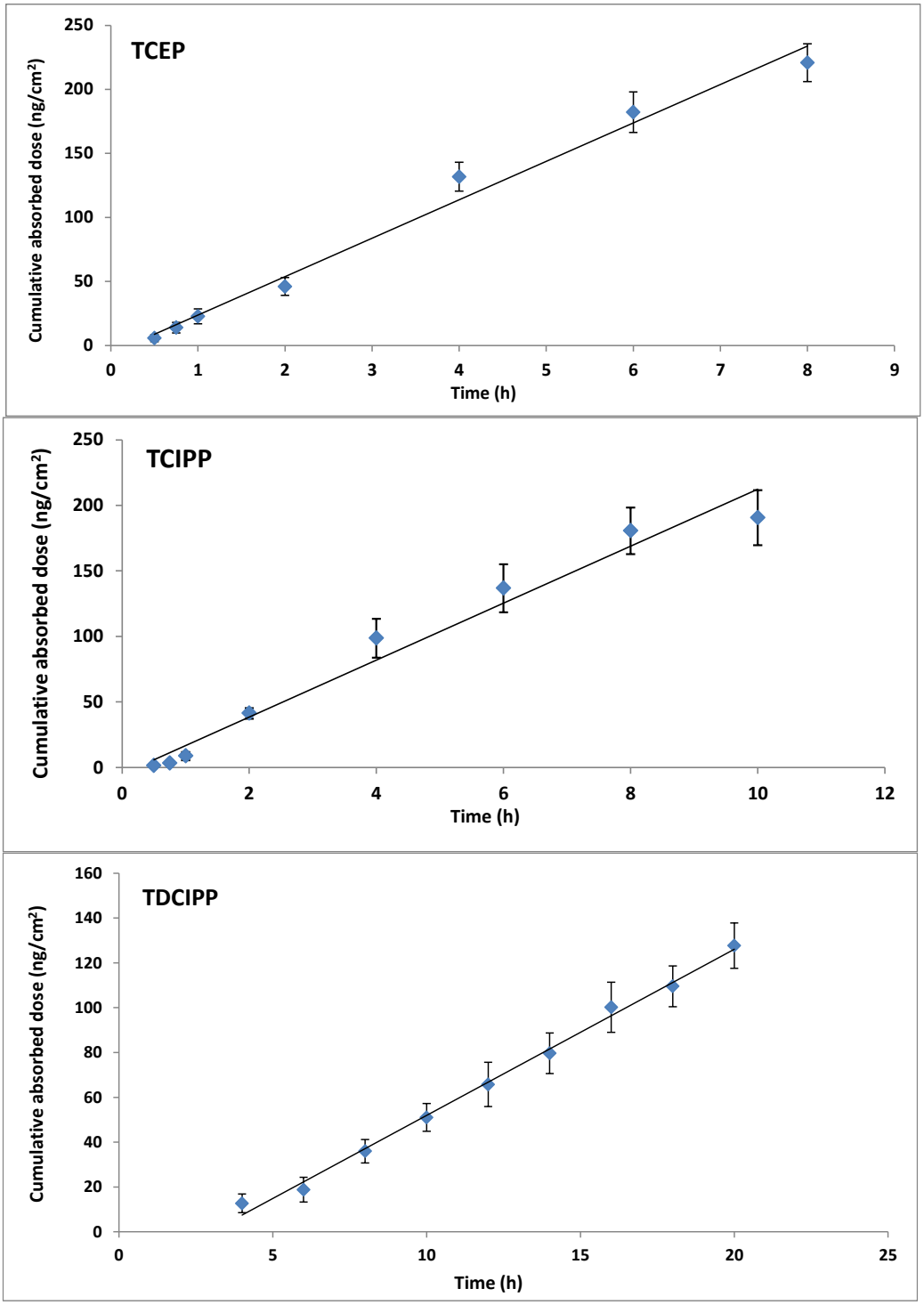

4.5.4: Other PFRs

4.5.4.1 TEHP & EHDPP

Tri-ethylhexyl phosphate (TEHP and 2-ethylhexyl-diphenyl phosphate (EHDPP) were applied at 1000 ng/cm^2 & 500 ng/cm^2 in acetone in triplicate to Episkin. The 24 h cumulative absorption values for TEHP and EHDPP across the Episkin model at 37 °C and 1000 ng/cm^2 dosing level were 0.50 ± 0.15 ng/cm^2, 62.1 ± 7.2 ng/cm^2 and 36.44 ± 3.4 ng/cm^2 respectively. A similar trend was observed for the 500 ng/cm^2 dosing level (Table 4.11). The results indicate that the absorption was highest in case of EHDPP and the least for TEHP. This behaviour could be attributed to the differences in the molecular weight and log K_{ow} values among these 3 target compounds. TEHP has the highest molecular weight of 434.65 g/mol and Log K_{ow} of 9.49. The transport of highly lipophilic chemical like TEHP occurs predominantly due to lipid rich stratum corneum and subsequent transfer into the aqueous epidermis is very slow or it could remain largely in the stratum corneum. The molecular weight & Log K_{ow} for EHDPP (362.4, 5.73) are lower than TEHP resulting in higher absorption across the skin. The amount remaining in the skin reservoir was higher for TEHP i.e. 750.43 ± 12.0 ng/cm^2 and 278.0 ± 9.5 ng/cm^2 for 1000 ng/cm^2 and 500 ng/cm^2 respectively. This is followed by EHDPP (578.12 ± 12.7 for 1000 ng/cm^2, 202.49 ± 7.0 for 500 ng/cm^2). Again this is due to high lipophilicity and molecular weight of TEHP. Significant amounts remained unabsorbed in all cases at both dosing levels.

Table 4.11: Distribution of target PFRs (expressed as ng/cm^2 ± standard deviation of exposure dose) in different fractions of the *in vitro* diffusion system following 24 h exposure to 1000 ng/cm^2 & 500 ng/cm^2 of the studied PFRs.

	TEHP						EHDPP					
	1000 ng/cm^2			500 ng/cm^2			1000 ng/cm^2			500 ng/cm^2		
Receptor fluid (24h)	0.30	±	0.1	0.22	±	0.08	35.24	±	2.5	47.25	±	3.5
Receptor rinse	0.20	±	0.05	0.08	±	0.02	1.20	±	0.9	2.0	±	1.2
Directly absorbed fraction	0.50	±	0.15	0.30	±	0.1	36.44	±	3.4	49.25	±	4.7
Skin-Epidermis (Depot)	750.43	±	12.0	278.0	±	9.5	578.12	±	12.7	202.49	±	7.0
Skin wash (unabsorbed)	182.0	±	6.0	197.63	±	13.5	91.0	±	14.0	99.0	±	9.0
Donor rinse (unabsorbed)	ND	±	ND	ND	±	ND	ND	±	ND	ND	±	ND
Total Recovery	93.29	±	17.56	95.17	±	15.0	70.39	±	1.2	70.0	±	10.0

Table 4.12: Flux rates (Jss, ng/cm^2 h), permeability constants (Kp, cm/h), lag times (t_{lag},h) and linear ranges (h) estimated from infinite exposure of EPISKIN^{TM} to 1000 ng/cm^2 of target PFRs for 24 h.

	J_{ss}	K_p
TEHP	0.0042	4.4 ± 0.28 (10^{-6})
EHDPP	1.30	2.29 ± 1.38 (x 10^{-3})

4.5.4.2: TCP isomers

The TCP isomers were dosed at infinite concentration (1000 ng/cm^2) in acetone in triplicate using Episkin. The cumulative absorption profiles for the neat isomers across the Episkin at 37 °C are shown in Fig 4.22 Each TCP isomer was found to continuously permeate for the full 24 h (i.e. steady state was not reached in 24 h). The cumulative amount in the receptor fluid was found to be 687 ± 15.25 ng/cm^2, 679 ± 11.23 ng/cm^2, 532 ± 19.7 ng/cm^2 for ToCP, TmCP and TpCP respectively. Thus the cumulative amount of isomers permeated at 24 h follows the order of ortho = meta > para but there is no statistically significant difference in the permeation between the three isomers. The amount remaining in the skin reservoir was similar i.e. 140-143 ng/cm^2 in case of ToCP and TmCP respectively. However, this amount was slightly higher for TpCP (163 ng/cm2). This could be attributed to the fact that the para isomer of tricresyl phosphate has a slightly lower water solubility and higher lipophilicity than the ortho and meta isomers. Therefore the partitioning of the *para* isomer to the lipid-rich *stratum corneum* is expected to be higher than the others. The unabsorbed amount was found to be 78.56 ± 1.06 ng/cm^2, 94.2 ± 3.70 ng/cm^2, 90.63 ± 3.31 ng/cm^2 for T*o*CP, T*m*CP and T*p*CP respectively. Flux values range from 22.14 ng/cm^2.h for *ortho* to 17.58 ng/cm^2.h for *para* isomer (Table 4.13).

The Kp (cm/hr) was found to be slightly similar i.e. for T*o*CP (2.22 cm/h); T*m*CP (2.14 cm/h); T*p*CP (1.80 cm/h). This could be due to the similar molecular weight (368 g/mol) and log K_{ow} (5.1) but the positioning of the methyl group on the benzyl ring may influence the permeability and toxicity of the different TCP isomers. Overall we achieved good recovery ranging from 75-87 % for all the isomers in the skin set up. However, a slight decrease in recovery for the TpCP isomer might be due to metabolism. It is therefore recommended to investigate potential dermal metabolism in future dermal exposure studies for each isomer.

Table 4.13: Distribution of TCP isomers in different fractions of the *in vitro* diffusion system following 24 h exposure to 1000 ng/cm^2 of the studied compounds.

EPISKIN™ (ng/cm^2)	ToCP	TmCP	TpCP
Receptor fluid	687 ± 15.25	679 ± 11.2	532 ± 19.7
Receptor Rinse	18.0 ± 3.8	5.0 ± 1.8	6.0 ± 0.89
Unabsorbed (Bud)	78.56 ± 1.0	94.2 ± 3.7	90.63 ± 3.31
Skin	143 ± 6.0	140.0 ± 0.16	163 ± 3.98
Recovery (%)	86.0 ± 5.6	87.3 ± 5.1	75 ± 11.5

Fig 4.25: Cumulative absorption of TCP isomers over 24 h

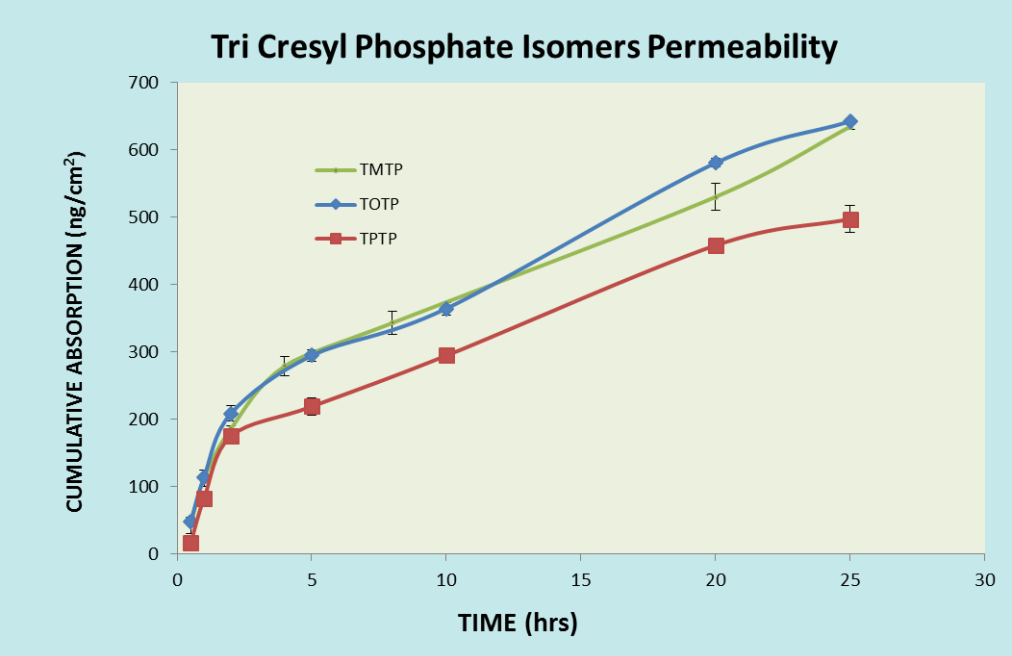

Table 4.14: Flux rates (J, ng/cm^2 h), permeability constants (Kp, cm/h) and linear ranges (h) estimated from infinite exposure of EPISKIN^{TM} to 1000 ng/cm^2 of TCP isomers for 24 h.

Episkin	J	K_p x 10^{-2}	R^2
T*o*CP	22.14	2.2	0.94
T*m*CP	21.44	2.1	0.95
T*p*CP	17.58	1.8	0.92

Fig 4.26: Linear cumulative permeation range (ng/cm^2) of TCP isomers following infinite exposure of Episkin to 1000 ng/cm^2 for 24 hours.

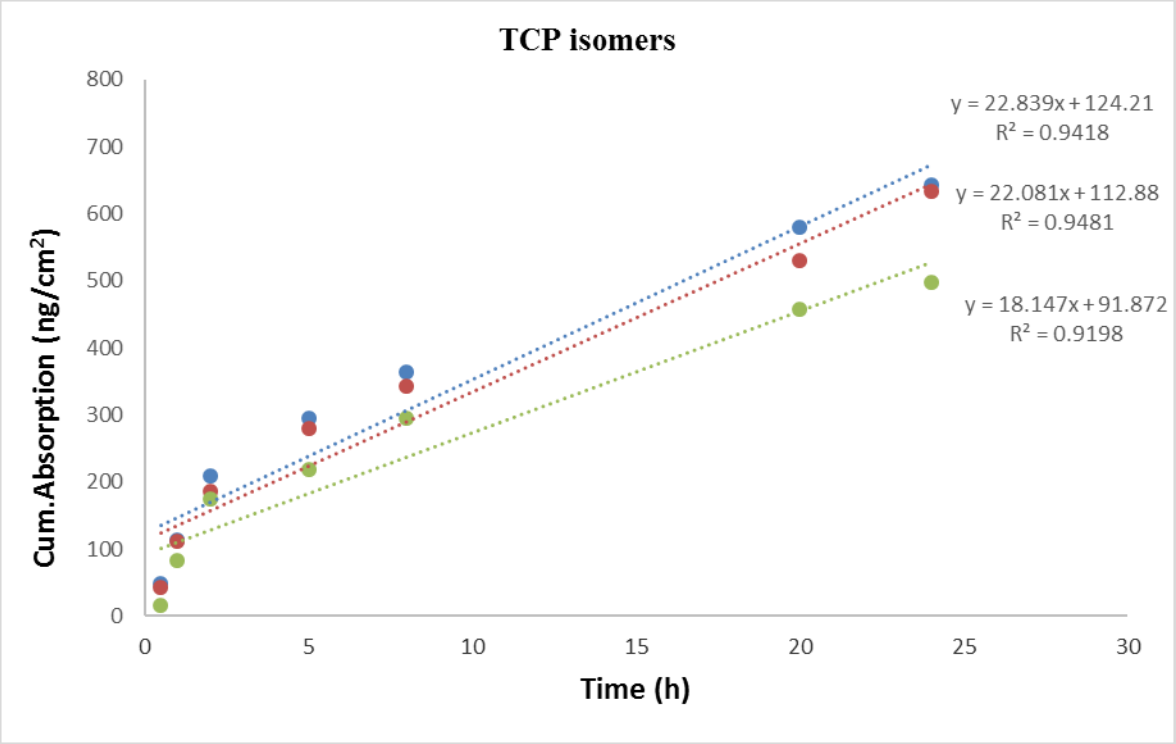

4.5.5: Human dermal absorption of Fire master -550 components (TPhP, EHTBB and BEHTEBP)

For TPhP and TBB the % absorption was higher at the lowest dosing concentration i.e. at 500 ng/cm^2 and lowest at the higher concentration i.e. at 2500 ng/cm^2. The % of absorption was 4.6, 9.6, and 18 (TPhP) and 0.37, 0.64, and 0.70 (EHTBB) at 2500 ng/cm^2, 1250 ng/cm^2 and 500 ng/cm^2 respectively. Kp was found to be constant at all the 3 dosing levels for TPhP i.e. 0.23 cm/hr and for EHTBB approx. 0.06 cm/hr. Kp is higher for TPhP than EHTBB as it is lighter molecule (higher diffusion rate) than EHTBB and TPhP possesses a log Kow of 4.65 which favours permeability according to LIPINSKI's rule of FIVE. BEHTBP was not detected in either the receptor fluid, receptor rinse or skin after 30 h of exposure at 3 concentration levels. This may be attributed to the high M.Wt (706 g/mol) and large molecular size of BEHTBP in addition to its high hydrophobicity. Further studies need to be carried out at lower dosing levels and for durations exceeding 30 hrs without losing the integrity of the skin. These studies are important as it may result in more substantial systemic circulation uptake especially for TPhP over chronic dermal exposure.

Table 4.15: Distribution in different fractions of the *in vitro* diffusion system following 12 h exposure for TPhP & 30 h exposure for EHTBB and TBPH at 2500 ng/cm^2 & 500 ng/cm^2

1200 ng/cm^2	**TPhP**	**EHTBB**	**BEHTEBP**
Absorbed*	4.6 ± 9.1	0.37 ± 0.15	ND
Unabsorbed#	24.0 ± 3.6	71.0 ± 13.8	60.0 ± 15.0
Skin	61.0 ± 14.5	18.0 ± 12.4	14 ± 10.0
Sum	89.6 ± 6.0	89.37 ± 3.5	74 ± 6.0
500 ng/cm^2	**TPhP**	**EHTBB**	**BEHTEBP**
Absorbed	18.1 ± 5.0	0.70 ± 0.30	ND
Unabsorbed	22.0 ± 16.5	69.0 ± 2.5	66.0 ± 12.0
Skin	55.0 ± 13.0	12.68 ± 3.8	10.5 ± 5.6
Sum	95.1 ± 7.5	92.38 ± 11.0	76.5 ± 17.0

4.5.6: Positive (2, 4, 6 TBP) and negative (DBDPE) controls

The validity and suitability of permeability assays were confirmed by reference compounds for high and low absorption. In this study, 2, 4, 6-tribromophenol was used as a high permeability reference (positive control) since it is a brominated phenol with increased polarity in the structure which would help the molecule to diffuse across the polar domain i.e. the epidermis of the skin. We also used DBDPE as a low permeability reference (negative control) because of its high molecular weight and lipophilic nature. These controls were run with every batch of permeability experiments.

When Episkin was dosed at 1250 ng/cm^2 , the cumulative amount absorbed was found to be 645.0 ± 8.3 ng/cm^2 and 2.71 ± 1.5 ng/cm^2 in case of 2,4,6 TBP and DBDPE respectively. The huge difference in this behaviour is due to differences in the physicochemical properties of these chemicals. For DBDPE the molecular weight is 971.22 g/mol and LogKow =11.1 whereas 2, 4, 6-TBP is a polar compound having a mol wt = 330.799 g/mol and Log Kow = 4.13. A higher amount i.e. 708.24 ± 112.58 ng/cm^2 of DBDPE remained on the skin unabsorbed due to its inability to penetrate the stratum corneum layers as a result of its high molecular weight. The proportion found in the skin depot was found to be higher for 2, 4, 6-TBP (201.0 ± 5.9 ng/cm^2) as compared to DBDPE (34.61 ± 8.8 ng/cm^2), while the flux for 2, 4, 6-TBP was 375.0 ng/cm^2.h and Kp was found to be 4.0 X 10^{-2} cm/hr. Due to the low permeability and inconsistency of cumulative absorption of DBDPE over 24 hr, the flux and Kp values could not be calculated. In study by Gabriel Knudsen et al (Knudsen, Sanders and Birnbaum 2016a) the potential dermal uptake of DBDPE was assessed using human and rat skin, with results revealing penetration to be 4% of the applied dose of 2.7 nmol/cm^2 with a major proportion (~ 12%) of the DBDPE remaining in the dermis as a skin depot. Compared to this study, our results showed only 0.59% of the initial dose absorbed across the skin; this could be due to the fact that in the previous study the DBDPE was dermally applied in an

organic solvent – namely toluene - resulting in higher permeability, whereas in our study we dosed in acetone which has minimal effect on the skin integrity as it easily evaporates at skin temperature when applied on the skin leaving the penetrant chemical behind to diffuse.

Table 4.16: Distribution in different fractions of the *in vitro* diffusion system following 12 h exposure for 2, 4, 6-TBP & 24 h exposure for DBDPE at 1250 ng/cm^2.

1250 ng/cm^2	2,4,6 TBP*	DBDPE**
Receptor fluid	645.0 ± 8.3	2.71 ± 1.5
Receptor rinse	27.0 ± 4.1	4.71 ± 0.66
Skin-Epidermis (Depot)	201.0 ± 5.9	34.61 ± 8.8
Skin wash (unabsorbed)	8.15 ± 1.6	708.24 ± 112.58
Donor rinse (unabsorbed)	1.5 ± 0.6	ND ± ND
Total Recovery	70.6 ± 4.1	60.02 ± 4.89

* 12 hr study ** 24 hr study

Fig 4.27: Linear cumulative permeation range (ng/cm^2) of 2, 4, 6 TBP following infinite exposure of Epikin to 1250 ng/cm^2 for 12 hours.

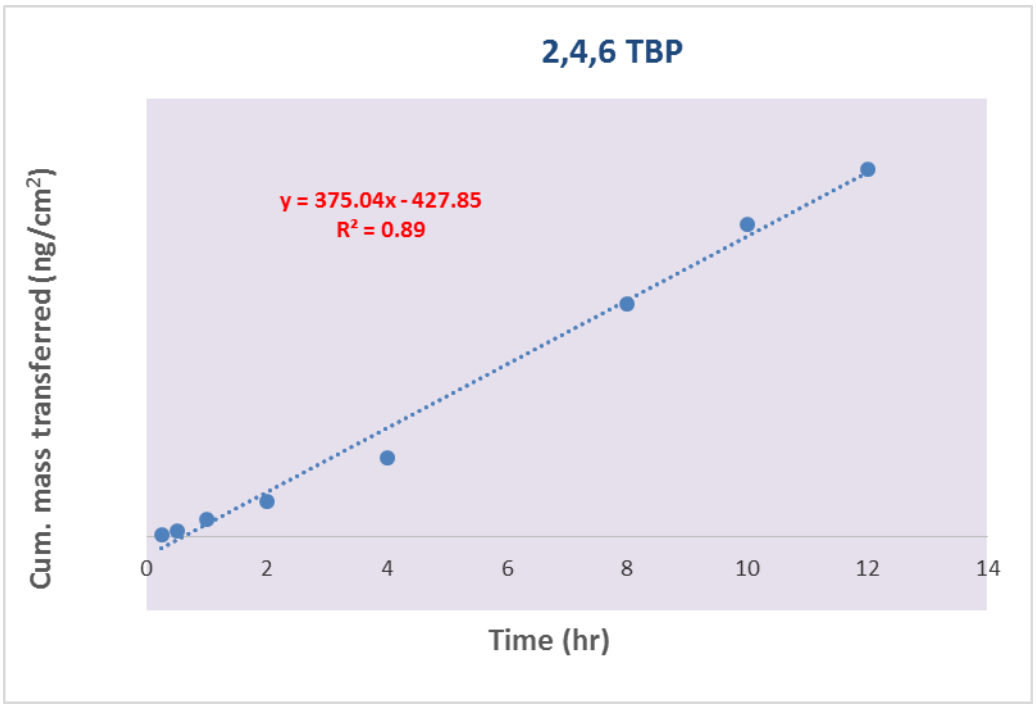

4.5.7: Dermal absorption of emerging brominated flame retardants (PBEB, PBBz, PBT, HBB, α, β-TBECH, *syn, anti*-Dechlorane plus)

The directly absorbed dose i.e. cumulative concentration in the receptor fluid over 24 hr (plus receptor compartment rinse) and the unabsorbed dose (skin surface wipes plus donor compartment rinse) were estimated for the following emerging flame retardants: pentabromoethylbenzene (PBEB), pentabromobenzene (PBBz), pentabromotoluene (PBT), hexabromobenzene (HBB), 1,2-dibromo-4-(1,2-dibromoethyl)cyclohexane and the chlorinated flame retardants *syn* and *anti* dechlorane plus (Table 4.5). The efficiency of the experimental approach was investigated using a mass balance exercise. The cumulative directly absorbed amount was found to be highest for α-TBECH and β-TBECH followed by PBEB, PBBz, PBT and HBB. The penta and hexa bromo series have slightly closer values i.e. 1.4-2.06 ng/cm^2. Surprisingly, the *syn* and *anti* dechlorane plus showed no penetration across the skin layers at both the concentrations over 24 hrs. This could be attributed to the high lipophilicity of dechlorane plus (LogKow – 9.0) and molecular weight (653.72). In contrast to this behaviour, TBECH has a lower mass and higher water solubility than dechloranes and penta and hexa brominated compounds. TBECH isomers have molecular weight < 500 (399.74) and a Log Kow <5.0 (3.73) which aids easy diffusion through the polar layers of epidermis. A significant proportion remained in the skin as a depot for all the compounds studied, which could penetrate the deeper layers of the skin and ultimately reach the systemic circulation after a period of time.

This highlights the influence of physicochemical properties on the human dermal bioavailability of a chemical. Flux (Jss) values ranged from 0.07–0.09 ng/cm^2·h for α-TBECH and β-TBECH respectively at 1000 ng/cm^2 (Table 4.17). Flux values for other EFRs studied were: HBB (0.0342 ng/cm^2·h), PBT (0.0583 ng/cm^2·h), PBZ (0.034 ng/cm^2·h) and

PBEB (0.067 ng/ cm^2·h). A decreasing trend of Kp with the increasing Log Kow was observed. (Table 4.18)

Table 4.17: Distribution in different fractions of the *in vitro* diffusion system following 24 h exposure for EFRs at 1000 and 500 ng/cm^2.

	PBEB		PBBz	
	1000 ng/cm^2	**500 ng/cm^2**	**1000 ng/cm^2**	**500 ng/cm^2**
Receptor fluid (24 h)	2.06 ± 0.8	1.8 ± 0.9	1.95 ± 0.85	1.55 ± 0.9
Receptor rinse	ND ± ND	ND ± ND	ND ± ND	ND ± ND
Skin-Epidermis (Depot)	699.0 ± 8.3	441.0 ± 10.5	592.3 ± 7.3	344.0 ± 4.17
Skin wash (unabsorbed)	81.76 ± 3.06	21.71 ± 8.67	203.5 ± 11.9	101.0 ± 9.0
Total Recovery	78.28 ± 11.5	88.21 ± 9.5	79.78 ± 16.7	89.21 ± 9.5
	PBT		**HBB**	
	1000 ng/cm^2	**500 ng/cm^2**	**1000 ng/cm^2**	**500 ng/cm^2**
Receptor fluid (24 h)	1.70 ± 0.8	1.5 ± 0.5	1.4 ± 0.74	1.2 ± 0.4
Receptor rinse	ND ± ND	ND ± ND	ND ± ND	ND ± ND
Skin-Epidermis (Depot)	593.4 ± 8.3	345.0 ± 6.7	811.6 ± 17.4	379.0 ± 11.0
Skin wash (unabsorbed)	111.5 ± 1.29	90.0 ± 5.8	76.89 ± 12.8	48.75 ± 5.6
Total Recovery	71.0 ± 4.0	87.3 ± 8.9	88.98 ± 13.0	85.7 ± 9.2
	α-TBECH		**β-TBECH**	
	1000 ng/cm^2	**500 ng/cm^2**	**1000 ng/cm^2**	**500 ng/cm^2**
Receptor fluid (24h)	1.97 ± 0.5	2.10 ± 1.2	1.80 ± 0.9	2.3 ± 1.2
Receptor rinse	2.46 ± 1.2	3.0 ± 2.0	2.20 ± 1.4	2.8 ± 3.0
Skin-Epidermis (Depot)	682.2 ± 13.7	300.0 ± 5.6	589.0 ± 16.2	318.0 ± 5.6

Skin wash (unabsorbed)	249.9	±	6.97	88.41	±	6.0	189.0	± 14.5	90.0	±	12.5
Total Recovery	93.4	±	7.0	78.63	±	8.5	78.2	± 19.0	82.6	±	11.0

	***Syn*-DP**				***Anti* –DP**			
	1000 ng/cm^2		**500 ng/cm^2**		**1000 ng/cm^2**		**500 ng/cm^2**	
Receptor fluid (24h)	ND	± ND	ND	± ND	ND	± ND	ND	± ND
Receptor rinse	ND	± ND	ND	± ND	ND	± ND	ND	± ND
Skin-Epidermis (Depot)	517.0	± 11.0	312.0	± 8.5	482.0	± 16.0	298.0	± 6.0
Skin wash (unabsorbed)	188.2	± 19.0	74.0	± 9.0	176.0	± 14.0	64.0	± 7.0
Total Recovery	70.0	± 16.0	77.2	± 8.7	66.0	± 17.0	72.4	± 11.0

Table 4.18: Flux rates (Jss, ng/cm^2 h), permeability constants (Kp, cm/h) and linear ranges (h) estimated from infinite exposure of EPISKIN^{TM} to 1000 ng/cm^2 of EFRs for 24 h.

Episkin	J_{ss}	$K_p * 10^{-5}$	R^2
PBEB	**0.067**	**6.7**	**0.89**
PBBz	**0.0340**	**3.40**	**0.80**
PBT	**0.0583**	**5.8**	**0.99**
HBB	**0.0342**	**3.42**	**0.89**
α-TBECH	**0.0705**	**7.05**	**0.74**
β-TBECH	**0.0965**	**9.65**	**0.98**
***Syn*, *Anti*-Dechlorane Plus**	**NM**	**NM**	**NM**

4.5.8: Summary

Overall our neat compound application for all the FRs (with varying physicochemical properties) to the HSE models results showed a significant negative correlation between the permeability constant of FRs and their Log K_{OW} values i.e. lower the molecular weight of the chemical (< 500 g/mol) and if the LogKow is within the ideal range (3-5), the dermal absorption would be higher. For some of the chemicals which have got high molecular weight and high lipophilicity like BDE 209, DBDPE and syn, anti DP we have observed no absorption or penetration through the skin where as other high molecular weight compounds like were found to be highly accumulated in the stratum corneum layer with very low dermal absorption.

Fig 4.28: Correlation between Log Kp and Log Kow values of the studied FRs. (R^2 = 0.7198 and P < 0.01)

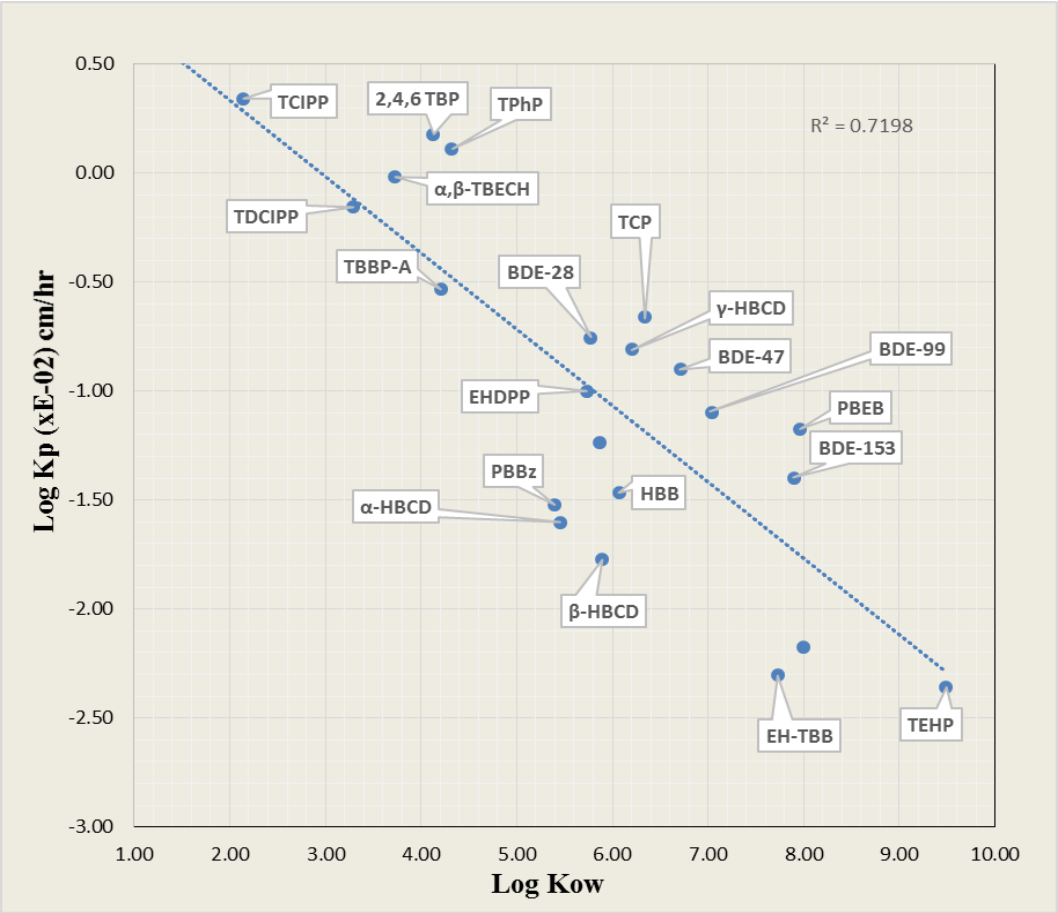

CHAPTER V

TOWARDS UNDERSTANDING THE ROLE OF SKIN MOISTURE AND OILINESS ON DERMAL UPTAKE OF FLAME RETARDANT CHEMICALS

This chapter contains some material taken verbatim from Pawar, G., M. A. Abdallah, et al. (2016). Dermal bioaccessibility of flame retardants from indoor dust and the influence of topically applied cosmetics. J Expo Sci Environ Epidemiol 6(10): 84.

5.1: INTRODUCTION

We spend the majority of our day indoors, where we are frequently exposed to flame retardants (FRs) due to the presence of such chemicals in consumer goods like furniture, electronics and building materials (van der Veen and de Boer 2012a).This is illustrated by numerous studies showing significant concentrations of HBCDs & PFRs in indoor dust (Abdallah and Covaci 2014a, Brommer and Harrad 2015, Abdallah et al. 2008b).

Humans are exposed to FRs mainly via diet, dust inhalation/ingestion and dermal contact with dust or consumer products (Abdallah et al. 2008b, Frederiksen et al. 2009, Watkins et al. 2011, Xu et al. 2016). Few studies have characterised the concentrations of HBCD isomers in indoor dust (Roosens et al. 2009), human blood (Li et al. 2014, Xiao et al. 2011) and breast milk (Eljarrat et al. 2009). (Roosens et al. 2009) reported positive correlation of HBCD concentrations in human serum with those in indoor dust samples and also other studies (Johnson et al. 2010, Watkins et al. 2012) reported positive correlations for PBDEs (BDE 47, 99 and 100).Wu et al. (Wu et al. 2007) reported correlations between breast milk and dust

concentrations of tetra-hexaBDEs.In contrast to these studies one study even (Cequier et al. 2015) reported negative correlation between dust concentrations and serum levels where as the diet indicated a higher contributions to the body burdens compared to the indoor environment. However Roosens et al reported no such correlation for HBCDs dietary exposure. Despite highlighting the importance of the internal and external body burdens and the pathways of exposure like dust ingestion or diets contribution, previous studies have not provided conclusive evidence of how external exposure drives human body burdens of FRs.

Other research findings (Stapleton et al. 2014, Stapleton et al. 2012b, Watkins et al. 2013) suggested that handwipes were a strong predictor of serum PBDE levels. In another study (Hoffman et al 2015) TDCIPP and TPhP were detected frequently in hand wipes and dust. One of the recent study analysed hand wipes which are more likely to reflect exposures for PFRs arising from contact with surfaces (Hammel et al. 2016). Such exposures may arise from hand-to-mouth contact and/or dermal absorption as concentrations of PFRs on hand wipes were associated with concentrations of their metabolites in urine (Stapleton et al. 2008a). Potential metabolites of PFRs have been studied in human biological matrices like urine. (Butt et al. 2014a, Meeker et al. 2013, Hoffman, Daniels and Stapleton 2014, Van den Eede et al. 2013, Van den Eede et al. 2015). These studies have correlated the concentration found in dust and its metabolites in urine, albeit little is known about the potential route of exposure. Even non-invasive samples like hair (Kucharska et al. 2015b) and nails (Liu et al. 2016) were also found to be contaminated with PFRs.

Recent studies have provided estimates of external human exposure to PFRs via inhalation (Bergh et al. 2011), ingestion of indoor dust (Abdallah and Covaci 2014b) and diet (Malarvannan et al. 2015). However, very little is known about the relative contribution of dermal exposure pathway to the overall human body burdens of these contaminants. Furthermore, pharmacokinetic modelling of the extensively studied PBDEs suggested the

potential significance of dermal contact with indoor dust as a pathway of human exposure to these FRs (Lorber 2008b, Trudel et al. 2011a). Despite this, as of now there remains a paucity of data testing the hypothesis that contaminants are transferred from dust to the skin and its subsequent absorption to reach the systemic circulation.

We have studied the *bioaccessibility* (the amount of the chemical that is potentially available for absorption and is dependent on the rate of release from the dust particles and its solubility into the physiological fluids like sweat/sebum) and *bioavailability* (the amount of chemical absorbed and is available for physiological function) for HBCDs and PFRs compounds applied in "neat" form to shed some light on the importance of dermal exposure in risk assessment however this exposure will differ from the real life exposure scenario where contaminants are present not as standards in organic solvents but in "real-world" matrices like dust particles, fibres or hard plastic pellets etc. Exposure to standard chemicals can occur during handling the chemicals or at the work place but majority of the chemicals are exposed to humans via indoor dust or consumer goods. The uptake of the chemicals from the vehicle /organic solvent would be different from that of dust exposure because the chemicals adsorbed on the dust particles needs to partition first to the sweat or the sebum (oily phase) on the skin surface and then the stratum corneum. Also in case of neat compound application, the partitioning/diffusibility would be faster. The dust particles adhered to the skin surface could be the potential source of highly lipophilic flame retardants which could be absorbed by the skin. Another factor which prompted us to go beyond the neat application study is the presence of cosmetics on the skin surface. Cosmetics (e.g. sunscreen creams) may contain certain ingredients (e.g. surfactants) which can increase the oiliness of the skin, remain on the skin and become incorporated within the skin surface film liquid. This in turn, may alter the lipid domain of the skin thereby increasing the partitioning of chemicals to the stratum corneum. Furthermore, the presence of natural surface active agents in this human skin

surface film (sweat/sebum mixture) (Stefaniak, Harvey and Wertz 2010), may influence the dermal absorption of these PFRs.

Against this background, the aim of this chapter is to mimic real life scenarios to study uptake of HBCDs and PFRs from indoor dust in the presence of sweat/ sebum and topically applied moisturising cream.

Fig 5.1: Schematic diagram showing the concept of dermal exposure

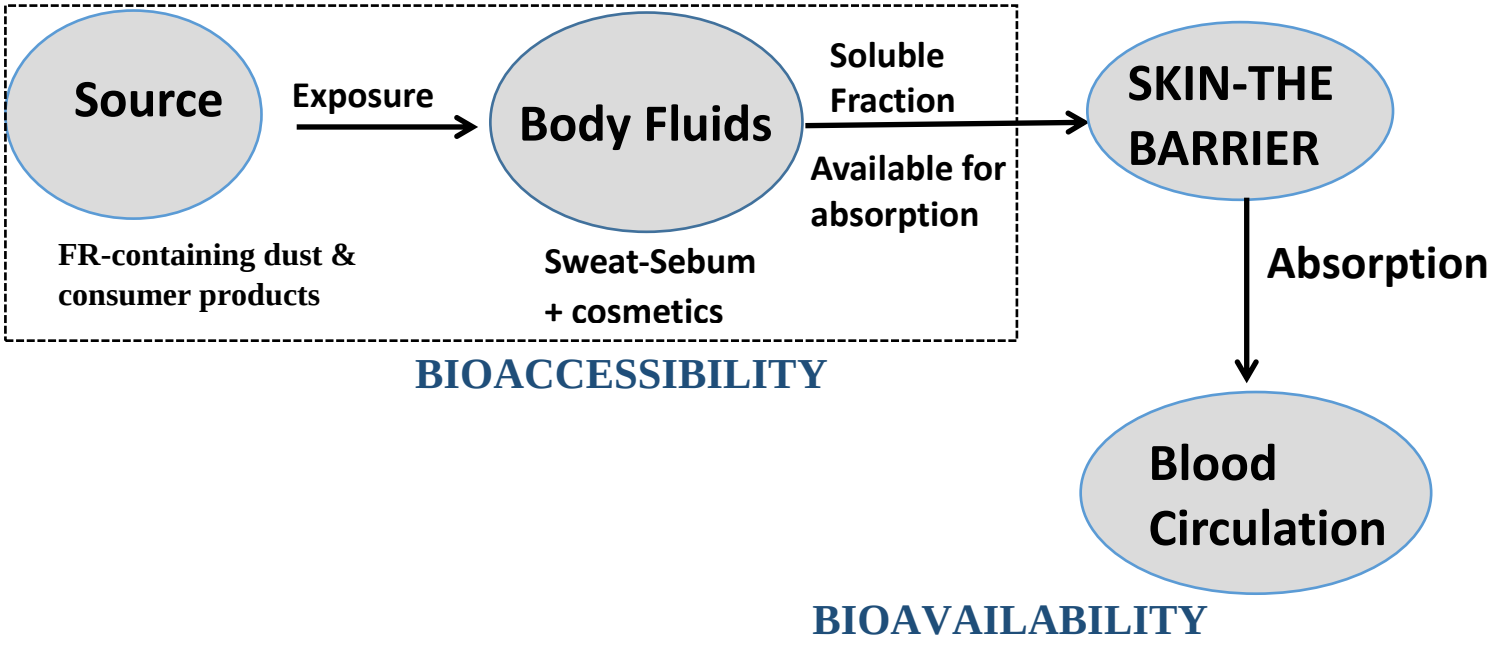

5.2: METHODOLOGY

5.2.1: Dust SRM2585 with the indicative values for HBCDs and OPFRs was used to study the dermal uptake of these compounds.

5.2.2: Synthetic Sweat and Sebum formulation

A synthetic sweat solution was prepared by dissolving electrolytes, organic acids, carbohydrates, amino acids, nitrogenous substances and vitamins in 500 mL of 18 MΩ-cm distilled and deionised water at 32 ºC to mimic the temperature of human skin. A synthetic sebum mixture was likewise prepared according to Stefaniak and Harvey (2008) by dissolving physiologically-relevant proportions of squalene, cholesterol oleate, triolein

(unsaturated), and palmityl oleate in hexane (quantity sufficient). The detailed composition of both the synthetic sweat and sebum mixtures are to be found in Chapter 2 Section 2.2.2.

5.2.3: Episkin Dust Exposure

Episkin was equilibrated in 12 co-star well plates in 2.5mL culture media at 37 °C. After 30 mins equilibration, the skin surface was exposed to 50-60 mg of SRM-2585 dust uniformly with the help of a spatula and a brush under 4 different scenarios: (a) just dust; (b) dust in presence 100µL of (1:1 v/v) of sweat: sebum mix; (c) dust in presence of 100 µL of 20% Tween 80, and (d) dust in presence of 50 mg of moisturising cream. Each of the scenarios was examined in triplicates. (Fig 5.2). After 15 mins of gentle shaking the plate was incubated at 37°C with humidified air containing 5% CO_2. In case of moisturising cream, 50 mg of cream was weighed in a tared clean glass tube and then with the help of a spatula, the cream was applied on the surface of the skin before spreading or exposing the dry dust on the skin surface. For all the 12 wells at serial time points, the receptor fluid was collected up to termination of exposure at 24 hr by removing the dust from the skin surface with a cotton bud soaked in hexane. At termination, the skin patches were removed with forceps and subjected to tape stripping (n=5) (Fig 2) and receptor compartments were washed separately (5 × 2 mL) with PBS. All samples (Receptor fluid, skin, cotton buds, well wash and tape strips) were stored at −20 °C until chemical analysis.

5.2.4: Extraction-Clean-up and Analysis

Receptor fluid, well wash, tape strips, cotton buds and the epidermis (after homogenisation) were spiked with 30 µL of ^{13}C-isotopically labelled α-HBCD, β-HBCD, γ-HBCD and TPhP-d15 (1 ng/µL), prior to extraction with 3 mL of hexane: ethyl acetate (1:1 v/v) mixed with 200 µL acetone (protein precipitation) using a QuEChERS-based method. Sample tubes were vortexed on a multi-positional mixer for 5 mins, followed by ultra-sonication for 5 mins and centrifugation at 3000 rpm for 5 mins. The extraction cycle was repeated twice before the

pooled supernatant was collected in a clean tube. The receptor fluids crude extracts were dried completely and reconstituted in 150 µL of methanol containing 50 pg/µL of d_{18}-α-HBCD and analysed later on LC-MS/MS. Target PFRs were reconstituted in 100 µL of isooctane containing 13C-BDE-100 used as RDS prior to GC/MS analysis according to a previously reported method (Abdallah and Covaci 2014b).

Fig 5.2 Schematic Diagram Plate A: The first three skin patches were applied with 50 mg of dry SRM-2585 dust to mimic " dry" skin condition and other 3 skin patches were dosed with 100µL of sweat and sebum (1:1 v/v) mixture before applying 50 mg of SRM-2585 dust uniformly. Plate-B: 50 mg of SRM -2585 dust was applied on the skin surface in presence of 20% Tween 80 (100µL) in triplicate and moisturising cream was applied uniformly with the help of spatula on skin surface and then 50 mg SRM-2585 dust was applied to cover the surface.

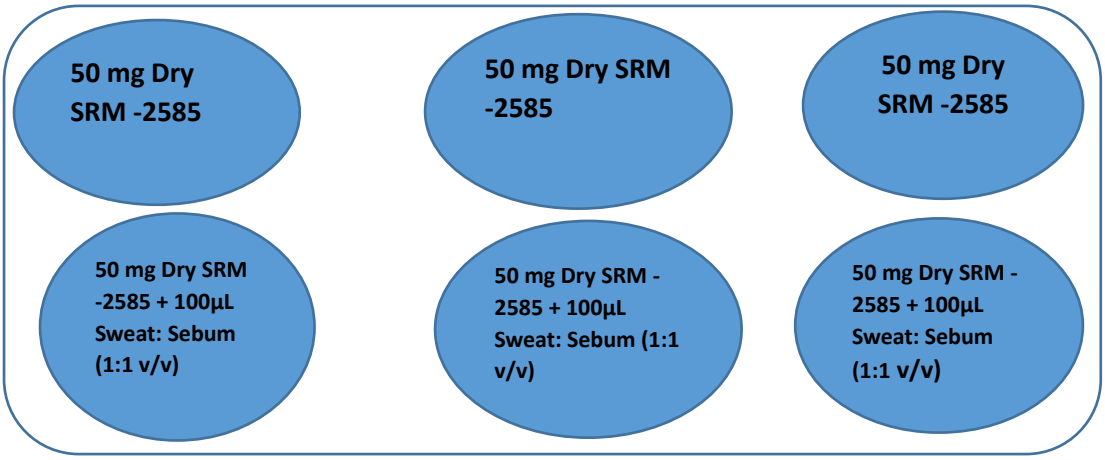

Plate A

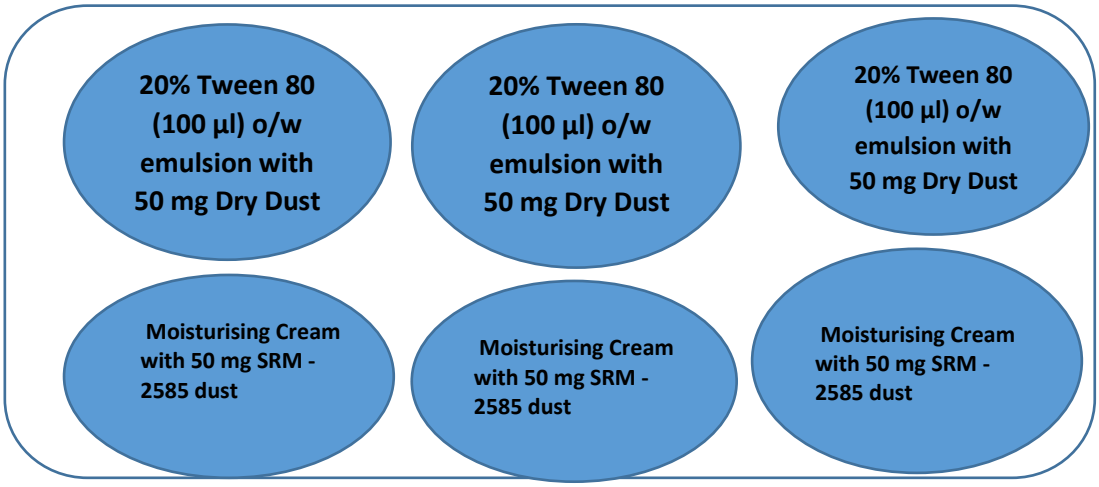

Fig 5.3: Tape stripping with the help of 3M adhesive tape (Pic 1-4).

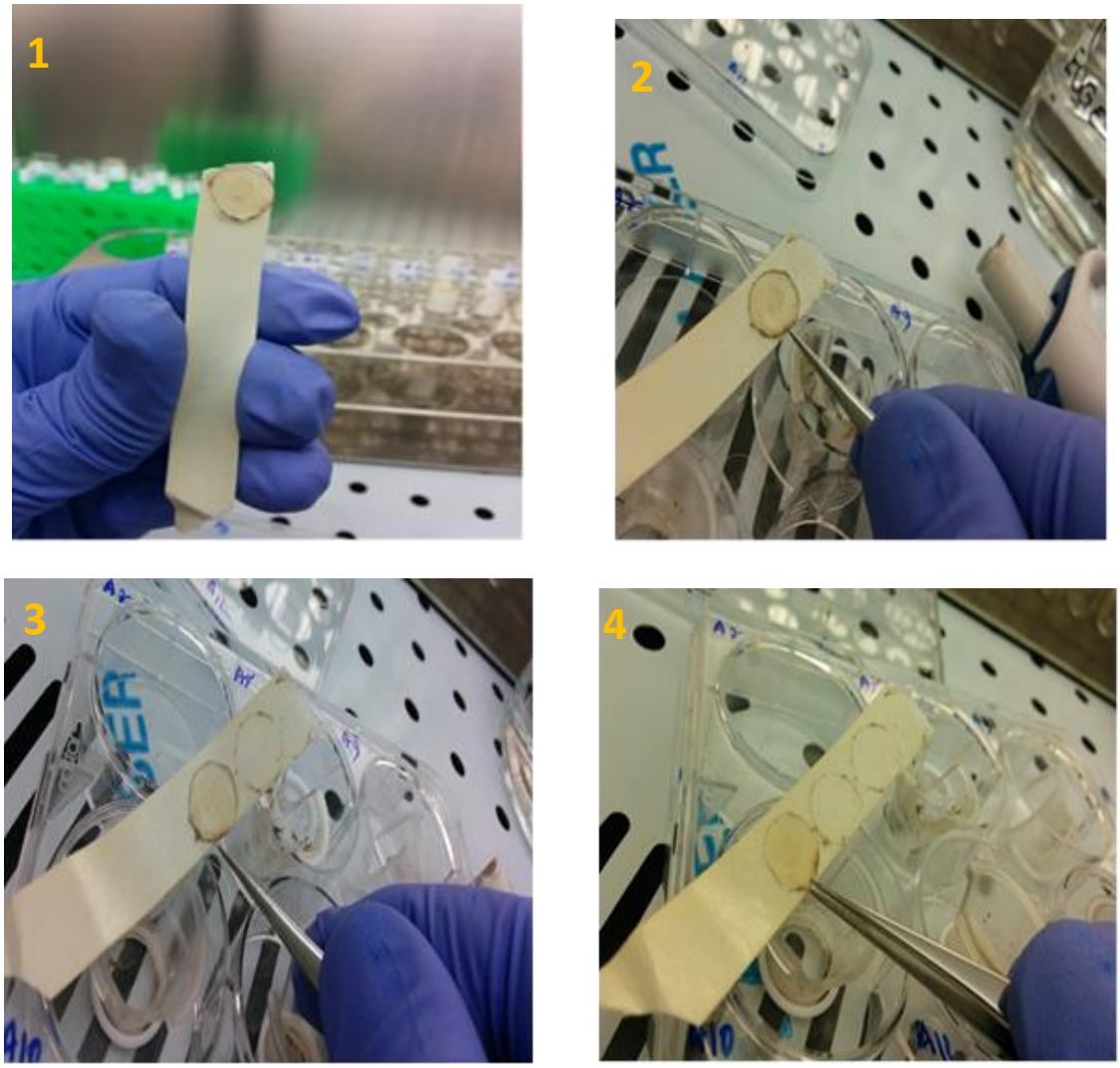

After terminating the exposure, the Episkin patch was dismantled from the Transwell "O" ring and with the help of clean forceps (rinsed in acetone between each stripping) the upper stratum corneum surface (1 cm^2) was placed towards the adhesive film for 2 mins and removed gently. In this way the stripping was carried out 5 times. After the sampling the tapes were placed in a clean test tube for further analysis. The tape strip contains the amount of corneocytes and the corresponding amount of penetrated target chemicals which were determined later by LC-MS/MS.

The crude extract of tape strips , cotton buds containing dust, sebum, moisturising cream & 20% Tween 80 (~1 mL) was cleaned up by loading onto a Florisil SPE cartridge (pre-conditioned with 6 mL of hexane). Fractionation was achieved by eluting with 8 mL of hexane (Fraction 1:F1 for HBCDs) followed by 10 mL of ethyl acetate (Fraction 2: F2 for PFRs). F1 was washed with ~ 2 mL of 95 % H_2SO_4 to remove lipids. The organic layer and washings were combined and evaporated to incipient dryness under N_2.Target analytes were reconstituted in 150 µL of methanol containing 50 pg/µL of d_{18}-α-HBCD used as recovery determination (Abdallah et al. 2014b). Fraction F_2 was evaporated to incipient dryness under N_2. Target PFRs were reconstituted in 100 µL of isooctane containing ^{13}C-BDE-100 used as RDS prior to GC/MS analysis according to a previously reported method (Abdallah and Covaci 2014b). Further details of instrumental analysis are provided in Chapter 2.1.3

5.3: QA/QC

We evaluated the mass balance for each exposure experiment by dividing the sum of FR masses found in all skin compartments by the initial mass (ng) applied on the skin surface. We also checked for the level of PFRs in the 3M adhesive tapes before using it and the PFRs were not detected. The recovery of initially applied FR mass was between 60-95 % across all tested FRs and exposure scenarios. (Table 5.2) The reasons for the obtained recoveries might be due to the possible dermal metabolism, losses during extraction/clean-up steps and analytical variabilities. Statistical analysis of the data was conducted using Excel (Microsoft Office 2003) and SPSS version 13.0. ANOVA tests were performed on concentrations in the receptor fluids and the skin. ($P \leq 0.05$, if differences are significant)

5.4: RESULTS & DISCUSSION

Concentrations of target FRs measured in all the compartments under all four exposure scenarios are shown in Figure 5.4 and Table 5.1. When dry dust was exposed to the Episkin, in 24 hrs time the cumulative absorption (receptor fluid plus receptor rinse) was found to be 0.85 ± 0.14 ng/cm^2, 0.079 ± 0.05 ng/cm^2 & 0.408 ± 0.36 ng/cm^2 for α-HBCD, β-HBCD and

γ-HBCD respectively. The absorption was higher in α-isomer followed by γ-isomer and then least for β-isomer. This behaviour could be due to lower water solubility of the γ-isomer (2 μg/L) compared to that of β–HBCD (15 μg/ L) and α-HBCD (49 μg/ L) (Abdallah et al. 2012). Surprisingly the absorbed amount is higher in γ-isomer as compared to the β isomer even though it has the lowest water solubility this may be due to the lesser concentration of β isomer than the γ-isomer in the SRM-2585 dust. This trend is more evident in the wet exposure scenario where in the presence of sweat/sebum mixture the amount absorbed was increased as compared to dry condition, it was found to be 5.19 ± 2.74 ng/cm^2, 0.77 ± 0.40 ng/cm^2, 0.75 ± 0.30 ng/cm^2 for α-HBCD, β-HBCD & γ-HBCD respectively. We also analysed the skin after removing the 5 outermost layers of the stratum corneum, the rationale behind performing only 5 stripping is that in the real life scenario these layers are considered as outside the body (not absorbed) and undergoes desquamation regularly. The rest of the contaminants in the stratum corneum layers can be considered as the "stored within the skin". The amount remained in the skin layers for α-HBCD, β-HBCD & γ-HBCD are 4.13 ± 0.55 ng/cm^2, 2.56 ± 0.14 ng/cm^2 & 4.40 ± 0.81 ng/cm^2 respectively. This amount is slightly increased in presence of sweat and sebum mixture. The effect of exposure conditions had increased the permeability of the FRs from the dust but statistically not so significant (P >0.05). The cumulative absorption values in the presence of 20% Tween 80 were 10.55 ± 6.48 ng/cm^2, 1.43 ± 0.94 ng/cm^2, 10.19 ± 5.73 ng/cm^2 for α-HBCD, β-HBCD & γ-HBCD respectively. However this amount penetration decreased in presence of 50 mg applied moisturising cream (3.31 ±1.76 ng/cm^2, 0.42 ± 0.27 ng/cm^2 and 0.42 ± 0.24 ng/cm^2 for α-HBCD, β-HBCD & γ-HBCD respectively) due to the retention of lipophilic HBCDs in the moisturising cream's lipids.

In case of dry dust exposure the receptor compartment concentration was found to be 1.7 ± 1.2 ng/cm^2, 6.43 ± 3.45 ng/cm^2, 4.43 ± 1.74 ng/cm^2 for TCEP, TCIPP and TDCIPP

respectively. Interestingly we observed the cumulative absorption increased in case of wet scenario. The values were 9.98 ± 3.8 ng/cm^2, 321.78 ± 18.03 & 130.52 ± 20.01 ng/cm^2 for TCEP, TCIPP and TDCIPP.

The amount remained in the skin layers also increased in wet condition due to the sweat/sebum effect. It increased from 142.91 ± 12.67 ng/cm^2 to 344.64 ± 54.12 ng/cm^2 (TCEP), 114.0 ± 6.8 ng/cm^2 to 518.5 ± 8.9 ng/cm^2 (TDCIPP). These higher values may arise due to enhanced solubility or dissolution of these FRs in the presence of sweat and sebum. Alternatively and/or additionally, they may arise as a result of enhanced partitioning/ diffusion of sebum through stratum corneum layers and enhanced permeability of sweat through the epidermis, which in both instances could have enhanced the permeability of the chemicals. However this trend was not observed in TCIPP which could be due to metabolism or analytical variability. Interestingly the 20% Tween 80 and moisturising cream further decreased the penetration in comparison to the sweat/sebum mixture. In the presence of 20% Tween 80 the receptor fluid concentration was 5.46 ± 3.56 ng/cm^2 (TCEP), 92.69 ± 24.2 ng/cm^2 (TCIPP) & 90.59 ± 6.95 ng/cm^2 (TDCIPP) and in case of moisturising cream the concentration decreased to 3.0 ± 1.96 ng/cm^2 (TCEP), 19.54 ± 9.43 ng/cm^2 (TCIPP) & 42.62 ± 16.94 ng/cm^2 (TDCIPP).

In comparison to HBCDs, PFRs were found to be more absorbed in both the wet and dry scenarios. The first reason for this behaviour is due to higher water solubility for PFRs as compared to the HBCDs isomers which helps in higher solubility in sweat and then partitioning into the hydrophilic epidermis as compared to HBCDs. The second reason is that the PFRs have higher concentrations in the dust so the absorption rate is dependent on the concentration gradient for the chemical on the skin surface. Third, due to higher lipophilic nature of HBCDs, they were found to be stored in the skin preferentially in the epidermis layers resulting in prolonged release into the receptor fluid. PFRs showed higher absorption

in 24 hrs time as compared to the HBCDs in presence of Tween-80 and moisturising cream. This might be due to enhanced permeation of PFRs by Tween 80 or moisturising cream through the lipophilic stratum corneum layers. Whereas for HBCDs the viable epidermis would increase the resistance for permeation.

The increase in the target compound recovered from the tape stripping and the epidermis demonstrated that artificial sweat-sebum mixture and 20% Tween 80 enhanced the transfer of flame retardants from the dust particles.

5.5: Implications for human expsoure

The results of dermal absorption and penetration of HBCDs and PFRs from the dust across the skin layers were used to assess the daily internal dose of the target FRs using the general equation:

$$DED = \frac{C \text{ x } BSA \text{ x } DAS \text{ x } F_A \text{ x } IEF}{BW \text{ x } 1000} \quad \ldots (1)$$

Where DED = Daily exposure dose (ng/kg bw/day), C = PFR concentration in dust (ng/g), BSA =Body surface area exposed (cm^2), DAS = Dust adhered to skin (mg/cm^2), FA = fraction absorbed by the skin (unitless), IEF = indoor exposure fraction (hours spent over a day in a certain indoor environment) (unitless), BW = Body weight (kg).

We estimated the dermal exposure of 2 age groups (adults and toddlers) using three exposure scenarios i.e. dry expsoure, wet exposure and in presence of moisturising cream.

We used the concentrations in SRM-2585 Dust (Chapter 2, Table 2.5) and the parameter F_A in equation 1 was replaced by the experimental values obtained in this study for the uptake of each target HBCDs & PFR from the SRM-2585 dust using the Episkin model (Table 5.2). Values for other parameters in equation 1 were obtained from the USEPA exposure factors handbook (USEPA 2011) and summarized in Table Chapter 3, Table 3.7.

When the adults and toddlers group were compared for the dry skin, wet skin and in presence of moisturising creams scenario the differences were found to be slightly higher in toddlers

group (Table 5.3), however the differences between them were not statistically significant (P>0.05). This may be attributed to more dust adhering to the toddlers' skin and higher exposed skin surface area to body weight ratio compared to adults. We have also noticed that the daily dermal estimates for the FRs were found to be lower when we considered the data on the bioavailable fraction (subsequent dermal transfer of the studied FRs from sweat/sebum or in presence/absence of moisturising cream across the epidermis to the systemic circulation) as compared to the bioaccessible fraction of the FRs from the dust to the sweat/sebum mixture. This is obvious as the skin is the main barrier to the absorption and penetration of the FRs. Other important aspects of exposure is that of the applied moisturising creams, the daily dermal estimates in both the adults and toddlers were found to be lower than that of the dry and wet skin expsoure which could be due to the possible retention of the lipophilic FRs in the fatty formulation of cosmetics. Its worth to note that our dermal exposure estimates assume a fixed body area undergoing a constant exposure to FRs in indoor dust for a constant period of time and not for a chronic exposure. Such a rigid assumption may introduce uncertainty to our estimates of dermal exposure, more research is required to fully elucidate the toxicological implications of such exposure in both adults and toddlers. Our worst-case scenario exposure estimates for dermal exposure of adults and toddlers (Table 5.3) fall far below the HBLV values of No Significant Risk Level (NSRL) of 5.4 µg/day for TDCIPP (OEHHA 2015). No other health based limit values (HBLVs) of legislative standing for our target FRs were found in the literature. Our estimates of daily dermal uptake of FRs from the dust shows that the composition (i.e. sweat: sebum ratio) of skin fluids, as well as the presence/absence of commonly used skin cosmetics is demonstrated to exert a substantial influence on the efficiency with which our target FRs are released from dust and rendered available for dermal uptake.

	α-HBCD			β-HBCD			γ-HBCD			TCEP			TCIPP			TDCIPP		
Dry Dust Exposure (SRM-2585)																		
Receptor fluid (24hr)	0.68	±	0.05	0.039	±	0.02	0.0486	±	0.15	1.20	±	0.78	5.23	±	2.9	3.23	±	1.09
Receptor rinse	0.17	±	0.09	0.040	±	0.03	0.36	±	0.21	0.5	±	0.42	1.2	±	0.55	1.2	±	0.65
Tape Strip (S.Corneum)	0.019	±	0.02	0.34	±	0.17	1.29	±	0.8	25.48	±	13.09	91.53	±	8.9	393.96	±	12.42
Skin-Epidermis (Depot)	4.13	±	0.55	2.56	±	0.14	4.40	±	0.81	142.91	±	12.67	192.0	±	26.86	114.0	±	6.8
Cotton wipe (unabsorbed)	11.52	±	0.19	0.53	±	0.30	106.97	±	5.33	535.14	±	20.56	420.56	±	9.39	512.0	±	8.4
Total Recovery (%)	64.3	±	2.45	84.7	±	12.65	86.31	±	7.43	94.0	±	6.78	89.9	±	6.7	60.61	±	8.2
Dust Exposure (SRM-2585) in presence of 1:1 v/v Sweat and sebum mixture																		
Receptor fluid (24h)	5.06	±	2.67	0.58	±	0.36	0.6	±	0.25	6.16	±	1.8	316.88	±	16.80	123.02	±	17.21
Receptor rinse	0.13	±	0.07	0.19	±	0.04	0.15	±	0.05	3.82	±	2.0	4.90	±	1.23	7.5	±	2.8
Tape Strip (S.Corneum)	0.14	±	0.05	0.07	±	0.06	0.61	±	0.22	19.42	±	7.8	57.62	±	18.9	84.32	±	9.6
Skin-Epidermis (Depot)	4.33	±	0.03	2.27	±	0.11	4.51	±	0.58	344.64	±	54.12	151	±	8.36	518.5	±	8.9
Cotton wipe (unabsorbed)	7.65	±	3.45	0.46	±	0.05	89.43	±	14.5	183.61	±	26.92	211.31	±	67.0	314.32	±	5.0
Total Recovery (%)	82.42	±	1.76	83.4	±	3.56	73.0	±	7.8	74.35	±	11.3	93.88	±	13.21	61.99	±	13.43
Dust Exposure (SRM-2585) in presence of 20 % Tween 80 (aqueous)																		
Receptor fluid (24h)	9.32	±	5.61	1.23	±	0.89	8.65	±	5.0	3.05	±	2.89	86.2	±	21.0	89.25	±	6.5
Receptor rinse	1.23	±	0.87	0.20	±	0.05	1.54	±	0.73	2.41	±	0.67	6.49	±	3.2	1.34	±	0.45
Tape Strip (S.Corneum)	1.34	±	1.0	0.34	±	0.22	16.54	±	8.9	26.59	±	11.68	51.09	±	15.9	28.54	±	5.6
Skin-Epidermis (Depot)	5.2	±	2.3	0.81	±	0.45	23.56	±	11.8	509.41	±	45.6	256	±	7.32	634	±	11.8
Cotton wipe (unabsorbed)	0.87	±	0.5	0.78	±	0.56	37.9	±	11.4	100.61	±	36.7	314.7	±	24	429.15	±	6.7
Total Recovery (%)	94.5	±	16.43	78.1	±	15.63	67.32	±	18.9	85.6	±	8.92	77.7	±	11.2	64.67	±	7.8x
Dust Exposure (SRM-2585) in presence of moisturising cream																		
Receptor fluid (24h)	2.64	±	1.43	0.33	±	0.26	0.32	±	0.15	2.0	±	1.2	15.87	±	7.89	29.95	±	11.34
Receptor rinse	0.67	±	0.33	0.09	±	0.01	0.1	±	0.09	1.09	±	0.76	3.67	±	1.54	12.67	±	5.6
Tape Strip (S.Corneum)	1.45	±	0.82	0.56	±	0.24	11.6	±	5.8	3.5	±	2.8	8.7	±	1.67	128.45	±	12.45
Skin-Epidermis (Depot)	3.54	±	1.45	0.84	±	0.34	10.73	±	6.7	34.0	±	9.45	186	±	6.89	125.8	±	13.4
Cotton wipe (unabsorbed)	5.43	±	2.5	1.83	±	0.87	56.2	±	15.6	498.2	±	6.98	345.0	±	12.89	789.67	±	31.5
Total Recovery (%)	72.2	±	15.90	83.9	±	7.4	60.2	±	21.5	71.83	±	16.59	70.7	±	8.9	64.29	±	5.6

Table 5.1 Showing the cumulative absorption found in the receptor fluid, unabsorbed amount (cotton wipe), skin depot (both stratum corneum i.e. tape stripping and the epidermis) and receptor well rinse. (Note all results are in Mean ± SD ng/cm ^{2}, Recovery in %

Fig 5.4: Graph showing the cumulative amount absorbed after 24 hrs of Dry SRM-2585 exposure (Control) in presence of sweat/sebum (wet condition),20% Tween 80 and moisturising cream (Values are given in Mean ± SD , n=3 replicates , ng/cm^2 P > 0.05 for all the groups).

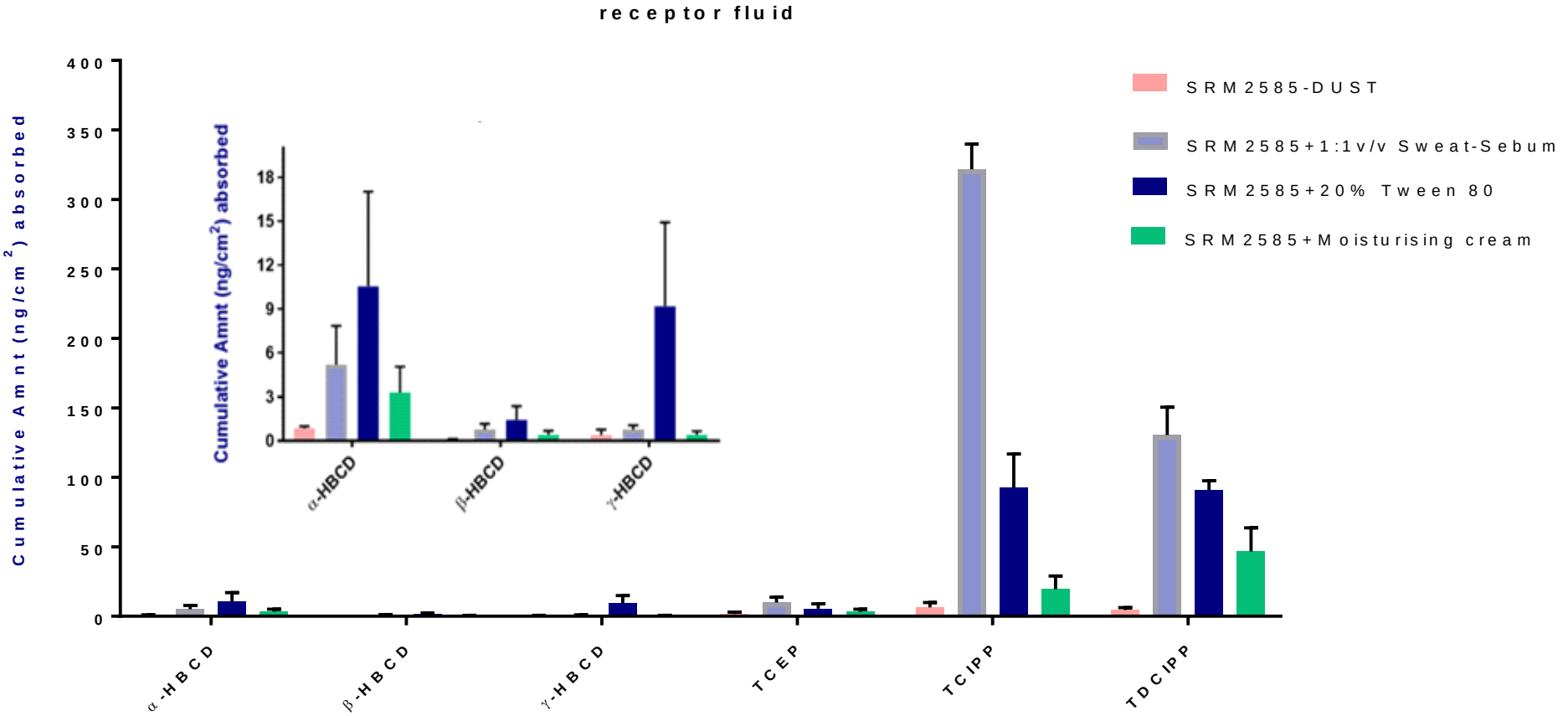

Fig 5.5: Graph showing the amount remained in the skin (sum of amount in stratum corneum and the epidermis) after 24 hrs of Dry SRM-2585 exposure (Control) in presence of sweat/sebum (wet condition),20% Tween 80 and moisturising cream (Values are given in Mean ± SD , n=3 replicates, (ng/cm^2), P > 0.05 for all the groups).

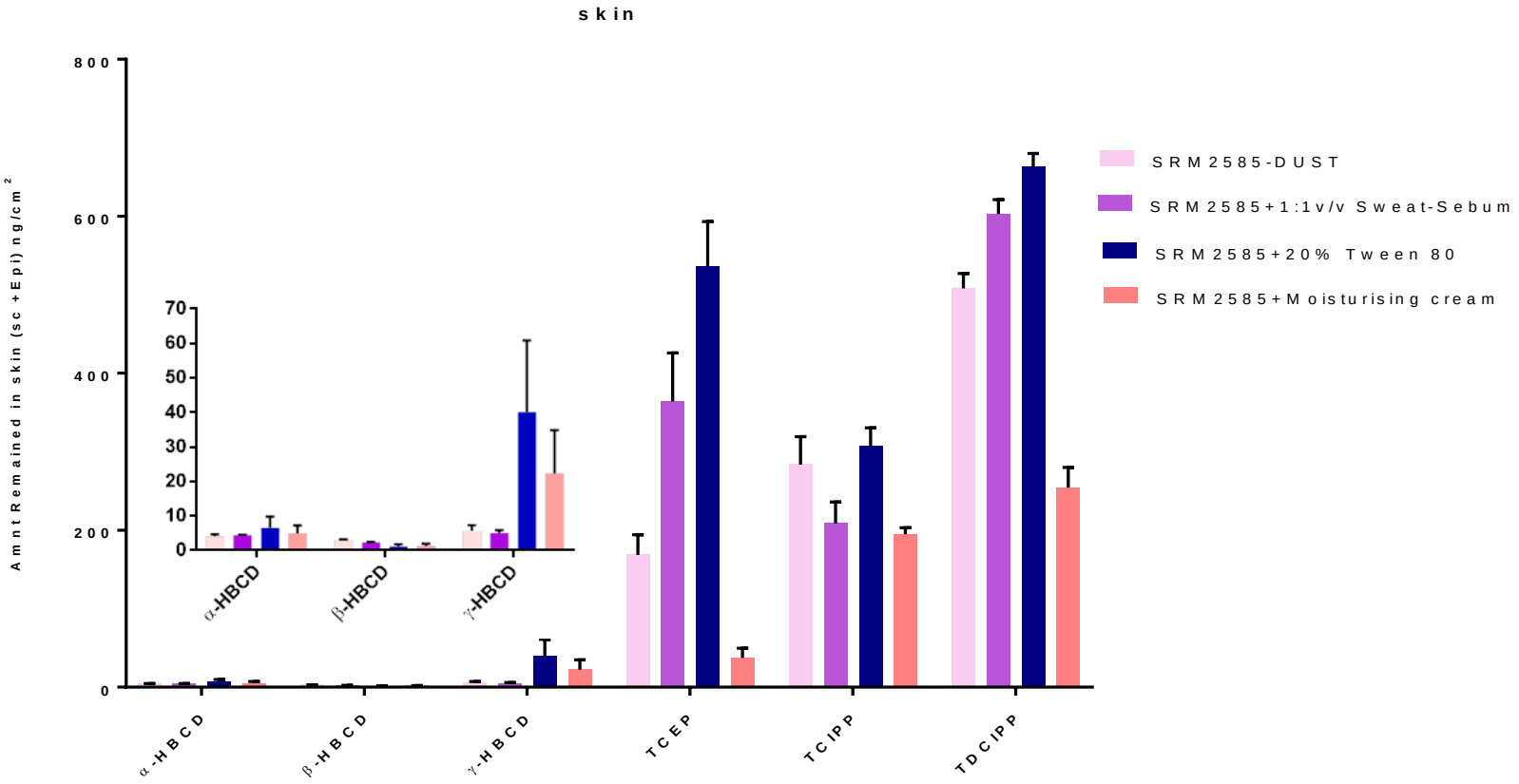

Table 5.2: Assessment of human dermal exposure (ng/kg bw/day) to FRs present in SRM-2585 dust upon contact with a skin surface at three different scenarios i.e dry skin, wet skin and in presence of moisturising creams.

Dermal exposure scenario	Dry skin exposure		Wet skin exposure		In presence of moisturising creams	
	Adults	Toddlers	Adults	Toddlers	Adults	Toddlers
α-HBCD	0.003	0.030	0.005	0.060	0.000036	0.00042
β-HBCD	0.001	0.016	0.002	0.020	0.000007	0.00008
γ-HBCD	0.0003	0.003	0.003	0.030	0.000058	0.00067
TCEP	0.100	0.868	0.200	2.130	0.000193	0.0022
TCIPP	0.100	1.194	0.247	2.840	0.001075	0.01236
TDCIPP	0.060	0.707	0.340	3.910	0.000882	0.0105

5.6: Summary

- Results demonstrated the importance of bridging and simultaneously considering factors like role of sweat/sebum and cosmetics in the dermal exposure of hazardous FRs from indoor dust. It shed light on how the adsorbed FRs (HBCDs & PFRs) on the dust particles gets dissolved in the human sweat or sebum and subsequently available for the partitioning into the outermost dead cell layers i.e. stratum corneum layer of the skin.
- For the first time we have mimicked the real life dermal exposure scenario by incorporating dry and wet conditions in our in vitro dermal experiment. The implication of this is to understand the type of skin i.e. dry skin and oily skin and it's prone to the hazardous chemicals. Dust was applied to the skin surface to show that dust could be a potential source of dermal exposure for FRs which would contribute to the overall body burdens. Our results suggested that the sweat/sebum mixture

increased the absorption of the lipophilic chemicals like HBCDs & PFRs thus it indicates that the wet or oiliness of the skin increases the exposure level, however it was not statistically significant as compared to the dry exposure which could be due to the moisture content of the skin.

- For the first time we developed a novel way of tape stripping method applied to the in vitro 3D-HSE skin. The results revealed that the substantial amount of the FRs remained in the skin. This bioaccumulation is important to know the behaviour of the chemicals and to correlate with the physicochemical properties of the substances accidentally exposed to the skin. Another importance is to understand the lag time of the chemicals to appear into the systemic circulations. We are in dermal contact with various cosmetics/personal care products on a daily basis and the oily fats of the formulations or the surfactants like Tween 80 may undergo retention on the skin surface. Due to the oiliness of the skin (which could be due to naturally secreting sebum or the intentionally applied skin creams) the dust particles might cling to the surface and the chemicals like FRs may act directly in the skin or be absorbed through the skin into the blood, accumulate in the body and exert toxic effects in various organs. It is important to monitor such exposure especially in toddlers group which are vulnerable due to their developmental status than is the general population.
- However future studies needs to be carried out to work on some of the uncertainties in dermal risk assessment. First, the amount of the chemicals (if any) in the personal care products which would further facilitates the body burdens in addition to the chemicals exposed via dust. Second, skin contact area and the frequency of events. Third, duration of contact and intensity of contact.

CHAPTER VI

DERMAL BIOACCESSIBILITY AND UPTAKE OF PBDEs FROM PLASTICS

6.1: INTRODUCTION

Plastics play an important role in the electrical and electronics (E&E) industry. E&E applications rely on thermo-plastics because of their unique features like light weight, resistance to physical, chemical, biological degradation and fire safety. Production of plastics for use in E&E applications grows globally and its demand reached 47.8 million tonnes/year in European countries according to *Plastics Europe* (Plastics 2016). Humans are likely to be exposed to many plastic products every day while using computers, laptops, TV-sets, fridges, cell phones, toys…etc. Moreover, plastics continuously degrade into smaller particles and highly increasing surface area is likely to become available for the desorption of persistent organic pollutants like PBDEs contained within the particles. Studies have suggested that plastics may also leach chemicals if they are scratched or heated and the chemicals can penetrate into cells, chemically interact with biologically important molecules and may disrupt the endocrine system (Teuten et al. 2009). PBDEs or other FRs may be present in plastic toys as contaminants during the manufacturing process or the chemicals could be transferred from indoor dust to the toy's external surfaces or to the soft foams/fillings when they are not added deliberately (Chen et al. 2009). During play time or hand-to-mouth behaviour of children, PBDEs could come in contact with physiological fluids like sweat/sebum on the skin. A recent study (Hoffman et al. 2016) showed that playing with plastic toys was associated with higher handwipe levels of PBDEs. Moreover, at e-waste dumping and recycling sites, workers regularly come into dermal contact with BFR-containing WEEE plastic. (Wu et al. 2016b, Wu et al. 2016a). Dermal exposure to chemicals

present as additives in polymers is of particular concern for pregnant women and children (Sutton et al.). When pregnant women are exposed to FRs, the maternal increase in body burdens can have detrimental effects on the fetus/baby via placental transfer or during lactation. Epidemiological research has linked prenatal exposure to the adverse outcomes; decrease in fecundability (Harley et al. 2010b), pregnancy loss, lower thyroid stimulating hormones (Chevrier et al. 2010), pre-term birth-low birth weight (Harley et al. 2011), childhood morbidity and impaired neurodevelopment (Herbstman et al. 2010). Children may be in frequent contact with plastic toys either by mouthing or via dermal contact.

A study performed by (Ionas et al. 2016) investigated the leaching behaviour of PBDEs from toys into saliva under simulated conditions. The results of this work revealed the leaching process to be congener dependent and that the proportion of lower brominated PBDEs leached was 4.5 times higher than the more brominated congeners. However, to our knowledge there are no studies where the leaching behaviour of PBDEs in other physiological fluids like sweat/sebum has been tested. Therefore, children's toys and child-care articles could be potential sources of dermal exposure to PBDEs. Despite a recent study by (Abdallah, Pawar and Harrad 2015a) highlighting the importance of dermal contact as a pathway of human exposure to brominated flame retardants, very little is currently known about human dermal exposure to additive FRs present in plastics.

Given this, the aim of this chapter is to test the hypothesis that the PBDEs in plastic can leach out upon contact with human SSFL and become available for absorption via penetration of the stratum corneum. For the first time, we simulated real life dermal exposure scenarios by exposing a 3D-HSE EPISKIN™ model to 75-85 mg/cm^2 of ERM micro-plastics (ERM-EC590 "low density polyethylene" & ERM-EC591 "polypropylene"). The tested micro-plastics were applied to the skin surface in the presence of 1:1 sweat sebum mixture (v/v) to mimic real-life exposure conditions (Pawar et al. 2016) (Stefaniak and Harvey 2008). The

concentrations of PBDEs in the SSFL were measured to assess the bioaccessibility of target compounds. This was followed by investigating their percutaneous penetration using the 3D Episkin model.

6.2 METHODOLGY

6.2.1 Dermal bioaccessibility of PBDEs from ERM-EC590, ERM-EC591 plastics

ERM-EC591 and ERM-EC590, obtained from the Institute for Reference Materials and Measurements (IRMM), were used as certified reference materials for the determination of BDE-28, BDE-47, BDE-99 & BDE-183 and BDE-209 in PP and PE matrices. The concentration range of the target compounds was between 87 mg/kg and 780 mg/kg in the two ERMs tested (Chapter 2, Table 2.12). Physiologically-simulated artificial sweat and sebum mixture (SSSM) was prepared according to a previously reported method (see section 3.2.2).

The ERM-EC590 plastic pellets (low density polyethylene polymer) and ERM-EC591 (polypropylene) were accurately weighed (80-90 mg) and placed in a mortar and ground using a heavy grinding ball with the Vibratory Micro Mill PULVERISETTE 0, which provided impact and friction at amplitude 3.0 mm. To achieve appropriately fine comminution, liquid nitrogen was used to render the plastic pellets brittle.

The resulting pulverised micro-plastics ERM-EC590 & ERM-EC591 were weighed (75-85 mg) in triplicate and transferred to clean test tubes. The samples were spiked with IS BDE-77, BDE-128 and ^{13}C-labelled BDE-209, and the mixture incubated in 5 mL of 1:1 v/v sweat and sebum mixture. The mixture was agitated with magnetic beads on a hot plate at 32 °C for 2 hrs exposure time to mimic the *in vivo* skin temperature. Due to the lower densities of the micro plastics they were found to be floating at the interface between the sweat and sebum layers.

Fig 6.1: The Vibratory Micro Mill PULVERISETTE 0

At the end of the exposure time, the liquid was collected using clean glass Pasteur pipettes (without the plastics) and the resulting samples generated (i.e. solid plastics and the liquid sweat/sebum mixture) were analysed separately and mass balance calculated.

6.2.2 Dermal uptake of PBDEs from pulverised ERM-EC590 and ERM-EC591 plastics (Fig 6.2) A dose (75-85 mg accurately weighed) of the pulverised ERM-EC590 plastic and ERM-EC591 (polypropylene) were applied on Episkin tissues and equilibrated in 12 co-star well plates in 2.5 mL culture media at 37 °C. After 30 mins equilibration, the skin surface was exposed to ERM-EC590 & ERM-EC591 spread uniformly on the skin surface in the presence of 100 µL of sweat: sebum mixture (1:1 v/v). At serial time points, the receptor fluid (2.5 mL) was collected and replaced (2.5 mL). The exposure was terminated at 24 hr by removing the microplastics from the skin surface with a cotton bud soaked in hexane. The skin patches were removed with forceps and subjected to tape stripping (n=5). The receptor compartments were washed separately (5 × 2 mL) with PBS. All samples (receptor fluid, skin, cotton buds with microplastics, well wash and tape strips) were stored at −20 °C until chemical analysis.

6.3 EXTRACTION AND CLEAN-UP

6.3.1 Bioaccessibility samples

The microplastics and the liquid phase (i.e. sweat/sebum) were separated and subjected to extraction and clean-up separately. The micro-plastics were extracted with 100% DCM three times and the pooled solvent extracts reduced to incipient dryness under N_2. Then the concentrated sample extracts were dissolved in 2 mL hexane and washed with ~ 2 mL of 95 % H_2SO_4 to remove lipids**.** The organic layer and washings were combined and evaporated to incipient dryness under N_2. Target analytes were reconstituted in 150 µL of isooctane containing 250 pg/µL of PCB-129 used as recovery determination standard (RDS) prior to GC-MS analysis using the method described in section 2.1.1. The liquid phase (i.e. sweat/sebum) samples were extracted with 3 mL hexane: ethyl acetate (1:1 v/v) and the pooled solvent treated via a procedure similar to that followed for the micro-plastics.

6.3.2 Episkin dermal exposure samples

Each permeation assay generated five different types of samples comprising: receptor fluid, skin tissue, cotton buds with microplastics (used to thoroughly wipe the skin surface), donor and receptor compartment solvent washes. The receptor fluid, skin tissue and cotton bud samples were extracted according to a previously reported QuEChERs based method (Abdallah et al. 2015). Briefly, each sample was spiked with 30 ng of BDE-77, BDE-128 and ^{13}C-BDE-209 used as internal (surrogate) standards.

Extraction was performed using 2 mL of (1:1) hexane: ethyl acetate mixture and vortexing for 2 minutes, followed by ultrasonication for 5 minutes and centrifugation at 4,000 g for 3 minutes. This extraction cycle was repeated twice before the combined organic extracts were evaporated under a gentle stream of N_2 and reconstituted into 100 µL of isooctane containing 100 pg/µL of PCB-129 used as recovery (syringe) standard for QA/QC purposes. The donor and receptor compartment washes were spiked with 30 ng of the internal standard mixture

and vortexed for 30 seconds prior to direct evaporation under a gentle stream of N_2. Target analytes were reconstituted into 100 µL of methanol containing 100 pg/µL of PCB-129 used as recovery (syringe) standard for QA/QC purposes. Quantification of target PBDEs was performed using a TRACE 1310™ GC coupled to a ISQ™ Single Quadrupole mass spectrometer (Thermo Fisher Scientific, Austin, TX, USA) operated in negative chemical ionisation (NCI) (Refer Chapter 2.1.1)

6.4 Bioaccessibility Results

The ERM-EC 590 & ERM-EC 591 pellets and the pulverised microplastics were subjected to incubation in the presence of 1:1 v/v sweat and sebum at 32°C to mimic normal physiological skin temperature. Both the pellets and the pulverised microplastics were chosen to study the effect of particle size on the release of PBDEs from the studied polymers. The reduced size of the pulverised plastics (~ 0.5 mm) resulted in higher surface area for easy dissipation of the polymers in the SSFL resulting in significantly higher bioaccessibility (%) for PBDEs (t-test, $P<0.01$, $n=3$) as compared to the intact pellet beads (~ 5 mm) for both the ERM-EC 590 & ERM-EC 591 reference plastics (Fig 6.4 & 6.5).The bioaccessibility ranged from 61% to ~ 83% in ERM-EC590 in case of pellets and significantly increased to 70% to 94% when the size of the pellets were reduced (microplastics). Both the lower PBDEs as well as the higher PBDEs were able to dissolve efficiently in the sweat and sebum mixture. The reasons for this may be attributed to the unique composition of the SSFL which contains lipophilic sebum that would facilitate the dissolution of highly lipophilic congeners (e.g. 183 and 209) together with the electrolyte-rich sweat which may favour the leaching of less hydrophobic congeners (e.g. 17 and 28) from the pulverised plastics. It is noteworthy that the increase in % bioaccessibility was also dependent on the varying concentrations or amount of PBDE congeners in both the polymers. For example, BDE-28 was present only in ERM-EC 591 polymer at a concentration of 2,500 ng/g whereas the concentration of BDE-209 was found to

be even at a higher concentration i.e. 780,000 ng/g than BDE-28. This difference in concentration for BDE 28 & BDE-209 resulted in bioaccessibility of 22.3 % to 31 % & 84 % to 93 % respectively. However there was no clear trend of increase in bioaccessibility due to increase in lipophilicity of the PBDEs which may again be attributed to the formulation reason because the formulation contains both the lipophilic sebum that facilitates the dissolution of highly lipophilic congeners together with the electrolyte-rich sweat which may favour the solubility of less hydrophobic congeners (e.g. 17 and 28) from the pulverised plastics. Our bioaccessibility results imply that in real life PBDEs could be bioaccessible to human sweat and sebum from low density polyethylene (LDPE) and polypropylene. Moreover, our data suggest it is invalid to assume 100% bioavailability for the chemicals when the rate limiting factor is their dissolution into physiological fluids (bioaccessibility).

6.5 *In vitro* Dermal Exposure (microplastics)

Due to the experimental costs and other technical reasons like lower surface area and particle size of intact ERM-EC 590 & ERM-EC 591 pellets, we performed the experiment only with pulverised (micro) plastics. When ERM-EC591 micro plastics were exposed to the Episkin model, the absorbed mass of PBDEs with increasing Br content from BDE-28 to BDE-154 revealed a broad decrease in dermal absorption (fig 6.6). The former trend i.e. broad decrease from BDE-28 to BDE-47 was not observed for ERM-EC590 because BDE-28 is not present in the ERM-EC590 reference material. Maximal penetration was achieved for Tetra-BDE and Penta-BDE, however Octa-BDE and Deca-BDE showed no penetration, although they were found to be more highly accumulated in the skin than the less brominated PBDEs studied (Fig 6.7). This is because the less hydrophobic lower brominated PBDEs penetrated faster through the water-rich viable epidermis than Octa-BDEs and Deca-BDE which were instead found in the lipid-rich stratum corneum and showed no discernible penetration due to their higher hydrophobicity. The PBDEs thus accumulated represent a depot from which they may

be released to the systemic circulation over a prolonged period or could be metabolised to lower congeners. The reason for higher penetration of less brominated PBDEs and higher accumulation of more highly brominated congeners in the skin could be due to the differences in physicochemical properties between the congeners. In spite of the differences in the concentrations of the PBDE congeners in the both ERMs, we found no statistical differences ($P>0.05$) between the % absorption of PBDE congeners from the two ERMs. Our data are in good agreement with previous studies that show the tetra congener BDE-47 and the penta congener BDE-99 to be well absorbed and highly distributed to fatty tissues like adipose, adrenal glands, gastrointestinal tract, skin and liver (Hakk and Letcher 2003) when administered orally in Sprague Dawley rats.

The higher dermal absorption for lower PBDEs could lead to higher toxicity concerns and the metabolism of the accumulated higher congeners to lower congeners might increase the overall toxicity by lower congeners.

Fig 6.2 Schematic diagram for the Dermal bioaccessibility and uptake of PBDEs from the ERM-EC 590 & ERM-EC 591 plastics

The Vibratory Micro Mill PULVERISETTE 0

ERM-EC590 (LDPE)

ERM-EC591 (polypropylene)

Pour liquid nitrogen for fine Communition impact, friction heavy ball @ 3 mm amplitude

Artificial Sweat/Sebum prepared

Equilibration

Twelve HSE patches were placed in 2.5 mL maintenance medium Incubated at 37°C with 5% CO_2 and 98% RH for 24 hrs

Exposure

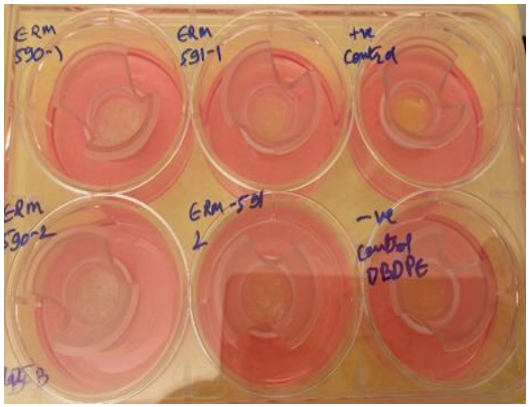

Co-star plate containing 2.5mL of Williams Medium E with 5 % FBS as a receptor fluid and were exposed with the micro plastics in triplicates for 24 hrs in presence of 100 µL sweat: sebum (1:1 v/v) to wet the plastics followed by incubation.

Sampling

- **Receptor fluid collected at serial time points up to 24 hr**
- **Exposure terminated at 24 hr by removing the micro plastics using the cotton swabs soaked in hexane: Ethyl acetate (1:1v/v)**
- **Skin patches were removed and homogenised in same solvent**

Sample Extraction

Clean-up

Cotton swabs with the micro plastics were extracted with DCM and cleaned-up with ~ 2 mL of 95 % H_2SO_4 to remove lipids

Samples of skin, receptor fluid, and PBS fluid were analysed by GC-MS after extraction with hexane: ethyl acetate (1:1 v/v)

Fig 6.3: Dermal bioaccessibility for PBDEs from ERM-EC 590 pellets and pulverised microplastics.

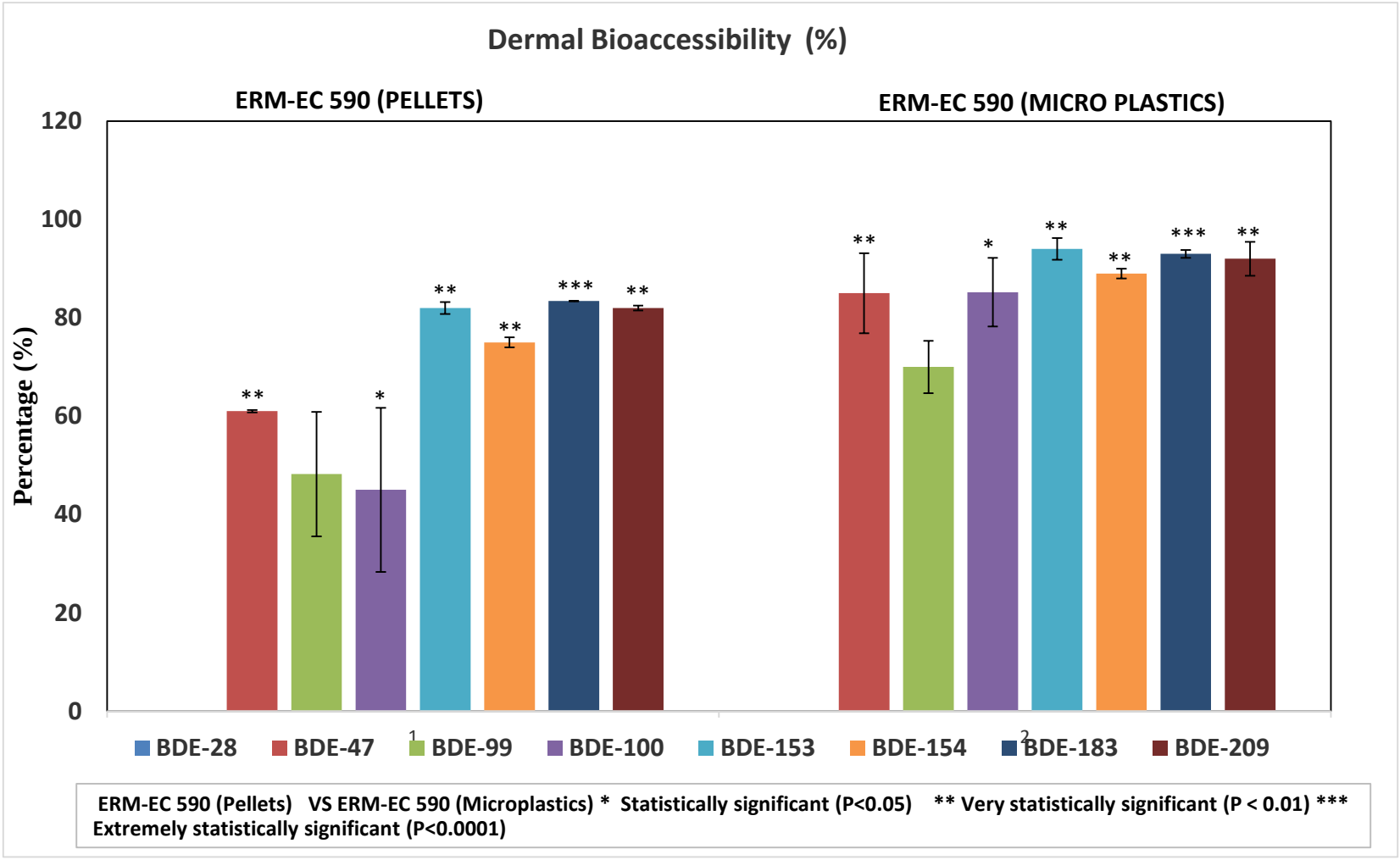

Fig 6.4: Dermal bioaccessibility for PBDEs from ERM-EC 591 full pellets and pulverised microplastics.

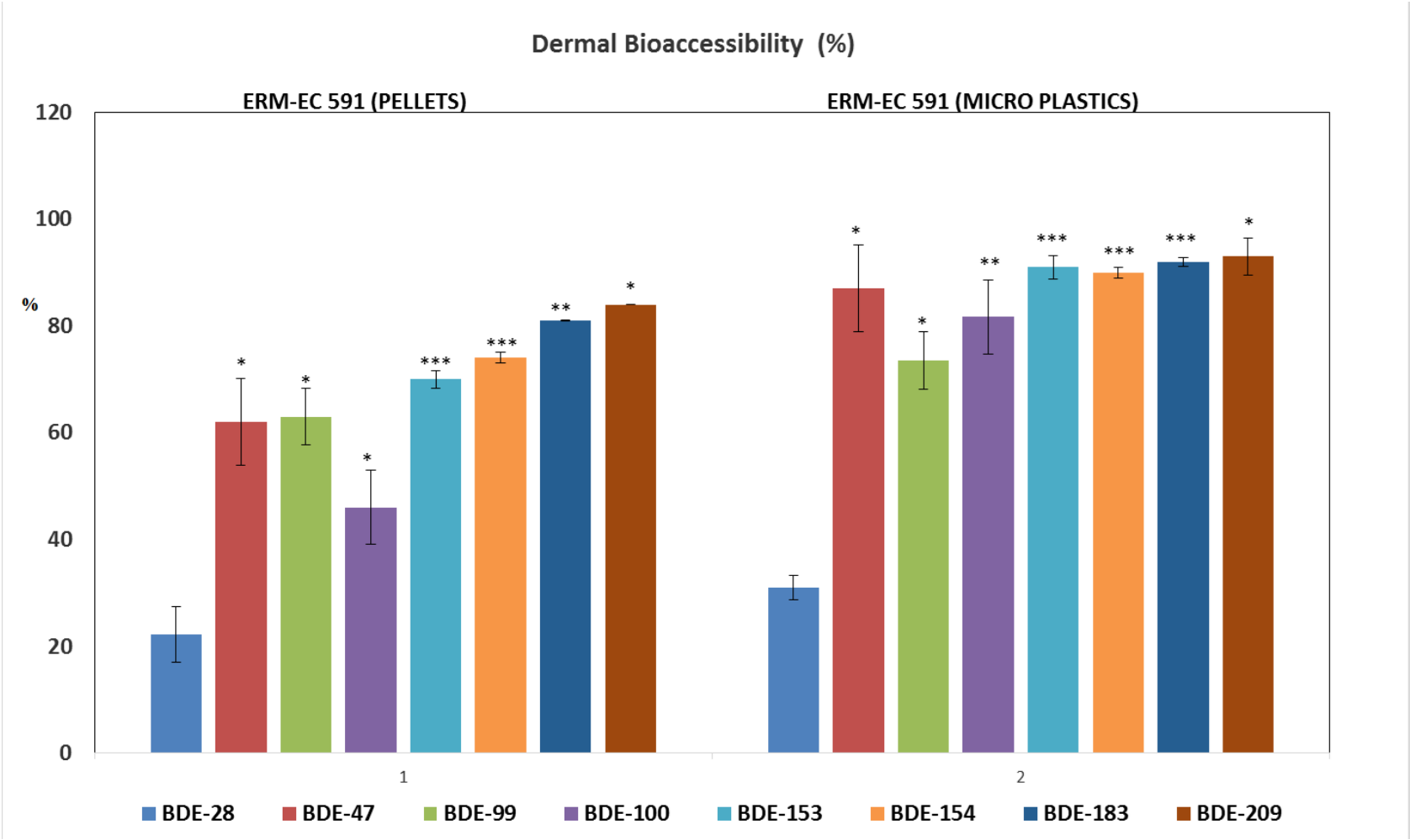

ERM-EC 590 (Pellets) VS ERM-EC 590 (Microplastics) * Statistically significant (P<0.05) ** Very statistically significant (P < 0.01) *** Extremely statistically significant (P<0.0001)

Fig 6.5: Dermal penetration (%) of each PBDE congeners found in the receptor compartment. (n =3)

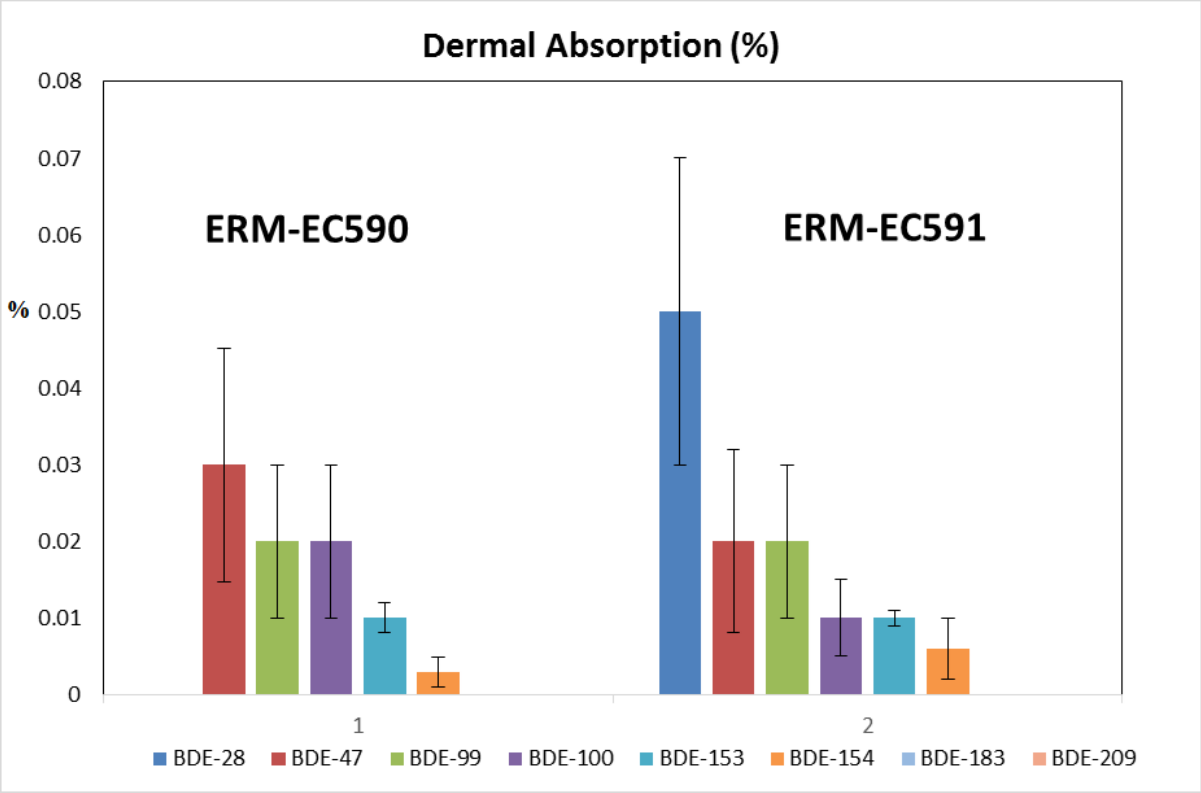

Fig 6.6: Dermal accumulation (%) of each PBDE congeners (n =3)

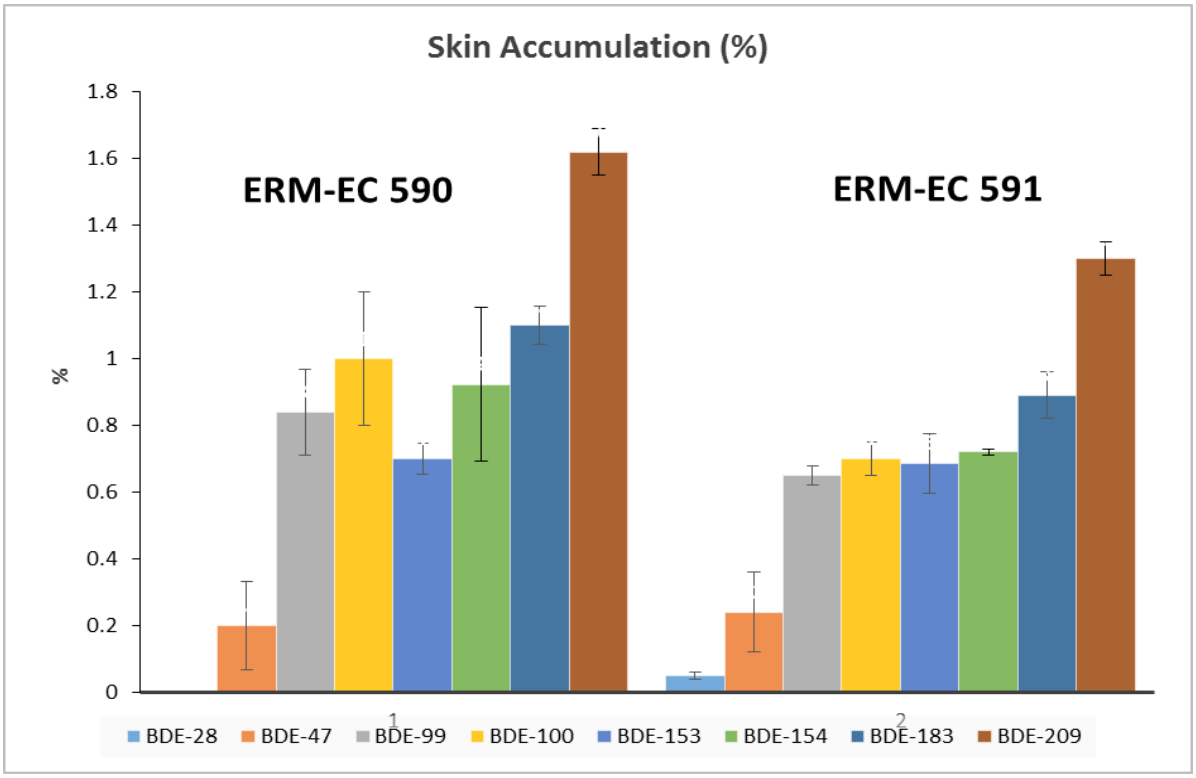

6.6: Estimation of Human dermal exposure

We estimated the dermal exposure of 2 age groups, adults and toddlers. Adults are exposed to plastics every day and are in constant contact with electronic gadgets (such as mobile phones or computer keyboards) made up of plastic materials. Typically toddlers are also exposed to plastics every day while playing with toys containing recycled plastics. In both age groups, chemicals like PBDEs might leach from plastics and dissolve in the SSFL and become available for subsequent dermal absorption. For the purposes of assessment of exposure via dermal uptake of PBDEs resulting from contact with plastics containing these BFRs, we presume that the highly exposed parts of the human body to plastics are the palms and the back of the hands. The palms and the hands contain many sebaceous glands that secrete both sweat and sebum, which facilitate absorption of PBDEs through the skin. Studies have not considered the influence of skin moisture on the adherence of the chemicals like PBDEs laden on the skin surface. Skin moisture varies for an individual depending on factors such as activity level and surrounding temperature/humidity.

Incorporation of our dermal absorption of PBDEs from plastics (bioavailable fraction) into risk assessment models is hampered by the current lack of reliable information on the degree of contact between plastics and skin and the frequency and duration of such contact. Notwithstanding these caveats, a model is presented here that incorporates reasonable assumptions for such parameters.

$$Ep = \frac{\mathbf{Cp\ x\ BSA\ x\ PAS\ x}\ Fb\ x\ NxF}{BW\ x\ 1000} \quad \textbf{.....Eqn-1}$$

Where **Ep** = Estimated daily dermal exposure; ng/kg.bw/day, **Cp** = Concentration of PBDEs in plastics; ng/g of plastic, ***BSA*** = Body surface area exposed; cm^2, **PAS** = Plastic adhered to the skin surface; mg/cm^2, **Fb** = fraction absorbed by the skin (unitless) after 24 hr of micro

plastic exposure; **N** = Number of plastic exposure events per day; day^{-1}**, F** = fraction of day exposed per exposure event (unitless), **BW**= bodyweight of the consumer; kg

Table 6.1 Parameters used in dermal exposure assessment of target PBDEs in pulverised plastics.

Parameter	Adult	Toddler
Age	>18 years	2-3 years
Body weight **Skin surface exposed to plastics (US EPA 2011)**	70 Kg 820 cm^2 (palms, back of hands)	15 Kg 230.4 cm^2 (palms, back of hands)
Plastics adhered to skin (Assumed)	1 mg/cm^2	1 mg/cm^2
Number of plastic exposure events per day (Assumed)	1 day^{-1}	1 day^{-1}
Fraction of day exposed to plastics per exposure event (Assumed)	5/24	3/24

Note: We assumed the palms and back of the hands to be the first point of contact to plastic articles (like toys or mobiles) so the exposed surface area of 820 cm^2 (adults) and 230.4 cm^2 was assumed in the exposure model. For other factors like the amount of plastic adhered to the skin, we have assumed it a "Unit" value. The exposure frequency and duration values are assumed based on experience.

Table 6.2: Assessment of human dermal exposure (ng/kg bw/day) to PBDEs present in micro plastics upon contact with a skin surface film composed of 1:1 sweat sebum mixture.

	ADULTS		TODDLERS	
	ERM-EC 590	ERM-EC 591	ERM-EC 590	ERM-EC 591
BDE-28	-	0.0003	-	0.0002
BDE-47	0.166	0.112	0.131	0.088
BDE-99	0.146	0.146	0.115	0.115
BDE-100	0.036	0.015	0.028	0.012
BDE-153	0.011	0.011	0.009	0.009
BDE-154	0.002	0.003	0.001	0.003
BDE-183	-	-	-	-
BDE-209	-	-	-	-

Fig 6.7: Estimations of daily dermal intake (ng/kg bw/day) of PBDEs from the ERM-EC 590 and ERM-EC 591 micro plastics in adults and toddlers.

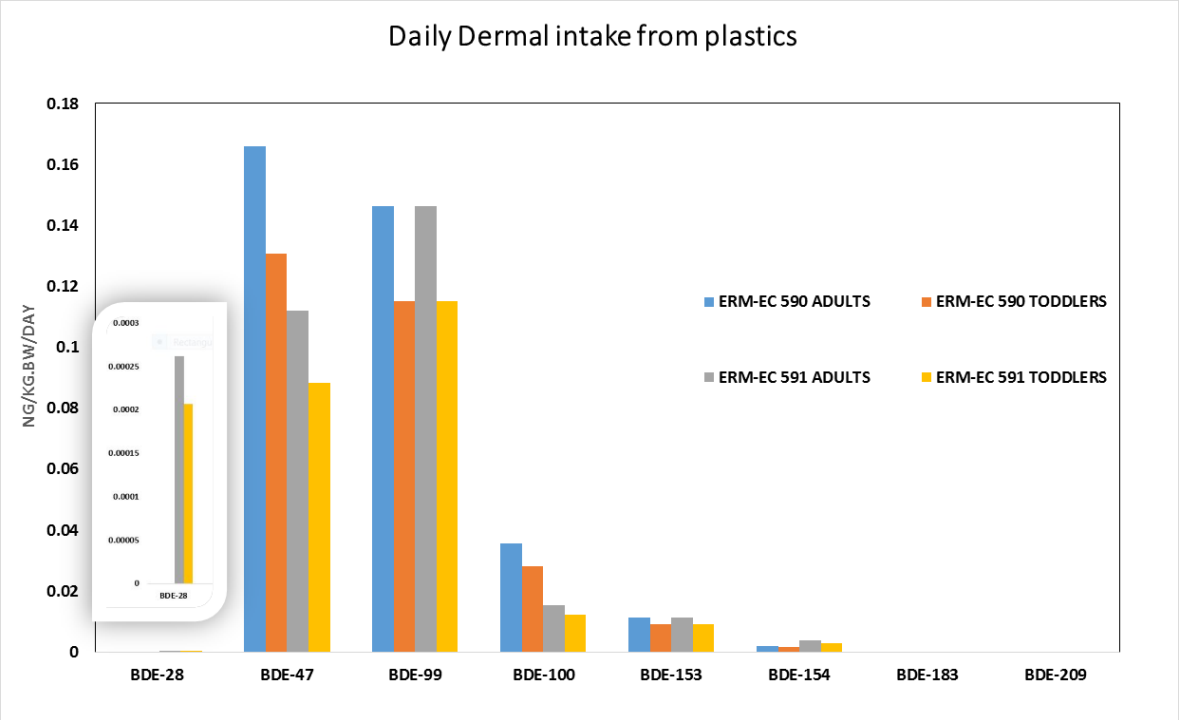

Table 6.2 & fig 6.8 summarise the exposure estimates of adults and toddlers to the studied PBDEs via dermal exposure via plastics. It is important to compare the estimates of exposure to PBDEs via dust and the plastics. Based on our daily human dermal exposure (ng/kg bw/day) results we observe that we cannot compare the exposure via dust (Chapter 3 Table 3.11) to that of plastics because, the dust exposure estimates include only bioaccessibility but not bioavailability, while our plastics exposure estimates include both the bioaccessibility and bioavailability. Another key factor to consider in exposure estimates is how representative the PBDE concentrations in the reference plastics and the real plastics because in real plastics the concentrations will be up to 2-3 % or more as opposed to the much lower concentrations (e.g. concentrations in ERM-EC 590 are 0.32 ± 0.04 g/kg and 0.78 ± 0.09 g/kg for BDE-99 and BDE-209 respectively), which means our dermal exposure will be greater if contact is with plastics containing PBDE concentrations.

All the estimated values in both the scenarios i.e. dust exposure and plastics exposure are found to be below the current USEPA'S Rfd health-based limit values (BDE-47 & BDE-99 HBLVs < 0.1 µg/kg/d) for PBDEs. For BDE-183 & BDE-209, we were unable to calculate the dermal exposure via plastics in humans due to its inability to penetrate the skin in the presence of sweat/sebum. Another factor worth discussing is the adherence factor for dust particles and plastic to the skin surface, as we apply some stress on the plastics while using the consumer products. We recommend future studies to elucidate the impact of stress on the transfer of chemicals from the plastics to the skin surface.

It is obvious that the human skin poses a barrier to human exposure to these hazardous chemicals, however the dermal pathway should definitely be considered, along with other routes, when assessing the overall human exposure to FRs and the potential risk arising from it.

6.7: Summary

In real life the exposure to plastics occurs mainly during direct contact with the consumer products made up of intact plastics, however sometimes we are exposed to the abraded plastics or microbeads for example in cosmetics. Such micro plastics have higher surface area for exposure and results in higher dissipation of PBDEs from the polymers leading to increase bioaccessibility to the skin fluids like sweat and sebum. This hypothesis is supported by our findings in bioaccessibility experiments where we found that PBDEs could be bioaccessible to human sweat and sebum from low density polyethylene (LDPE) and polypropylene. When ERM-EC591 micro plastics were exposed to the Episkin model, the absorbed mass of PBDEs with increasing Br content from BDE-28 to BDE-154 revealed a broad decrease in dermal absorption. Maximal penetration was achieved for Tetra-BDE and Penta-BDE, however Octa-BDE and Deca-BDE showed no penetration, although they were found to be more highly accumulated in the skin than the less brominated PBDEs studied. The higher PBDEs accumulated could undergo metabolism to the lower, toxic congeners or metabolites in the skin. At the end we tried to develop a risk assessment model by incorporating our dermal absorption of PBDEs from plastics. The exposure estimates of adults and toddlers were found to be below the USEPA's HBLV values. However we recommend future dermal exposure studies with real life plastics which might contain higher levels of PBDEs.

CHAPTER VII

DERMAL BIOACCESSIBILITY AND UPTAKE OF ORGANOPHOSPHATE FLAME RETARDANTS FROM UPHOLSTERED FABRICS

This chapter contains some material taken verbatim from Pawar, G., M. A. Abdallah, et al. (2016). "Dermal bioaccessibility of flame retardants from indoor dust and the influence of topically applied cosmetics. J Expo Sci Environ Epidemiol 6(10): 84.

7.1: INTRODUCTION

In the UK, British Standard 5852:2006 applies to fabrics used to upholster domestic furnishings, primarily sofas and chairs. This standard requires testing of the fabric to ensure that fire or flame caused by a match or lit cigarette would not ignite the material. Fabrics tested under this standard require use for its intended purpose, which is to upholster furnishings. It is impossible to list accurately the application levels because of the diversity of formulations and fabric structures available. However, there are three methods of rendering synthetic fibres flame retardant:

• Use of FR monomers during copolymerization,

• Introduction of an additive FR during extrusion,

• Application of flame retardant finishes or coatings.

There are different standards used for commercial and domestic fabrics. For example, for normal domestic upholstery, the fabric should withstand match or lit cigarette testing however for the upholstery used in public buildings should comply more stringent (Crib 5 &

Crib 7) laboratory tests. Tris (1-chloro-2-propyl) phosphate (TCIPP) is currently the preferred FR used in the production of UK PUF due to lower production costs than other similar FRs such as tris (1, 3 –dichloropropyl) phosphate (TDCIPP) (EU RAR, 2008c).Tris-2-chloroethyl phosphate (TCEP) has not been used in the production of UK PUF since the introduction of the 1988 flammability regulations. However, TCEP is known to form as a reaction by-product in the manufacture of TDCIPP and can be present as an impurity (EU RAR, 2008b). The substances TDCIPP and TCIPP have similar use patterns and chemical similarity. The three substances are predominantly used in various types of polyurethane foam applications in the EU (> 97.5% of TCIPP, > 85% of TDCIPP and > 75% of 2, 2-bis (chloromethyl) propane-1, 3-diyltetrakis (2-chloroethyl) bisphosphate -V6, which is another flame retardant used in flexible PUF for making expensive automative and furniture articles). However, PFRs such as TCIPP, TDCIPP, and TCEP were reported to be both hazardous and multi-organ toxic (van der Veen and de Boer 2012a). Furthermore, the EU has classified TCEP as a "potential human carcinogen" (category 3) and TDCIPP as suspected of causing cancer. Moreover, TCIPP is structurally related to TDCIPP and TCEP (chemical structures given in Chapter 1 Table 1.1) and could therefore cause similar effects. (ECHA, 2010).

Further afield, TDCIPP is more commonly used as a flame retardant in US furniture where it was used as a replacement for Penta-BDE to meet the stringent California Technical Bulletin 117 standard that comprises a series of flammability performance tests (Stapleton et al. 2012c).

Additive FR chemicals may migrate/leach from the FR treated fabrics by abrasion or volatilisation or by physical stress ultimately leading to the skin deposition. However there is a paucity of data on the level of migration of PFRs from the underneath foams to the superficial fabrics in the upholstered furnitures. In 2005 a report by National Research Council (US) Subcommittee on Flame-Retardant Chemicals indicated that considerable time

(approx. 5 h) is spent in contact with the flame retarded fabrics and these fabrics renders this contact a potential pathway for human exposure. The paucity of data on human dermal absorption of PFRs and the extent of exposure to consumers is a research gap in accurate risk assessment. Thus the aims of this chapter were to:

- Quantify FR release from the fabrics and subsequently dissolved in sweat/sebum mixture (Bioaccessible fraction)
- Quantify FR penetration through the skin surface in the presence of moisture or sweat/sebum mixture
- Estimate daily dermal intake of target FRs for adults and toddlers when exposed to FR-containing fabrics

7.1.1: Determination of PFRs in upholstered fabrics

The upholstery fabrics from chairs and sofas were collected from the waste piles at University of Birmingham. Our bioaccessibility and dermal uptake experiments employed the 3 fabric samples shown below in Figure 7.1.

Fig 7.1: a) Fabric arm chair b) Domestic sofa fabric c) Office desk chair

a) b) c)

To quantify the identity and concentrations of the FRs present in these samples, the fabrics were first weighed (50-60 mg), spiked with 50 µL IS (d_{15}-TPHP) and soaked in 5 mL hexane: ethyl acetate (1:1 v/v) overnight. Following soaking, the extract was filtered with Whatman® No.1 filter paper to remove colourants or pigments. The filtrate was subjected to incipient dryness under N_2 (Turbovap) evaporator Target PFRs were reconstituted in 100 µL of

methanol and injected onto a LC-MS/MS. (Chapter 2 Section 2.1.2).Our analysis revealed the following PFRs concentrations in the three fabric samples. Note each sample was analysed in triplicate.

Table 7.1 Concentrations (average ± standard deviation ng/g) for TCEP, TCIPP and TDCIPP in the upholstered fabrics

Sample	Conc (ng/g)		
	TCEP	TCIPP	TDCIPP
Sofa	**390 ± 10**	**27000 ± 20**	**38780 ± 34**
Arm chair	**1344 ± 19**	**1793904 ± 11**	**25447 ± 6**
Office desk chair	**520 ± 5**	**79601 ± 17**	**42002 ± 13**

7.2: Methodology for dermal bio accessibility test for contaminated fabrics

The fabrics in triplicates were first weighed (50-60 mg) and were spiked with 50 µL IS (d_{15}-TPHP) of 1 ng/µL concentration and were incubated in the clean test tube containing 5 mL of 1:1 v/v sweat-sebum mixture and agitated for 5 h with magnetic beads with agitation on a hot plate at 32 ºC to mimic the normal skin temperature. Fabrics were removed and the supernatant liquids subjected to extraction and clean-up (QuEChERS) and later the samples were analysed. As above, each sample was studied in triplicate.

7.3: Methodology for *in vitro* dermal exposure test for contaminated fabrics

Episkin was equilibrated in 12 co-star well plates in 2.5 mL culture media at 37 °C. After 30 mins equilibration, skin surface was exposed to 100 µL of 1:1 v/v sweat/sebum and immediately 1 cm^2 round cut out of the fabrics (facing the surface which will be contact with the human skin in real life scenario) is placed on the skin surface. In similar manner all the three type of fabrics were exposed to the skin surface in triplicates. A control skin experiment was also conducted consisting of the same experiment but without any exposure of the skin

model to fabric. Then followed by 15 mins of gentle shaking; the plate was incubated at 37 °C with humidified air containing 5% CO_2. The receptor fluid was collected at time points 5, 10, 20, 30 hour & the exposure was terminated at 30 hour by removing the fabrics from the skin surface with tweezers and any residual chemical remaining on the skin surface removed with cotton swabs soaked in hexane. The skin patches were removed with forceps and stored, receptor compartments were washed separately (5 × 2 mL) with PBS. All samples receptor fluid, skin, cotton buds, well wash and fabrics) were stored at −20 °C until chemical analysis.

7.4: Extraction and Clean-up

The receptor fluid, skin tissue and cotton bud samples were extracted according to a previously reported QuEChERs based method (Abdallah et al., 2015). Briefly, each sample was spiked with 1 ng of 30 µL IS (d_{15}-TPHP) used as internal (surrogate) standards. Extraction was performed using 2 mL of (1:1) hexane: ethyl acetate mixture and vortexing for 2 minutes, followed by ultrasonication for 5 minutes and centrifugation at 4,000 g for 3 minutes. This extraction cycle was repeated twice before the combined organic extracts were evaporated under a gentle stream of N_2 and reconstituted into 100 µL of methanol. The donor and receptor compartment washes were spiked with 30 ng of the d_{15}-TPHP prior to direct evaporation under a gentle stream of N_2. Target analytes were reconstituted into 100 µL of methanol. The exposed fabrics were also extracted in a fashion similar to that described in section 7.1.1

7.5: Determination of PFRs by LC-MS/MS

The details of the analytical procedures employed to determine concentrations of PFRs are provided in Chapter 2, Section 2.1.2.

7.6: Assessment of dermal exposure via contact with fabrics

We estimated daily dermal exposure to PFRs as a result of contact with the fabrics via the equation below;

$$E\,fabric\_derm = \frac{Cfabric \text{ x BSA x } FAS \text{ x IEF x } Fbioavail}{BW \text{ x } 1000} \quad \text{.....Eqn-1}$$

$E\,fabric\_derm$ = ng/kg .bw/day, $Cfabric$ = ng of chemical /g of fabric

BSA = Body surface area exposed (cm^2), as a worst case scenario the body area in contact with the sofa or chair was assumed to be $1/4^{th}$ of the bare upper torso

F_{AS} = Mass of fabric adhered to the skin surface per unit surface area (mg/cm^2)

***IEF* =** indoor exposure fraction (hours spent over a day on a sofa/ chair) (unitless)

$Fbioavail$ = fraction absorbed by the skin (unitless) after 5 hr of fabric exposure

BW = bodyweight of the consumer (kg)

Table 7.2: Exposure parameters *(USEPA 2011)* and estimated dermal exposure (ng/kg bw.day) of UK adults and toddlers to the studied PFRs via contact with upholstered fabrics.

Parameter	Adult	Toddler
Age	**>18 years**	**2-3 years**
Body weight	**60 Kg**	**15 Kg**
Skin surface exposed	**8800 cm^2 (head, forearms, hands and trunk)**	**4800 cm^2 (head, forearms, hands trunk, legs and feet)**
Time spent on Sofa/ Chair (Conservative Assumption)	**5 hrs/day**	**5 hrs/day**

7.7: RESULTS:

7.7.1: Bioaccessibility of PFRs from fabrics

The first rate limiting step in dissolution of PFRs from the treated fabrics to the sweat/sebum mixture is the release or migration rate of FRs from the interwoven fabric fibres. However the wear and tear or abrasion during the physical stress exerted while sitting on a sofa or

upholstered fabric and the presence of sufficient sweat /sebum on the skin surface during summer days could assist in dissolution of PFRs to facilitate human exposure. Our *in vitro* bioaccessibility test data indicated that migration/leaching of TCIPP from different fabrics to the sweat: sebum were: 57 ± 7.28 %, 22.4 ± 4.42 % and 15 ± 1.91% of the initial concentration for domestic sofa, office chair fabric and domestic arm chair fabric respectively.

For TCEP, the bioaccessible fraction was found to be 1.56 ± 0.18 %, 0.65 ± 0.08 % and 3.84 ± 2.8 % for arm chair fabric, sofa fabric and office desk chair fabric respectively. However TDCIPP was found be more bioaccessible than TCEP for 2 types of fabrics i.e. 2.36 ± 0.30 % (arm chair) and 5.56 ± 4.64 % (sofa fabric) but less so for office desk chair fabric at 1.16 ± 0.20 %. Bioaccessibility is higher for TCIPP as compared to TDCIPP & TCEP**.**

Our previous report (Pawar et al. 2016) on bioaccessibility from dust of the same PFRs revealed bioaccessible fractions of 10.4 ± 1.8, 17.4 ± 2.7 & 18.6 ± 0.8 % for TCEP, TCIPP and TDCIPP respectively. This was attributed to the easy dissolution of PFRs from the dust particles and was found to be concentration dependent. The bioaccesibility for PFRs from the fabrics are lower than that of the bioaccessibility of PFRS from the dust. This could be due to the fact that FRs applied to the fabrics might have different physical or chemical forms and also due to the back coating treatments or polymerisation or derivatization of the parent molecule, in case if the FR are treated on the surface it would be easily bioaccessible.

Table 7.3: $F_{BIOACCESSIBLE}$ of PFRs from upholstered fabrics in presence of 1:1 sweat/sebum mixture

Acronym	Water Solubility (van der Veen and de Boer 2012b) (µg/L)	Log K_{ow} (van der Veen and de Boer 2012b)	$F_{bioaccessible}$ (%)-1:1 Sweat:Sebum		
			Arm chair Fabric	Sofa Fabric	Office Desk chair
TCEP	7×10^6	1.44	1.56 ± 0.181	0.65 ± 0.08	3.84 ± 2.8
TCIPP	1.6×10^6	2.59	15.00 ± 1.91	57.00 ± 7.28	22.38 ± 4.42
TDCIPP	1.5×10^3	3.80	2.36 ± 0.30	5.56 ± 4.64	1.16 ± 0.20

7.7.2: Bioavailability of PFRs from upholstered fabrics in presence of sweat: sebum mixture

Following 30 hours exposure of Episkin to the 1 cm^2 arm chair fabric, sofa fabric and office desk chair fabric (in triplicates) in the presence of 100 µL synthetic sweat/sebum mixture which was applied to the skin surface before placing the fabrics on to the skin surface, TCIPP showed the highest cumulative absorption (ng/cm^2) with 523.58 ± 1.44, 414.29 ± 5.81, 64.9 ± 0.34 in case of domestic arm chair fabric, office desk chair and sofa fabric respectively in the receptor fluid. For TCEP, cumulative absorption (ng/cm^2) was found to be: 150.3 ± 0.94, 59.5 ± 12.09 & 37.0 ± 3.2 for arm chair fabric, sofa fabric and office desk chair respectively. Compared to TCIPP and TCEP, TDCIPP was less abundant in receptor fluid at a concentration of 37.8 ± 9.8, 37.0 ± 3.84 and 31.4 ± 1.68 for arm chair fabric, office chair fabric and sofa fabric respectively. Considerable quantities remained on the skin surface (Table 7.5) Analysis of the skin tissue resulted in recovery (%) of TCEP (12.43 ± 4.89, 18.76 ± 2.2, 31.46 ± 1.40), TCIPP (1.55 ± 0.13, 0.2 ± 0.01, & 2.67 ± 0.19) and TDCIPP (0.62 ± 0.15, 0.48 ±0.034, 0.039 ± 0.014), for sofa fabric, arm chair fabric and office desk chair fabric respectively after 30 h exposure.

Table 7.4: Distribution of target PFRs (expressed as average percentage ± standard deviation of exposure dose) in different fractions of the *in vitro* diffusion system following 30 h exposure to 500 ng/cm^2 (finite dose) of the studied compound.

SOFA FABRIC	TCEP	TCIPP	TDCIPP
Absorbed*	20.59 ± 3.57	0.30 ± 0.07	0.13 ± 0.006
Unabsorbed#	33.57 ± 16.21	83.9 ± 5.6	94.6 ± 8.9
Skin	12.43 ± 4.89	1.55 ± 0.13	0.62 ± 0.15
Sum (Recovery)	66.59 ± 24.67	85.8 ± 5.75	95.35 ± 9.06
ARM CHAIR FABRIC	**TCEP**	**TCIPP**	**TDCIPP**
Absorbed*	15.18 ± 2.09	0.03 ± 0.002	0.233 ± 0.06
Unabsorbed#	41.62 ± 0.6	77.1 ± 15.2	88.33 ± 3.3
Skin	18.76 ± 2.2	0.2 ± 0.01	0.48 ± 0.034
Sum (Recovery)	75.56 ± 4.89	77.3 ± 15.2	89.04 ± 3.39
OFFICE DESK CHAIR FABRIC	**TCEP**	**TCIPP**	**TDCIPP**
Absorbed*	16.25 ± 3.15	0.52 ± 0.005	0.12 ± 0.03
Unabsorbed#	35.56 ± 0.68	86.34 ± 7.85	98.1 ± 24.81
Skin	31.46 ± 1.40	2.67 ± 0.19	0.39 ± 0.014
Sum (Recovery)	83.27 ± 5.23	89.53 ± 8.04	98.61 ± 24.85

***** Comprises cumulative concentrations in the receptor fluid over 30 h + receptor compartment rinse.

[#] comprises concentrations in the skin surface wipes after 30 h + donor compartment rinse

Fig 7.2: Cumulative absorption of TCEP detected in receptor fluid up to 30 h.

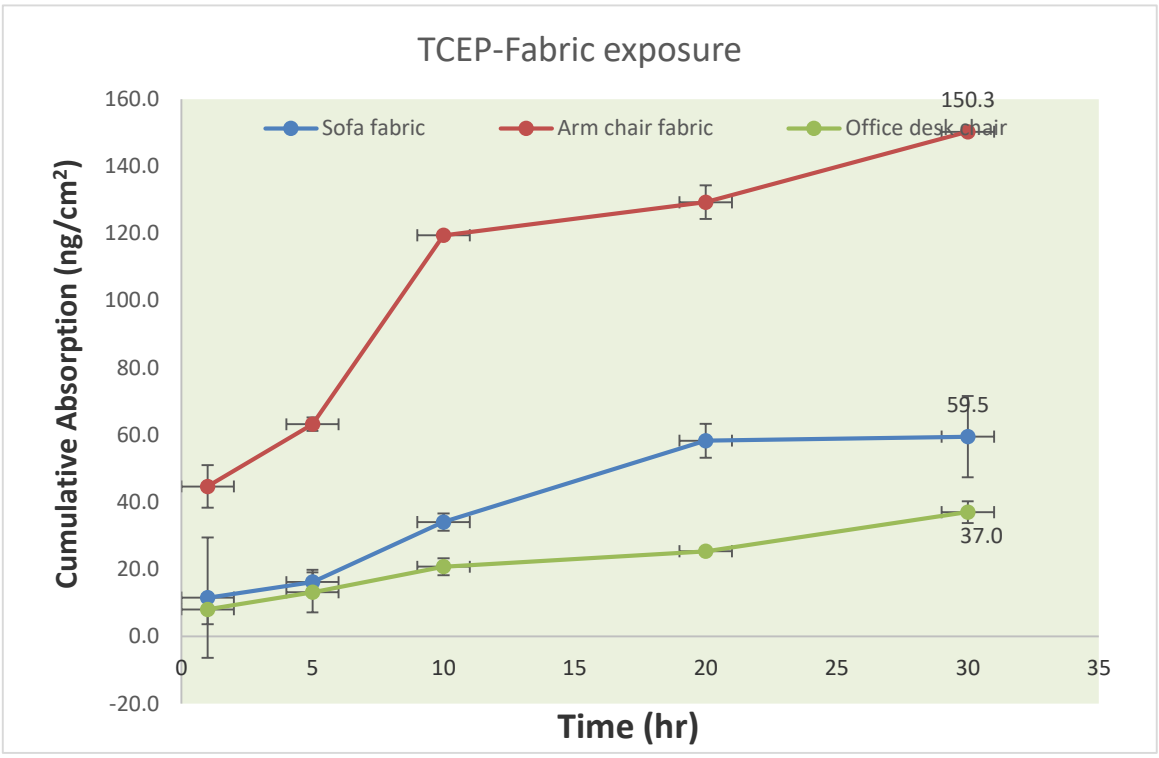

Fig 7.3: Cumulative absorption of TCIPP detected in receptor fluid up to 30 h.

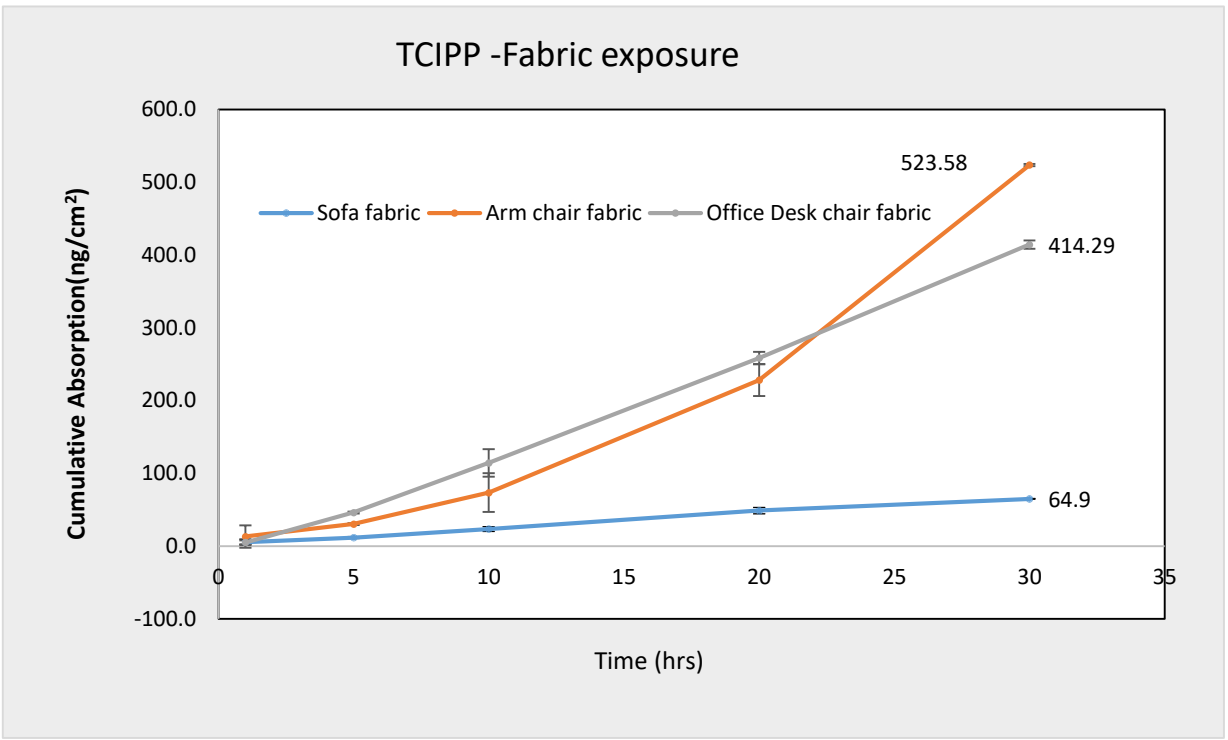

Fig 7.4: Cumulative absorption of TDCIPP detected in receptor fluid up to 30 h.

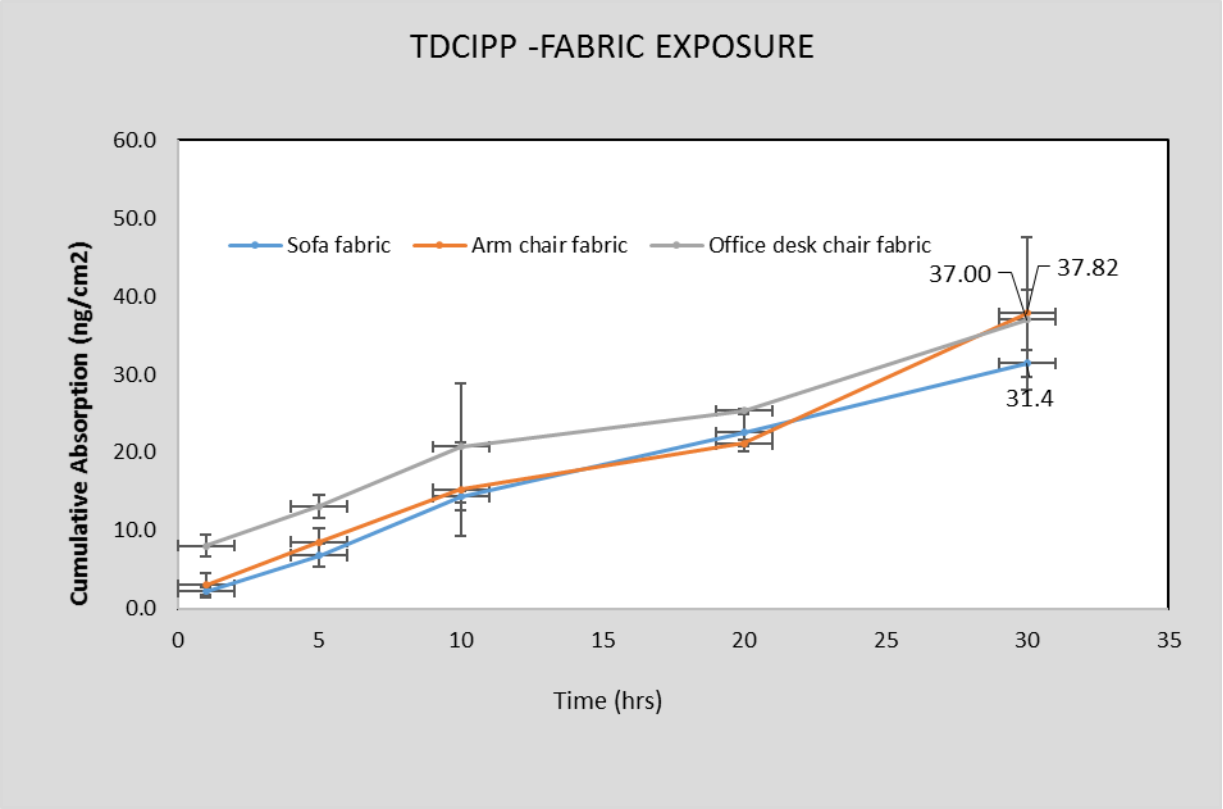

7.7.3 Estimated human dermal exposure (ng/kg bw/day) to TCEP, TCIPP & TDCIPP in fabrics (Fig 7.5, 7.6 and 7.7)

The average estimated human dermal exposure (ng/kg bw/day) for TCEP, TCIPP & TDCIPP in toddlers was found to be higher in toddlers than for adults which could be attributed to factors like higher body surface area by weight in toddlers.

In case of sofa fabric, TCEP contributed more to the daily dermal intake i.e. 31.5 and 106.79 ng/kg bw/day in both UK adults and toddlers respectively. In case of TCIPP, fabric from the domestic arm chair contributed more to the exposure whereas in case of TDCIPP, the contribution is more from the office chair.

Fig 7.5: Estimated daily dermal intake (ng/kg bw/day) of TCEP from upholstered fabrics

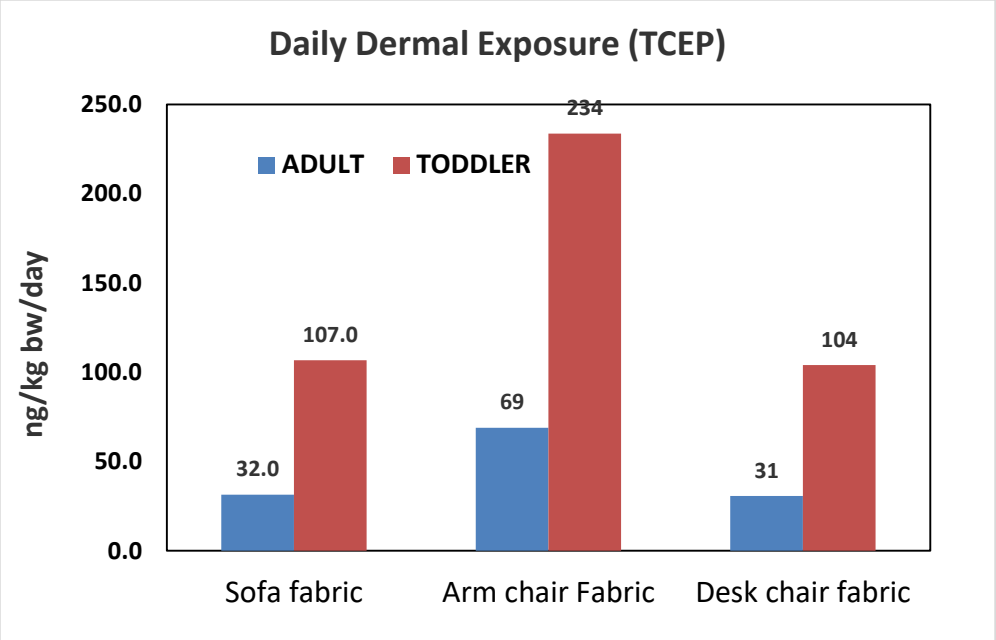

Fig 7.6: Estimated daily dermal intake (ng/kg bw/day) of TCIPP from upholstered fabrics.

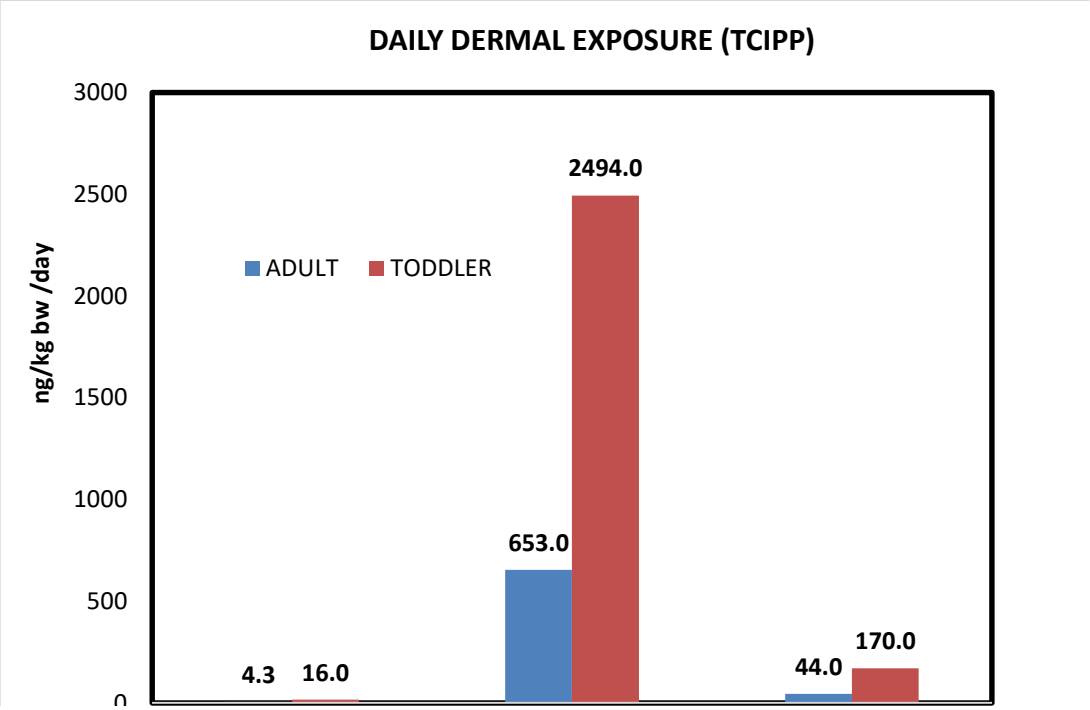

Fig 7.7: Estimated daily dermal intake (ng/kg bw/day) of TDCIPP from upholstered fabrics.

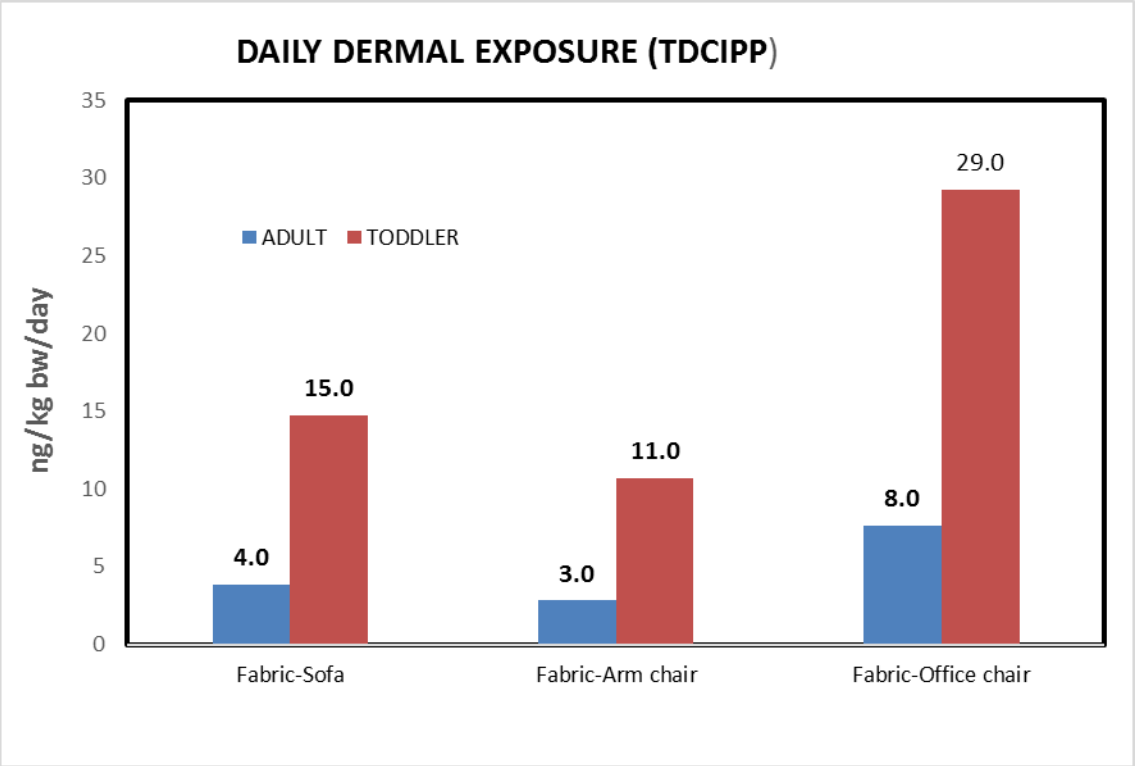

7.8: Summary

The paucity of data on human dermal absorption of PFRs and the extent of exposure to upholstered fabrics is a research gap hindering their accurate risk assessment. Thus we studied the transfer of FRs from upholstered fabrics. Bioaccessibility for TCIPP (~ 15-57 %) exceeds that of TDCIPP (~ 1-6%) and TCEP (~ 0.65-4%) for all three types of upholstered fabrics studied, suggesting that these flame retarded fabrics could act as a potential source of dermal exposure. The SSFL (sweat/sebum) influences the bioaccessibility of PFRs from fabrics. Bioaccessibility is higher for TCIPP from the fabrics as compared to TDCIPP

The bioaccessibility of PFRs from fabrics is lower than from dust. This could be due to the fact that FRs applied to the fabrics might have different physical or chemical forms and also due to the back coating treatments or polymerisation or derivatization of the parent molecule.

We tried to mimic real life dermal exposure of upholstered fabrics to the Episkin surface in presence of sweat and sebum under controlled conditions and we found that among the PFRs studied, the cumulative absorption was higher for TCIPP and followed by TCEP and TDCIPP. This is due to higher amount of TCIPP applied in all the three fabrics.

These data confirm the potential importance of the dermal route as a pathway of human exposure to TCEP, TCIPP & TDCIPP from upholstered fabric.

Dermal exposure estimates fell far below the reported health based limit values (HBLVs) for TDCIPP (5.4 µg/day according to OEHHA, 2015). No other health based limit values (HBLVs) of legislative standing for TCEP and TCIPP. Interestingly for toddlers for TCIPP uptake from arm chair fabric, as it is 2.5 µg/kg bw/day, so for a 10 kg toddler this is 250 µg/day. However, future research may erode this margin of safety.

Detailed studies are required to study the forensic microscopic details of fabrics to know the extent of distribution of applied PFRs either on the superficial layers or deep layers of the fabrics and subsequently its dissolution into the sweat on the skin surface. Also it would help us to clarify whether the chemicals are migrating from PUR foams to the covering fabrics and contributing to the dermal exposure of PFRs.

CHAPTER VIII

Summary and conclusions

Organic flame retardants (FRs) are widely added to polyurethane foam, plastics, electric and electronic equipment and textile coatings in furniture. The capacity of these chemicals to leach out from these consumer goods by volatilisation/abrasion and pollute the indoor environment coupled with evidence of their persistent, bioaccumulative and toxic properties is a cause of concern. Although many studies have examined the relationship between concentrations of FRs in indoor dust and in human biological fluids/tissues, we do not yet fully understand the exact mechanism via which FRs transfer from the indoor dust or the consumer goods to the body (i.e. whether it is ingestion of dust or dermal contact with dust and/or the consumer goods themselves). To date, the role of the dermal pathway has been somewhat overlooked, although some authors have suggested that it may be of importance.

This need for data on human dermal uptake of FRs coupled with the ethical and scientific problems associated with extrapolation of dermal data obtained from animals to humans, provided the driver for this research to evaluate alternative *in vitro* approaches to studying the dermal uptake of FRs. Specifically, we evaluated commercially-available 3D-HSE (human skin equivalent) models developed and applied widely in the cosmetics and pharmaceuticals sectors. Initially we evaluated the bioaccessibility of FRs from source matrices to skin fluids using artificial sweat and sebum. Then we developed a standard protocol according to the guidelines of OECD- 428 for dermal absorption of FRs as a neat compounds. The protocol was applied to two commercially available 3D HSE models namely, EpiDerm^{TM} and EPISKIN^{TM}. To evaluate the barrier function of 3D-HSE models, the permeability coefficients for FRs obtained from two models were evaluated against the ex *vivo* human skin. After establishing the protocol we tried to mimic the real life exposure scenario by

exposing the Episkin model to the potential sources of FRs like dust (dry or wet condition or in presence of moisturising cream), reference material plastics and contaminated upholstered fabrics. Finally we applied the PK model to predict the daily dermal intake of different FRs for UK adults and toddlers with contaminated dust, plastics and upholstered fabrics using different exposure scenarios.

8.1: SUMMARY AND CONCLUSIONS

The main achievements and outcomes of this research are summarised below:

- We successfully designed and applied an *in vitro* physiologically based extraction test to provide new insights into the dermal bioaccessibility of various FRs from indoor dust, upholstered fabrics and powdered plastic pellets to a synthetic sweat/sebum mixture (SSSM). The composition of the SSSM, compound-specific physicochemical properties (e.g. K_{OW}) and matrix properties (e.g. organic carbon content, FR concentration) were the major factors influencing FR bioaccessibility.
- Average bioaccessible fractions of α-, β-, γ- HBCD and TBBPA from indoor house dust to a physiologically-relevant 1:1 (sweat: sebum) mixture were: 41 %, 47 %, 50 % and 40 %, respectively. For TCEP, TCIPP and TDCIPP, the bioaccessible fractions were 10 %, 17 % and 19 % respectively.
- For BDE-209, the bioaccessibility to 100% sweat was 0.04 ± 0.01 %. This was the lowest value obtained for our target PBDEs, and is likely due to its low water solubility (<0.0001 mg/L) compared to other congeners. The reverse trend was observed for bioaccessibility to 100% sebum, with $f_{BIOACCESSSIBLE}$ highest for BDE-209 (98.5 ± 7.78 %), followed by BDE-28 (98.2 ± 7.08 %) and BDE-47 (87.18 ± 3.13 %). At the most physiologically relevant SSSM (i.e. 1:1 sweat: sebum), $f_{BIOACCESSSIBLE}$ was highest for BDE-209 (79.37 ± 7.66 %); however, no significant

relationship was observed between the degree of congener bromination and the $f_{BIOACCESSSIBLE}$.

- Previous studies have shown certain sunscreen lotions to act as inadvertent enhancers of the dermal penetration of potentially harmful chemicals (Pont et al. 2004, Walters et al. 1997). Therefore, we investigated the effect of topically-applied cosmetics on the dermal bioaccessibility of FRs in indoor dust. The results indicated that except for TBBPA, the presence of cosmetics (moisturising cream, sunscreen lotion, body spray, and shower gel) had a significant negative effect ($P < 0.05$) on the bioaccessibility of the studied FRs. The presence of cosmetics decreased the bioaccessibility of HBCDs and PBDEs from indoor dust, while shower gel and sunscreen lotion enhanced the bioaccessibility of target PFRs. The decrease in bioaccessibility for HBCDs and PBDEs was due to the retention of these lipophilic chemicals by skin cream products.
- A recent study (Hoffman et al. 2016) showed that playing with plastic toys was associated with higher handwipe levels of PBDEs. We hypothesise that the PBDEs in plastic can leach out upon contact with human SSFL and become available for absorption via penetration of the stratum corneum. The bioaccessibility ranged from 61 % to ~ 83 % in ERM-EC590 (LDPE) in case of pellets and significantly increased to 70 % to 94 % when the size of the pellets were reduced (microplastics). Both the lower PBDEs as well as the higher PBDEs were able to dissolve efficiently in the sweat and sebum mixture. The reasons for this may be attributed to the unique composition of the SSFL which contains lipophilic sebum that would facilitate the dissolution of highly lipophilic congeners (e.g. BDEs-183 and 209) together with the electrolyte-rich sweat which may favour dissolution of less hydrophobic congeners (e.g. 17 and 28) from the pulverised plastics. The reduced size of the pulverised plastics (~ 0.5 mm) resulted in a higher surface area for easy dissipation of the

polymers in the SSFL resulting in significantly higher bioaccessibility (%) for PBDEs (t-test, $P<0.01$, $n=3$) as compared to the intact pellet beads (~ 5 mm) for both the ERM-EC 590 & ERM-EC 591 reference plastics. Our results imply that in real life PBDEs could be bioaccessible to human sweat and sebum from low density polyethylene (LDPE) and polypropylene.

- The paucity of data on human dermal absorption of PFRs and the extent of exposure to consumers is a research gap hindering their accurate risk assessment. Thus we studied the transfer of FRs from upholstered fabrics. Bioaccessibility for TCIPP (~ 15-57 %) exceeds that of TDCIPP (~ 1-6%) and TCEP (~ 0.65-4%) for all three types of upholstered fabrics studied, suggesting that these flame retarded fabrics could act as a potential source of dermal exposure. The bioaccessibility of PFRs from fabrics is lower than from dust. This could be due to the fact that FRs applied to the fabrics might have different physical or chemical forms and also due to the back coating treatments or polymerisation or derivatization of the parent molecule.

In the second phase of the research we developed a protocol for studying dermal uptake of legacy and novel brominated flame retardants using two 3D-HSE models, EpiDerm™ and EPISKIN™ in compliance with the OECD guidelines 428. The results were then validated against a viable human *ex vivo* skin model to evaluate the barrier function of the 3D-HSE for the studied FRs.

- Our results showed a significant negative correlation between the permeability constant of FRs and their Log K_{OW} values. (Fig 4.27)
- For the first time we have mimicked real life dermal exposure *in vitro* by incorporating dry and wet conditions in our experiments. This provided insights into the influence on dermal uptake of the type of skin e.g. dry or oily. Dust was applied to the skin surface to show that it could be a potential source of dermal exposure to FRs.

Our results suggested that dermal absorption of lipophilic chemicals like HBCDs and PFRs was enhanced when the skin model was treated with a sweat: sebum mixture compared to a "dry" skin scenario. However, this effect was not significant.

- When ERM-EC591 micro plastics were exposed to the Episkin model, the absorbed mass of PBDEs with increasing Br content from BDE-28 to BDE-154 revealed a broad decrease in dermal absorption. Maximal penetration was achieved for Tetra-BDE and Penta-BDE, however Octa-BDE and Deca-BDE showed no penetration, although they were found to be more highly accumulated in the skin than the less brominated PBDEs studied.
- We applied our data on dermal bioaccessibility in worst case scenarios and bioavailability to estimate the internal exposure of UK adults and toddlers to our target FRs via dermal contact with dust, plastics and upholstered fabrics.

  The high concentrations of PBDEs in the ERM-EC 590 and ERM-EC 591 plastic matrices studied resulted in higher estimated dermal exposure than for dust but are still reassuringly below the current USEPA's health-based limit values (BDE-47 & BDE-99 HBLVs < 0.1 µg/kg/d) for PBDEs. For BDE-183 & BDE-209, we were unable to calculate the dermal exposure via plastics in humans due to its inability to penetrate the skin in presence of sweat/sebum.

  For the sofa fabrics studied, TCEP contributed more than other PFRs like TCIPP & TDCIPP to the daily dermal intake i.e. TCEP (31.5 and 106.79 ng/kg bw/day in both UK adults and toddlers respectively). In case of TCIPP, fabric from the domestic arm chair contributed 653.0 ng/kgbw/day & 2494 ng/kgbw/day in adults & toddlers respectively more to the exposure whereas in case of TDCIPP, the contribution is more from the office chair 29.0 ng/kg bw/day in toddlers group. These data confirm

the potential importance of the dermal route as a pathway of human exposure to TCEP, TCIPP & TDCIPP from upholstered fabric.

8.2: Future research recommendations

Although current commercially available HSE models may provide a useful alternative to study human dermal absorption of FRs, there remain several challenges and research gaps that need to be addressed in the near future. These include:

- Further improvements like the presence of hair follicles, sweat and sebaceous glands in the 3D-HSE models are still required to provide further potential pathways for percutaneous penetration. Vascularised full thickness models would allow the models to more closely mimic *in vivo* skin.
- More realistic repeated chronic exposures of the skin models are required to closely mimic the real life exposure scenarios without compromising the stability/viability of the 3D-HSE models. This would be helpful to study the tissue perturbations due to repeated and intermittent exposure, degradation/metabolism due to skin deposition and sustained release into the systemic circulation.
- To employ dynamic models like flow-through diffusion cells that offer an important advantage over static models i.e. the continuous flow of receptor fluid through the receiver compartment which helps to maintain the skin condition for compounds having large permeability coefficients. Also this set up helps to mimic the *in vivo* subcutaneous vasculature.
- Currently, very little is known about the dermal biotransformation of FRs so the conduct of future studies in this area is strongly recommended. Such work would enhance understanding of percutaneous metabolic pathways and identification of the metabolites thus formed.

- Further improvements can be made by mimicking real life exposure scenarios – e.g. using environmentally relevant exposure concentrations present in exposure media like soil, dust and different consumer products treated with FRs.

REFERENCES

(1984) **NTP** Toxicology and Carcinogenesis Studies of Tris(2-ethylhexyl)phosphate (CAS No. 78-42-2) In F344/N Rats and B6C3F1 Mice (Gavage Studies). *Natl Toxicol Program Tech Rep Ser,* 274**,** 1-178.

Abdallah, M. A.-E. & A. Covaci (2014a) Organophosphate Flame Retardants in Indoor Dust from Egypt: Implications for Human Exposure. *Environmental Science & Technology,* 48**,** 4782-4789.

Abdallah, M. A.-E. & S. Harrad (2011a) Tetrabromobisphenol-A, hexabromocyclododecane and its degradation products in UK human milk: Relationship to external exposure. *Environment International,* 37**,** 443-448.

Abdallah, M. A.-E., S. Harrad & A. Covaci (2008a) Hexabromocyclododecanes and Tetrabromobisphenol-A in Indoor Air and Dust in Birmingham, UK: Implications for Human Exposure. *Environmental Science & Technology,* 42**,** 6855-6861.

Abdallah, M. A.-E., G. Pawar & S. Harrad (2015a) Effect of Bromine Substitution on Human Dermal Absorption of Polybrominated Diphenyl Ethers. *Environmental Science & Technology,* 49**,** 10976-10983.

Abdallah, M. A.-E., C. Uchea, J. K. Chipman & S. Harrad (2014a) Enantioselective Biotransformation of Hexabromocyclododecane by in Vitro Rat and Trout Hepatic Sub-Cellular Fractions. *Environmental Science & Technology,* 48**,** 2732-2740.

Abdallah, M. A.-E., A. H. Zaky & A. Covaci Levels and profiles of organohalogenated contaminants in human blood from Egypt. *Chemosphere*.

Abdallah, M. A. & A. Covaci (2014b) Organophosphate flame retardants in indoor dust from Egypt: implications for human exposure. *Environmental Science & Technology,* 48**,** 4782-9.

Abdallah, M. A. & S. Harrad (2011b) Tetrabromobisphenol-A, hexabromocyclododecane and its degradation products in UK human milk: relationship to external exposure. *Environ Int,* 37**,** 443-8.

--- (2014) Polybrominated diphenyl ethers in UK human milk: implications for infant exposure and relationship to external exposure. *Environ Int,* 63**,** 130-6.

Abdallah, M. A., S. Harrad & A. Covaci (2008b) Hexabromocyclododecanes and tetrabromobisphenol-A in indoor air and dust in Birmingham, U.K: implications for human exposure. *Environ Sci Technol,* 42**,** 6855-61.

Abdallah, M. A., G. Pawar & S. Harrad (2015b) Effect of Bromine Substitution on Human Dermal Absorption of Polybrominated Diphenyl Ethers. *Environ Sci Technol,* 49**,** 10976-83.

--- (2015) Evaluation of 3D-human skin equivalents for assessment of human dermal absorption of some brominated flame retardants. *Environ Int,* 84**,** 64-70.

Abdallah, M. A., E. Tilston, S. Harrad & C. Collins (2012) In vitro assessment of the bioaccessibility of brominated flame retardants in indoor dust using a colon extended model of the human gastrointestinal tract. *J Environ Monit,* 14**,** 3276-83.

Abdallah, M. A., C. Uchea, J. K. Chipman & S. Harrad (2014b) Enantioselective Biotransformation of Hexabromocyclododecane by in Vitro Rat and Trout Hepatic Sub-Cellular Fractions. *Environmental Science & Technology,* 48**,** 2732-2740.

Abdallah, M. A., J. Zhang, G. Pawar, M. R. Viant, J. K. Chipman, K. D'Silva, M. Bromirski & S. Harrad (2015) High-resolution mass spectrometry provides novel insights into products of human metabolism of organophosphate and brominated flame retardants. *Anal Bioanal Chem,* 407**,** 1871-83.

Abdelouahab, N., Y. Ainmelk & L. Takser (2011) Polybrominated diphenyl ethers and sperm quality. *Reprod Toxicol,* 31**,** 546-50.

Abou-Donia, M. B. (1981) Organophosphorus ester-induced delayed neurotoxicity. *Annu Rev Pharmacol Toxicol,* 21**,** 511-48.

Abou-Elwafa Abdallah, M., G. Pawar & S. Harrad (2016) Human dermal absorption of chlorinated organophosphate flame retardants; implications for human exposure. *Toxicol Appl Pharmacol,* 291**,** 28-37.

Abou-Elwafa Abdallah, M., E. Tilston, S. Harrad & C. Collins (2012) In vitro assessment of the bioaccessibility of brominated flame retardants in indoor dust using a colon extended model of the human gastrointestinal tract. *Journal of Environmental Monitoring,* 14**,** 3276-3283.

Abrams, K., J. D. Harvell, D. Shriner, P. Wertz, H. Maibach, H. I. Maibach & S. J. Rehfeld (1993) Effect of organic solvents on in vitro human skin water barrier function. *J Invest Dermatol,* 101**,** 609-13.

Ackermann, K., S. L. Borgia, H. C. Korting, K. R. Mewes & M. Schafer-Korting (2010) The Phenion full-thickness skin model for percutaneous absorption testing. *Skin Pharmacol Physiol,* 23**,** 105-12.

Aggarwal, M., M. Battalora, P. Fisher, A. Huser, R. Parr-Dobrzanski, M. Soufi, V. Mostert, C. Strupp, P. Whalley, C. Wiemann & R. Billington (2014) Assessment of in

vitro human dermal absorption studies on pesticides to determine default values, opportunities for read-across and influence of dilution on absorption. *Regul Toxicol Pharmacol,* 68**,** 412-23.

Alaee, M., P. Arias, A. Sjödin & Å. Bergman (2003) An overview of commercially used brominated flame retardants, their applications, their use patterns in different countries/regions and possible modes of release. *Environment International,* 29**,** 683-689.

Ali, N., A. C. Dirtu, N. V. Eede, E. Goosey, S. Harrad, H. Neels, A. t Mannetje, J. Coakley, J. Douwes & A. Covaci (2012a) Occurrence of alternative flame retardants in indoor dust from New Zealand: Indoor sources and human exposure assessment. *Chemosphere,* 88**,** 1276-82.

Ali, N., S. Harrad, E. Goosey, H. Neels & A. Covaci (2011) "Novel" brominated flame retardants in Belgian and UK indoor dust: implications for human exposure. *Chemosphere,* 83**,** 1360-5.

Ali, N., N. Van den Eede, A. C. Dirtu, H. Neels & A. Covaci (2012c) Assessment of human exposure to indoor organic contaminants via dust ingestion in Pakistan. *Indoor Air,* 22**,** 200-211.

Alves, A., A. Covaci & S. Voorspoels (2017) Method development for assessing the human exposure to organophosphate flame retardants in hair and nails. *Chemosphere,* 168**,** 692-698.

Antignac, J. P., R. Cariou, D. Maume, P. Marchand, F. Monteau, D. Zalko, A. Berrebi, J. P. Cravedi, F. Andre & B. Le Bizec (2008) Exposure assessment of fetus and newborn to brominated flame retardants in France: preliminary data. *Mol Nutr Food Res,* 52**,** 258-65.

Auletta, C. S., M. L. Weiner & W. R. Richter (1998) A dietary toxicity/oncogenicity study of tributyl phosphate in the rat1. *Toxicology,* 128**,** 125-134.

Bartosova, L. & J. Bajgar (2012) Transdermal drug delivery in vitro using diffusion cells. *Curr Med Chem,* 19**,** 4671-7.

Bergh, C., K. Magnus Aberg, M. Svartengren, G. Emenius & C. Ostman (2011) Organophosphate and phthalate esters in indoor air: a comparison between multi-storey buildings with high and low prevalence of sick building symptoms. *J Environ Monit,* 13**,** 2001-9.

Boelsma, E., S. Gibbs, C. Faller & M. Ponec (2000) Characterization and comparison of reconstructed skin models: morphological and immunohistochemical evaluation. *Acta Derm Venereol,* 80**,** 82-8.

Bramwell, L., A. Fernandes, M. Rose, S. Harrad & T. Pless-Mulloli (2014) PBDEs and PBBs in human serum and breast milk from cohabiting UK couples. *Chemosphere,* 116**,** 67-74.

Brandsma, S. H., J. de Boer, P. E. G. Leonards, W. P. Cofino & A. Covaci (2013) Organophosphorus flame-retardant and plasticizer analysis, including recommendations from the first worldwide interlaboratory study. *TrAC Trends in Analytical Chemistry,* 43**,** 217-228.

Breitkreutz, D., I. Koxholt, K. Thiemann & R. Nischt (2013) Skin Basement Membrane: The Foundation of Epidermal Integrity—BM Functions and Diverse Roles of Bridging Molecules Nidogen and Perlecan. *BioMed Research International,* 2013**,** 16.

Brommer, S. (2014) Characterising human exposure to organophosphate ester flame retardants. *Ph.D. thesis. University of Birmingham. etheses.bham.ac.uk/5292/5/Brommer14PhD.pdf.*

Brommer, S. & S. Harrad (2015) Sources and human exposure implications of concentrations of organophosphate flame retardants in dust from UK cars, classrooms, living rooms, and offices. *Environ Int,* 83**,** 202-7.

Brommer, S., S. Harrad, N. Van den Eede & A. Covaci (2012a) Concentrations of organophosphate esters and brominated flame retardants in German indoor dust samples. *Journal of Environmental Monitoring,* 14**,** 2482-2487.

Bruchajzer, E., B. Frydrych, S. Sporny & J. A. Szymańska (2010) Toxicity of penta- and decabromodiphenyl ethers after repeated administration to rats: a comparative study. *Archives of Toxicology,* 84**,** 287-299.

Buckley, W. R. & C. E. Lewis (1960) The "ruster" in industry. *J Occup Med,* 2**,** 23-31.

Buist, H. E., J. A. van Burgsteden, A. P. Freidig, W. J. Maas & J. J. van de Sandt (2010) New in vitro dermal absorption database and the prediction of dermal absorption under finite conditions for risk assessment purposes. *Regul Toxicol Pharmacol,* 57**,** 200-9.

Butt, C. M., J. Congleton, K. Hoffman, M. Fang & H. M. Stapleton (2014a) Metabolites of organophosphate flame retardants and 2-ethylhexyl tetrabromobenzoate in urine from paired mothers and toddlers. *Environ Sci Technol,* 48**,** 10432-8.

Carignan, C. C., W. Heiger-Bernays, M. D. McClean, S. C. Roberts, H. M. Stapleton, A. Sjödin & T. F. Webster (2013) Flame Retardant Exposure among Collegiate United States Gymnasts. *Environmental Science & Technology,* 47**,** 13848-13856.

Cequier, E., R. M. Marcé, G. Becher & C. Thomsen (2015) Comparing human exposure to emerging and legacy flame retardants from the indoor environment and diet with concentrations measured in serum. *Environment International,* 74**,** 54-59.

Chan, W. K. & K. M. Chan (2012) Disruption of the hypothalamic-pituitary-thyroid axis in zebrafish embryo-larvae following waterborne exposure to BDE-47, TBBPA and BPA. *Aquat Toxicol,* 108**,** 106-11.

Chao, H. R., S. L. Wang, W. J. Lee, Y. F. Wang & O. Papke (2007) Levels of polybrominated diphenyl ethers (PBDEs) in breast milk from central Taiwan and their relation to infant birth outcome and maternal menstruation effects. *Environ Int,* 33**,** 239-45.

Chen, J. X., L. L. Xu, J. H. Mei, X. B. Yu, H. B. Kuang, H. Y. Liu, Y. J. Wu & J. L. Wang (2012) Involvement of neuropathy target esterase in tri-ortho-cresyl phosphate-induced testicular spermatogenesis failure and growth inhibition of spermatogonial stem cells in mice. *Toxicol Lett,* 211**,** 54-61.

Chen, S.-J., Y.-J. Ma, J. Wang, D. Chen, X.-J. Luo & B.-X. Mai (2009) Brominated Flame Retardants in Children's Toys: Concentration, Composition, and Children's Exposure and Risk Assessment. *Environmental Science & Technology,* 43**,** 4200-4206.

Chevrier, J., K. G. Harley, A. Bradman, M. Gharbi, A. Sjödin & B. Eskenazi (2010) Polybrominated Diphenyl Ether (PBDE) Flame Retardants and Thyroid Hormone during Pregnancy. *Environmental Health Perspectives,* 118**,** 1444-1449.

Choy, Y. B. & M. R. Prausnitz (2011) The rule of five for non-oral routes of drug delivery: ophthalmic, inhalation and transdermal. *Pharm Res,* 28**,** 943-8.

Chu, I., D. C. Villeneuve, B. McDonald, V. E. Secours & V. E. Valli (1987) Pentachlorotoluene and pentabromotoluene: results of a subacute and a subchronic toxicity study in the rat. *J Environ Sci Health B,* 22**,** 303-17.

Covaci, A., A. C. Gerecke, R. J. Law, S. Voorspoels, M. Kohler, N. V. Heeb, H. Leslie, C. R. Allchin & J. De Boer (2006a) Hexabromocyclododecanes (HBCDs) in the environment and humans: a review. *Environ Sci Technol,* 40**,** 3679-88.

Covaci, A., S. Harrad & M. A. Abdallah (2011a). *Environ Int,* 37**,** 532.

Covaci, A., S. Harrad, M. A. E. Abdallah, N. Ali, R. J. Law, D. Herzke & C. A. de Wit (2011b) Novel brominated flame retardants: A review of their analysis, environmental fate and behaviour. *Environment International,* 37**,** 532-556.

Covaci, A., S. Voorspoels, M. A.-E. Abdallah, T. Geens, S. Harrad & R. J. Law (2009) Analytical and environmental aspects of the flame retardant tetrabromobisphenol-A and its derivatives. *Journal of Chromatography A,* 1216**,** 346-363.

Darnerud, P. O. (2008) Brominated flame retardants as possible endocrine disrupters. *Int J Androl,* 31**,** 152-60.

Davies, D. J., J. R. Heylings, T. J. McCarthy & C. M. Correa (2015) Development of an in vitro model for studying the penetration of chemicals through compromised skin. *Toxicology in Vitro,* 29**,** 176-181.

De Saeger, S., H. Sergeant, M. Piette, N. Bruneel, W. Van de Voorde & C. Van Peteghem (2005) Monitoring of polychlorinated biphenyls in Belgian human adipose tissue samples. *Chemosphere,* 58**,** 953-60.

Dishaw, L. V., C. M. Powers, I. T. Ryde, S. C. Roberts, F. J. Seidler, T. A. Slotkin & H. M. Stapleton (2011) Is the PentaBDE replacement, tris (1,3-dichloro-2-propyl) phosphate (TDCPP), a developmental neurotoxicant? Studies in PC12 cells. *Toxicol Appl Pharmacol,* 256**,** 281-9.

Du, M., D. Zhang, C. Yan & X. Zhang (2012) Developmental toxicity evaluation of three hexabromocyclododecane diastereoisomers on zebrafish embryos. *Aquat Toxicol,* 113**,** 1-10.

Duling, M., A. Stefaniak, R. Lawrence, S. Chipera & M. Abbas Virji (2012) Release of beryllium from mineral ores in artificial lung and skin surface fluids. *Environmental Geochemistry and Health,* 34**,** 313-322.

Egloff, C., D. Crump, S. Chiu, G. Manning, K. K. McLaren, C. G. Cassone, R. J. Letcher, L. T. Gauthier & S. W. Kennedy (2011) In vitro and in ovo effects of four brominated flame retardants on toxicity and hepatic mRNA expression in chicken embryos. *Toxicol Lett,* 207**,** 25-33.

Eljarrat, E., P. Guerra, E. Martinez, M. Farre, J. G. Alvarez, M. Lopez-Teijon & D. Barcelo (2009) Hexabromocyclododecane in human breast milk: levels and enantiomeric patterns. *Environ Sci Technol,* 43**,** 1940-6.

Ertl, H. & W. Butte (2012a) Bioaccessibility of pesticides and polychlorinated biphenyls from house dust: in-vitro methods and human exposure assessment. *J Expos Sci Environ Epidemiol,* 22**,** 574-583.

Esa, A. H., G. A. Warr & D. S. Newcombe (1988) Immunotoxicity of organophosphorus compounds. Modulation of cell-mediated immune responses by inhibition of monocyte accessory functions. *Clin Immunol Immunopathol,* 49**,** 41-52.

Esser, C. & C. Gotz. *Filling the gaps: need for research on cell-specific xenobiotic metabolism in the skin*. Arch Toxicol. 2013 Oct;87(10):1873-5. doi: 10.1007/s00204-013-1031-7. Epub 2013 Mar 8.

EU Risk Assessment Report (2006) European Union Risk Assessment Report on 2,2',6,6'-tetrabromo-4,4'-isopropylidenediphenol(tetrabromobisphenol-A or TBBP-A). Part II, Human health. *European Commission, Joint Research Centre, European Chemicals Bureau, EUR22161E, 2006.,* vol. 63.

Fang, M. & H. M. Stapleton (2014) Evaluating the Bioaccessibility of Flame Retardants in House Dust Using an In Vitro Tenax Bead-Assisted Sorptive Physiologically Based Method. *Environmental Science & Technology,* 48**,** 13323-13330.

Fautz, R. & H. G. Miltenburger (1994) Influence of organophosphorus compounds on different cellular immune functions in vitro. *Toxicol In Vitro,* 8**,** 1027-31.

Franz, T. J. (1975) Percutaneous absorption on the relevance of in vitro data. *J Invest Dermatol,* 64**,** 190-5.

Frederiksen, M., K. Vorkamp, N. M. Jensen, J. A. Sorensen, L. E. Knudsen, L. S. Sorensen, T. F. Webster & J. B. Nielsen (2016) Dermal uptake and percutaneous penetration of ten flame retardants in a human skin ex vivo model. *Chemosphere,* 162**,** 308-14.

Frederiksen, M., K. Vorkamp, M. Thomsen & L. E. Knudsen (2009) Human internal and external exposure to PBDEs--a review of levels and sources. *Int J Hyg Environ Health,* 212**,** 109-34.

Freudenthal, R. I., L. J. McDonald, J. V. Johnson, D. L. McCormick & R. T. Henrich (2000) Comparative Metabolism and Toxicokinetics of 14C-ResorcinoI Bis-Diphenylphosphate (RDP) in the Rat, Mouse, and Monkey. *International Journal of Toxicology,* 19**,** 233-242.

Fromme, H., G. Becher, B. Hilger & W. Volkel (2016) Brominated flame retardants - Exposure and risk assessment for the general population. *Int J Hyg Environ Health,* 219**,** 1-23.

Garner, C. E., J. Demeter & H. B. Matthews (2006a) The effect of chlorine substitution on the disposition of polychlorinated biphenyls following dermal administration. *Toxicology and Applied Pharmacology,* 216**,** 157-167.

Garner, C. E. & H. B. Matthews (1998) The effect of chlorine substitution on the dermal absorption of polychlorinated biphenyls. *Toxicol Appl Pharmacol,* 149**,** 150-8.

Ghosh, R., K. J. Hageman & E. Bjorklund (2011) Selective pressurized liquid extraction of three classes of halogenated contaminants in fish. *J Chromatogr A,* 14**,** 7242-7.

Gibbs, S., E. Corsini, S. W. Spiekstra, V. Galbiati, H. W. Fuchs, G. DeGeorge, M. Troese, P. Hayden, W. Deng & E. Roggen (2013) An epidermal equivalent assay for identification and ranking potency of contact sensitizers. *Toxicol Appl Pharmacol,* 272**,** 529-541.

Gill, U., I. Chu, J. J. Ryan & M. Feeley (2004) Polybrominated diphenyl ethers: human tissue levels and toxicology. *Rev Environ Contam Toxicol,* 183**,** 55-97.

Godin, B. & E. Touitou (2007) Transdermal skin delivery: Predictions for humans from in vivo, ex vivo and animal models. *Advanced Drug Delivery Reviews,* 59**,** 1152-1161.

Gundert-Remy, U., U. Bernauer, B. Blomeke, B. Doring, E. Fabian, C. Goebel, S. Hessel, C. Jackh, A. Lampen, F. Oesch, E. Petzinger, W. Volkel & P. H. Roos (2014) Extrahepatic metabolism at the body's internal-external interfaces. *Drug Metab Rev,* 46**,** 291-324.

Guth, K., M. Schafer-Korting, E. Fabian, R. Landsiedel & B. van Ravenzwaay (2015) Suitability of skin integrity tests for dermal absorption studies in vitro. *Toxicol In Vitro,* 29**,** 113-23.

Hakk, H. & R. J. Letcher (2003) Metabolism in the toxicokinetics and fate of brominated flame retardants--a review. *Environ Int,* 29**,** 801-28.

Hallgren, S., T. Sinjari, H. Håkansson & P. Darnerud (2001) Effects of polybrominated diphenyl ethers (PBDEs) and polychlorinated biphenyls (PCBs) on thyroid hormone and vitamin A levels in rats and mice. *Archives of Toxicology,* 75**,** 200-208.

Hamers, T., J. H. Kamstra, E. Sonneveld, A. J. Murk, M. H. Kester, P. L. Andersson, J. Legler & A. Brouwer (2006) In vitro profiling of the endocrine-disrupting potency of brominated flame retardants. *Toxicol Sci,* 92**,** 157-73.

Hammel, S. C., K. Hoffman, T. F. Webster, K. A. Anderson & H. M. Stapleton (2016) Measuring Personal Exposure to Organophosphate Flame Retardants Using Silicone Wristbands and Hand Wipes. *Environmental Science & Technology,* 50**,** 4483-4491.

Harley, K. G., J. Chevrier, R. Aguilar Schall, A. Sjodin, A. Bradman & B. Eskenazi (2011) Association of prenatal exposure to polybrominated diphenyl ethers and infant birth weight. *Am J Epidemiol,* 174**,** 885-92.

Harley, K. G., A. R. Marks, J. Chevrier, A. Bradman, A. Sjodin & B. Eskenazi (2010a) PBDE concentrations in women's serum and fecundability. *Environ Health Perspect,* 118**,** 699-704.

Harrad, S., S. Brommer & J. F. Mueller (2016) Concentrations of organophosphate flame retardants in dust from cars, homes, and offices: An international comparison. *Emerging Contaminants,* 2**,** 66-72.

Harrad, S., C. A. de Wit, M. A. Abdallah, C. Bergh, J. A. Bjorklund, A. Covaci, P. O. Darnerud, J. de Boer, M. Diamond, S. Huber, P. Leonards, M. Mandalakis, C. Ostman, L. S. Haug, C. Thomsen & T. F. Webster (2010a) Indoor contamination with hexabromocyclododecanes, polybrominated diphenyl ethers, and perfluoroalkyl compounds: an important exposure pathway for people? *Environ Sci Technol,* 44**,** 3221-31.

Harrad, S. & M. Diamond (2006) New Directions: Exposure to polybrominated diphenyl ethers (PBDEs) and polychlorinated biphenyls (PCBs): Current and future scenarios. *Atmospheric Environment,* 40**,** 1187-1188.

Harrad, S., E. Goosey, J. Desborough, M. A. Abdallah, L. Roosens & A. Covaci (2010b) Dust from U.K. primary school classrooms and daycare centers: the significance of dust as a pathway of exposure of young U.K. children to brominated flame retardants and polychlorinated biphenyls. *Environ Sci Technol,* 44**,** 4198-202.

Harrad, S., C. Ibarra, M. Diamond, L. Melymuk, M. Robson, J. Douwes, L. Roosens, A. C. Dirtu & A. Covaci (2008) Polybrominated diphenyl ethers in domestic indoor dust from Canada, New Zealand, United Kingdom and United States. *Environ Int,* 34**,** 232-8.

Hartung, T., S. Bremer, S. Casati, S. Coecke, R. Corvi, S. Fortaner, L. Gribaldo, M. Halder, S. Hoffmann, A. J. Roi, P. Prieto, E. Sabbioni, L. Scott, A. Worth & V. Zuang (2004) A modular approach to the ECVAM principles on test validity. *Altern Lab Anim,* 32**,** 467-72.

Hedberg, Y., K. Midander & I. O. Wallinder (2010) Particles, sweat, and tears: a comparative study on bioaccessibility of ferrochromium alloy and stainless steel particles, the pure metals and their metal oxides, in simulated skin and eye contact. *Integr Environ Assess Manag,* 6**,** 456-68.

Herbstman, J. B., A. Sjodin, M. Kurzon, S. A. Lederman, R. S. Jones, V. Rauh, L. L. Needham, D. Tang, M. Niedzwiecki, R. Y. Wang & F. Perera (2010) Prenatal exposure to PBDEs and neurodevelopment. *Environ Health Perspect,* 118**,** 712-9.

Hillwalker, W. E. & K. A. Anderson (2014) Bioaccessibility of metals in alloys: evaluation of three surrogate biofluids. *Environ Pollut,* 185**,** 52-8.

Hoath, S. B. & D. G. Leahy (2003) The Organization of Human Epidermis: Functional Epidermal Units and Phi Proportionality. *Journal of Investigative Dermatology,* 121**,** 1440-1446.

Hoffman, K., J. L. Daniels & H. M. Stapleton (2014) Urinary metabolites of organophosphate flame retardants and their variability in pregnant women. *Environ Int,* 63**,** 169-72.

Hoffman, K., T. F. Webster, A. Sjodin & H. M. Stapleton (2016) Toddler/'s behavior and its impacts on exposure to polybrominated diphenyl ethers. *J Expos Sci Environ Epidemiol*.

Hughes, M. F., B. C. Edwards, C. T. Mitchell & B. Bhooshan (2001) In vitro dermal absorption of flame retardant chemicals. *Food Chem Toxicol,* 39**,** 1263-70.

Ionas, A. C., J. Ulevicus, A. B. Gómez, S. H. Brandsma, P. E. G. Leonards, M. van de Bor & A. Covaci (2016) Children's exposure to polybrominated diphenyl ethers (PBDEs) through mouthing toys. *Environment International,* 87**,** 101-107.

Ismail, N., S. B. Gewurtz, K. Pleskach, D. M. Whittle, P. A. Helm, C. H. Marvin & G. T. Tomy (2009) Brominated and chlorinated flame retardants in Lake Ontario, Canada, lake trout (Salvelinus namaycush) between 1979 and 2004 and possible influences of food-web changes. *Environ Toxicol Chem,* 28**,** 910-20.

Jackh, C., V. Blatz, E. Fabian, K. Guth, B. van Ravenzwaay, K. Reisinger & R. Landsiedel (2011) Characterization of enzyme activities of Cytochrome P450 enzymes, Flavin-dependent monooxygenases, N-acetyltransferases and UDP-glucuronyltransferases in human reconstructed epidermis and full-thickness skin models. *Toxicol In Vitro,* 25**,** 1209-14.

Jakasa, I. & S. Kezic (2008) Evaluation of in-vivo animal and in-vitro models for prediction of dermal absorption in man. *Hum Exp Toxicol,* 27**,** 281-8.

Jin, S., F. Yang, Y. Hui, Y. Xu, Y. Lu & J. Liu (2010) Cytotoxicity and apoptosis induction on RTG-2 cells of 2,2',4,4'-tetrabromodiphenyl ether (BDE-47) and decabrominated diphenyl ether (BDE-209). *Toxicol In Vitro,* 24**,** 1190-6.

Johnson-Restrepo, B., D. H. Adams & K. Kannan (2008) Tetrabromobisphenol A (TBBPA) and hexabromocyclododecanes (HBCDs) in tissues of humans, dolphins, and sharks from the United States. *Chemosphere,* 70**,** 1935-1944.

Johnson-Restrepo, B. & K. Kannan (2009) An assessment of sources and pathways of human exposure to polybrominated diphenyl ethers in the United States. *Chemosphere,* 76**,** 542-548.

Johnson, P. I., H. M. Stapleton, B. Mukherjee, R. Hauser & J. D. Meeker (2013) Associations between brominated flame retardants in house dust and hormone levels in men. *Sci Total Environ,* 446**,** 177-84.

Johnson, P. I., H. M. Stapleton, A. Sjodin & J. D. Meeker (2010) Relationships between Polybrominated Diphenyl Ether Concentrations in House Dust and Serum. *Environmental Science & Technology,* 44**,** 5627-5632.

Jonsson, O. B. & U. L. Nilsson (2003) Determination of organophosphate ester plasticisers in blood donor plasma using a new stir-bar assisted microporous membrane liquid-liquid extractor. *Journal of Separation Science,* 26**,** 886-892.

Kademoglou, K., F. Xu, J. A. Padilla-Sanchez, L. S. Haug, A. Covaci & C. D. Collins Legacy and alternative flame retardants in Norwegian and UK indoor environment: Implications of human exposure via dust ingestion. *Environment International*.

Kandarova, H., S. Letasiova, T. Milasova & M. Klausner (2013) Analysis of the validated epiderm skin corrosion test (EpiDerm SCT) and a prediction model for sub-categorization according to the UN GHS and EU CLP. *Toxicology Letters,* 221, Supplement**,** S141.

Karlsson, M., A. Julander, B. van Bavel & L. Hardell (2007) Levels of brominated flame retardants in blood in relation to levels in household air and dust. *Environment International,* 33**,** 62-69.

KEMI (2008) National Chemicals Inspectorate, EU Risk Assessment Report on Hexabromocyclododecane. *R044_0710_env_hh.doc; Sundbyberg, Sweden*

Khalaf, H., A. Larsson, H. Berg, R. McCrindle, G. Arsenault & P. E. Olsson (2009) Diastereomers of the brominated flame retardant 1,2-dibromo-4-(1,2 dibromoethyl)cyclohexane induce androgen receptor activation in the hepg2 hepatocellular carcinoma cell line and the lncap prostate cancer cell line. *Environ Health Perspect,* 117**,** 1853-9.

Kitamura, S., N. Jinno, S. Ohta, H. Kuroki & N. Fujimoto (2002) Thyroid hormonal activity of the flame retardants tetrabromobisphenol A and tetrachlorobisphenol A. *Biochem Biophys Res Commun,* 293**,** 554-9.

Knudsen, G. A., M. F. Hughes, K. L. McIntosh, J. M. Sanders & L. S. Birnbaum (2015) Estimation of tetrabromobisphenol A (TBBPA) percutaneous uptake in humans using the parallelogram method. *Toxicology and Applied Pharmacology,* 289**,** 323-329.

Knudsen, G. A., J. M. Sanders, M. F. Hughes, E. P. Hull & L. S. Birnbaum (2016b) The biological fate of decabromodiphenyl ethane following oral, dermal or intravenous administration. *Xenobiotica***,** 1-9.

Kojima, H., S. Takeuchi, T. Itoh, M. Iida, S. Kobayashi & T. Yoshida (2013) In vitro endocrine disruption potential of organophosphate flame retardants via human nuclear receptors. *Toxicology,* 314**,** 76-83.

Kucharska, A., E. Cequier, C. Thomsen, G. Becher, A. Covaci & S. Voorspoels (2015a) Assessment of human hair as an indicator of exposure to organophosphate flame retardants. Case study on a Norwegian mother–child cohort. *Environment International,* 83**,** 50-57.

Kucharska, A., A. Covaci, G. Vanermen & S. Voorspoels (2015b) Non-invasive biomonitoring for PFRs and PBDEs: New insights in analysis of human hair externally exposed to selected flame retardants. *Science of The Total Environment,* 505**,** 1062-1071.

Kulthong, K., S. Srisung, K. Boonpavanitchakul, W. Kangwansupamonkon & R. Maniratanachote (2010) Determination of silver nanoparticle release from antibacterial fabrics into artificial sweat. *Part Fibre Toxicol,* 7**,** 8.

Kuriyama, S. N., C. E. Talsness, K. Grote & I. Chahoud (2005) Developmental Exposure to Low-Dose PBDE-99: Effects on Male Fertility and Neurobehavior in Rat Offspring. *Environmental Health Perspectives,* 113**,** 149-154.

Lane, M. E. (2013) Skin penetration enhancers. *Int J Pharm,* 447**,** 12-21.

Law, R. J., A. Covaci, S. Harrad, D. Herzke, M. A. Abdallah, K. Fernie, L. M. Toms & H. Takigami (2014) Levels and trends of PBDEs and HBCDs in the global environment: status at the end of 2012. *Environ Int,* 65**,** 147-58.

Lee, E., T. H. Kim, J. S. Choi, P. Nabanata, N. Y. Kim, M. Y. Ahn, K. K. Jung, I. H. Kang, T. S. Kim, S. J. Kwack, K. L. Park, S. H. Kim, T. S. Kang, J. Lee, B. M. Lee & H. S. Kim (2010) Evaluation of liver and thyroid toxicity in Sprague-Dawley rats after exposure to polybrominated diphenyl ether BDE-209. *J Toxicol Sci,* 35**,** 535-45.

Lema, S. C., I. R. Schultz, N. L. Scholz, J. P. Incardona & P. Swanson (2007) Neural defects and cardiac arrhythmia in fish larvae following embryonic exposure to 2,2′,4,4′-tetrabromodiphenyl ether (PBDE 47). *Aquatic Toxicology,* 82**,** 296-307.

Li, P., J. Jin, Y. Wang, J. Hu, M. Xu, Y. Sun & Y. Ma (2017) Concentrations of organophosphorus, polybromobenzene, and polybrominated diphenyl ether flame retardants in human serum, and relationships between concentrations and donor ages. *Chemosphere,* 171**,** 654-660.

Li, P., C. Q. Yang, J. Jin, Y. Wang, W. Z. Liu & W. W. Ding (2014) Correlations between HBCD and thyroid hormone concentrations in human serum from production source area]. *Huan Jing Ke Xue,* 35**,** 3970-6.

Li, Y., L. Yu, J. Wang, J. Wu, B. Mai & J. Dai (2013) Accumulation pattern of Dechlorane Plus and associated biological effects on rats after 90 d of exposure. *Chemosphere,* 90**,** 2149-2156.

Liang, X., W. Li, C. J. Martyniuk, J. Zha, Z. Wang, G. Cheng & J. P. Giesy (2014) Effects of dechlorane plus on the hepatic proteome of juvenile Chinese sturgeon (Acipenser sinensis). *Aquat Toxicol,* 148**,** 83-91.

Lignell, S., M. Aune, P. O. Darnerud, A. Hanberg, S. C. Larsson & A. Glynn (2013) Prenatal exposure to polychlorinated biphenyls (PCBs) and polybrominated diphenyl ethers (PBDEs) may influence birth weight among infants in a Swedish cohort with background exposure: a cross-sectional study. *Environ Health,* 12**,** 12-44.

Liu, L.-Y., K. He, R. A. Hites & A. Salamova (2016) Hair and Nails as Noninvasive Biomarkers of Human Exposure to Brominated and Organophosphate Flame Retardants. *Environmental Science & Technology,* 50**,** 3065-3073.

Liu, X., K. Ji & K. Choi (2012) Endocrine disruption potentials of organophosphate flame retardants and related mechanisms in H295R and MVLN cell lines and in zebrafish. *Aquat Toxicol,* 115**,** 173-81.

Lorber, M. (2007) Exposure of Americans to polybrominated diphenyl ethers. *J Expos Sci Environ Epidemiol,* 18**,** 2-19.

Luu-The, V., D. Duche, C. Ferraris, J. R. Meunier, J. Leclaire & F. Labrie (2009) Expression profiles of phases 1 and 2 metabolizing enzymes in human skin and the reconstructed skin models Episkin and full thickness model from Episkin. *J Steroid Biochem Mol Biol,* 116**,** 178-86.

Lyubimov, A. V., V. V. Babin & A. I. Kartashov (1998) Developmental neurotoxicity and immunotoxicity of 2,4,6-tribromophenol in Wistar rats. *Neurotoxicology,* 19**,** 303-12.

Main, K. M., H. Kiviranta, H. E. Virtanen, E. Sundqvist, J. T. Tuomisto, J. Tuomisto, T. Vartiainen, N. E. Skakkebaek & J. Toppari (2007) Flame retardants in placenta and breast milk and cryptorchidism in newborn boys. *Environ Health Perspect,* 115**,** 1519-26.

Malarvannan, G., C. Belpaire, C. Geeraerts, I. Eulaers, H. Neels & A. Covaci (2015) Organophosphorus flame retardants in the European eel in Flanders, Belgium: Occurrence, fate and human health risk. *Environmental Research,* 140**,** 604-610.

Mankidy, R., B. Ranjan, A. Honaramooz & J. P. Giesy (2013) Effects of Novel Brominated Flame Retardants on Steroidogenesis in Primary Porcine Testicular Cells. *Toxicol Lett,* 24**,** 01361-1.

Mayes, B. A., G. L. Brown, F. J. Mondello, K. W. Holtzclaw, S. B. Hamilton & A. A. Ramsey (2002) Dermal absorption in rhesus monkeys of polychlorinated biphenyls from soil contaminated with Aroclor 1260. *Regul Toxicol Pharmacol,* 35**,** 289-95.

Meeker, J. D., E. M. Cooper, H. M. Stapleton & R. Hauser (2013) Urinary metabolites of organophosphate flame retardants: temporal variability and correlations with house dust concentrations. *Environ Health Perspect,* 121**,** 580-5.

Meeker, J. D., P. I. Johnson, D. Camann & R. Hauser (2009) Polybrominated diphenyl ether (PBDE) concentrations in house dust are related to hormone levels in men. *Sci Total Environ,* 407**,** 3425-9.

Merk, H. F. (2009) Drug skin metabolites and allergic drug reactions. *Curr Opin Allergy Clin Immunol,* 9**,** 311-5.

Mertsching, H., M. Weimer, S. Kersen & H. Brunner (2008) Human skin equivalent as an alternative to animal testing. *GMS Krankenhhyg Interdiszip,* 3.

Mynster Kronborg, T., J. Frohnert Hansen, C. H. Nielsen, L. Ramhøj, M. Frederiksen, K. Vorkamp & U. Feldt-Rasmussen (2016) Effects of the Commercial Flame Retardant Mixture DE-71 on Cytokine Production by Human Immune Cells. *PLOS ONE,* 11**,** e0154621.

Nakari, T. & S. Huhtala (2010) In vivo and in vitro toxicity of decabromodiphenyl ethane, a flame retardant. *Environ Toxicol,* 25**,** 333-8.

Ni, Y., K. Kumagai & Y. Yanagisawa (2007) Measuring emissions of organophosphate flame retardants using a passive flux sampler. *Atmospheric Environment,* 41**,** 3235-3240.

Nicolaides, N. (1974) Skin lipids: their biochemical uniqueness. *Science,* 186**,** 19-26.

Niedorf, F., E. Schmidt & M. Kietzmann (2008a) The automated, accurate and reproducible determination of steady-state permeation parameters from percutaneous permeation data. *Altern Lab Anim* 36**,** 201-213.

OEHHA (2015) Office of Environmental Health Hazard Assessment, State of California, Environmental Protection Agency, Safe drinking water and toxic enforcement act of 1986safe drinking water and toxic enforcement act of 1986, PROPOSITION 65. *http://oehha.ca.gov/prop65/prop65_list/files/P65single082515.pdf*.

Oesch, F., E. Fabian, K. Guth & R. Landsiedel (2014) Xenobiotic-metabolizing enzymes in the skin of rat, mouse, pig, guinea pig, man, and in human skin models. *Arch Toxicol,* 88**,** 2135-90.

Oulhote, Y., J. Chevrier & M. F. Bouchard (2016) Exposure to Polybrominated Diphenyl Ethers (PBDEs) and Hypothyroidism in Canadian Women. *J Clin Endocrinol Metab,* 101**,** 590-8.

Patisaul, H. B., S. C. Roberts, N. Mabrey, K. A. McCaffrey, R. B. Gear, J. Braun, S. M. Belcher & H. M. Stapleton (2013a) Accumulation and endocrine disrupting effects of the flame retardant mixture Firemaster(R) 550 in rats: an exploratory assessment. *J Biochem Mol Toxicol,* 27**,** 124-36.

Pawar, G., M. A.-E. Abdallah, E. V. de Saa & S. Harrad (2016) Dermal bioaccessibility of flame retardants from indoor dust and the influence of topically applied cosmetics. *J Expos Sci Environ Epidemiol*.

Pereira, L. C., A. O. de Souza & D. J. Dorta (2013) Polybrominated diphenyl ether congener (BDE-100) induces mitochondrial impairment. *Basic Clin Pharmacol Toxicol,* 112**,** 418-24.

Pont, A. R., A. R. Charron & R. M. Brand (2004) Active ingredients in sunscreens act as topical penetration enhancers for the herbicide 2,4-dichlorophenoxyacetic acid. *Toxicol Appl Pharmacol,* 195**,** 348-54.

Proksch, E., J. M. Brandner & J. M. Jensen (2008) The skin: an indispensable barrier. *Exp Dermatol,* 17**,** 1063-72.

Regnery, J. & W. Püttmann (2010) Occurrence and fate of organophosphorus flame retardants and plasticizers in urban and remote surface waters in Germany. *Water Research,* 44**,** 4097-4104.

Regnery, J., W. Puttmann, C. Merz & G. Berthold (2011) Occurrence and distribution of organophosphorus flame retardants and plasticizers in anthropogenically affected groundwater. *J Environ Monit,* 13**,** 347-54.

Roosens, L., M. A.-E. Abdallah, S. Harrad, H. Neels & A. Covaci (2009) Exposure to Hexabromocyclododecanes (HBCDs) via Dust Ingestion, but Not Diet, Correlates with Concentrations in Human Serum: Preliminary Results. *Environmental Health Perspectives,* 117**,** 1707-1712.

Roper, C. S., A. G. Simpson, S. Madden, T. L. Serex & J. A. Biesemeier (2006) Absorption of [14C]-Tetrabromodiphenyl Ether (TeBDE) Through Human and Rat Skin In Vitro. *Drug and Chemical Toxicology,* 29**,** 289-301.

Ruby, M. V., A. Davis, R. Schoof, S. Eberle & C. M. Sellstone (1996) Estimation of lead and arsenic bioavailability using a physiologically based extraction test. *Environmental Science & Technology,* 30**,** 422-430.

Saunders, D. M., E. B. Higley, M. Hecker, R. Mankidy & J. P. Giesy (2013) In vitro endocrine disruption and TCDD-like effects of three novel brominated flame retardants: TBPH, TBB, & TBCO. *Toxicol Lett,* 223**,** 252-9.

Saunders, D. M. V., M. Podaima, G. Codling, J. P. Giesy & S. Wiseman (2015) A mixture of the novel brominated flame retardants TBPH and TBB affects fecundity and transcript profiles of the HPGL-axis in Japanese medaka. *Aquatic Toxicology,* 158**,** 14-21.

Schafer-Korting, M., U. Bock, W. Diembeck, H. J. Dusing, A. Gamer, E. Haltner-Ukomadu, C. Hoffmann, M. Kaca, H. Kamp, S. Kersen, M. Kietzmann, H. C. Korting, H. U. Krachter, C. M. Lehr, M. Liebsch, A. Mehling, C. Muller-Goymann, F. Netzlaff, F. Niedorf, M. K. Rubbelke, U. Schafer, E. Schmidt, S. Schreiber, H. Spielmann, A. Vuia & M. Weimer (2008) The use of reconstructed human epidermis for skin absorption testing: Results of the validation study. *Altern Lab Anim,* 36**,** 161-87.

Schafer-Korting, M., U. Bock, A. Gamer, A. Haberland, E. Haltner-Ukomadu, M. Kaca, H. Kamp, M. Kietzmann, H. C. Korting, H. U. Krachter, C. M. Lehr, M. Liebsch, A. Mehling, F. Netzlaff, F. Niedorf, M. K. Rubbelke, U. Schafer, E. Schmidt, S. Schreiber, K. R. Schroder, H. Spielmann & A. Vuia (2006) Reconstructed human epidermis for skin absorption testing: results of the German prevalidation study. *Altern Lab Anim,* 34**,** 283-94.

Schiffer, R., M. Neis, D. Holler, F. Rodriguez, A. Geier, C. Gartung, F. Lammert, A. Dreuw, G. Zwadlo-Klarwasser, H. Merk, F. Jugert & J. M. Baron (2003) Active influx transport is mediated by members of the organic anion transporting polypeptide family in human epidermal keratinocytes. *J Invest Dermatol,* 120**,** 285-91.

Schindler, B. K., S. Koslitz, T. Weiss, H. C. Broding, T. Bruning & J. Bunger (2014) Exposure of aircraft maintenance technicians to organophosphates from hydraulic fluids and turbine oils: a pilot study. *Int J Hyg Environ Health,* 217**,** 34-7.

Schmid, P., F. Bühler & C. Schlatter (1992) Dermal absorption of PCB in man. *Chemosphere,* 24**,** 1283-1292.

Shi, T., S.-J. Chen, X.-J. Luo, X.-L. Zhang, C.-M. Tang, Y. Luo, Y.-J. Ma, J.-P. Wu, X.-Z. Peng & B.-X. Mai (2009) Occurrence of brominated flame retardants other than polybrominated diphenyl ethers in environmental and biota samples from southern China. *Chemosphere,* 74**,** 910-916.

Spalt, E. W., J. C. Kissel, J. H. Shirai & A. L. Bunge (2009) Dermal absorption of environmental contaminants from soil and sediment: a critical review. *J Expo Sci Environ Epidemiol,* 19**,** 119-48.

Stapleton, H. M., S. Eagle, A. Sjodin & T. F. Webster (2012a) Serum PBDEs in a North Carolina toddler cohort: associations with handwipes, house dust, and socioeconomic variables. *Environ Health Perspect,* 120**,** 1049-54.

Stapleton, H. M., S. M. Kelly, J. G. Allen, M. D. McClean & T. F. Webster (2008a) Measurement of Polybrominated Diphenyl Ethers on Hand Wipes: Estimating Exposure from Hand-to-Mouth Contact. *Environmental Science & Technology,* 42**,** 3329-3334.

Stapleton, H. M., S. Klosterhaus, A. Keller, P. L. Ferguson, S. van Bergen, E. Cooper, T. F. Webster & A. Blum (2011) Identification of Flame Retardants in Polyurethane Foam Collected from Baby Products. *Environmental Science & Technology,* 45**,** 5323-5331.

Stapleton, H. M., J. Misenheimer, K. Hoffman & T. F. Webster (2014) Flame retardant associations between children's handwipes and house dust. *Chemosphere,* 116**,** 54-60.

Stapleton, H. M., S. Sharma, G. Getzinger, P. L. Ferguson, M. Gabriel, T. F. Webster & A. Blum (2012c) Novel and High Volume Use Flame Retardants in US Couches Reflective of the 2005 PentaBDE Phase Out. *Environmental Science & Technology,* 46**,** 13432-13439.

Staskal, D. F., J. J. Diliberto, M. J. DeVito & L. S. Birnbaum (2005) Toxicokinetics of BDE 47 in Female Mice: Effect of Dose, Route of Exposure, and Time. *Toxicological Sciences,* 83**,** 215-223.

Stefaniak, A. B., M. G. Duling, L. Geer & M. A. Virji (2014) Dissolution of the metal sensitizers Ni, Be, Cr in artificial sweat to improve estimates of dermal bioaccessibility. *Environmental Science: Processes & Impacts*, 16**,** 341-351.

Stefaniak, A. B. & C. J. Harvey. 2008. Artificial skin surface film liquids. Google Patents.

Stefaniak, A. B., C. J. Harvey & P. W. Wertz (2010) Formulation and stability of a novel artificial sebum under conditions of storage and use. *International journal of cosmetic science*, 32**,** 347-55.

Stuart, H., C. Ibarra, M. A.-E. Abdallah, R. Boon, H. Neels & A. Covaci (2008) Concentrations of brominated flame retardants in dust from United Kingdom cars, homes, and offices: Causes of variability and implications for human exposure. *Environment International*, 34**,** 1170-1175.

Sutton, P., T. J. Woodruff, J. Perron, N. Stotland, J. A. Conry, M. D. Miller & L. C. Giudice Toxic environmental chemicals: the role of reproductive health professionals in preventing harmful exposures. *American Journal of Obstetrics & Gynecology*, 207**,** 164-173.

Suzuki, G., H. Takigami, M. Watanabe, S. Takahashi, K. Nose, M. Asari & S.-i. Sakai (2008) Identification of Brominated and Chlorinated Phenols as Potential Thyroid-Disrupting Compounds in Indoor Dusts. *Environmental Science & Technology*, 42**,** 1794-1800.

Tao, F., M. A.-E. Abdallah & S. Harrad (2016a) Emerging and legacy flame retardants in UK indoor air and dust: evidence for replacement of PBDEs by emerging flame retardants? *Environmental Science & Technology*.

--- (2016b) Emerging and Legacy Flame Retardants in UK Indoor Air and Dust: Evidence for Replacement of PBDEs by Emerging Flame Retardants? *Environmental Science & Technology*, 50**,** 13052-13061.

Teuten, E. L., J. M. Saquing, D. R. U. Knappe, M. A. Barlaz, S. Jonsson, A. Björn, S. J. Rowland, R. C. Thompson, T. S. Galloway, R. Yamashita, D. Ochi, Y. Watanuki, C. Moore, P. H. Viet, T. S. Tana, M. Prudente, R. Boonyatumanond, M. P. Zakaria, K. Akkhavong, Y. Ogata, H. Hirai, S. Iwasa, K. Mizukawa, Y. Hagino, A. Imamura, M. Saha & H. Takada (2009) Transport and release of chemicals from plastics to the environment and to wildlife. *Philosophical Transactions of the Royal Society of London B: Biological Sciences*, 364**,** 2027-2045.

Tilson, H. A., B. Veronesi, R. L. McLamb & H. B. Matthews (1990) Acute exposure to tris(2-chloroethyl)phosphate produces hippocampal neuronal loss and impairs learning in rats. *Toxicol Appl Pharmacol,* 106**,** 254-69.

Tornier, C., C. Amsellem, A. d. B. d. Fraissinette & N. Alépée (2010) Assessment of the optimized SkinEthic™ Reconstructed Human Epidermis (RHE) 42 bis skin irritation protocol over 39 test substances. *Toxicology in Vitro,* 24**,** 245-256.

Trudel, D., M. Scheringer, N. von Goetz & K. Hungerbuehler (2011a) Total Consumer Exposure to Polybrominated Diphenyl Ethers in North America and Europe. *Environmental Science & Technology,* 45**,** 2391-2397.

Tseng, L.-H., C.-W. Lee, M.-H. Pan, S.-S. Tsai, M.-H. Li, J.-R. Chen, J.-J. Lay & P.-C. Hsu (2006) Postnatal exposure of the male mouse to 2,2′,3,3′,4,4′,5,5′,6,6′-decabrominated diphenyl ether: Decreased epididymal sperm functions without alterations in DNA content and histology in testis. *Toxicology,* 224**,** 33-43.

Turyk, M. E., V. W. Persky, P. Imm, L. Knobeloch, R. Chatterton & H. A. Anderson (2008) Hormone disruption by PBDEs in adult male sport fish consumers. *Environ Health Perspect,* 116**,** 1635-41.

Ulsamer, A. G., W. K. Porter & R. E. Osterberg (1978) Percutaneous absorption of radiolabeled TRIS from flame-retarded fabric. *J Environ Pathol Toxicol,* 1**,** 543-9.

Umezu, T., J. Yonemoto, Y. Soma & T. Suzuki (1998) Tris(2-chloroethyl)phosphate Increases Ambulatory Activity in Mice: Pharmacological Analyses of Its Neurochemical Mechanism. *Toxicology and Applied Pharmacology,* 148**,** 109-116.

Usenko, C., E. Abel, A. Hopkins, G. Martinez, J. Tijerina, M. Kudela, N. Norris, L. Joudeh & E. Bruce (2016) Evaluation of Common Use Brominated Flame Retardant **(BFR)** Toxicity Using a Zebrafish Embryo Model. *Toxics,* 4**,** 21.

USEPA (2011) Exposure factors handbook. *www.epa.gov/ncea/efh/pdfs/efh-complete.pdf*.

Van den Eede, N., A. L. Heffernan, L. L. Aylward, P. Hobson, H. Neels, J. F. Mueller & A. Covaci (2015) Age as a determinant of phosphate flame retardant exposure of the Australian population and identification of novel urinary PFR metabolites. *Environ Int,* 74**,** 1-8.

Van den Eede, N., H. Neels, P. G. Jorens & A. Covaci (2013) Analysis of organophosphate flame retardant diester metabolites in human urine by liquid chromatography electrospray ionisation tandem mass spectrometry. *Journal of Chromatography A,* 1303**,** 48-53.

van der Veen, I. & J. de Boer (2012a) Phosphorus flame retardants: Properties, production, environmental occurrence, toxicity and analysis. *Chemosphere,* 88**,** 1119-1153.

Veronesi, B., S. Padilla & D. Newland (1986) Biochemical and neuropathological assessment of triphenyl phosphite in rats. *Toxicology and Applied Pharmacology,* 83**,** 203-210.

Viberg, H., A. Fredriksson & P. Eriksson (2003) Neonatal exposure to polybrominated diphenyl ether (PBDE 153) disrupts spontaneous behaviour, impairs learning and memory, and decreases hippocampal cholinergic receptors in adult mice. *Toxicology and Applied Pharmacology,* 192**,** 95-106.

Vizcaino, E., J. O. Grimalt, A. Fernandez-Somoano & A. Tardon (2014) Transport of persistent organic pollutants across the human placenta. *Environ Int,* 65**,** 107-15.

Walters, K. A., K. R. Brain, D. Howes, V. J. James, A. L. Kraus, N. M. Teetsel, M. Toulon, A. C. Watkinson & S. D. Gettings (1997) Percutaneous penetration of octyl salicylate from representative sunscreen formulations through human skin in vitro. *Food Chem Toxicol,* 35**,** 1219-25.

Wang, Q., K. Liang, J. Liu, L. Yang, Y. Guo, C. Liu & B. Zhou (2013) Exposure of zebrafish embryos/larvae to TDCPP alters concentrations of thyroid hormones and transcriptions of genes involved in the hypothalamic-pituitary-thyroid axis. *Aquat Toxicol,* 126**,** 207-13.

Wang, W., K. O. Abualnaja, A. G. Asimakopoulos, A. Covaci, B. Gevao, B. Johnson-Restrepo, T. A. Kumosani, G. Malarvannan, T. B. Minh, H. B. Moon, H. Nakata, R. K. Sinha & K. Kannan (2015) A comparative assessment of human exposure to tetrabromobisphenol A and eight bisphenols including bisphenol A via indoor dust ingestion in twelve countries. *Environ Int,* 83**,** 183-91.

Watkins, D. J., M. D. McClean, A. J. Fraser, J. Weinberg, H. M. Stapleton, A. Sjodin & T. F. Webster (2011) Exposure to PBDEs in the office environment: evaluating the relationships between dust, handwipes, and serum. *Environ Health Perspect,* 119**,** 1247-52.

Watkins, D. J., M. D. McClean, A. J. Fraser, J. Weinberg, H. M. Stapleton, A. Sjödin & T. F. Webster (2012) Impact of Dust from Multiple Microenvironments and Diet on PentaBDE Body Burden. *Environmental Science & Technology,* 46**,** 1192-1200.

Watkins, D. J., M. D. McClean, A. J. Fraser, J. Weinberg, H. M. Stapleton & T. F. Webster (2013) Associations between PBDEs in Office Air, Dust, and Surface Wipes. *Environment International,* 0**,** 124-132.

Wiegand, C., N. J. Hewitt, H. F. Merk & K. Reisinger (2014) Dermal xenobiotic metabolism: a comparison between native human skin, four in vitro skin test systems and a liver system. *Skin Pharmacol Physiol,* 27**,** 263-75.

Wikoff, D. S. & L. Birnbaum. 2011. Human Health Effects of Brominated Flame Retardants. In *Brominated Flame Retardants,* eds. E. Eljarrat & D. Barceló, 19-53. Berlin, Heidelberg: Springer Berlin Heidelberg.

Wilkinson, S. C. & F. M. Williams (2002) Effects of experimental conditions on absorption of glycol ethers through human skin in vitro. *Int Arch Occup Environ Health,* 75**,** 519-527.

Wu, C.-C., L.-J. Bao, S. Tao & E. Y. Zeng (2016a) Dermal Uptake from Airborne Organics as an Important Route of Human Exposure to E-Waste Combustion Fumes. *Environmental Science & Technology*.

Wu, N., T. Herrmann, O. Paepke, J. Tickner, R. Hale, E. Harvey, M. La Guardia, M. D. McClean & T. F. Webster (2007) Human Exposure to PBDEs: Associations of PBDE Body Burdens with Food Consumption and House Dust Concentrations. *Environmental Science & Technology,* 41**,** 1584-1589.

Xiao, Z., J. Feng, Z. Shi, J. Li, Y. Zhao & Y. Wu (2011) Determination of three brominated flame retardants in human serum using solid-phase extraction coupled with ultra-performance liquid chromatography-tandem mass spectrometry and gas chromatography-mass spectrometry. *Se Pu,* 29**,** 1165-72.

Xu, F., G. Giovanoulis, S. van Waes, J. A. Padilla-Sanchez, E. Papadopoulou, J. Magner, L. S. Haug, H. Neels & A. Covaci (2016) Comprehensive Study of Human External Exposure to Organophosphate Flame Retardants via Air, Dust, and Hand Wipes: The Importance of Sampling and Assessment Strategy. *Environ Sci Technol,* 50**,** 7752-60.

Yamada-Okabe, T., H. Sakai, Y. Kashima & H. Yamada-Okabe (2005) Modulation at a cellular level of the thyroid hormone receptor-mediated gene expression by 1,2,5,6,9,10-hexabromocyclododecane (HBCD), 4,4'-diiodobiphenyl (DIB), and nitrofen (NIP). *Toxicol Lett,* 155**,** 127-33.

Yamaguchi, Y., M. Kawano & R. Tatsukawa (1988a) Tissue distribution and excretion of hexabromobenzene and its debrominated metabolites in the rat. *Arch Environ Contam Toxicol,* 17**,** 807-12.

Yamaguchi, Y., M. Kawano, R. Tatsukawa & S. Moriwaki (1988b) Hexabromobenzene and its debrominated compounds in human adipose tissues of Japan. *Chemosphere,* 17**,** 703-707.

Zalko, D., C. Jacques, H. Duplan, S. Bruel & E. Perdu (2011) Viable skin efficiently absorbs and metabolizes bisphenol A. *Chemosphere,* 82**,** 424-30.

Zendzian, R. P. (2000) Dermal Absorption of Pesticides in the Rat. *AIHAJ - American Industrial Hygiene Association,* 61**,** 473-483.

Zhang, X., F. Yang, C. Xu, W. Liu, S. Wen & Y. Xu (2008) Cytotoxicity evaluation of three pairs of hexabromocyclododecane (HBCD) enantiomers on Hep G2 cell. *Toxicol In Vitro,* 22**,** 1520-7.

Zhang, Z. & B. B. Michniak-Kohn (2012) Tissue Engineered Human Skin Equivalents. *Pharmaceutics,* 4**,** 26-41.

Zheng, J., K.-H. Chen, X.-J. Luo, X. Yan, C.-T. He, Y.-J. Yu, G.-C. Hu, X.-W. Peng, M.-Z. Ren, Z.-Y. Yang & B.-X. Mai (2014) Polybrominated Diphenyl Ethers (PBDEs) in Paired Human Hair and Serum from e-Waste Recycling Workers: Source Apportionment of Hair PBDEs and Relationship between Hair and Serum. *Environmental Science & Technology,* 48**,** 791-796.

Zhou, S. N., A. Buchar, S. Siddique, L. Takser, N. Abdelouahab & J. Zhu (2014) Measurements of Selected Brominated Flame Retardants in Nursing Women: Implications for Human Exposure. *Environmental Science & Technology,* 48**,** 8873-8880.

Zhou, T., D. G. Ross, M. J. DeVito & K. M. Crofton (2001) Effects of short-term in vivo exposure to polybrominated diphenyl ethers on thyroid hormones and hepatic enzyme activities in weanling rats. *Toxicol Sci,* 61**,** 76-82.

National Research Council (US) Subcommittee on Flame-Retardant Chemicals. Toxicological Risks of Selected Flame-Retardant Chemicals. Washington (DC): National Academies Press (US); 2000. Available from: http://www.ncbi.nlm.nih.gov/books/NBK225647/ doi: 10.17226/9841